University of Alberta

The Design, Synthesis and Evaluation of Multivalent Heterobifunctional Ligands Specific for Shiga Toxin 1 and Shiga Toxin 2

by

Jared Matthew Jacobson

A thesis submitted to the Faculty of Graduate Studies and Research
in partial fulfillment of the requirements for the degree of

Doctor of Philosophy

Department of Chemistry

Spring 2014
Edmonton, Alberta

Abstract

Hemolytic uremic syndrome (HUS) is a potential life-threatening condition caused by infection with Shiga toxin-producing *Escherichia coli* O157:H7. There are two major types of Shiga toxins, namely, Shiga toxin 1 (Stx1) and Shiga toxin 2 (Stx2), of which, Stx2 is clinically most closely associated with enterohemorrhagic *E. coli* O157:H7-mediated HUS. The ability to express the toxin has been acquired by other *E. coli* strains and outbreaks of food poisoning have caused significant mortality rates. Shiga toxins, are AB_5 toxins that gain entry into human cells by recognizing and binding to the P^k trisaccharide component of the membrane glycosphingolipid receptor Gb_3.

A bifunctional ligand that incorporates P^k trisaccharide and a cyclic pyruvate acetal that binds to human serum amyloid P component (HuSAP), facilitates simultaneous binding of the B_5 subunit of Shiga toxins with HuSAP as a supramolecular complex. The incorporation of the heterobifunctional ligand into a polymeric scaffold affords an increase in binding avidity over the low affinity of the trisaccharide ligand. When the multivalent bifunctional ligand was tested in a mouse model of Shigatoxemia, it was protective at low microgram doses.

The synthesis of a disaccharide P^k analogue is described whereby α-GalNAc replaces the terminal α-Gal residue and is co-crystallized with Stx2. This co-crystal structure confirms previous inferences that two of the primary binding sites identified in the B_5 pentamer of Stx1 are also functional in Stx2. This knowledge provides a rationale for the synthesis and evaluation of heterobifunctional antagonists for *E. coli* toxins that target Stx2.

Acknowledgements

I would like to thank my supervisor, Prof. David Bundle for the opportunity to pursue my Ph.D. in his group and for the guidance he has provided me throughout. I am very grateful for all the amazing opportunities I have been given to further expand upon my knowledge and expertise such as attending the Gordon Research conference and the International Carbohydrate Symposium and being given the opportunity to teach having substituted for him on occasion.

I would also like to thank all past and present members of the Bundle group for all their support and help. Most notably I would like to thank Dr. Pavel Kitov for his invaluable help and guidance. We are very fortunate in the Chemistry department to have a number of facilities to assist in our data acquisition and analysis available to us such as the analytical instrumentation lab, NMR services and mass spectrometry lab. I am very appreciative of all their help and time with my samples.

Lastly, I would like to thank my family: father, mother and brother, and all my friends for their support, understanding and patience while I pursued my Ph.D. You have helped me more than you will ever know.

Table of Contents

List of Tables

List of Figures

List of Schemes

Abbreviations

-CN	cyano
A/E	“attaching-and-effacing”
AA	aggregative adherence
Ac2O	acetic anhydride
ADP	adenosine diphosphate
AgOTf	silver trifluoromethanesulfonate
Ala	Alanine
AllBr	allyl bromide
Arg	Arginine
Asn	Asparagine
Asp	Aspartic acid
BF_3•OEt_2	boron trifluoride diethyl etherate
BH_3•THF	borane tetrahydrofuran complex
BnBr	benzyl bromide
BSA	bovine serum albumin
BzCl	benzoyl chloride
CAMKII	calmodulin-dependent protein kinase II
CFTR	cystic fibrosis transmembrane regulator
cGMP	cyclic guanosine monophosphate
CH_2Cl_2	dichloromethane
CH_3CN	acetonitrile
CH_3COOH	acetic acid

CH_3NO_2	nitromethane
CH_3OH	methanol
CH_3ONa	sodium methoxide
Cl_3CCN	trichloroacetonitrile
CP	cyclic pyruvate
CSA	camphor sulfonic acid
CT	cholera toxin
DA	diffuse adherence
DAEC	diffusely-adherent *E. coli*
DBU	1,8-diazabicyclo[5.4.0]undec-7-ene
DMF	*N,N*-dimethylformamide
DTT	dithiothreitol
E. coli	*Escherichia coli*
EAEC	Enteroaggregative *E coli*
EAF	EPEC adherence factor
EAST-1	*E. coli* associated heat stable toxin 1
EC_{50}	half minimal effective concentration for binding
EHEC	Enterohemorrhagic *E. coli*
EIEC	Enteroinvasive *E. coli*
ELISA	enzyme linked immunosorbent assay
EPEC	Enteropathogenic *E. coli*
ER	endoplasmic reticulum
Esp	EPEC-secreted protein

Et_2O	diethyl ether
Et_3N	triethylamine
Et_3SiH	triethylsilane
ETEC	Enterotoxigenic *E. coli*
FT-ICT-MS	Fourier-transform ion cyclotron resonance mass spectrometry
Gal	D-galactose
GalNAc	*N*-acetylgalactosamine, 2-acetamido-2-deoxy-D-galactose
Gb3	globotriaosylceramide
GC-C	guanylate cyclase C
Glc	D-glucose
Glu	Glutamic acid
Gly	Glycine
GM_1	monosialotetrahexosylganglioside
GPP130	Golgi phosphoprotein of 130 kDa
H-bond	hydrogen bond
HC	Hemorrhagic colitis
HF-Pyr	hydrogen fluoride in pyridine
$Hg(CN)_2$	mercury(II) cyanide
$HgBr_2$	mercury(II) bromide
HUS	Hemolytic uremic syndrome
HuSAP	Human serum amyloid P component
HuSAP-tg	HuSAP-transgenic
I.P.	intraperitoneal injection

IC_{50}	inhibitor concentration required to give 50 % inhibition
IDCP	iodonium dicollidine perchlorate
Ipa	invasion plasmid associated
ITC	isothermal titration calorimetry
K_2CO_3	potassium carbonate
KCN	potassium cyanide
LA	localized adherence
LEE	locus of enterocyte effacement
LPS	lipopolysaccharide
LT	heat labile toxin
Lys	Lysine
MALDI-TOF	matrix assisted laser desorption ionization time of flight
MCO	*O*-methoxycarbonyl octane
mg	milligram
MHz	Megahertz
ml	milliliter
$NaBH_3CN$	sodium cyanoborohydride
NaCl	sodium chloride
NaH	sodium hydride
nanoES	nano electrospray
NETs	neutrophil extracellular traps
ng	nanogram
NIS	*N*-iodosuccinimide

NMO	*N*-methylmorpholine *N*-oxide
NMR	nuclear magnetic resonance
OsO_4	osmium tetraoxide
Pet	plasmid encoded toxin
pg	picogram
Phe	Phenylalanine
P^k	α-Gal*p*-(1→4)-β-Gal*p*-(1→4)-β-Gal*p*-(1→*O*)
P^kNAc	α-GalNAc*p*-(1→4)-β-Gal*p*-(1→4)-β-Gal*p*-(1→*O*)
Pyr	pyridine
RES	reticuloendothelial system
RIPs	ribose inactivating proteins
rRNA	ribosomal ribonucleic acid
RTA	Ricin toxin A
Ser	Serine
SLT	Shiga-like toxin
$SOCl_2$	thionyl chloride
SPR	surface plasmon resonance
ST	heat stable toxin
STD	saturation transfer difference
Stx1	Shiga toxin 1
Stx2	Shiga toxin 2
Stxs	Shiga toxins
T3SS	type III secretion system

TBAB	tetra-*n*-butylammonium bromide
TBDPS	*tert*-butyl diphenylsilyl
TBDPSCl	*tert*-butyl diphenylsilyl chloride
TBMB	2-*tert*-butyl-2-methyl-1,3-benzodiazole-4-carboxylate
TDS	(dimethyl)thexylsilyl
TEMED	tetramethylethylenediamine
Tf_2O	trifluomethanesulfonic anhydride
TFA	trifluoroacetic acid
TfOH	trifluomethanesulfonic acid
THF	tetrahydrofuran
Thr	Threonine
TLC	thin layer chromatography
TMSOTf	trimethylsilyl trifluoromethane sulfonate
tRNA	transfer ribonucleic acid
trNOE	transfer nuclear Overhauser effect
Trp	Tryptophan
UDP	uridinium diphosphate
UV	ultraviolet
VT	Verotoxin

Chapter 1

Introduction

1.1. *Escherichia coli*

Escherichia coli (*E. coli*) are gram-negative, rod-shaped bacteria of the Enterobacteriaceae family. *E. coli* are facultative anaerobes and are the predominant species of human colonic flora.[1,2] They have been found to colonize the human colon within the first few hours of life.[3] Most commonly, *E. coli* remains harmlessly in the gut but in some cases, immuno-compromised or debilitated individuals can develop infection even from strains known to be non-pathogenic.[3] Upon infection with pathogenic forms of *E. coli*, three general clinical syndromes occur from naturally pathogenic strains.

1. The development of urinary tract infections.
2. Sepsis and/or meningitis
3. Enteric or diarrheal disease.

Due to the wide variety of types of *E. coli*, classification and identification of specific variants plays an important role in the study of these organisms. As such, many methods and characteristics may be used for the identification of subtypes of the species but the most common method is that of serotyping.[4]

1.1.1. Serotyping of *E. coli*

The serotyping of *E. coli* species was first used and introduced by Kaufman *et al*.[5] Kaufmann's approach is based on the identification of O, H, and K surface antigen profiles.[3,6] The specific combination of O, H and K antigens defines the serotype of an *E. coli* isolate.

The O antigen (also referred to as the somatic antigen) is a polymer of immunogenic repeating oligosaccharides and is a component of the bacterial lipopolysaccharide (LPS).[7] LPS consists of lipid A, an inner core oligosaccharide, an outer core oligosaccharide and lastly the O antigen [Figure 1.1].[7] It is the structure of the repeating units of the O-specific chain of polysaccharides that defines the specificity of the O antigens.[4]

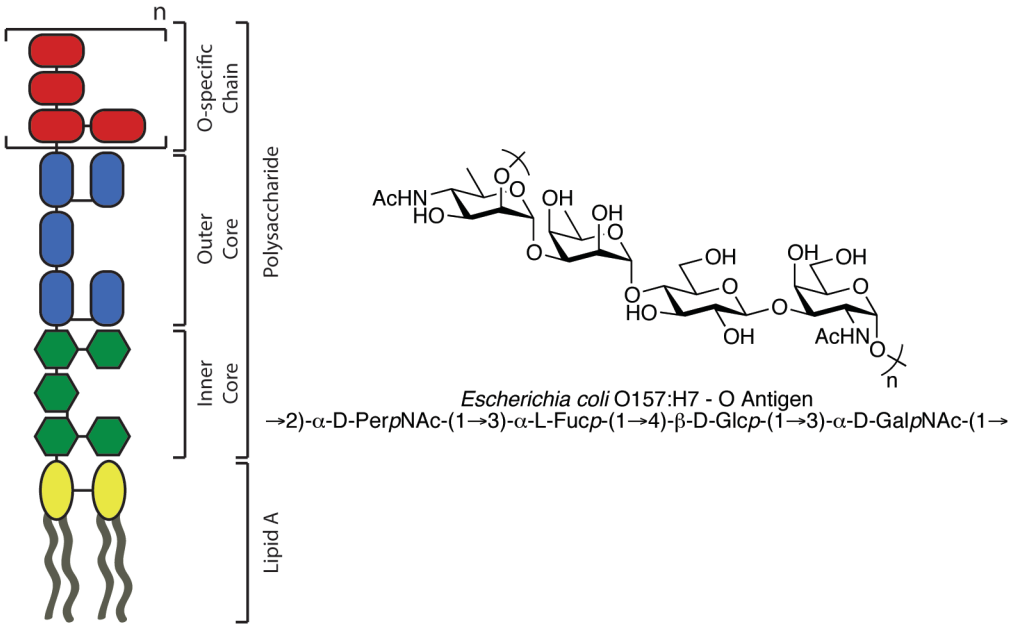

Figure 1.1. (Left) General structure of bacterial lipopolysaccharides. Oval and hexagonal do not represent specific carbohydrates. (Right) The structure of the *E. coli* O157:H7 O-antigen polysaccharide.

The H antigens of *E. coli* are flagellar antigens.[4] The flagella of *E. coli* are responsible for the movement of the bacteria and are composed of the protein flagellin.[8]

The K antigens[9] are also polysaccharide polymers on the surface of the cell although what distinguishes them from being characterized as O antigens is their acidic character. Consequently, K antigens are composed of acidic capsular polysaccharides and as such have been labeled as a unique serotype.[3,4]

The specific combination of O and H antigens in defining a serotype of *E. coli* is important, as H antigens may occur with many combinations of O antigens. Therefore, the distinct determination of both the O and H antigens is necessary as a marker for any pathogenic *E. coli* serotypes.[3,4]

1.1.2. Classification of *E. coli* based on virulence

The term enteropathogenic *E. coli* (EPEC) was first applied by Neter[10] to define characterized *E. coli* strains associated with enteric disease. For many years, the term EPEC was used for a variety of organisms that were associated with diarrheal disease but with unknown pathogenic mechanisms. Since then, the discovery of *E. coli* pathogenic mechanisms has allowed for a more specific classification of EPEC and other types of enteric pathogenic *E. coli* based on their respective virulence properties in human disease. To date, six classes of pathogenic *E. coli* have been recognized; enteropathogenic *E. coli* (EPEC), enterotoxigenic *E. coli* (ETEC), enteroinvasive *E. coli* (EIEC), enteroaggregative *E. coli* (EAEC), diffusely-adherent *E. coli* (DAEC) and enterohemorrhagic *E. coli* (EHEC).[11] Below is a description of the first five classes while EHEC will be addressed in section 1.2.

1.1.2.1. Enteropathogenic *E. coli*

EPEC infections are characterized by the development of watery diarrhea, vomiting and fever, particularly in infants and young children.[2,11] The hallmark of EPEC infection is the development of an "attaching–and–effacing" (A/E) lesion

as a result in part from the intimate adherence between the bacterium and the epithelial cell membrane.

A three-stage model of EPEC infection has been proposed by Donnenberg and Kaper:[12]

1. Localized adherence [Figure 1.2a]

In 1979, Cravioto *et al*. tested the adherence of various EPEC and ETEC strains to HEp-2 cells. Their results indicated that EPEC had acquired the unique ability to adhere to HEp-2 cells, whereas ETEC and other types of pathogenic *E. coli* were unable to do so.[13] These findings suggested a specific factor associated with EPEC that enabled the localized adherence of these bacteria to the outer membrane of epithelial cells. Baldini *et al*. discovered the factor involved in EPEC adherence was plasmid encoded and was later coined the EPEC adherence factor (EAF).[14]

2. Signal transduction

Adherence of EPEC to intestinal epithelial cells induces a variety of signal transduction pathways and is associated with an increase of intracellular calcium levels.[15,16] An increase in the concentration of calcium within the cell inhibits the absorption of sodium and chloride thereby increasing the extracellular concentration of chloride leading to the secretion of water from the cell and the development of diarrhea.[17,18]

3. Intimate adherence

The intimate adherence of EPEC is dependent on an approximately 94 kDa outer membrane protein called Intimin encoded by the *eae* gene.[19] Intimin has been found to be present in all EPEC and EHEC and is one of many possible contributors involved in the development of the A/E lesion. The *eae* gene has been found to be required for full virulence of EPEC. Intimin has been implicated in the rearrangement of actin within the host epithelial cell causing sever distortions to the host cell structure and resulting in inflammation.[20]

At least four proteins have been discovered and investigated that are secreted from EPEC that could explain pathogenicity. EPEC-secreted protein A or EspA, EspB, EspC and EspD.[21-24] All but EspC were found to be required for the development of the A/E lesion and the induction of pathogenesis.[25]

1.1.2.2. Enterotoxigenic *E. coli*

ETEC are defined by their ability to express at least one member of two defined groups of enterotoxins: heat-stable toxin (ST) and heat-labile toxin (LT).[2] ETEC are found to be the major cause of infantile diarrhea. Fever, abdominal cramps, vomiting and watery diarrhea characterize ETEC infections.[3] LT is an AB_5, high molecular weight protein that resembles cholera toxin (CT).[26] Both LT and CT possess an enzymatically active A subunit joined to five receptor binding B subunits.[27] The natural ligand for LT is GM_1 present of the surface of epithelial cells.[28] Once incorporated into the cell, the toxin is transferred through the cell *via*

trans-Golgi vesicular transport.[29] The A subunit of LT possesses adenosine diphosphate (ADP)-ribosyltransferase activity and through a series of intracellular mechanisms, activates cystic fibrosis transmembrane regulator (CFTR – a defective ion channel in cystic fibrosis).[3,30,31] Activation of CFTR, induces the secretion of chloride from the cell and thereby increasing the extracellular concentration of chloride, causing water secretion and the onset of diarrhea.[3,32]

In contrast to LT's, ST's are a family of small oligomeric peptides. There are two unrelated classes of ST's: STa and STb and both have been found to be plasmid encoded.[33] STa is approximately 18-19 amino acids long with a molecular mass of approximately 2 kDa.[32,34] STa's method of action involves binding to its natural receptor, guanylate cyclase C (GC-C) on intestinal epithelial cells.[35,36] GC-C is an apical transmembrane protein and binding on its outer surface induces its intracellular activity.[3] Activation of GC-C results in an increase of guanylate cyclase activity, which increases the intracellular cyclic guanosine monophosphate (cGMP) concentration. An increase in cGMP concentration ultimately leads to the secretion of chloride and/or the inhibition of sodium chloride absorption resulting in a net secretory state.[3,32,33] STb is a 48 amino acid protein with a molecular mass of 5.2 kDa and is not homologous to STa.[37] Studies have shown that STb induces damage in the intestinal epithelium and increases the secretion of intracellular calcium.[30,38] Evidence suggests that increasing concentrations of calcium within the cell activates calmodulin-dependent protein kinase II (CAMKII). CAMKII opens a calcium activated

chloride channel leading to the loss of chloride resulting in the secretion of water from the cells and the development of diarrhea.[32,38]

1.1.2.3. Enteroinvasive *E. coli*

In 1971, it was discovered that certain *E. coli* strains, serotypically distinct from ETEC and EPEC, caused severe diarrhea.[39] Their primary pathogenic trait was found to be their ability to invade and proliferate *within* epithelial cells. As such they were coined EIEC.[3,39] EIEC have been found to be very similar to *Shigella* and much of what is understood about EIEC pathogenesis has been pioneered by work done on *Shigella*.[40] The ability of EIEC to invade epithelial cells is the result of a large plasmid pINV (~140 MDa) that encodes invasion plasmid associated (Ipa) proteins, required for invasion.[41-44] Upon entering the epithelial cells of the colon, EIEC lyse the phagosomal vacuole and multiply within the cytoplasm, resulting in cell death.[44,45] In addition, it has been hypothesized that EIEC serotypes may express an enterotoxin that mediates severe diarrhea, but this is still under investigation.[3]

1.1.2.4. Enteroaggregative *E. coli*

Cravioto *et al*. discovered that certain *E. coli* serotypes displayed adherence to HEp-2 cells.[13] This discovery led to further research, investigating the adherence properties of other *E. coli* serotypes to HEp-2 cells. Subsequently it was shown that certain, non-EPEC serotypes, also adhered to these cells and did so in a manner distinguishable from traditional EPEC.[46,47] The adherence pattern

of EPEC is described as localized adherence (the presence of clusters or microcolonies on the surface of the cells) whereas non-EPEC morphology is described as "diffuse".[46,48] It was later found that the "diffuse" category could be subdivided into two subtypes of adherence:[48]

1. aggregative adherence (EAEC)
2. diffuse adherence (DAEC)

EAEC pathogenesis is defined by bacteria that display aggregative adherence: to each other, to the surface of epithelial cells and additionally the glass coverslip when being analyzed.[3] These all occur in a characteristic "stacked brick" pattern [Figure 1.2b].[49] In doing so, EAEC have the ability to form biofilms and studies have shown that EAEC adheres to the intestinal mucosa of the small bowel surface and forms a mucoid biofilm.[50]

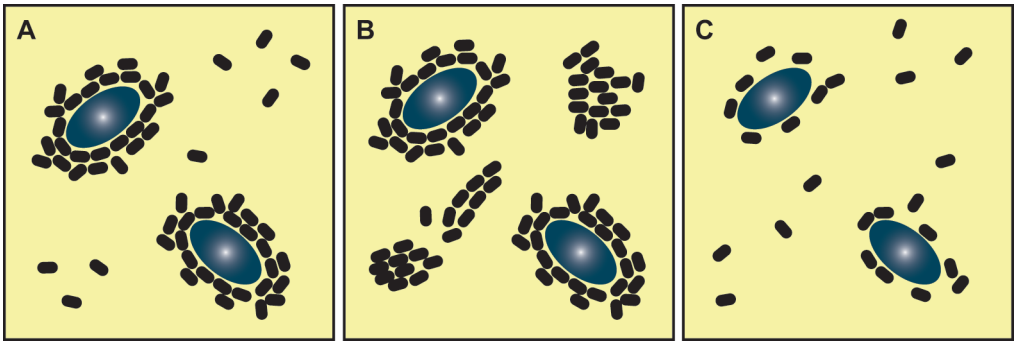

Figure 1.2: Adapted representation of adherence patterns of *E. coli*. (a) Localized adherence (LA), typical of EPEC; (b) Aggregative adherence (AA), bacteria adhere to each other as well as to the surface of cells (EAEC); (c) Diffuse adherence (DA), bacteria are dispersed over surface of the cell (DAEC).[3]

EAEC possess the ability to produce several potentially pathogenic toxins including *E. coli* associated heat stable toxin 1 (EAST-1). However, the role of EAST-1 in the development of diarrhea remains inconclusive.[51] In addition, EAEC can encode for Pet (plasmid-encoded toxin). Pet is a type V serine protease transporter which is known to induce the release of mucous and the development of crypt abscesses.[52] However, there is still much to be understood about EAEC pathogenesis.

1.1.2.5. Diffusely-adherent *E. coli*

DAEC serotypes are a group of isolates, all of which exhibit diffuse adherence to epithelial cells [Figure 1.2c]. Little is known about the pathogenic features of DAEC.[3] Although recently, research has shown that DAEC can induce the formation of neutrophil extracellular traps (NETs) causing epithelial cell inflammation and additionally result in unfavorable effects on actin cytoskeleton structure.[53]

1.2. Enterohemorrhagic *E. coli*

Enterohemorrhagic *E. coli* (EHEC) are technically a subset of a pathogenic class labeled Shiga toxin producing *E. coli* (STEC) in that they both produce Shiga toxins (Stxs). However, the term EHEC has a clinical connotation whereby EHEC denotes a subset of STEC that produce Stxs, form A/E lesions and possess a 60 MDa plasmid. Lacking these additional characteristics, forming A/E lesions and possessing the specific plasmid, while being able to produce

Shiga toxins does not cause serious disease in humans. To further understand the role of EHEC, one must take a closer look at the history and research that led to the discovery of the prototypical EHEC *E. coli* O157:H7 and its cytotoxins.

1.2.1. Discovery of *Escherichia coli* O157:H7

In 1977, Konowalchuk *et al.* reported the discovery of a toxin distinct from LT that showed particular virulence against kidney epithelial cells from the African green monkey, also known as Vero cells. They named this toxin verotoxin or VT.[54] The year 1983 proved to be a productive year for the investigation of *E. coli* O157:H7, firstly, Riley *et al*. investigated an outbreak of severely bloody diarrhea from across the United States after consumption of contaminated hamburgers from a nation-wide fast food chain. They reported that a previously rare *E. coli* serotype, *E. coli* O157:H7 was the major causative agent that resulted in Hemorrhagic colitis (HC) and did so in a manner distinct from EIEC or ETEC after testing.[55] In the same year, Karmali *et al.* reported the association of the development of hemolytic uremic syndrome (HUS) with an isolated fecal cytotoxin from a cytotoxin producing *E. coli* in analyzed stool samples.[56] Prior work done by O'Brien *et al.* in 1977 and 1980 found that extracts from certain *E. coli* strains were cytotoxic to HeLa cells (an immortal cell line derived from cervical cancer cells). In addition, they reported that this cytotoxicity could be neutralized by an antitoxin serum specific for crude Shiga toxin from *Shigella dysenteriae I*.[57,58] As a result of their earlier endeavors, they later showed that many *E. coli* strains isolated from patients suffering from severe

diarrhea produced a Shiga-like toxin (SLT).[59] O'Brien *et al.* subsequently proved that VT and SLT were one and the same and that the *E. coli* serotype O157:H7 described by Riley produced this toxin.[60] Independently and at the same time, Johnson *et al.* found that *E. coli* O157:H7 strains isolated from patients suffering from hemorrhagic colitis, produced a cytotoxin, toxic to Vero cells.[61] Lastly, Karmali *et al.* concluded the year by proposing that SLT/VT was the common virulence factor between HC and HUS and was responsible for the damage observed to both intestinal and renal tissues.[62]

1.2.2. Pathology of *E. coli* O157:H7

1.2.2.1. Shiga toxins

Infection with *E. coli* O157:H7 can result in the development of hemorrhagic colitis HC and potentially the development of a severe complication, hemolytic uremic syndrome (HUS).[63,64] HC is characterized by severe abdominal pain, watery diarrhea followed by grossly bloody diarrhea and little-to-no fever. The development of potentially life-threatening HUS is attributed to the ability of EHEC to produce Shiga toxins. There are two major types of Shiga toxins, Shiga toxin 1 (Stx1) and Shiga toxin 2 (Stx2). Within each family of Shiga toxins there exist subtypes of Stx1 and Stx2, although not all have been associated with human disease (Table 1.1).[63]

Toxin	Source	Synonym	A Subunit Homology[a]	B Subunit Homology[a]
Shiga toxin[65]	*S. dysenteriae* Type I	Stx		
Shiga toxin 1a[66,67]	*E. coli* O157:H7	Stx1, Stx1a, VT1, SLTI	99%	100%
Shiga toxin 1c[68]	*E. coli* O128:H2	Stx1c, VT1c, SLTIc	97%	97%
Shiga toxin 1d[69]	*E. coli* ONT:H19	Stx1d, VT1d, SLTId	94%	92%
Shiga toxin 2a[70]	*E. coli* O157:H7	Stx2, Stx2a, VT2, SLTIIa	Stx hom.: 55%	Stx hom.: 57%
Shiga toxin 2b[71]	*E. coli* O118:H12	Stx2b, VT2b, SLTIIb	94%	89%
Shiga toxin 2c[72]	*E. coli* O157:H7	Stx2c, VT2c, SLTIIc	100%	97%
Shiga toxin 2d[73]	*E. coli* O91:H21	Stx2d, VT2d, SLTIId	99%	97%
Shiga toxin 2e[74]	*E. coli* O139	Stx2e, VT2e, SLTIIe	94%	87%
Shiga toxin 2f [75]	*E. coli* O128:H2	Stx2f, VT2f, SLTIIf	71%	83%
Shiga toxin 2g[76]	*E. coli* O2:H25	Stx2g, VT2g, SLTIIg	96%	94%

Table 1.1: Table of Stx1 and Stx2 subtypes and their % homology.

[a] Sequence homology to prototype Shiga toxin subtype of particular family (Stx or Stx2a). Adapted from Bergan *et al*.[63]

Stx1 is almost identical to Shiga toxin produced by *Shigella dysenteriae I*, save for a single amino acid in the A subunit, whereas greater sequence variation exists within the Stx2 family of toxins.[3] Shiga toxins are AB_5 toxins consisting of an enzymatically active A subunit and a pentamer of receptor binding B subunits [Figure 1.3a and 1.3b].[63,77] The A subunit of Shiga toxins, consist of an enzymatically active A1 chain associated to an A2 chain, which facilitates association of the A subunit to the B_5 subunit. Each B subunit contains three distinct binding sites, sites 1 – 3 [Figure 1.3c], consequently each B_5 moiety can bind up to 15 molecules of its natural ligand, globotriaosylceramide (Gb_3).[78]

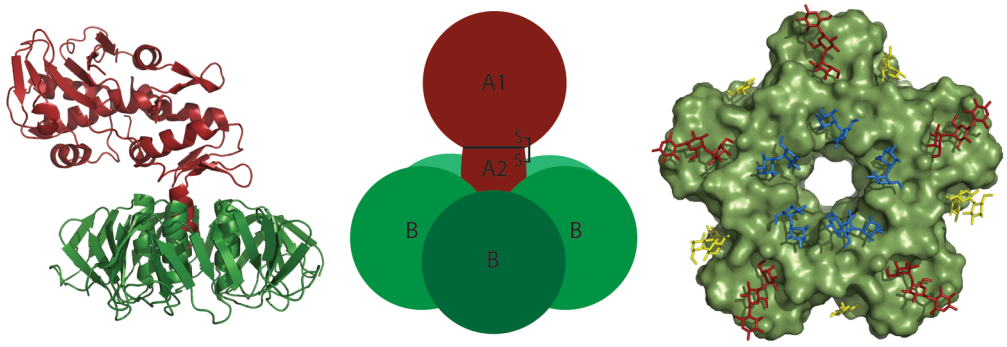

Figure 1.3. Shiga toxin structure: (a) Crystal structure of Stx holotoxin (PDB 1DMO).[77] (b) Graphical representation of the Shiga toxin structure. (c) Crystal structure surface representation of Stx1 with bound Gb_3 analog ligands (PDB 1BOS).[78] Ligands are colored according to binding site, yellow (Site 1), red (Site 2), blue (Site 3).

Most Stx variants have high binding affinity for the glycolipid Gb_3 [Figure 1.4]. Gb_3 consists of a trisaccharide responsible for binding to the B subunit of Stx1/2, also known as P^k trisaccharide. The reducing end of Gb_3 is attached to ceramide consisting of a sphingosine, branched at C-2 of the alkyl chain with an *N*-acylated fatty acid group. Analysis of binding preferences of Gb_3 analogs for $Stx1B_5$ subunit have shown that site 2 displays the highest occupancy followed by site 1, with site 3 showing little to no occupancy.[79]

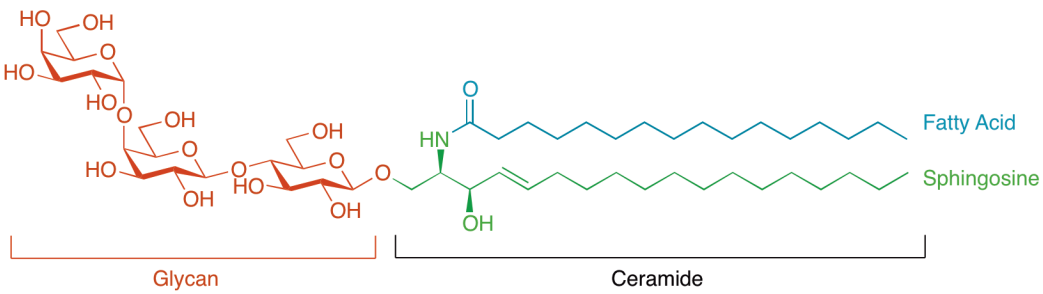

Figure 1.4. Structure of Gb_3, consisting of the Stx binding moiety, P^k trisaccharide αGal-(1→4)-βGal-(1→4)-βGlc.

Shiga toxins are ribose-inactivating proteins (RIPs) that have been found to cleave a single adenosine residue from the sarcin loop of 28S rRNA.[80] The removal of this single residue results in the inactivation of the ribosome and prevents further protein synthesis in the host cell causing eventual cell death.[81]

Shiga toxins are encoded by genes localized on the genomes of lambdoid bacteriophages which are termed Stx-phages.[82] Stx-phages contain a Shiga toxin operon, which encompasses genetic elements capable of integration into the host chromosome. Bacterial host cells are capable of carrying multiple Stx-phages allowing bacteria to produce one or more Stx variants.[83] The genes encoding the production of Shiga toxins are termed *stx* and are located in the late gene region.[63] The *stx* genes are generally not expressed until the bacterial lytic cycle has been induced, usually as a product of the bacterial SOS repair response. The bacterial SOS repair response can be induced by host DNA damage and upon activation results in greater Stx-phage production and Stx release.[63]

This thesis will deal exclusively with Shiga toxins responsible for disease in humans, that is, Stx1 and Stx2a (referred to as Stx2) and their specific interactions.

1.2.2.2. Additional Virulence Factors

The ability of EHEC to produce Shiga toxins is not in itself sufficient to cause HC or HUS. *E. coli* O157:H7 possesses other factors that have been found

to contribute to the virulence of this serotype. The first such feature is a virulence plasmid pO157. pO157 is a 60 MDa plasmid that encodes enterohemolysin[3]. Enterohemolysin is found in nearly all O157:H7 strains and is widely distributed among non-O157 strains. Enterohemolysin is encoded on the *ehxA* gene and may allow *E. coli* O157:H7 to use blood released into the intestine as a source of iron.[84] The second feature is the locus of enterocyte effacement (LEE).[3,63] The LEE contains genes that encode for adhesion, particularly Intimin. Intimin is an attaching-effacing protein excreted from *E. coli* capable of forming A/E lesions that facilitates the tight binding of the bacteria to the host epithelial cells. Studies have shown that intimin is required for full colonization of O157:H7 and the development of A/E lesions.[85-87]

1.2.2.3. Mechanism of Action

Upon ingestion of either EHEC contaminated food, most often beef, or water, *E. coli* O157:H7 adheres to intestinal epithelial cells of the large bowel, disrupting the brush border (microvilli-covered surface of intestinal epithelial cells).[64] The number of organisms that are required to establish an infection is estimated to be approximately 100 bacteria.[63,64] The *E. coli* cells intimately adhere to the epithelium through the use of intimin. As mentioned previously, intimin has been found to be responsible for the development of A/E lesions in EHEC pathogenesis. It is encoded on the LEE, which additionally encodes for the intimin receptor Tir and a type III secretion system (T3SS) which facilitates the

release of intimin and its receptor into the cell, causing further adherence and colonization.[88]

As colonization has been established in the intestine, the bacteria start to express Stx1 and/or Stx2. Once the toxins are in the intestine, they pass through the intestinal mucosal barrier and enter the blood stream where they will eventually reach their target organs. Shiga toxins primarily bind Gb_3 found in large amounts on kidney epithelial cells.[89] Upon binding to Gb_3 the toxin is endocytosed *via* a variety of endocytotic pathways within eukaryotic cells.[90,91] Subsequently, they are transported *via* a retrograde mechanism to the Golgi apparatus.[92-95] Once inside the Golgi, the toxin undergoes further retrograde transport to the endoplasmic reticulum (ER) *via* a mechanism that has been reported to be actin based.[94,96] Upon entering the ER, the A subunit is proteolytically cleaved by furin to an A1-A2-B_5 complex that is held together by a single disulfide bond between A1 and A2. Due to the reducing conditions of the ER, the disulfide bond keeping the enzymatic A1 moiety connected to the A2-B5 complex is cleaved. The A1 subunit is subsequently translocated to the cytosol where it can perform its *N*-glycosidase activity on the 60S ribosome, specifically a single adenosine (A-4324) from the 3' region of 28S rRNA.[80,97,98] Cleavage of A4324 results in inactivation of the ribosome, cessation of protein synthesis and eventual cell death.[63]

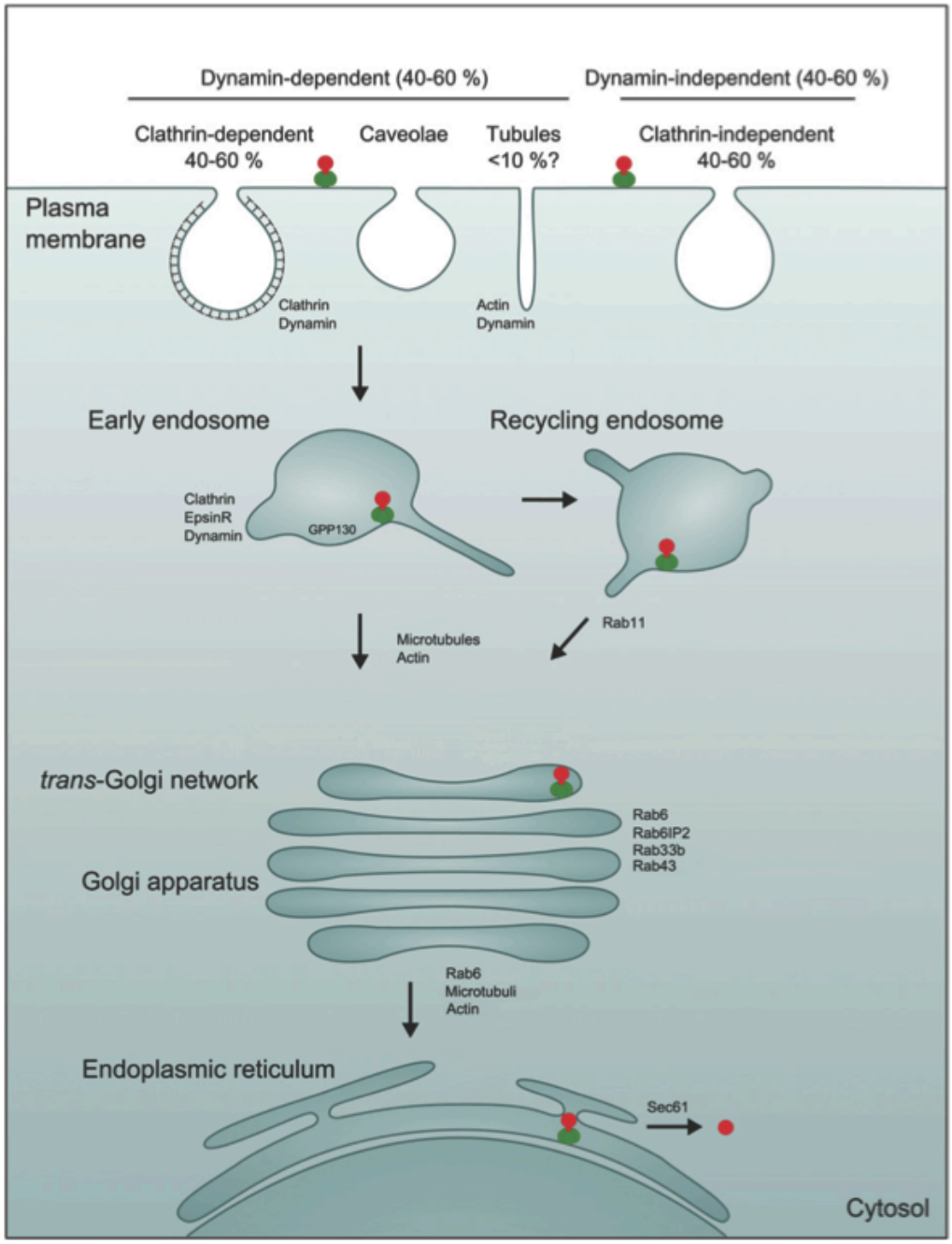

Figure 1.5. Process of Shiga toxin incorporation into the cell, intracellular trafficking and processing. Adapted from Bergan *et al*.[63]

1.2.3. Hemolytic Uremic Syndrome

Hemolytic uremic syndrome is a post-diarrheal complication associated with infection by EHEC. HUS comprises the clinical triad of thrombocytopenia, thrombotic microangiopathy, and hemolytic anemia.[99] HUS is mostly associated with acute kidney damage as Gb_3 is expressed at higher density on glomerular endothelial cells.[100] Of those infected with EHEC such as *E. coli* O157:H7, the very young (<5) and the elderly (>60) are the most susceptible to complications and death.[99,101] In the United States, infection with *E. coli* O157:H7 is the leading cause of acute renal failure in children with an average infection rate of 1/100,000, however globally this pathogen has become a growing problem as well. The largest outbreak of O157:H7 mediated HUS to date occurred in 1996 in Sakai, Japan.[102] The outbreak resulted in 121 confirmed cases of HUS out of 12,680 infected individuals, that culminated in the death of three children. The source of the infection was traced to contaminated bean sprouts in elementary school lunches. The largest non-O157:H7 mediated outbreak occurred in 2011 in Hamburg, Germany.[103] This outbreak was the result of an EAEC strain, *E. coli* O104:H4 that has acquired the ability to produce Shiga toxins and as such is both EAEC and EHEC. Traditionally, EAEC cause self-limiting diarrhea characterized by intestinal mucosa adherence. The Germany outbreak resulted in 3816 individuals infected in northern Germany, of which 845 involved the development of HUS and resulted in the death of 54 individuals. The cause of this outbreak was traced to the consumption of sprouts.[104] HUS typically develops in 5 % - 15 % of patients infected with *E. coli* O157:H7. The severity of an outbreak is usually

measured by the rate of HUS per infection.[99] What distinguishes the outbreak in Hamburg was the abnormally high rate of HUS, ~22 %, occurring mostly in adults, ~88 %.[103]

The rate of mortality of EHEC infection is fairly low at approximately 3 % - 5% when compared to other infectious diseases but morbidity associated with kidney injury is significant. Of those infected, approximately 12 % of patients with diarrhea-associated HUS, will progress to end-stage renal failure and 25 % of patients will suffer long term renal impairment that may require constant medical treatment.[105,106]

The treatment of HUS is a matter of debate, as traditional approaches would indicate that the administering of antibiotics for a bacterial infection would result in resolution of the infection. However, studies have shown that in many cases, antibiotic treatment results in a higher incidence of HUS.[107] This is most likely due to the increased production of Shiga toxins upon bacteria death. For the O157:H7 strain, antibiotics increase toxin production due to the location of *stx* genes within the bacteriophages, as expression of lambdoid bacteriophages is antibiotic-inducible.[108] Current strategies toward the treatment of HUS are supportive. Most treatments focus on renal replacement therapy, which encompasses hemodialysis, peritoneal dialysis, hemofiltration, and in some cases renal transplantation.[109]

1.3. Non-antibiotic therapeutic approaches

The use of antibiotics is traditionally the preferred treatment for bacterial infections. However, treatment of *E. coli* O157:H7 with antibiotics may indeed increase the production of Shiga toxins and cause further disease.[110] Consequently, alternative therapeutic strategies are of great interest. There are several advantages in exploring the therapeutic potential of inhibition of bacterial virulence factors rather than the bacteria themselves.[111] Firstly, treatment of bacterial virulence factors and not the bacteria themselves incurs less evolutionary pressure on the host pathogen.[110] As a consequence the likelihood of the development of drug-resistant strains of *E. coli* is reduced. Secondly, if one were to use antibiotics to kill the pathogenic bacteria, the toxins themselves would remain unaffected therefore still able to cause disease even after bacterial cell death. Lastly, the use of antibiotics is a nonspecific attack on all bacterial strains in the body, including normal flora. The use of non-antibiotic therapies, does not affect normal microbiota.[112]

Many research groups have explored a variety of mechanisms to which Shiga toxins could be neutralized. Strategies employed target mechanisms of disease rather than the bacterium itself. In order to achieve potent inhibitors of Shiga toxins, a good understanding of the mechanism of disease is required. Most often, alternative strategies target Shiga toxins ability to bind to and therefore enter the cell or to inhibit the enzymatic activity of the A1 subunit.

1.3.1. Potential inhibition strategies

Analysis of the mechanism of infection and transportation of *E. coli* O157:H7 and Stx suggests a number of different routes for the possible inhibition of pathogenesis [Figure 1.6]. For example, inhibition of the proteins ability to bind Gb_3 on the surface of cells could prevent endocytosis and infection. Additionally, the introduction of small molecule inhibitors that inhibit the *N*-glycosidase activity of Stx could prevent inactivation of protein synthesis.

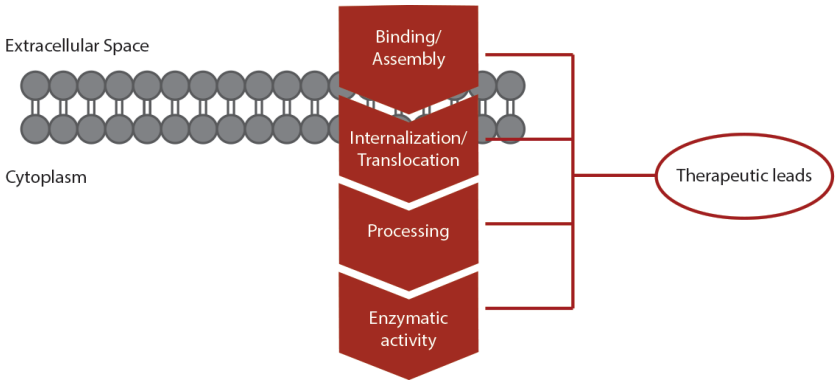

Figure 1.6. Representation of pathogenesis of *E. coli* O157:H7 and potential therapeutic targets within. These include, inhibition of binding to cell surface, inhibition of internalization of the toxin, inhibition of the processing of the toxin, and lastly inhibition of specific enzymatic activity. Reproduced from Ivarsson *et al.*[112]

In the following sections, various strategies are presented that have been developed for the potential treatment of *E. coli* O157:H7 Shiga toxin infection.

1.3.2. Inhibitors of Enzymatic Activity

Various attempts to develop small molecule inhibitors of Shiga toxins have been developed. This is an attractive area of research due to the ease of synthesis of potential targets.

One area of focus has been toward the development of molecules designed to target/inhibit the ultimate causative agent of *E. coli* O157:H7 cellular disruption, the enzymatic portion of Stxs.

Shiga toxins produced by *E. coli*, are Ribosome inactivating proteins that are among the most thoroughly studied *N*-glycosidase bacterial toxins.[112] RIPs cleave a single adenine residue from 28S rRNA resulting in a depurinated base that inhibits the ability of the ribosome to bind aminoacyl-tRNA and thereby ceases protein translation [Scheme 1.1].[97]

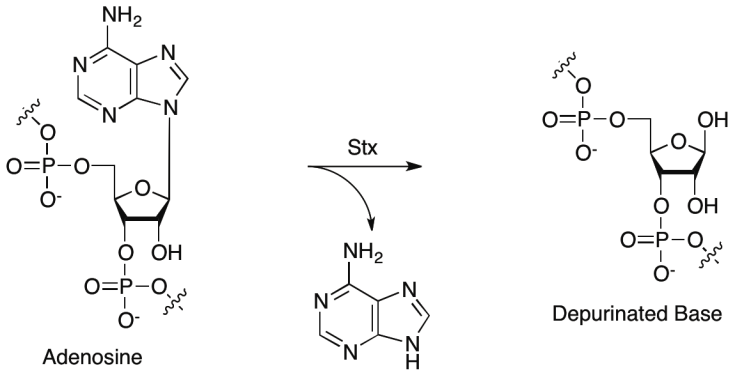

Scheme 1.1. Shiga toxin *N*-glycosidase mechanism.

The majority of research done for the development of inhibitors of RIPs, has been focused on Ricin toxin A (RTA), also an A-B type toxin, that resembles Stx in its catalytic activity and A subunit structure.[113] Most lead compounds are designed to bind to and distort the catalytic active sites of RTA and Stx, thereby preventing the adenosine moiety of 28S rRNA from being cleaved. Some examples of RIP inhibitors are presented below with their experimentally determined half maximal inhibitory concentrations (IC_{50}) [Figure 1.7].

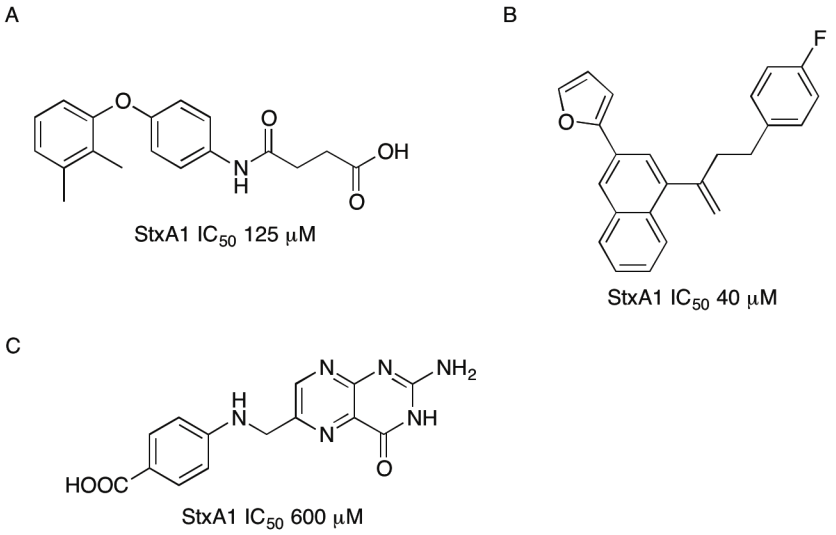

Figure 1.7. Representative RIPs that have been investigated to date: A[113], B[114] and C[115] have all been developed to mimic the binding of the A subunit to adenosine and prevent biological activity.

A common challenge associated with the development of these inhibitors is that mimicking the adenine substrate, often yields molecules with poor solubility characteristics, and as a result low inhibitory activity.[113] In addition, these molecules are often cytotoxic themselves however, further development of

these molecules could provide an attractive method for the treatment of Shiga toxin mediated HUS.

1.3.3. Inhibitors of Toxin Trafficking

While the development of *N*-glycosidase inhibitors is an active area of research, other efforts have been made to develop inhibitors of intracellular toxin activities. Upon endocytosis, Shiga toxins are moved from the cell membrane to the Golgi apparatus and subsequently the ER *via* a retrograde transport mechanism. The identification and elaboration of inhibitors that inhibit the movement of the toxin vacuole is another area of ongoing research.

Recently, Mukhopadhyay *et al*. showed that manganese blocks intracellular trafficking of Stx.[116] They had previously shown that exposure of cells to a wide range on concentrations of manganese, induced degradation of GPP130 (Golgi phosphoprotein of 130 kDa). GPP130 is a membrane protein that cycles between the Golgi and endosomes and has been found to play an undefined role in Stx trafficking [Figure 1.5].[116-118] Consequently, the authors investigated the ability of Mn^{2+} to inhibit shigatoxemia in both a cell survival model and a mouse model of disease. Mn^{2+} protected Stx1-treated HeLa cells at concentrations as high as 2000 times the LD_{50} for Stx1 (LD_{50} Stx1 = 0.05 ng/ml). In addition to these promising results, it was shown that Mn^{2+} did not compromise cell viability. Mn^{2+} was also shown to protect Stx1-treated mice from Shiga toxin infection, at 50 mg/kg mouse Mn^{2+}. Over the course of the experiment, varying concentrations

of Mn^{2+} were shown to be protective, 10, 25, and 50 mg/kg and resulted in 100% mouse survival with little-to-no changes in body mass. The authors suggested that inactivation of GPP130, caused Stx to accumulate in endosomes and were found to not reach the ER. The caveat of this approach is the treatment of shigatoxemia with an inherently toxic chemical. The authors, found that in mice the LD_{50} of Mn^{2+} was 125 mg/kg proving that the concentrations used to afford protection were well within the toxic threshold of Mn^{2+}.[116] While it may be possible this approach would prove successful against Stx2 infection, no studies have been undertaken by the authors to confirm its applicability towards Stx2.

Nishikawa *et al*. have screened a series of tetravalent peptides that displayed the ability to bind to the Stx2 B-subunit.[119] One major hit designated PPP-tet [Figure 1.8] was found and assessed *in vivo* and was found to protect mice from *E. coli* O157:H7 infection, even when administered orally after the establishment of infection. In addition, the acetylated form of PPP-tet, Ac-PPP-tet displayed proteolytic resistance and showed an increase in protective activity against EHEC infection.[120] The authors originally designed PPP-tet and Ac-PPP-tet to bind the B-subunit of Stx2 and in doing so, inhibiting its ability to be incorporated into the cell. However, their studies revealed that both inhibitors bound Stx2 and the complex was still incorporated into the cell. PPP-tet and Ac-PPP-tet were found to prevent the retrograde transport of the toxin from the Golgi apparatus to the ER and therefore prevented the onset of shigatoxemia.[119,120]

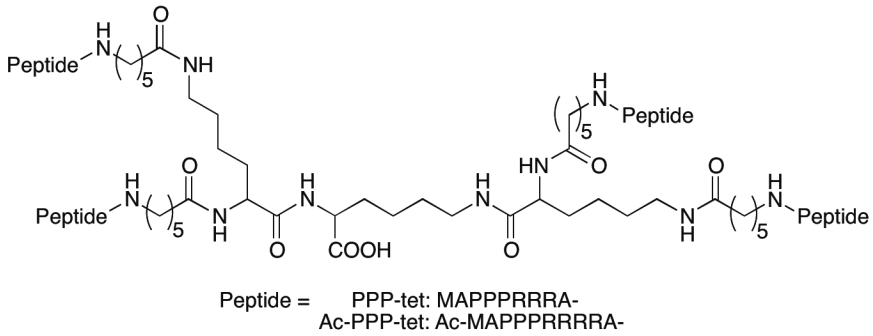

Figure 1.8. Structure of PPP-tet and Ac-PPP-tet developed to inhibit intracellular trafficking of Stx.

1.3.4. Inhibitors of Toxin Binding

Various approaches to inhibit the ability of Stxs to bind to Gb_3 have been investigated. Some include sequestering the toxin in the gut and others target the toxin in the circulation. A common theme to those that have been studied is their incorporation of P^k trisaccharide from Gb_3 as a ligand to either monomers or polymers to inhibit binding. The intrinsic affinity of monovalent carbohydrate ligands is low, typically in the mM range and therefore the use of polymers is necessary to increase ligand avidity through the use of multivalency such as linear polymers and dendrimers. The following section will cover various strategies designed to inhibit the Gb_3 binding B-subunits of Shiga toxins.

As Shiga toxins are released in the gut after infection with EHEC, one potential therapeutic approach has been to introduce an insoluble adsorbent into the stomach to sequester the toxin. Synsorb-P^k was designed for this purpose. Synsorb-P^k consisted of the Stx1-B_5 binding ligand P^k trisaccharide linked to Chromosorb-P, a diatomite used in chromatography [Figure 1.9].[121] Synsorb-P^k

was tested in Phase II trials but ultimately failed to diminish the severity of HUS in pediatric patients.[122] It has been proposed that the lack of efficacy of Synsorb-P^k *in vivo* could be due to its lower activity to Stx2 than Stx1.[121]

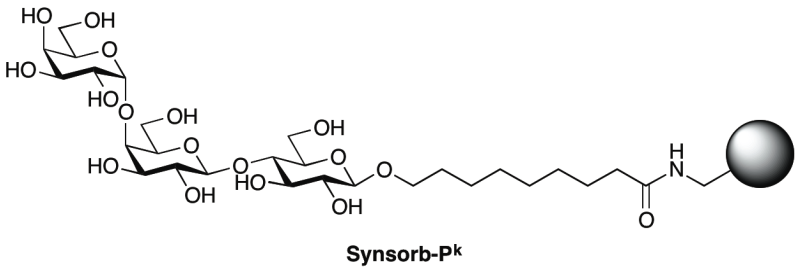

Figure 1.9. Structure of Synsorb-P^k. Its structure consists of P^k trisaccharide conjugated to a diatomite, Chromosorb-P.

Paton *et al.* utilized a probiotic approach by genetically engineering a harmless bacterium that was engineered to express Gb_3 on its outer surface. They hypothesized that "designer probiotics", when administered orally, would bind to and neutralize toxins in the gut lumen [Figure 1.10].[123] Paton *et al.* used a harmless mutant host *E. coli* strain CWG308 and *via* gene insertion, engineered it to express P^k trisaccharide on its outer surface. By introducing plasmids that directed the addition of galactose moieties to an already existing cell surface glucose, they were able to create a chimeric LPS that is incorporated onto the cell surface. *In vitro* analysis of the bacteria and their ability to bind to Stx were undertaken. They found the specific binding capacity of their substrates were approximately 10,000 times stronger than Synsorb-P^k and similar to other multivalent templates discussed herein. The authors suggested that the increased activity of the probiotic approach could in large part be due to the high density of

receptor mimics displayed on the bacterial cell surface. *In vivo* analysis showed that administration of the receptor-mimic bacteria to mice infected with a lethal dose of highly virulent Stx producing *E. coli*, was completely effective at preventing fatal disease.[124]

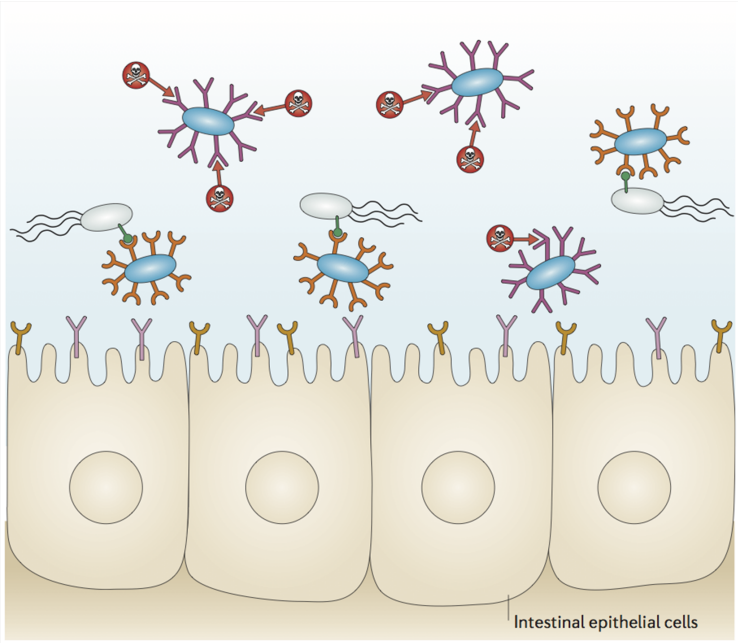

Figure 1.10. Reproduced graphical representation of the probiotic approach.[123] The strategy depends on interfering with pathogen-receptor or toxin-receptor interactions for their inhibition. The latter strategy was used by Paton *et al*. to design a harmless bacterium to sequester Stx1 and Stx2 (Red skull) in the gut.

Dohi *et al*. synthesized a series of fluorescent polymers designed to bind Stxs.[125] The polymers were co-polymers containing acrylamide, the ligand, and the fluorescent chromophore of TBMB carboxylic acid (2-*tert*-butyl-2-methyl-1,3-benzodiazole-4-carboxylate) on a galactose residue [Figure 1.10]. The authors tested their ability to prevent the binding of either Stx1 or Stx2 to human kidney cells. Polymer **III** was found to inhibit the binding of Stx1 and neutralize its

activity *in vitro*. However, the authors note polymer **III** was ineffective and showed no activity against Stx2. Their results suggested that P^k trisaccharide, and by extension Gb_3, is not the natural ligand for Stx2 due to its low affinity to the toxin.[125]

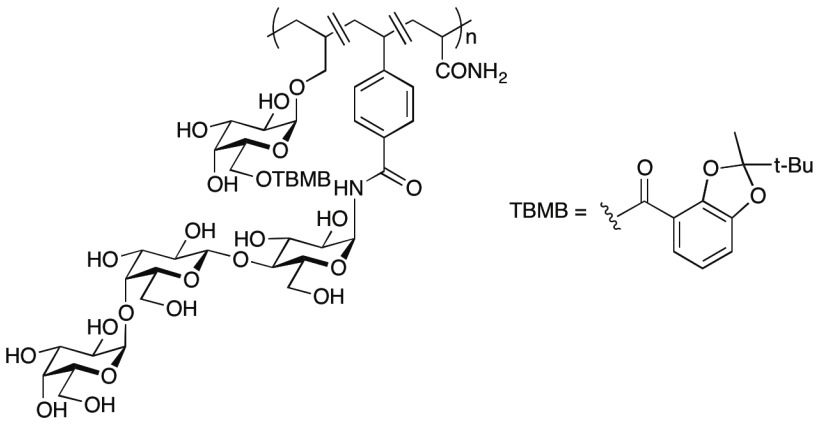

Figure 1.11. Fluorescent polymer **III**. Synthesized by Dohi *et al.* bound to Stx1 *in vitro* but not Stx2.[125]

Nishikawa *et al*. developed a series of carbosilane dendrimers called SUPER TWIGs designed to express defined amounts of P^k trisaccharide. An advantage of this approach is that the structures are easy to manipulate and thus a variety of P^k densities can be expressed. Three targets were synthesized, designated SUPER TWIGs (0)3, (1)6, and (1)12, the first number in parenthesis indicating the generation of SUPER TWIG and corresponding number of displayed P^k trisaccharides respectively [Figure 1.11].[126] *In vitro* testing of the compounds revealed SUPER TWIG (1)12 bound Stx2 with higher affinity than (1)6 and inhibited the cytotoxicity of Stx2 against Vero cells. However, SUPER TWIG (1)12 did not inhibit the cytotoxicity of Stx2 *in vivo*. In a mouse model of

infection, SUPER TWIG (1)6 completely suppressed the lethal effects of Stx2 in mice after intravenous administration. Even more importantly, it protected mice from a lethal dose of EHEC that produces Stx1 and Stx2, even if it was administered after the onset of infection. As such, intravenous SUPER TWIG (1)6 was the first Stx1 and Stx2 neutralizer that completely suppressed the effects of Stx2.[127] More recently, the same research group introduced SUPER TWIG (2)18.[128] Analysis of its activity found that SUPER TWIG (2)18 was another potent inhibitor in suppressing Stx1 and Stx2 toxicity of Vero cells. Additionally, intravenous administration of SUPER TWIG (2)18 completely suppressed the lethal effects of Stx2 in mice.[128] The authors propose that efficacy of SUPER TWIGs is due to their binding to Shiga toxins which stimulate their aggregation and subsequent degradation by phagocytotic macrophages within the reticuloendothelial system.[127]

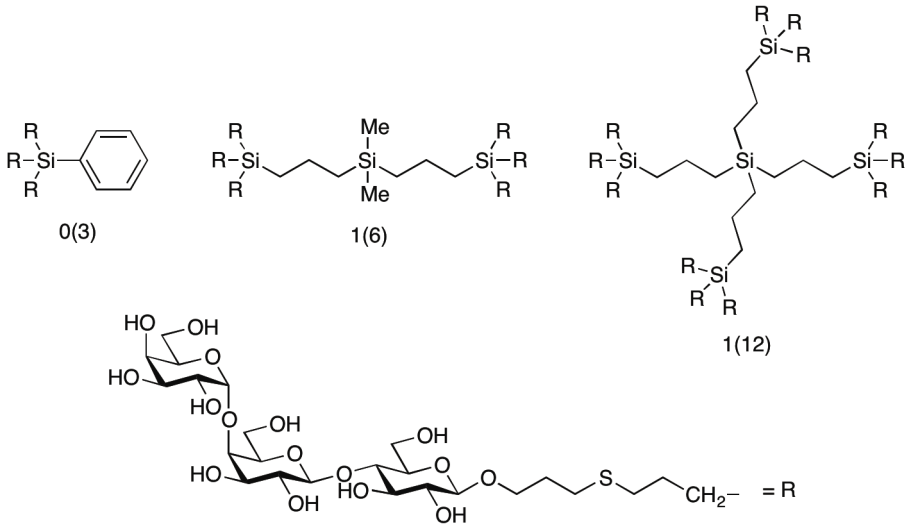

Figure 1.12. Structure of SUPER TWIGs (0)3, (1)6 and (1)12. SUPER TWIGs are a series of carbosilane dendrimers with controllable amounts of P^k trisaccharide expressed on their outer surfaces.

Watanabe *et al.*[129] previously developed an effective strategy utilizing P^k trisaccharides on a linear polymer to effectively bind Shiga toxins in the gut. Their strategy involved the synthesis of a series of polymers of acrylamide, each expressing a different density of P^k trisaccharide. They synthesized four different polymers consisting of either only P^k trisaccharide or varying amounts of P^k trisaccharide with lactose and lastly a fifth consisting of only lactose as a control [Figure 1.13]. Analysis of binding preferences for both Stx1-B_5 and Stx2-B_5 were done by surface plasmon resonance (SPR). Their results show that polymer 1:0 (refers to ratio of P^k trisaccharide:lactose) bound both Stx1-B_5 and Stx2-B_5 with K_d's of 0.34 and 0.68 μM respectively. These values were found to be half of those found on the previously synthesized SUPER TWIG (1)6 (0.72 and 1.3 μM respectively) synthesized by the same group. *In vivo* testing was done first by infecting mice with a fatal dose *E. coli* O157:H7 and subsequent oral

administration of polymer 1:0 protected mice from the development of shigatoxemia with an observable reduction in the serum level of Stx2. The authors proposed that the Gb_3 polymers entrap Stx in the gut and prevent its entrance into the circulation.[129]

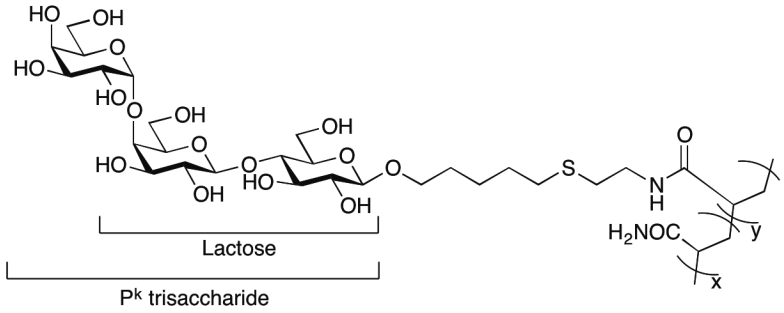

Figure 1.13. Orally administered polymers designed for sequestering Stxs in the gut before entrance into host circulation.

Early work done by Kitov *et al*. was focused on the effective inhibition of Shiga toxins *via* a multivalent dendrimeric scaffold. The first such inhibitor developed was Starfish.[130] Starfish is a pentameric display of P^k trisaccharides connected to a glucose core by five radiating spacers. Each spacer is terminated by two P^k trisaccharides [Figure 1.14].

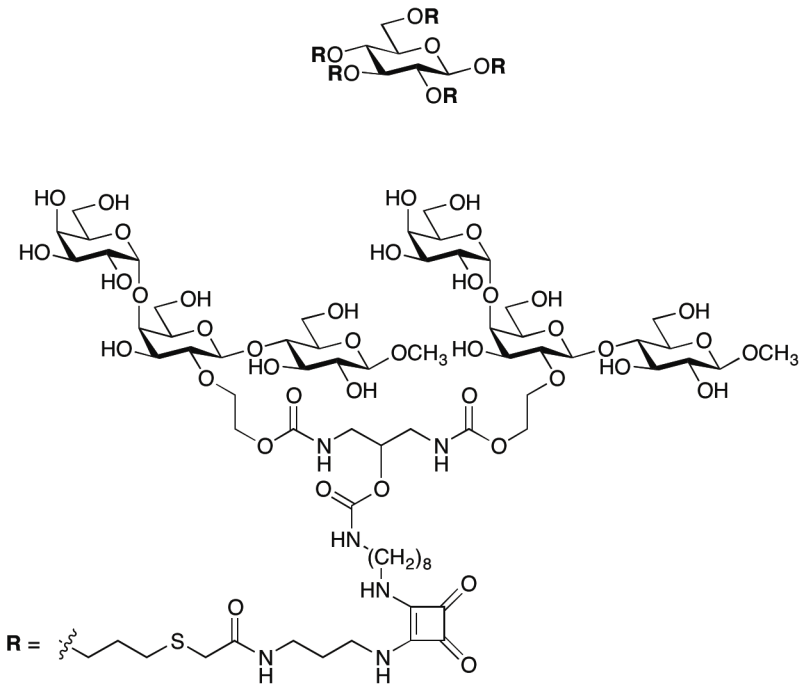

Figure 1.14. Dendrimeric Starfish. Consists of a glucose core radiating five spacers terminated with two P^k trisaccharides.

Starfish was originally designed to bind both Site 1 and Site 2 simultaneously. A crystal structure of Starfish in complex with Stx1 revealed that Starfish was "sandwiched" between two Stx1 B-subunits as a supramolecular assembly. P^k trisaccharides at the end of each tether, engaged both distinct B_5 subunits *via* Site 2 [Figure 1.15].[130]

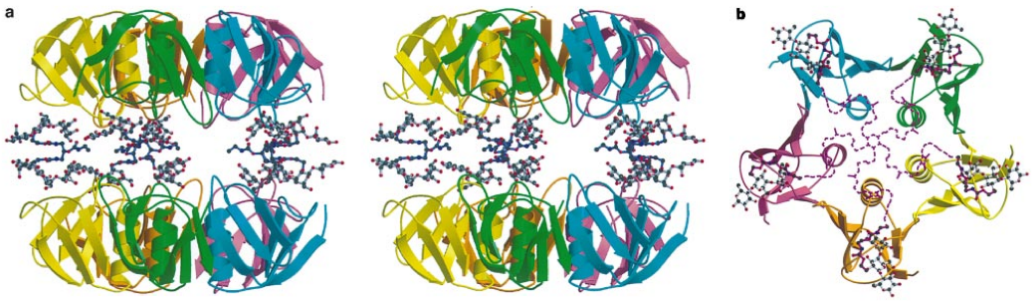

Figure 1.15. Crystal structure of Starfish with Stx1 (PDB 1QNU). a) Side profile of "sandwiched" structure clearly shows tether bound trisaccharide engaging each B_5 subunit.

In vitro experiments were performed to assess Starfish's ability to bind to and inhibit both Stx1 and Stx2. An Enzyme Linked Immunosorbent Assay (ELISA) showed Starfish exhibited subnanomolar activity for both Stx1 (IC_{50} = 0.4 nM) and Stx2 (IC_{50} = 6 nM). The ability of Starfish to protect host cells against a lethal dose of Stx1 or Stx2 was measured by Vero cell cytotoxicity assay. Starfish provided effective protection of Vero cells against lethal doses of Stx1 (IC_{50} = 1.19 mM) and Stx2 (IC_{50} = 1.58 mM) over the course of the experiment.

In an attempt to simplify the synthesis of Starfish, the Bundle group synthesized an alternative dendrimeric inhibitor of Stxs termed Daisy. Structurally similar to Starfish, Daisy employed a strategy whereby the P^k trisaccharides were covalently linked to the linker *via* the anomeric position [Figure 1.16]

Shortly thereafter, Mulvey *et a*l. in collaboration with the Bundle group tested the inhibitory potential of both Starfish and Daisy in solid-phase inhibition

assay and a mouse model of disease. ELISA assays were performed to assess both Starfish's and Daisy's potential to inhibit Stx1 and Stx2 binding to immobilized Gb_3 analog on the surface of the plates. Starfish was found to inhibit both Stx1 and Stx2 with IC_{50}'s of 0.4 nM and 6 nM respectively. Daisy was found to inhibit both Stx1 and Stx2 with IC_{50}'s of 8.1 nM and 295 nM respectively.

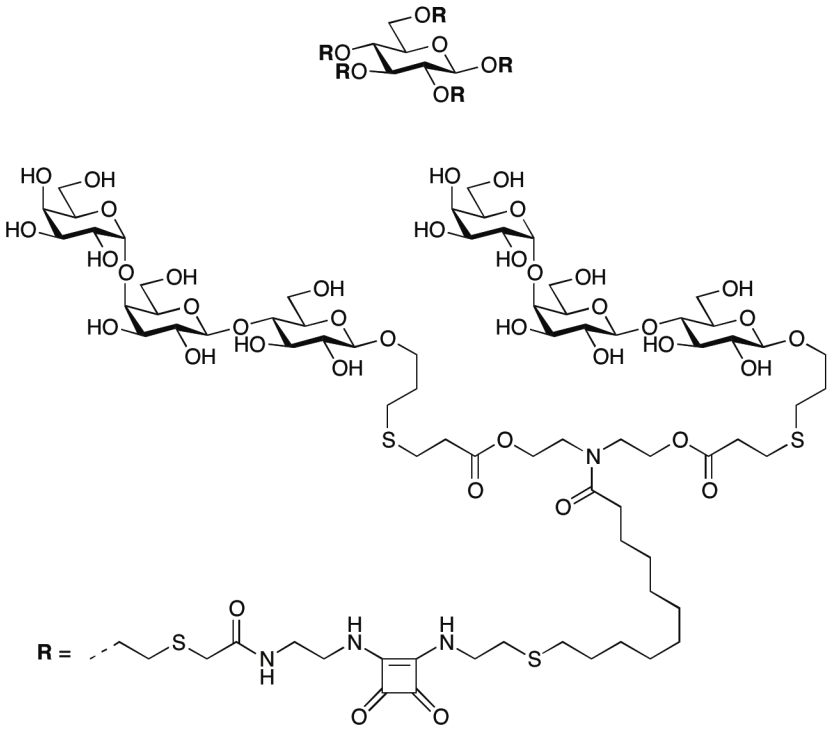

Figure 1.16. Structure of Daisy.

In a mouse model of disease, mice were challenged with a lethal dose of either Stx1 or Stx2 and treated with either Starfish or Daisy. Starfish was found to be effective at preventing shigatoxemia in all mice infected with Stx1 but failed to protect mice challenged with a lethal dose of Stx2. In contrast, Daisy was found to protect mice against both Stx1 and Stx2, an interesting result due to ELISA assay results suggesting Daisy's weaker interaction with Stx2 compared to Starfish.

Therefore attempts to inhibit Stx1 with the Starfish yielded inconclusive results and showed only a moderate increase in activity.[130,131]

In recent years, there has been a growing interest in the use of specific aggregation for the inhibition of bacterial toxins, which can result in increased potency of the inhibition of antagonists of multivalent receptors.[130,132-134] In principle, the use of a template protein with a suitable ligand that can bind to both the target and template proteins simultaneously could form a *supramolecular complex* and sequester the target protein. This is depicted graphically in Figure 1.17, where the ligand is a heterobifunctional polymeric ligand. The ligand should posses the binding motifs to simultaneously bind both the target and template proteins to form a *supramolecular complex*.

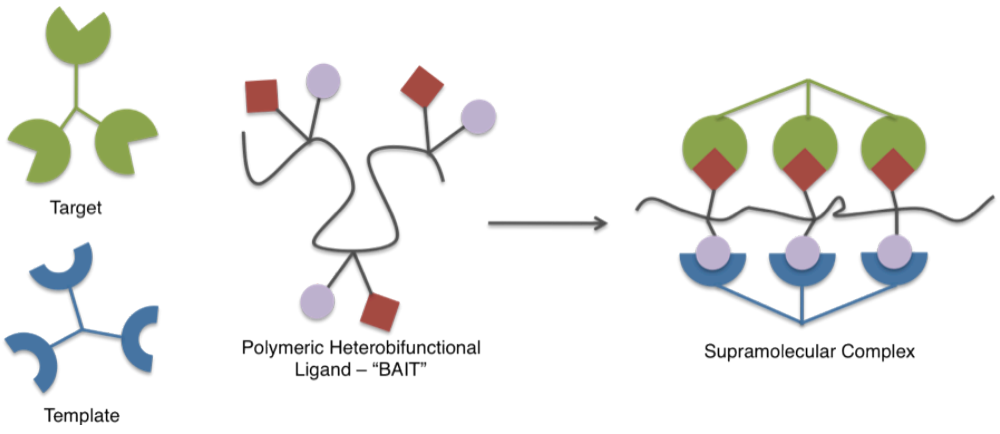

Figure 1.17. Use of a heterobifunctional ligand for the formation of a supramolecular complex.

To adopt the strategy of utilizing a template protein to achieve specific aggregation Solomon *et al*.[132] synthesized the polymeric heterobifunctional ligand

"BAIT" [Figure 1.18]. The structure was created to form a dendrimeric like structure in the same manner as Starfish and its ability to bring two units of Stx1 together. BAIT possessed an Stx1 binding P^k trisaccharide moiety as well as a cyclic pyruvate (CP) acetal moiety, known to be a millimolar binder to the innate immune system protein Human serum amyloid P component (HuSAP).[133] Although there is a large size disparity between HuSAP and Stx1, the radial distance to the Ca^{2+}-dependent binding site in HuSAP matches that for Site 2 of Stx1 and therefore their respective binding sites are found to be in register [Figure 1.19a-d]. Hence, a heterobifunctional ligand could potentially enable binding to both proteins simultaneously.

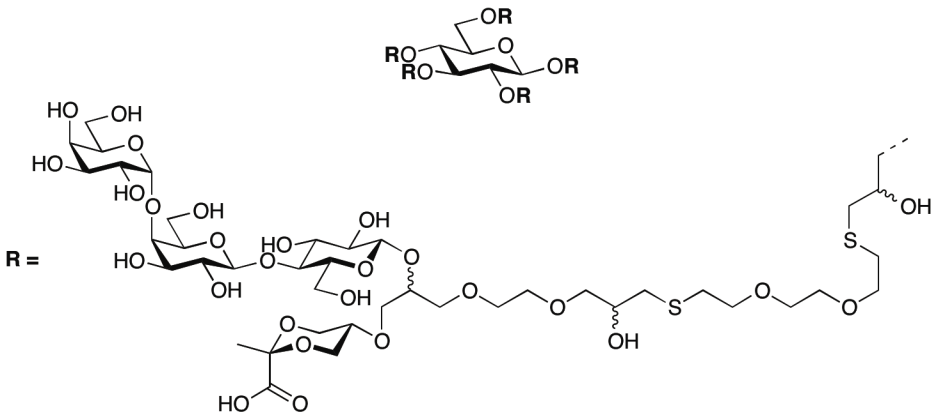

Figure 1.18. Structure of BAIT – a dendrimeric heterobifunctional ligand.

An ELISA was done to assess BAIT's ability to inhibit binding of Stx1 to P^k coated on the surface of the wells. The results suggested that while a moderate increase in inhibitory activity could be achieved, the dendrimeric scaffold does not greatly support a large multivalency effect. These results suggested that ligand-induced aggregation is a promising approach for sequestering multivalent

receptors. Additionally, the combination of the supramolecular effect with the multivalency effect does result in an overall increase in activity.[132]

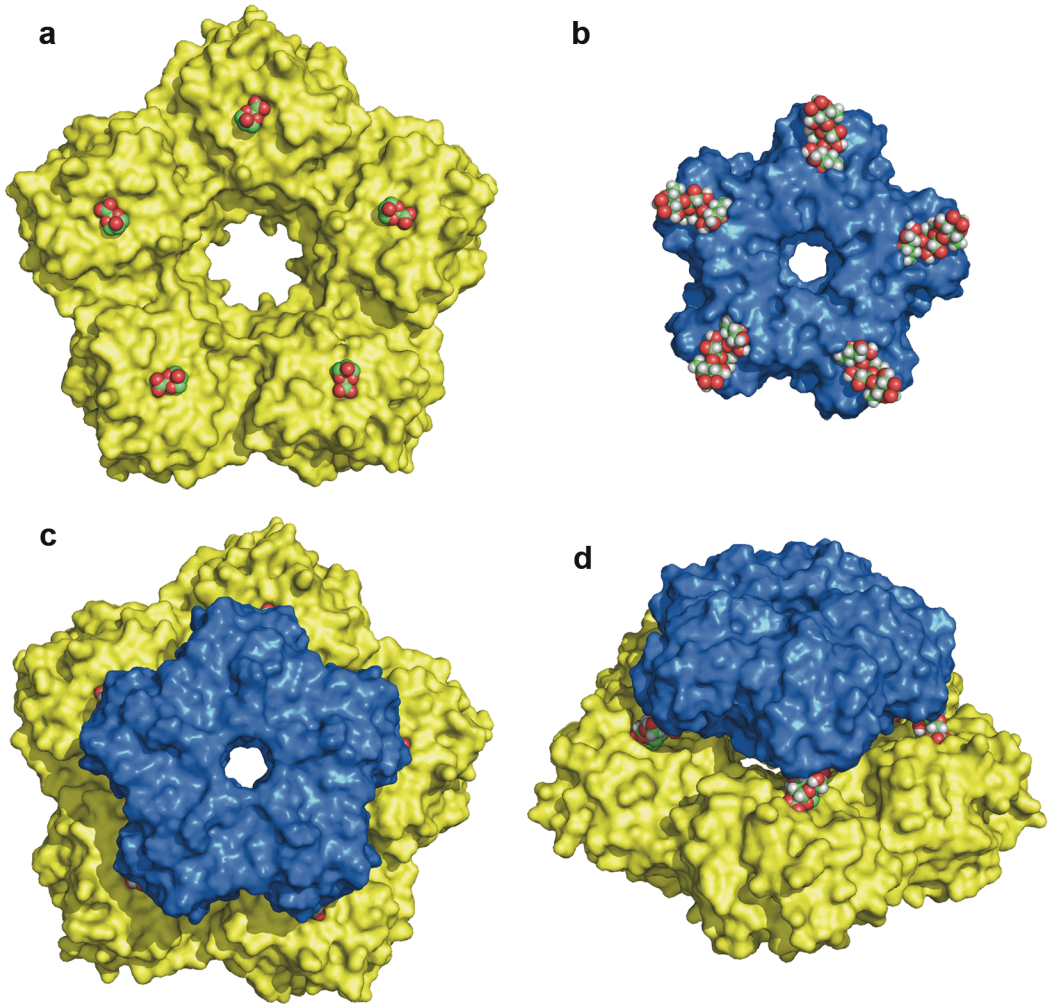

Figure. 1.19a-d. Structure of Stx1 and HuSAP in supramolecular complex. (a) Top profile of HuSAP with pyruvate ligand. (b) Bottom profile of Stx1 B_5 homopentamer with ligand. (c) and (d) Two views from above of the Stx1, HuSAP complex mediated by a heterobifunctional ligand.

To simplify the synthesis of the inhibitor of Stx1, BAIT, a more compact inhibitor was designed (*S*)-BAIT [Figure 1.20].[135] This inhibitor once again

contained the necessary P^k trisaccharide and CP moieties required for binding but were now condensed to a singular trisaccharide derivative. Through the use of molecular modeling, it was found that for the CP moiety to have the correct orientation to bind HuSAP, it must adopt the (*S*)- or *exo* configuration.

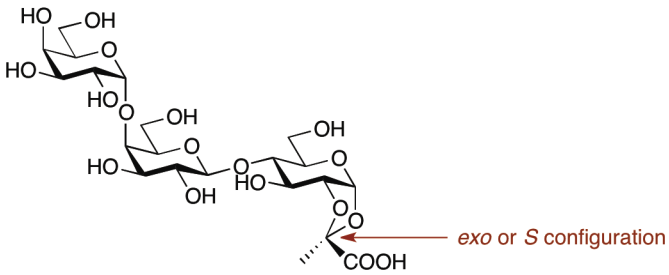

Figure 1.20. Structure of (*S*)-BAIT. The monomeric heterobifunctional ligand consists of the required P^k trisaccharide (Stx1 binding) and a cyclic pyruvate moiety (HuSAP binding) for supramolecular complex formation.

Solid phase binding assay data revealed that (*S*)-BAIT (IC_{50} = 5.6 x 10^{-7} M) showed an approximate 50-fold gain in activity compared to a BAIT monomer (IC_{50} = 3.0 x 10^{-5} M). This source of the apparent gain in activity may have been from the elimination of the short but flexible arm from the original BAIT, which through single bond rotations can adopt 243 possible conformations. As such the overall gain in entropy when eliminating the flexible linker in (*S*)-BAIT contributed to its higher inhibitory activity. To compare the activity of (*S*)-BAIT to the previously discussed Starfish, a Vero cell cytotoxicity assay was performed in the presence of HuSAP. Although (*S*)-BAIT is univalent with respect to Starfish and has a nearly 15-fold lower molecular weight, (*S*)-BAIT, in the presence of HuSAP, was found to be as active as Starfish [Figure 1.14]. A

possible rationale behind this finding could be due to the high physiological concentration of HuSAP in contrast to Stx1, which would make the binding of (*S*)-BAIT to HuSAP and Stx1 thermodynamically favorable compared to an Stx1-BAIT-Stx1 complex. Lastly, (*S*)-BAIT's ability to inhibit Stx1 *in vivo* was assessed in transgenic mice.[135] However, it was found to be ineffective at protecting mice against shigatoxemia due to its low molecular weight. Analysis of the serum after injection yielded that (*S*)-BAIT has a very low half-life and is rapidly cleared from mice circulation; it is nearly undetectable after two hours post injection.

1.4. Carbohydrate-Protein Interactions

The interaction of a carbohydrate ligand with its respective protein receptor results in an equilibrium between bound and unbound species in solution. This interaction involves many attractive and repulsive forces that affect the binding enthalpy and in addition the state of disorder of the system, the overall binding entropy. The following sections will address the thermodynamics of a carbohydrate-protein binding interaction and the concept of multivalency.

1.4.1. Thermodynamics of Carbohydrate-Protein Interactions

Let us consider a binding event between a ligand, L and its receptor protein, P. We can express the binding equilibrium as in equation (1):

$$P + L \leftrightarrows PL \tag{1}$$

Where P and L represent the unbound protein P and the ligand L respectively and PL represents the bound complex.

The association constant K_a indicates the position of the equilibrium expressed in equation (1) and is the reciprocal to the dissociation constant K_d. K_a and K_d are defined as in equation (2).

$$K_a = \frac{1}{K_d} = \frac{[PL]}{[P][L]} \tag{2}$$

[PL], [P] and [L] indicate the concentrations of the different species in solution. A larger K_a indicates the equilibrium in (1) is favored in the forward direction and therefore there is a higher concentration of complex PL than protein P or ligand L. Inversely, a lower K_d indicates the same and suggests a good binding interaction. The association constant K_a is also related to the Gibbs free energy (ΔG) by equation (3):

$$\Delta G = -RT \ln K_a \tag{3}$$

In the above reaction R and T are the universal gas constant and the absolute temperature in Kelvin respectively. From the equation it is evident that a greatly negative ΔG is a more favorable process, therefore a larger K_a results in a more favorable binding event. Additionally, ΔG is the sum binding enthalpy (ΔH) and entropy (ΔS) as expressed in equation (4) where T is once again the temperature in degrees Kelvin:

$$\Delta G = \Delta H - T\Delta S \tag{4}$$

The enthalpy of binding (ΔH) accounts for changes in the attractive ($\Delta H_{attract}$) and repulsive forces ($\Delta H_{repulse}$) between the ligand and the protein and can be expressed as equation (5):

$$\Delta H = \Delta H_{attract} + \Delta H_{repulse} \tag{5}$$

$\Delta H_{attract}$ accounts for a variety of cohesive or non-covalent chemical forces which, as individuals are characteristically weak. However cumulatively, a large number of these non-covalent interactions can result in an overall larger binding energy. $\Delta H_{attract}$ encompasses non-covalent forces that can be either non-specific such as van der Waals forces, or specific such as hydrogen bonds.

A hydrogen bond (H-bond) is a non-covalent interaction involving a hydrogen bond donor and a hydrogen bond acceptor. A hydrogen bond donor

consists of a hydrogen atom covalently bound to an electronegative atom that can accept an electron lone pair. The hydrogen donor consists of a second row electronegative atom such as nitrogen or oxygen, which has a lone pair of electrons for interaction with the corresponding hydrogen [Figure 1.21]. Therefore the terminology of hydrogen bond acceptors or donors refers to the donation and acceptance of the hydrogen atom and not the lone pair of electrons of the hydrogen bond acceptor. The distance between the hydrogen of the donor and the lone pair of electrons on the acceptor is denoted as *r*. The D-H-A angle is denoted as θ and the Y-A-H angle denoted as ϕ.

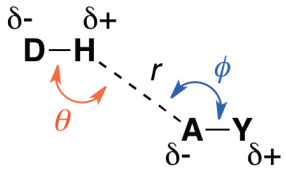

Figure 1.21. A prototypical hydrogen bond interaction. The hydrogen bond (dashed line) forms between an H, covalently bound to an electronegative atom D, and another electronegative atom A.

Commonly, hydrogen bond distances range from 1.5 to 3.0 Å with θ = 180º. The bond angle ϕ is dependant on the geometry on the molecular orbitals of A. The energy of a hydrogen bond has been estimated to be within 1.0 – 4.0 kcal·mol^{-1}. Due to the large number of hydroxyl groups around the carbohydrate ring, hydrogen bonds play an important role in carbohydrate-protein binding interactions. Hydrogen bonds can form between the protein side chains and backbone to create positive binding interactions; in addition, water molecules can mediate hydrogen bonding when both ligand and protein are solvated.

Dispersive forces or van der Waals forces play another important role in binding. The formation of temporary dipoles in atoms and in even mildly non-polar components of a ligand, can contribute to $\Delta H_{attract}$ when interaction occurs between the ligand and the protein. The strength of the interaction and its contribution to $\Delta H_{attract}$ is dependant on the surface area of the interaction; usually a larger surface area is required to form a stronger interaction.

The total entropy change (ΔS_{tot}) in a protein-ligand binding event, equation (6), is the sum of the changes in translational, rotational and conformational entropies for both the protein and the bound ligand. In addition, the change of solvation entropy is taken into account for those interactions that are solvated.

$$\Delta S_{tot} = \Delta S_{trans} + \Delta S_{rot} + \Delta S_{conf} + \Delta S_{sol} \qquad (6)$$

The translational entropy (ΔS_{trans}) of a molecule is its ability to freely translate through space and is related to its molecular weight and concentration. A larger molecular weight or a lower concentration leads to a higher change in ΔS_{trans}. Rotational entropy (ΔS_{rot}) refers to the freedom of a molecule to rotate around its principle axis. Conformational entropy (ΔS_{conf}) refers to changes in the conformations of both ligand and protein upon binding. In an aqueous solution, the change in total entropy (ΔS_{tot}) is also dependent on the change in solvation entropy (ΔS_{sol}). When the respective proteins and ligands are dissolved in water,

water molecules are attracted to polar surfaces of the protein or ligand *via* hydrogen bonding; or are attracted to and are highly ordered around hydrophobic regions. When a binding event occurs, the protein-ligand interaction releases or desolvates the ligand and protein around the areas of association. The desolvation process results in the release of bound water molecules and therefore causes large increases in solvation entropy. Consequently, this process can result in a large ΔS_{sol} and by extension a larger ΔS_{tot} creating a more favorable binding event.

1.4.2. Thermodynamics of Multivalent Binding Interactions

In the above sections, various examples of potential Shiga toxin inhibitors were described. A common theme among those examples utilizes the exploitation of the P^k trisaccharide of Gb_3 for sequestering the toxin *via* multivalent display of ligands. The affinity of carbohydrate ligands for their respective receptors is innately low, for example, a univalent P^k trisaccharide has an association constant (K_a) for Stx1-B_5 of 3.6 x 10^2 M^{-1}.[136] One of the most important strategies employed by chemists to overcome the weak affinity of carbohydrates for a protein receptor is the use of multivalency. Tailored multivalency, where a carefully constructed ligand displays a limited number of tethered branches designed to match adjacent sugar binding sites of a protein, can lead to large avidity gains. However, the thermodynamic basis for these gains has eluded thorough description. Assessing the strength of a multivalent interaction is not a trivial task. Many techniques have been developed to measure the association constants of complexes such as, ELISA, SPR spectroscopy and isothermal

titration calorimetry (ITC), although, this has led to the development of a controversy in describing the activity of multivalent ligands.[137-141] The same ligand may show different activity to the same receptor when measured by different analytical techniques. As a result, the nature of binding and activity measurements and the subsequent reporting of a binding constant, is flooded with adjectives such as "effective", "functional", "pseudo" and "observed". Consequently, the development of an unambiguous definition of a thermodynamic binding constant is necessary. A summary of the work accomplished to date investigating the thermodynamics of multivalent binding interaction are described below.

For an N^{th}-order binding interaction between a protein and a ligand containing N number of ligands and N number of receptors, the free energy can be presented as $\Delta G_{poly,N}$.[137] The average free energy of interaction $\Delta G_{poly,avg}$ between a single ligand and receptor moiety in a multivalent interaction can be described as in equation (7):

$$\Delta G_{poly,avg} = \frac{\Delta G_{poly,N}}{N} \qquad (7)$$

Consider the interaction of a monovalent ligand with a monovalent receptor; the free energy change can be presented as ΔG_{mono}. The average free energy of an interaction between a ligand and a receptor in a multivalent interaction ($\Delta G_{poly,avg}$) can be greater than, equal to, or less than the analogous free

energy interaction of the monovalent ligand (ΔG_{mono}). The ratio of $\Delta G_{poly,avg}$ and ΔG_{mono} is defined as cooperativity, α (Equation (8)).[137]

$$\Delta G_{poly,avg} = \alpha \Delta G_{mono} \quad (8)$$

Cooperativity can be described as either positive (when $\alpha>1$) or negative (when $\alpha<1$).[137] Positive cooperativity occurs when binding events contribute to the overall binding avidity in a synergistic manner. Negative cooperativity occurs when the individual interactions of a polyvalent ligand, interfere and hamper binding avidity. The combination of equations (7) and (8) describes the Gibbs free energy change of a polyvalent interaction, Equation (9):

$$\Delta G_{poly,N} = N \cdot \Delta G_{poly,avg} = N \cdot \alpha \Delta G_{mono} = N \Delta G_{mono} + N(\alpha - 1)\Delta G_{mono} \quad (9)$$

The term $N(\alpha - 1)\Delta G_{mono}$ describes the collective free energy contribution from favorable or unfavorable effects resulting from tethering in a polyvalent system. The avidity of free energy, previously introduced by Jencks as $\Delta G_{interaction}$, can be described as in Equation (10).[142]

$$\Delta G_{poly,N} = N \cdot \Delta G_{mono} + \Delta G_{interaction} \quad (10)$$

Mammen *et al.* previously proposed the substitution of free energy using the equation constant equation (3).[137] They suggested that the polyvalent association constant ($K_{a,poly,N}$) is the quantitative description of avidity, $K_{avidity}$, Equation (11). However, obtaining a quantitative value from this equation is unlikely.

$$K_{avidity} = K_{a,poly,N} = (K_{a,poly,avg})^N \quad (11)$$

More recently, Kitov and Bundle proposed a more stringent approach that considers the contribution of all bound species and their distribution.[143] A review of their approach follows.

Consider the formation of a *microscopic* complex rl(i) between a multivalent receptor R and multivalent ligand L, which has a unique arrangement of i binding sites on the receptor occupied by i branches of the ligand. A microscopic interaction is defined here as the interaction of one active unit of a multivalent ligand with one active unit of the receptor. According to Jencks, the free energy of formation of the complex rl(i) could be expressed as in Equation (12).[142]

$$\Delta g_i^\circ = i\Delta G_{mono}^\circ + \Delta G_{interaction}^\circ \quad (12)$$

$\Delta G^{\circ}_{\text{interaction}}$ is used to correct for imperfections in avidity arising from the difference in free energies of the initial *inter*molecular interaction and the subsequent *intra*molecular binding events. Rearrangement of Equation (12) to account for the origin of the interactions provides Equation (13).

$$\Delta g^{\circ}_{i} = i\Delta G^{\circ}_{\text{inter}} + (i-1)\Delta G^{\circ}_{\text{intra}} \tag{13}$$

Here, the contribution of the initial binding event is designated as the intermolecular free energy $\Delta G^{\circ}_{\text{inter}} = \Delta G^{\circ}_{\text{mono}}$ and is separated from all subsequent interactions. Therefore, the remaining intramolecular interactions can be expressed as $(i-1)\Delta G^{\circ}_{\text{intra}} = (i-1)\Delta G^{\circ}_{\text{mono}} + \Delta G^{\circ}_{\text{interaction}}$.

For this model, two limitations were placed on the interaction between an oligomeric protein receptor and a multivalent ligand. The first requires that only one multivalent ligand can bind to one oligomeric receptor at a time and therefore no aggregates are to be considered. Secondly, all *n* binding sites of the multimeric receptor and *m* branches of the multivalent ligand act independently and have identical binding properties. Consider Equation (13), since all binding units of the ligand and the receptor have identical binding properties, all microscopic complexes rl(*i*) formed with *i* binding sites engaged have identical free energies. As a result, the free energy of binding may be collectively represented as a macroscopic complex RL(*i*) as in Equation (14).

$$\Delta G_i^\circ = \Delta G_{\text{inter}}^\circ + (i-1)\Delta G_{\text{intra}}^\circ - RT\ln\Omega_i \quad (14)$$

The addition of the last term in Equation (14), $-RT\ln\Omega_i$, introduces the degeneracy coefficient Ω_i. It is necessary to account for degenerate binding energies due to RL(i) not being an individual molecule. Rather, the *macroscopic* complex RL(i) is an ensemble of *microscopically* distinguishable complexes rl(i). The relative contribution of each bound species RL(i) to the overall free energy of the complex is proportional to the weight coefficient w_i. The weight coefficient is the weight of each bound ligand species existing at equilibrium and is described in Equation (15).

$$w_i = \frac{e^{-\Delta G_i^\circ/RT}}{\sum_{i=1}^{i_{\max}} e^{-\Delta G_i^\circ/RT}} \quad (15)$$

In order to obtain an expression for the overall free energy of a multivalent interaction, it is first necessary to define the overall binding constant. A possible definition of the binding constant can be presented as a ratio between the concentration of products and reactants and can be expressed as a sum of all possible complexes (Equation (16)).

$$\text{R} + \text{L} \leftrightarrows \text{RL}(1) + \text{RL}(2) + \ldots + [\text{RL}(i)] + \ldots \quad (16)$$

Therefore, K_{avidity} may be expressed as in Equation (17).

$$K_{\text{avidity}} = \frac{\sum[\text{RL}(i)]}{[\text{R}][\text{L}]} = \frac{[\text{R}_{\text{bound}}]}{[\text{R}][\text{L}]} = \frac{[\text{R}]_{\text{o}} - [R]}{[\text{R}][\text{L}]} \tag{17}$$

Based on this approach, all bound species of the receptor are treated collectively and K_{avidity} represents their cumulative effect. The formation of a binding isotherm of Equation (17) presented in [R] and [L] coordinates assumes a Langmuir plot. At the midpoint of the graph, $[\text{R}] = 0.5[\text{R}]_{\text{o}} = \sum[\text{RL}(i)]$ and $[\text{L}] = \text{IC}_{50}$. Therefore, under excess ligand concentrations, K_{avidity} is the reciprocal of IC_{50} (Equation (18)).

$$K_{\text{avidity}} = \frac{1}{\text{IC}_{50}} \tag{18}$$

Equation (17) describes K_{avidity} as a sum of constants from each complex for individually bound species, as a consequence K_{avidity} can also be expressed as in Equation (19).

$$K_{\text{avidity}} = \sum_{i=1}^{i_{\max}} K_i \tag{19}$$

As an extension of this, the avidity free energy of binding can be expressed as in Equation (20).

$$\Delta G^{\circ}_{\text{avidity}} = -RT \ln \sum_{i=1}^{i_{\max}} K_i = -RT \ln \sum_{i=1}^{i_{\max}} e^{-\Delta G_i^{\circ}/RT} \tag{20}$$

Having equations (14), (15), and (20) allows for a final description of the avidity free energy of interaction $\Delta G^{\circ}_{\text{avidity}}$ *via* the combination of these mathematical descriptors to provide an important expression for the thermodynamic analysis of multivalent interactions, Equation (21).

$$\Delta G^{\circ}_{\text{avidity}} = \Delta G^{\circ}_{\text{inter}} + \Delta G^{\circ}_{\text{intra}} \sum_{i=1}^{i_{\max}} w_i (i-1) + RT \sum_{i=1}^{i_{\max}} w_i \ln\left(\frac{w_i}{\Omega_i}\right) \tag{21}$$

In the above equation, all enthalpic effects of a multivalent interaction, the enthalpy portions of both inter- and intramolecular binding energies, are contributed by the first two expressions. The first term $\Delta G^{\circ}_{\text{inter}}$, accounts for, and is similar to, the free energy of the intrinsic intermolecular monovalent interaction $\Delta G^{\circ}_{\text{mono}}$. The second and third terms consist of two aspects of multivalent interactions and the multivalency effect: additional specific interactions and the effect of a statistical factor.

In addition, the last term in Equation (21) agrees with a previously reported definition of statistical entropy.[144] This term is representative of the probability of interaction rather than bond strength and was coined “avidity entropy” or $\Delta S^{\circ}_{\text{avidity}}$ by the authors. This classification of entropy is specific for

multivalent systems and it represents a measure of disorder in the distribution of individual microscopic complexes. Avidity entropy, $\Delta S^{\circ}_{\text{avidity}}$, always favors the association of a multivalent receptor and ligand and is always positive. Expanding the expression for $\Delta S^{\circ}_{\text{avidity}}$ into two terms provides Equation (22).

$$\Delta S^{\circ}_{\text{avidity}} = -R\sum_{i=1}^{i_{\max}} w_i \ln w_i + R\sum_{i=1}^{i_{\max}} \ln \Omega_i \tag{22}$$

If we consider the extreme case where microscopic complexes have equal free energies and equal probabilities, for example when $\Delta G^{\circ}_{\text{intra}} = 0$. Then considering Equation (15), $w_i = 0$ and the degeneracy of the states is maximal $\Omega_i = \sum \Omega_i$. As a consequence, the first term in Equation (22) is zero and avidity entropy, $\Delta S^{\circ}_{\text{avidity}}$ can be expressed as Equation (23).

$$\Delta S^{\circ}_{\text{avidity}} = R \ln \Omega_i \tag{23}$$

If we consider the system to consist of an ensemble of individual bound states with equal probabilities w_i, then the summation must be conducted over $i_{\max} = \Omega$ equal states. As a consequence, the degeneracy of each individual state in the ensemble has $\Omega_i = 1$ and the second term in Equation (22) is zero and avidity entropy may be expressed as in Equation (24).

$$\Delta S^{\circ}_{\text{avidity}} = -R \sum_{i=1}^{i_{\max}} w_i \ln w_i \qquad (24)$$

According to the authors, both equations, (23) and (24), will provide the same mathematical result. However equation (23) is computationally simpler. Therefore the magnitude of the degeneracy factor, Ω_i must be considered.

The magnitude of Ω_i is dependent on the topology of the multivalent interaction. Those considered include *indifferent topology*, *linear topology*, and *radial topology* [Figure 1.22]. Recall, the complex RL(*i*) is composed of a protein receptor with *n* binding sites and a multivalent ligand with *m* branches.

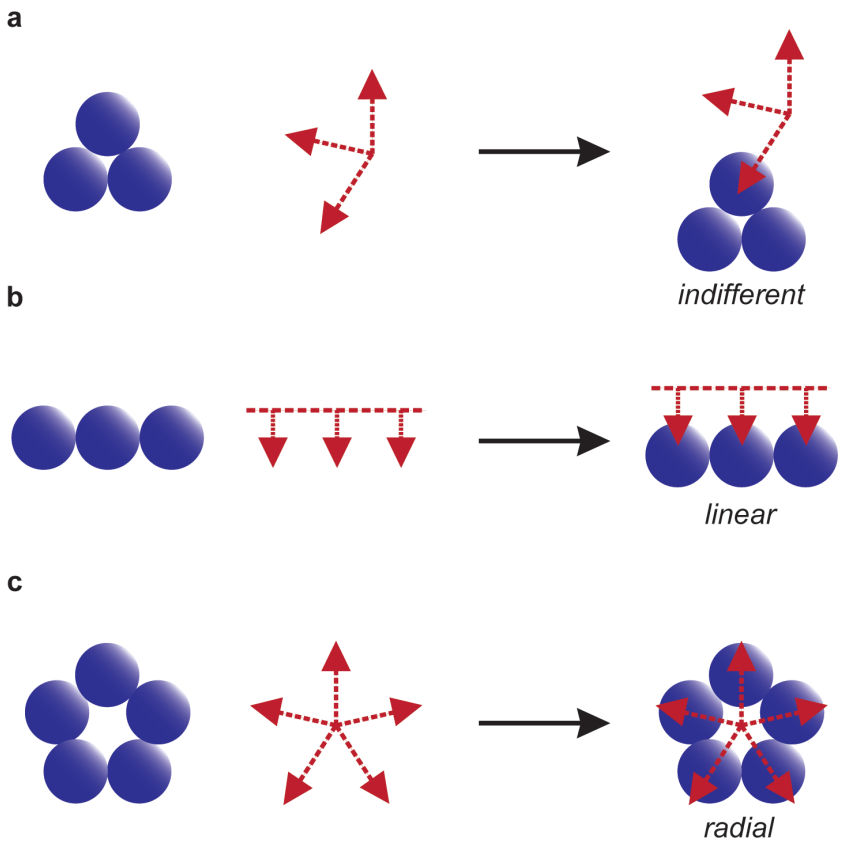

Figure 1.22. Three examples of multivalent ligand-receptor topologies. a. Indifferent. b. Linear. c. Radial.

In the case of indifferent topology, only one branch of a cluster of ligands can interact with the binding site at any one time. The ligand tethers are too short to allow other branches in the cluster to bind, regardless of arrangement of the active fragments of the ligand. No intramolecular interactions are possible and there is only one bound level therefore the activity enhancement is minimal and the degeneracy of this topology is Equation (25).

$$\Omega_i(\text{indifferent}) = nm \tag{25}$$

An example of linear topology, like Gb_3 on polyacrylamide, is the interaction of receptor and ligand between linear uniform complementary sequences. Due to the uniformity of bindings units, the number of complexes formed increases greatly due to a linear shift. For example, the ligand can move down the line in a linear manner and form new unique complexes. As such the degeneracy of the i^{th} level is expressed in Equation (26).

$$\Omega_i(\text{linear}) = (n - i + 1)(m - i + 1) \tag{26}$$

Radial topology, as seen in the dendrimeric Starfish, is typified by symmetrical or pseudo-symmetrical molecules with several copies of the active fragment tethered to a central core. The tethers must be of sufficient length to allow for interaction with all the binding sites on the receptor and each binding site is equally accessible to each receptor subunit. The degeneracy of radial topology may be expressed as in Equation (27).

$$\Omega_i(\text{radial}) = \frac{n!m!}{(n - i)!(m - i)!} \tag{27}$$

When compared to a monovalent interaction, the thermodynamic analysis of a multivalent system cannot be based on binding measurements for a single ligand-receptor pair. Alternatively, Kitov and Bundle used a goodness-of-fit function χ^2 (Equation 28) to compare the IC_{50}'s of various dendrimeric ligands for Stx1.

$$\chi^2 = \frac{\sum_{i=1}^{k}\left[\Delta G^{\circ}_{\text{exp,avidity}}(i) - \Delta G^{\circ}_{\text{avidity}}(i)\right]^2}{k} \qquad (28)$$

In the above equation, $\Delta G^{\circ}_{\text{exp,avidity}}$ represents the *experimental* avidity free energy and $\Delta G^{\circ}_{\text{avidity}}$ refers to the *calculated* avidity free energy.

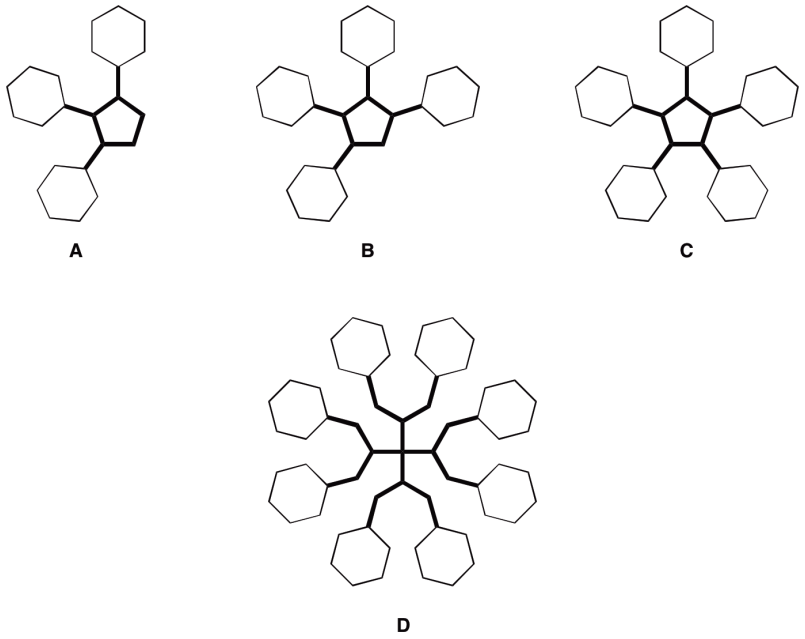

Figure 1.23. Graphical representation of ligands designed to confirm validity of the computational approach for thermodynamic investigation. Compounds **A**, **B**, and **C** were used to develop a goodness-of-fit graph. Compound D's activity was calculated and confirmed *via* ELISA assay and found to be in good agreement. Bold lines represent central cores (glucose for **A**, **B**, and **C** and a branched polyalkyl chain for **D**) attached to linkers. Hexagon's represent P^k trisaccharides.

Utilizing the parameters of the ligands **A**, **B** and **C** [Figure 1.23] for χ^2 minimization, they were able to effectively predict K_{avidity} for another ligand in the series, **D**, *via* their mathematical analysis of $\Delta G^{\circ}_{\text{avidity}}$ and subsequently confirm its

activity with ELISA. The activity of **D** was predicted to be $K_{avidity} = 1/IC_{50} = 1.26 \times 10^9\ M^{-1}$. The experimentally measured value was $1/IC_{50} = 1.4 \times 10^9$ confirming to accuracy and significance of this model.[143]

Lastly, Kitov *et al.* found that avidity entropy depends solely on the topology of binding, $\Delta S^{\circ}_{avidity}$ increases as the number of ligand branches *m* increases. In addition the influence of ΔG°_{intra} on the magnitude of $\Delta S^{\circ}_{avidity}$ is very limited [Figure 1.24]. Even at $\Delta G^{\circ}_{intra} = 0$, the model predicts an increase in binding energy.

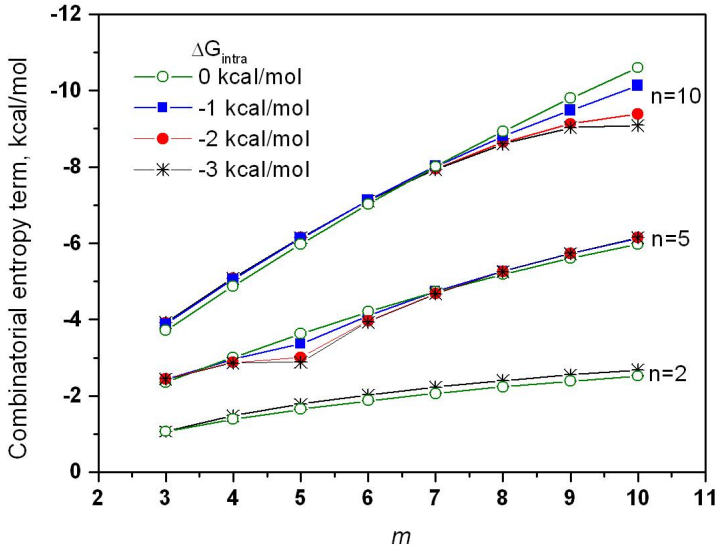

Figure 1.24. Dependence of avidity entropy, $\Delta S_{avidity}$, on the number of ligand branches *m* and the intramolecular free energy, ΔG_{intra}. The graph depicts that an increase in avidity entropy is almost independent of intramolecular free energy ΔG_{intra} and can provide a substantial contribution to overall binding energy.

Based on the compounds tested (A-D, Figure 1.23), it can further be observed that as the number of branches increases, the value of $\Delta S^{\circ}_{\text{avidity}}$ increases [Table 1.2]. However, it is subject to the natural limitations of the natural world in which the number of equivalent ligands cannot be infinitely increased.

Table 1.2 displays the relative contributions of the three terms in equation (21) to $\Delta G^{\circ}_{\text{avidity}}$. The last column of the table shows a large increase in $\Delta S^{\circ}_{\text{avidity}}$ based on the number of ligands resulting in a more favorable overall avidity binding energy.

$$\Delta G^{\circ}_{\text{avidity}} = \Delta G^{\circ}_{\text{inter}} + \Delta G^{\circ}_{\text{intra}} \sum_{i=1}^{i_{\max}} w_i (i-1) + RT \sum_{i=1}^{i_{\max}} w_i \ln\left(\frac{w_i}{\Omega_i}\right)$$

Compound	ΔG_{inter}	$\Delta G_{\text{intra}} \Sigma w_i(i\text{-}1)$	$RT \Sigma w_i \ln(w_i/\Omega_i)$
A	-2.61	-2.10	-2.68
B	-2.61	-3.10	-3.32
C	-2.61	-3.92	-3.83
D	-2.61	-4.32	-5.56

Table 1.2. Relative contributions to binding by ΔG_{intra} and avidity entropy. All units are in kcal/mol.

1.5. Scope of Project

This thesis will explore strategies to synthesize and investigate multivalent inhibitors of Shiga toxins from *E. coli* O157:H7 and investigate the nature of binding to Stx2.

1.5.1. The Development of an Stx1 Multivalent Heterobifunctional Inhibitor

The prevention of HUS *via* the inhibition of Stx1 or Stx2 *in vivo* is an attractive field of research. Many research groups have endeavored to develop potential therapies that include, but are not limited to, cell surface binding inhibition, intracellular trafficking inhibition and small molecule inhibitors of Stx enzymatic activity. (*S*)-BAIT, developed by Kitov *et al.*, displayed excellent inhibitory activity *in vitro* but otherwise failed to effectively inhibit shigatoxemia *in vivo*.[135] Analysis of its biodistribution in mice showed it had an extremely short half-life *in vivo*. A potential solution to this problem is the increase of (*S*)-BAIT's half-life *via* incorporation onto a polymer scaffold. As a result, this thesis will discuss the synthesis of a polymeric (*S*)-BAIT coined (*S*)-PolyBAIT and its inactive isomer (*R*)-PolyBAIT (Chapter 2). (*S*)-PolyBAIT's inhibitory activity will also be discussed.

1.5.2. Understanding Binding to Stx2

It has been previously shown that Stx2 and not Stx1 is the major cause of HUS in *E. coli* O157:H7 infected patients.[145] Structural information on Stx2 has been provided by the solved crystal structure of the holotoxin.[146] However, to date, there has been no solved crystal structure of Stx2 with a bound ligand in the cell surface binding B_5 homopentamer domain. Recent work by Kale *et al*. has shown that P^k trisaccharide derivatives expressing a terminal 2-acetamido-2-deoxy-galactopyranose residue can selectively bind Stx2 over Stx1.[147] This thesis

will explore the nature of binging to Stx2 (Chapter 3). The development of an Stx2 ELISA binding assay will be discussed to assess the selectivity of each protein to its respective ligand. In addition, the synthesis and co-crystallization of Stx2 with 2-acetamido-2-deoxy-galactopyranose derivative of P^k trisaccharide will be discussed.

1.5.3. The synthesis and analysis of Stx2 specific inhibitors

Continuing on the findings of Chapter 2 and Chapter 3, the synthesis and evaluation of Stx2 specific ligands will be presented and discussed (Chapter 4). Utilizing information obtained from the analysis of binding to Stx2, the synthesis of both PolyBAIT-P^kNAc and PolyBAIT-*di*NAc will be presented. This strategy incorporates both multivalency and the benefits of supramolecular complex formation for the inhibition of Stx2.

Chapter 2

Multivalent Heterobifunctional Ligands for the Sequestering of Shiga Toxin 1

2.1. Introduction

In this chapter, the use of synthetic carbohydrate chemistry for the formation of complex oligosaccharides will be explored. The inherent problems and challenges of carbohydrate synthesis will be covered. Finally, the synthesis and evaluation of two Stx1 heterobifunctional ligands will be described.

2.1.1. The Nature of Carbohydrates

In the growing area of chemical biology, the study of complex carbohydrates and glycoconjugates has become increasingly popular. As such access to these biomolecules to study their biochemical roles is very important and two such approaches to obtain these molecules have come to the forefront of modern research. One approach is the formation, isolation and purification of a target molecule from its biological source but this route is often very low yielding and time intensive.[148,149] The second approach is the synthesis of a target *via* chemical means. Until the late 1970s, this approach was largely limited to simple mono- and disaccharide structures as the synthesis of more complicated structures was a daunting task due to the lack of available methods for their formation.

However, due to the development and design of new synthetic techniques for obtaining complex oligosaccharides, this approach has become much more practical. The use of synthetic chemistry techniques is now the method of choice for acquiring complex carbohydrate structures as tools for chemical biology analysis. However, this approach does not come without its challenges. Due to the great structural diversity present in carbohydrates and the prevalence of many hydroxyl groups on the ring, the number of potential products varies greatly. An important contribution towards making these structures accessible has been extensive work on the glycosylation reaction.[150]

2.1.2. The Glycosidic Linkage

The glycosylation reaction involves the coupling of a glycosyl donor to a glycosyl acceptor. The donor has an attached labile leaving group which upon activation leaves creating a high energy intermediate, an oxocarbenium ion, which undergoes nucleophilic attack by an exocyclic oxygen of the glycosyl acceptor to form a glycosidic linkage [Scheme 2.1].[151-153]

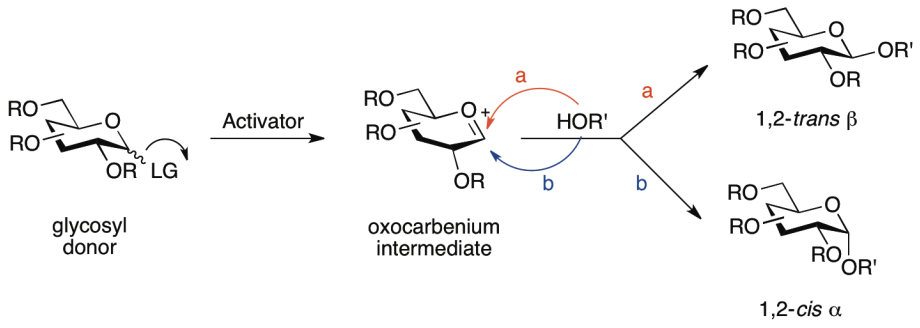

Scheme 2.1. A typical glycosylation reaction mechanism

The nucleophilic attack of the glycosyl acceptor on the oxocarbenium intermediate may occur from either (a) the top face, or (b) the bottom face resulting in different potential products based on the stereochemistry of the anomeric carbon, α or β products.[154] The designation of α and β anomers is dependent on the comparison of the relative configurations between the anomeric carbon and the reference atom, the furthest stereogenic carbon in the ring [Figure 2.1a]. For example in D-glucose, an axial substituent at C-1 is α – due to the relative configurations of the substituents on the C-1 and C-5 carbons being *cis* to each other when viewed in a Fisher projection. The opposite is said to hold if the substituent is equatorial whereby the configuration the substituents at C-1 and C-5 are *trans* to each other in a Fisher projection and are therefore β. Another view for interpretation is to compare the absolute configuration of the anomeric carbon with that of the reference atom [Figure 2.1b]. For example if the absolute stereochemistry of the anomeric carbon and the reference atom are different, then the isomer is α. In contrast, if the absolute stereochemistry of the anomeric carbon and the anomeric reference atom are the same, then the isomer is β.

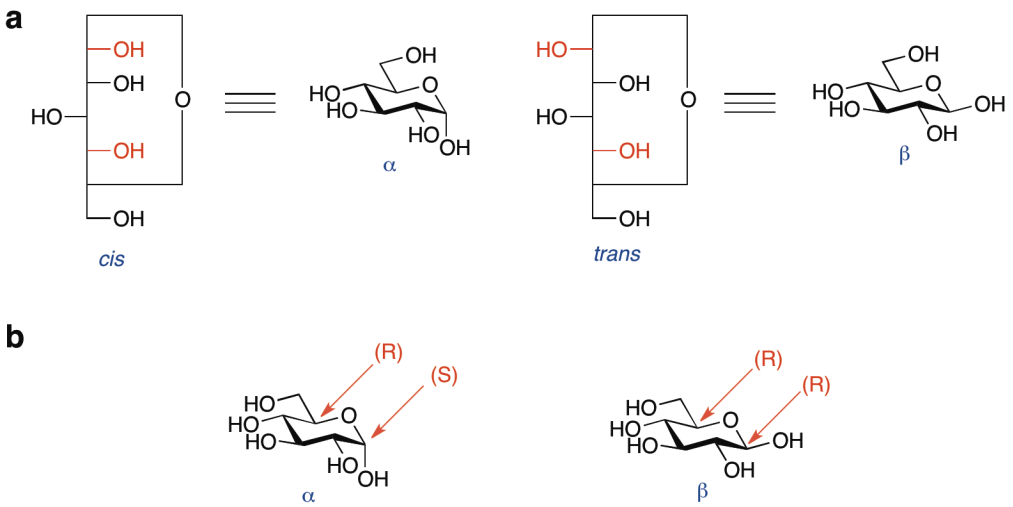

Figure 2.1. Graphical representation of α,β isomers. (a) Fisher projections of glucose indicating both α and β isomer designations. (b) α and β designations based on absolute configuration of anomeric carbon and anomeric reference atom.

If the configuration of the C-2 hydroxyl group is considered, the glycosidic linkage may have one of four general stereochemical characteristics, 1,2-*trans* α, 1,2-*trans* β, 1,2-*cis* α and 1,2-*cis* β [Scheme 2.2].[153] It is important to note that certain linkages are more challenging to synthesize than others. Often the resulting stereochemistry is dependent on the nature of the protecting group at C-2.

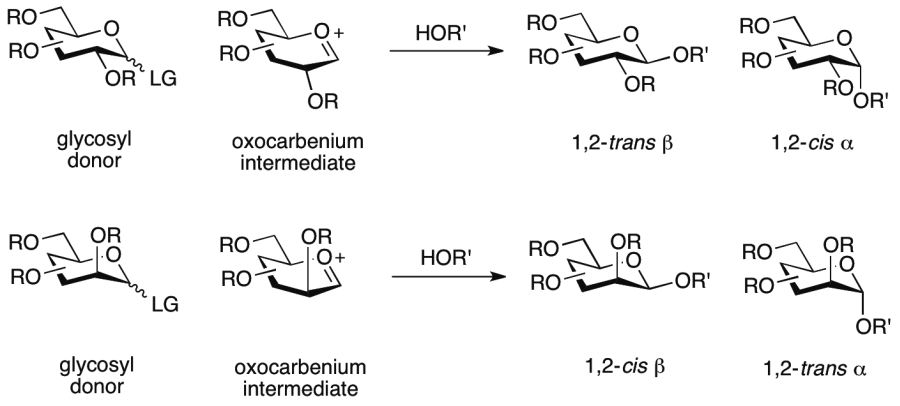

Scheme 2.2. Four possible stereochemical outcomes of a glycosylation reaction.

2.1.3. Types of Glycosylation Reactions

Late in the 19th Century, Fisher performed the first glycosylation reaction followed by the work of Koenigs and Knorr who performed the first controlled glycosylation reaction.[155,156] Since then, many new techniques and glycosyl donors have been discovered and successfully employed in a number of complex oligosaccharide syntheses. The most commonly employed glycosyl donors are glycosyl halides, thiogylcosides and glycosyl trichloroacetimidates [Figure 2.2].

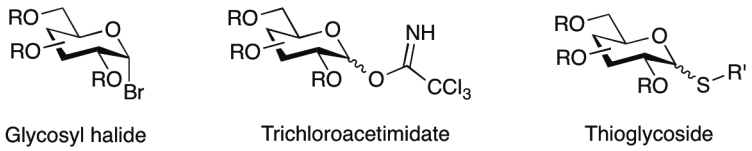

Figure 2.2. Types of glycosyl donor leaving groups.

Koenigs and Knorr reported the first use of glycosyl halides in a glycosylation reaction in 1901.[156] Consequently, glycosyl halides have become one of the most widely used methods for the formation of glycosidic linkages in what is essentially a Williamson ether synthesis. The traditional procedure has

become useful in that it allows for an easy and convenient method for the formation of 1,2-*trans* β linkages. Although this method does not allow for glycoside formation on a large scale (>10 g) due to the use of heavy metal salts and the formation of toxic heavy metal wastes.[154] Of the glycosyl halides, glycosyl bromides are the most commonly used whereas glycosyl iodides were often considered too reactive to be of practical use.[157,158] However, Gervay-Hague has shown that the use of glycosyl iodides can be very beneficial for glycosylation reactions, in some cases showing better yields and selectivity versus other more widely used donors.[159]

Until 1975, the formation of 1,2-*cis* α glycosides was not easily achieved. Lemiuex and coworkers published a series of papers describing a new technique for the formation of these linkages. The procedure employed by Lemieux was termed "halide-ion catalysis".[160-163]

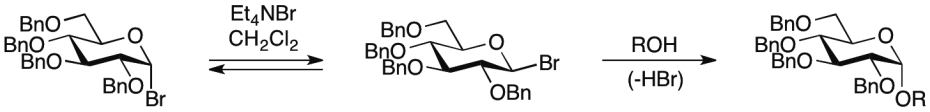

Scheme 2.3. Halide-ion catalyzed 1,2-*cis*-α glycosylation reaction.[160]

A great deal of work was done to assess the potential reaction mechanism for halide-ion catalysis by Lemieux and coworkers [Scheme 2.3], additionally when considering the mechanism [Scheme 2.4], one can see that it can be considered as a seminal reference for most glycosylation reactions. The preferential formation of the α-glycoside can be explained *via* the differences in

reactivity between **A**α and **A**β. In order for the new bond to be formed, the alcohol must attack C-1 from an angle that would leave a lone pair of electrons on O-5 *anti*-periplanar to the incoming nucleophile. The addition of the alcohol to **A**β occurs faster due to the intermediate **B**α having a chair-like structure after consideration of the stereoelectronic requirements for nucleophilic attack on C-1. In contrast addition of the alcohol to **A**α must occur in a manner that would force the intermediate **B**β to adopt an energetically unfavorable boat-like structure.

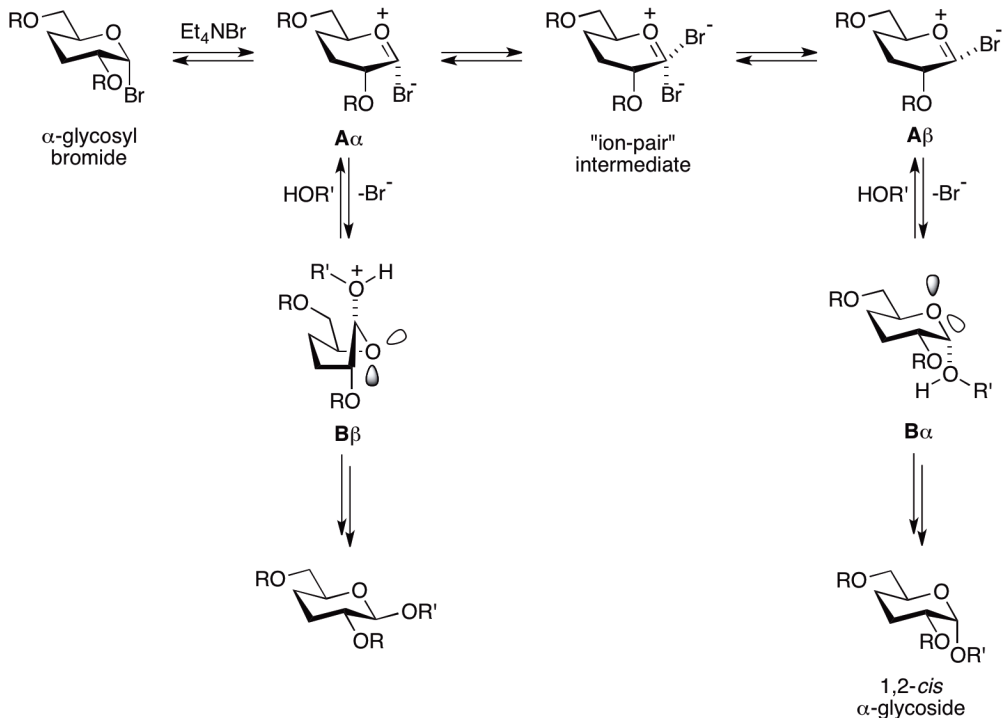

Scheme 2.4. Halide-ion catalyzed glycosylation reaction mechanism.

The use of imidates for the formation of glycosidic linkages was first described and utilized by Sinaÿ in 1977.[164] As an extension of this work, Schmidt introduced and utilized extensively, trichloroacetimidates, stable glycosyl donors that have become one of the most frequently used donors in carbohydrate

synthesis. The popularity of the trichloroacetimidate donor can in part be attributed to its ease of synthesis, as well as, its simplicity in use, often requiring only a Lewis acid activator as opposed to the heavy metal activators of glycosyl halides.[154] The synthesis of trichloroacetimidate donors can be readily and stereoselectively achieved *via* the treatment of a sugar hemi-acetal with trichloroacetonitrile in the presence of a suitable base [Scheme. 2.5].[165]

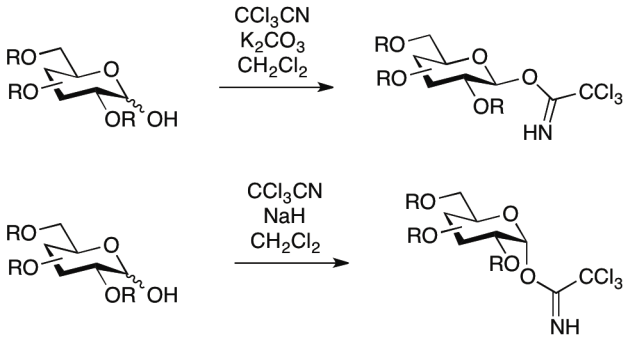

Scheme 2.5. Methods for the preparation of α and β trichloroacetimidates.

The use of potassium carbonate often yields more of the β-anomer whereas the use of sodium hydride (NaH) or 1,8-diazabicylco[5.4.0]undec-7-ene (DBU) often favors the formation of the α-anomer. A typical glycosylation reaction involving trichloroacetimidates requires the use of a Lewis acid promoter in a suitable solvent and therefore proves to be an easy and convenient method. The most common Lewis acid promoters of a glycosylation reaction involving the use of trichloroacetimidates are trimethylsilyl trifluoromethanesulfonate (TMSOTf) and boron trifluoride diethyl etherate (BF_3•OEt_2). A potential problem that arises when using trichloroacetimidates is the rearrangement of the imidate to the corresponding trichloroacetamide. This problem arises from the hydrogen on

the acetimidate nitrogen that may be abstracted to allow for rearrangement to the amide. As a potential solution to this problem, Yu and Tao[166] introduced *N*-phenyltrifluoroacetimidates as a replacement. The advantage of this donor lies in that it cannot be subject to rearrangement due to the replacement of hydrogen with an *N*-phenyl group. Additionally, these glycosyl donors have been found to be more stable for storage and long term use than their trichloroacetimidate counterparts. The preparation of these donors is achieved *via* the reaction of an aldose hemiacetal with *N*-phenyl acetimidoyl chloride under basic conditions [Scheme 2.6].[166,167]

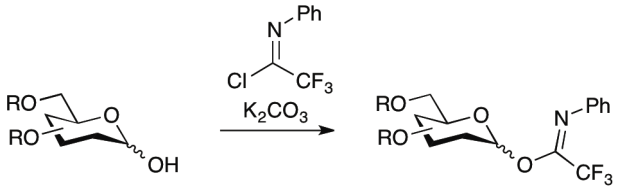

Scheme 2.6. The preparation of glycosyl *N*-phenyl trifluoroacetimidate donors.

The first reported synthesis of a thiogylcoside was published by Fischer and Delbrück in 1909.[168] Since then, thiogylcoside chemistry has been extensively explored and since the mid 1980s has become a frequently used glycosyl donor.[169] A major contributor to the widespread use of thiogylcosides is their stability under a wide variety of conditions such as various protecting group manipulations. Additionally due to their stability, not only can thioglycosides act as glycosyl donors, but under certain conditions can also be glycosyl acceptors.[150]

Thioglycosides are commonly prepared by treating the peracetylated monosaccharide with the desired thiol and a suitable Lewis acid, most often with BF_3•OEt_2 [Scheme 2.7].[170-172]

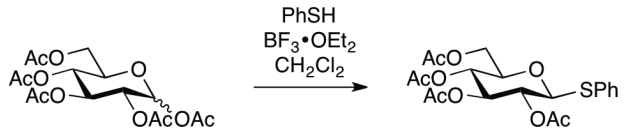

Scheme 2.7. A general procedure for the preparation of thioglycosides.

Over the years many different reagents for the activation of these donors have been introduced such as dimethyl sulfide (Me_2S_2)/Tf_2O[173], BSP/Tf_2O[174,175], Ph_2SO/Tf_2O[176,177] and many others [Figure 2.3].

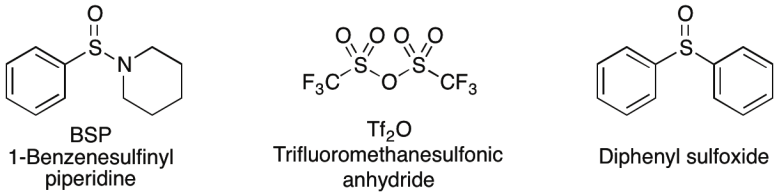

Figure 2.3. Activators for thioglycoside donors.

The most commonly used methods for the activation of thiogylcosides involve the thiophilic *N*-iodosuccinimide (NIS) in combination with a lewis acid such as silver triflate (AgOTf)[178] or triflic acid (TfOH).[179] In recent years thiogylcosides have proven to be very useful for the synthesis of complex oligosaccharides due to their stability, low reactivity and weak basicity. As a result, they can often survive a wide range of conditions that would allow for the activation of other glycosyl donors. Therefore, the stepwise coupling of multiple

donors and acceptors in a "one-pot" fashion is possible.[169] Also, early work by Veeneman and van Boom reported that thiogylcosides could be activated selectively with iodonium dicollidine perchlorate (IDCP) when the use of specific protecting groups were found on the ring.[179] The selective activation of thioglycosides was used with great success by Fraser-Reid and coworkers. Their work lead to the development of the concept of "armed" and "disarmed" donors that could be reacted in a stepwise and sequential manner (Section 2.1.4.4).

2.1.4. Factors Affecting Glycosylation Reactions

2.1.4.1. The Endo-Anomeric Effect

The anomeric effect can be described as the tendency of electronegative substituents at C-1 (the anomeric carbon) of an aldopyranose or pyranoside to adopt an axial orientation.[180] Traditionally, a substituted cyclohexyl ring can adopt one of two different chair conformations, the more stable being the chair conformation with the largest number of substituents being placed in the equatorial position to limit the number of steric interactions produced by 1,3-diaxial interactions [Figure 2.4].

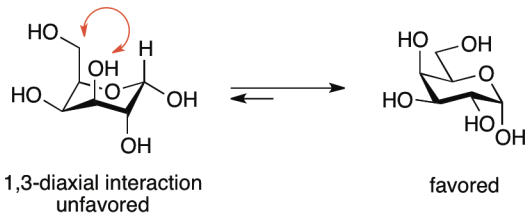

Figure 2.4. Conformational preferences based on steric 1,3-diaxial interactions.

However, for a substituent at C-1 of a pyranose it has been shown that the axial orientation is preferred. The term "anomeric effect" was introduced by Lemieux[181]. The preference was first described by Edward[182] and later elaborated by Kabayama and Patterson[183] who proposed that there exists a dipole-dipole repulsion between the lone pair of electrons of the ring oxygen and the dipole moment of the electronegative substituent on the anomeric carbon [Figure 2.5.]. Due to this interaction, the substituent on the anomeric carbon prefers the axial orientation to reduce the interaction between dipole moments.

Figure 2.5. The dipole-dipole repulsion theory of the anomeric effect.

An alternative to the dipole-dipole interaction theory is one based on molecular orbital theory [Figure 2.6]. The theory was originally proposed by Romers *et al.*[184] and further elaborated upon by Radom *et al.*[185] and Altona *et al.*[185] Its rationale is based on the interaction between the lone pair of electrons on O-5 back-bonding to the σ* antibonding orbital of the C-1-O-1 bond also known as hyperconjugation.

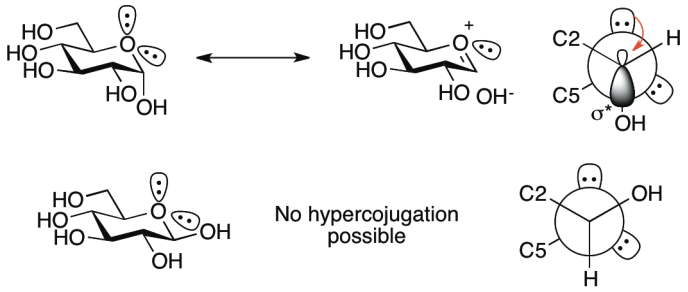

Figure 2.6. Hyperconjugation theory of the anomeric effect.

This effect is found to be possible due to the *anti*-periplanar orientation of the lone pair of electrons on O-5 to the C-1-O-1 bond, allowing for the donation of electron density into the σ* antibonding orbital.

2.1.4.2. Neighboring-Group Participation

Perhaps the most profound determinant influencing glycoside bond stereochemistry is neighboring group participation, also known as anchimeric assistance. As mentioned in section 2.1.2 the result of any glycosylation reaction can yield four possible products based on the stereochemistry of the glycosyl donor, namely 1,2-*trans* β, 1,2-*cis* α, 1,2-*cis* β, and 1,2-*trans* α [Scheme 2.2]. The nature of the resulting stereochemistry in most glycosylation reactions can often be determined by the stereochemistry and nature of protecting groups on C-2. 1,2-*Trans* β and 1,2-*trans* α linkages can easily be formed through the use of participating acyl (2-*O*-acetyl, 2-*O*-benzoyl) protecting groups on the C-2 hydroxyl [Scheme 2.8a]. For the formation of 1,2-*trans* β glycosides, the glycosyl donor, after mild acid activation, will leave the anomeric position to form a highly reactive oxocarbenium intermediate. Subsequent nucleophilic attack by the

carbonyl oxygen of an acetyl group at C-2 results in the formation of an acetoxonium ion intermediate. Consequently the incoming glycosyl acceptor is unable to approach *via* the bottom face of the ring and will therefore nucleophilically attack C-1 from the top face resulting in the formation of the β-glycosidic linkage. The opposite is to be said for the formation of 1,2-*trans* α glycosides [Scheme 2.8b], whereby the formation of the acetoxonium ion prevents nucleophilic attack from the top face of the ring and favors the formation of the α glycosidic linkage. One disadvantage of using the acyl group for the formation of 1,2-*trans* glycosides is the possibility for the formation of orthoester by-products [Scheme 2.8c].[186] In this case, nucleophilic attack occurs at the carbon of the acetoxonium ion intermediate. Products of this type are only stable under neutral or basic conditions.

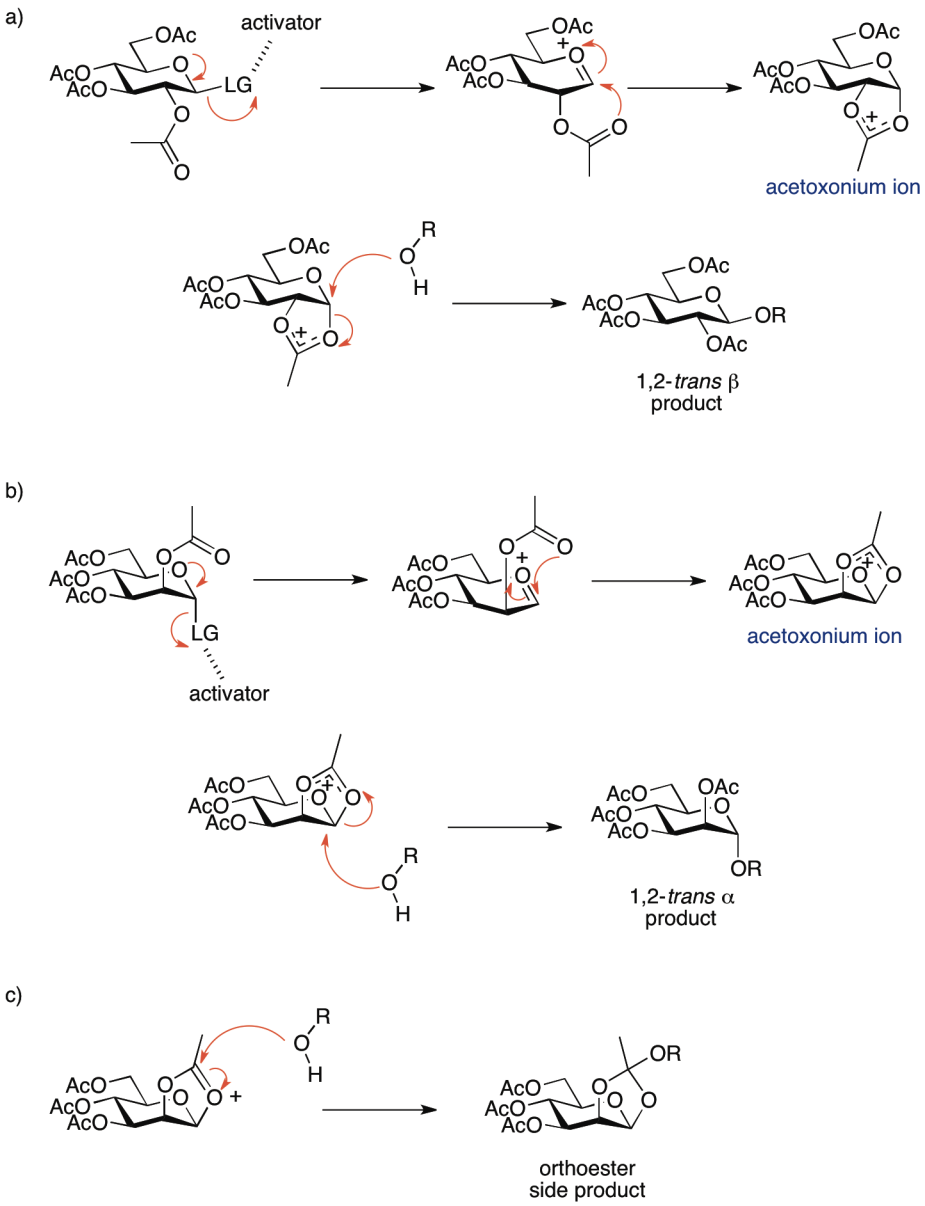

Scheme 2.8. Neighboring group participation. (a) 1,2-trans β products and (b) 1,2-trans α products. (c) Formation of orthoester side product.

The formation of 1,2-*cis* α and 1,2-*cis* β products often involve a lack of neighboring participating groups and are considered a much greater synthetic challenge. The use of non-participating ether groups is most often the preferred strategy for the formation of 1,2-cis α products in combination with solvent

effects and kinetic versus thermodynamic control. The most difficult glycosidic linkage to make is the 1,2-cis β linkage most notably those of mannose derivatives. The first direct synthesis of a β-mannosyl glycosylation reaction was performed by Gorin and Perlin in 1961,[187] since then, many other techniques have been introduced although no one technique has been embraced as a standard methodology.[188] As a consequence, the development of new methodologies for the formation of β-mannosyl linkages is an ongoing field of research.[188,189]

2.1.4.3. Solvent Effects

Typically, the use of polar aprotic solvents such as dichloromethane (CH_2Cl_2), nitromethane (CH_3NO_2) and tetrahydrofuran (THF) are preferred for glycosylation reactions, due to their being able to stabilize charges formed during the reaction.[169] However the solvent can also play an important role in determining the outcome of a glycosylation reaction. This can be used to great effectiveness in the synthesis of 1,2-*cis* glycosides based on the directing effect of intermediates formed within the reaction. The two most common solvents found to alter the stereochemical outcome of glycosylation reactions are diethyl ether (Et_2O)[190] and acetonitrile (CH_3CN)[191]. As an example, after the activation of the leaving group on a glycosyl donor, the formation of the oxocarbenium ion favors the nucleophilic attack of a nucleophile on C-1. In this case we have both the glycosyl acceptor and solvent in the reaction mixture and both are able to nucleophilically attack C-1. As the concentration of the solvent is much greater than that of the nucleophile, a glycosyl solvent intermediate is formed as an *in situ*

intermediate. For the use of Et_2O [Figure 2.7a], the β diethyl etherate intermediate is formed and is therefore mostly α directing. After the formation of the intermediate, the glycosyl acceptor can displace the Et_2O *via* an S_N2 type reaction to form the desired 1,2-*cis* α glycosylation product. Considering CH_3CN [Figure 2.7b], the solvent can attack C-1 of the oxocarbenium ion to form an α nitriluim ion and as such, the glycosyl acceptor will attack from the top face of the ring to form the desired β glycosylation reaction.

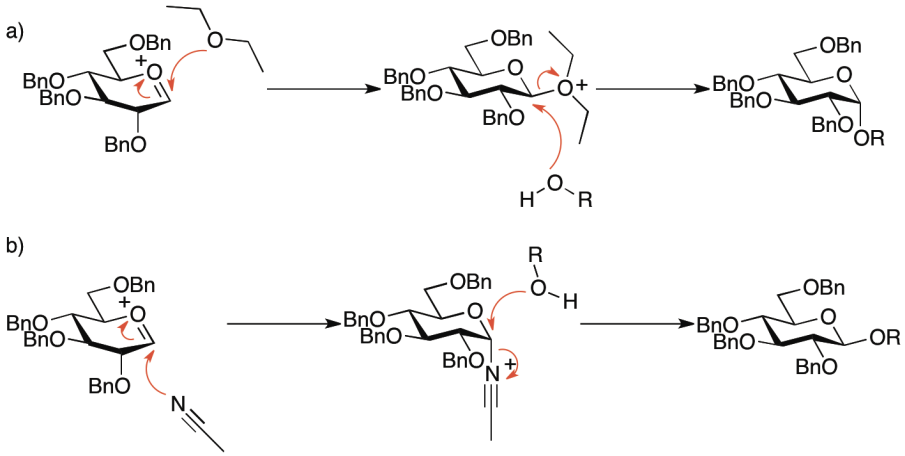

Figure 2.7. Solvent effects on glycosylation reaction outcomes. Solvents effects can play an important role in the stereochemical outcome of a glycosylation reaction when using (a) diethyl ether and (b) acetonitrile.

The principle behind the formation of a reactive intermediate that allows for stereochemical control of the resulting product has been explored to great extent particularly in the formation of 1,2-*cis* β glycosides. Crich and coworkers demonstrated that creating a glycosyl triflate under controlled reaction conditions can indeed favor the nucleophilic attack of the glycosyl acceptor to occur *via* the top face of the glycosyl triflate intermediate *via* an S_N2 type reaction to form 1,2-

cis β mannosides [Scheme 2.9a].[192] The reaction mechanism has been studied to great extent and the glycosyl triflate intermediate has been observed in nuclear magnetic resonance (NMR) studies [Scheme 2.9b].[174] It has also been shown that the effectiveness of this procedure relies heavily on the correct order of addition of the reactants.

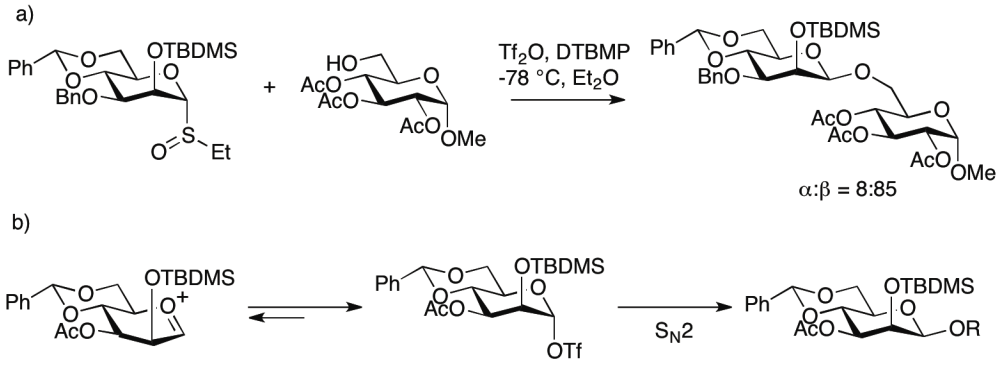

Scheme 2.9. 1,2-*cis* β mannoside formation. (a) Crich's method for the formation of 1,2-*cis* β mannosides (b) Proposed mechanism for the formation of the glycosyl triflate.

More recently Lu *et al*. have shown the ability of *N*,*N*-dimethylformamide (DMF) to form a glycosyl imidate intermediate of DMF, that directs the formation of an α glycosidic linkage [Figure 2.10].[193] This method was found to be successful as pre-activation of the donor in the presence of DMF resulted in the formation of an α-glycosyl imidate intermediate that can isomerize to the more reactive β-glycosyl imidate intermediate. Consequently, addition of the nucleophile after activation of the donor in the presence of DMF is required in order to allow for imidate formation and isomerization.

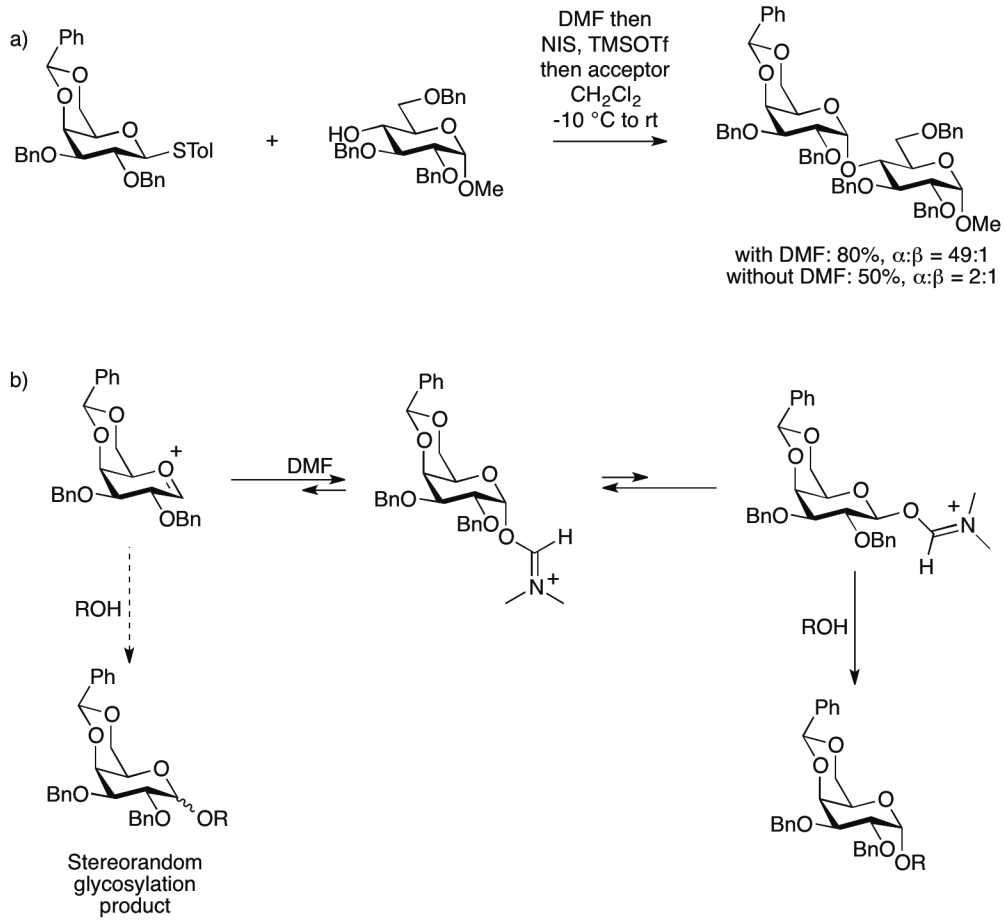

Scheme 2.10. Solvent mediated anomeric specificity. (a) General procedure for glycosylation reaction employing DMF as stereochemical directing agent. (b) Proposed mechanism of DMF directing action.

2.1.4.4. Armed and Disarmed Donors

Introduced in concept by van Boom and elaborated by Fraser-Reid, the *armed-disarmed* approach to oligosaccharide synthesis postulates that benzylated (i.e. electronically activated) glycosyl donors will react faster and chemoselectively over their acetylated or benzoylated (i.e. electronically deactivated) glycosyl donor counterparts. Therefore, those donors that are electronically activated are *armed* and those that are electronically deactivated are *disarmed*.[194,195] This method was originally developed in conjunction with the use

of pentenyl glycoside donors employed by Fraser-Reid and coworkers but has shown to be useful for thioglycoside syntheses as well. The concept of *armed* and *disarmed* donors has been used with great success in one-pot glycosylation strategies for oligosaccharide synthesis [Scheme 2.11].[179,196]

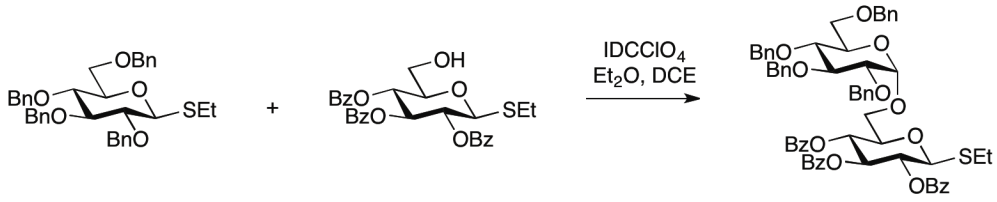

Scheme 2.11. Armed-disarmed approach to oligosaccharide synthesis.

2.2. The Synthesis of (*S*)- and (*R*)-PolyBAIT

As mentioned in Chapter 1 previous work by the Bundle group has been focused on the development of inhibitors to bind Shiga toxin in the circulation. One of the most promising candidates researched was (*S*)-BAIT, which showed excellent activity *in vitro* but failed to prevent shigatoxemia *in vivo* due to its short half-life in circulation.[135] Therefore in order to increase the lifetime of (*S*)-BAIT in circulation, it was hypothesized that incorporation of (*S*)-BAIT onto a polymer scaffold would firstly, increase its mass and therefore half life and as noted previously, and secondly improve binding *via* multivalency and avidity. Consequently, two synthetic targets were identified, the multivalent heterobifunctional ligand (*S*)-PolyBAIT, and as a negative control, its isomer (*R*)-PolyBAIT [Figure 2.8]. (*R*)-PolyBAIT can act as an ideal negative control as it still contains the necessary P^k trisaccharide for Stx binding but the cyclic pyruvate acetal is in the opposite configuration (*endo*) and therefore is no longer able to

bind HuSAP. As a consequence, (*R*)-PolyBAIT would not be able to form a supramolecular complex and would therefore behave as a linear polymer expressing ligands for Stx only.

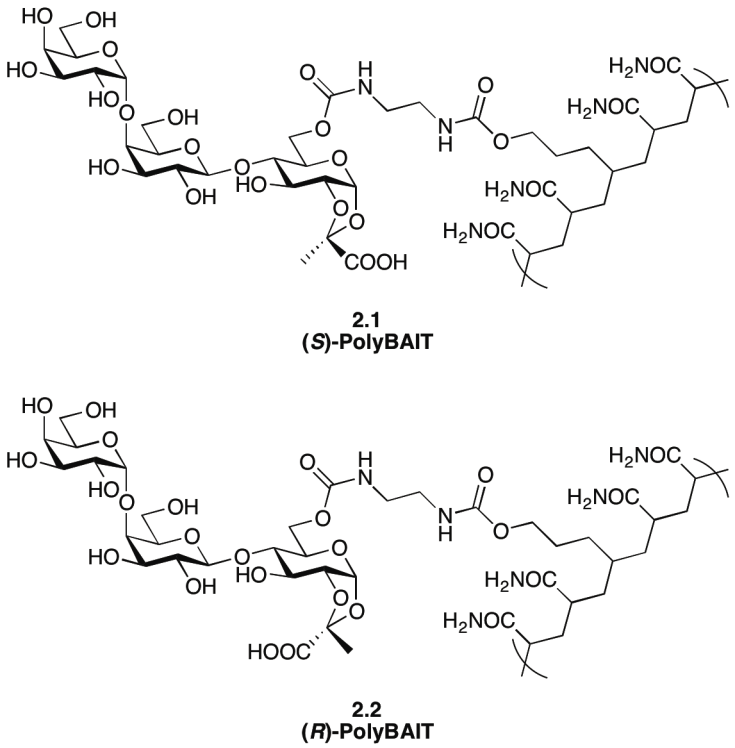

Figure 2.8. Synthetic targets, (*S*)-PolyBAIT **2.1** and (*R*)-PolyBAIT **2.2**.

The synthesis and evaluation of (*S*)-PolyBAIT **2.1** and its inactive isomer (*R*)-PolyBAIT **2.2** will be described in the sections to follow.

2.2.1. The Synthesis of (*S*)-PolyBAIT

The synthesis of (*S*)-PolyBAIT can be retrosynthetically approached as in Scheme 2.12.

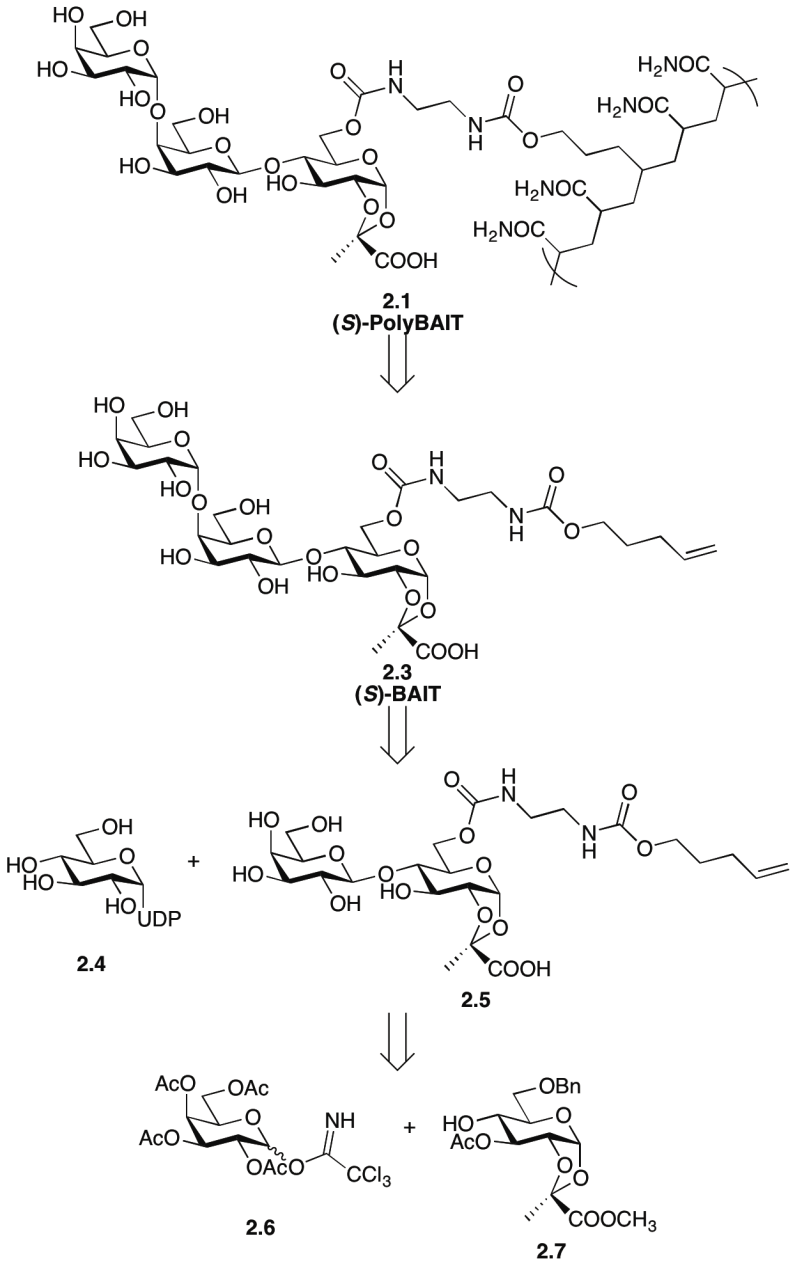

Scheme 2.12. Retrosynthetic analysis of (*S*)-PolyBAIT, **2.1**.

For the formation of the polymeric **2.1**, a suitable monomeric precursor would be required for copolymerization with acrylamide such as **2.3**. (*S*)-BAIT, **2.3**, contains the Stx binding P^k trisaccharide moiety as well as a cyclic pyruvate acetal necessary for interaction with HuSAP. In addition, the introduction of a

terminal alkene linker at 6-OH of the glucose moiety would allow for its polymeric incorporation. For the formation of the trisaccharide structure in **2.3**, two strategies may be considered for the formation of the α(1→4) glycosidic linkage. The first is by chemical means, whereby a suitably protected disaccharide glycosyl acceptor would need to be synthesized (i.e. with an unprotected 4'-OH, to allow for regioselective glycosidic bond formation). This approach would require further chemical modifications of both the acceptor and donor and as such would increase the complexity of the synthesis. The second approach is the formation of the α(1→4) glycosidic linkage *via* enzymatic means with a suitable enzyme and a commercially available uridinium diphosphate (UDP) glycosyl donor **2.4**. The fusion enzyme, α(1,4)-galactosyltranferase/4'-Gal-epimerase[197], is capable of both epimerization at C-4 of the relatively inexpensive UDP-glucose and the formation of the galactopyranosyl glycosidic linkage. Often, enzyme catalyzed glycosylation reactions are very *stereo*- and *regio*-selective and as such hold great promise in carbohydrate synthesis. The disaccharide **2.5** is envisioned to be accessible *via* the synthesis and glycosylation between the galactosyl trichloroacetimidate **2.6** and the glycosyl acceptor **2.7**.

The synthesis of (*S*)-PolyBAIT was started by the construction of the glycosyl acceptor **2.4** [Scheme 2.13].

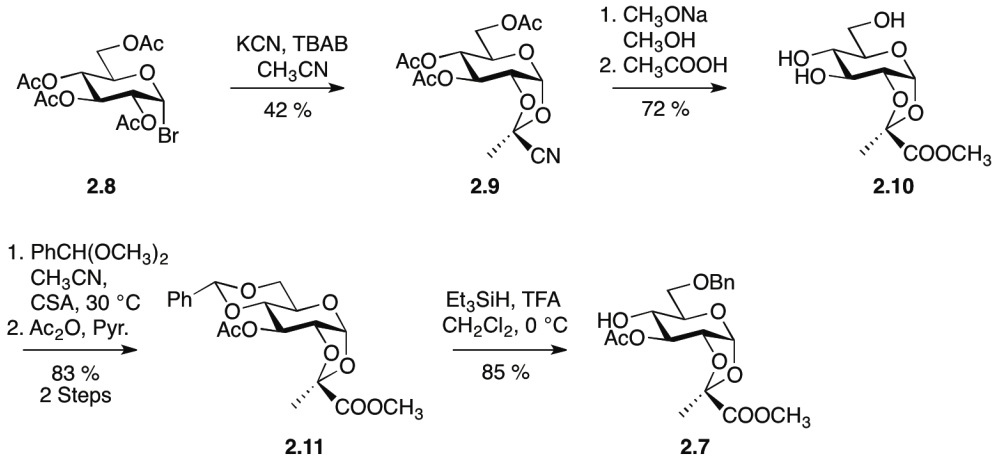

Scheme 2.13. The synthesis of glycosyl acceptor **2.5**.

The synthesis of **2.7** began with the formation of the (*S*)-cyanoethylidene derivative of glucose **2.9** *via* treatment of the glucosyl bromide **2.8** with potassium cyanide (KCN) and *tert*-butyl ammonium bromide (TBAB) in CH_3CN. This method, first introduced by Kochetkov and coworkers[198] provides a mixture of both *exo*-CN (cyano) and *endo*-CN isomers. Fortuitously the *exo*-CN or (*S*) derivative is crystalline, whereas the *endo*-CN or (*R*) derivative is a syrup. After column chromatography, each isomer can be selectively obtained and those fractions containing a mixture of both can be further resolved by the crystallization of the *exo*-CN isomer to achieve separation. The (*S*)-cyanoethylidene derivative **2.9** was obtained in 42 % yield as a white solid. The cyanoethylidene **2.9** was subsequently converted into the methyl ester *via* methanolysis and treated with glacial acetic acid (CH_3COOH) to convert the methoxy imidate intermediate to the methyl ester. This method also removed the acetyl protecting groups to provide the product **2.10** in 72 % yield, without the need for purification. The deprotected sugar **2.10** was subsequently treated with

α,α-dimethoxytoluene under acid catalysis at 30 °C to install the benzylidene acetal.[199] Treatment of the benzylidene intermediate with acetic anhydride (Ac_2O) and pyridine (Pyr) protected the free hydroxyl group at C-3 to give the benzylidene product **2.11** in 83 % yield over two steps. Lastly, the benzylidene acetal was selectively opened to yield the 4-OH and 6-OBn product **2.7** by treatment with triethylsilane (Et3SiH) and trifluoroacetic acid (TFA).[200] This method has become popular in recent years due to it not requiring the toxic sodium cyanoborohydride ($NaBH_3CN$) traditionally used for this regioselective opening of the benzylidene acetal. The glycosyl acceptor **2.7** was synthesized in 85 % yield over two steps from **2.11**.

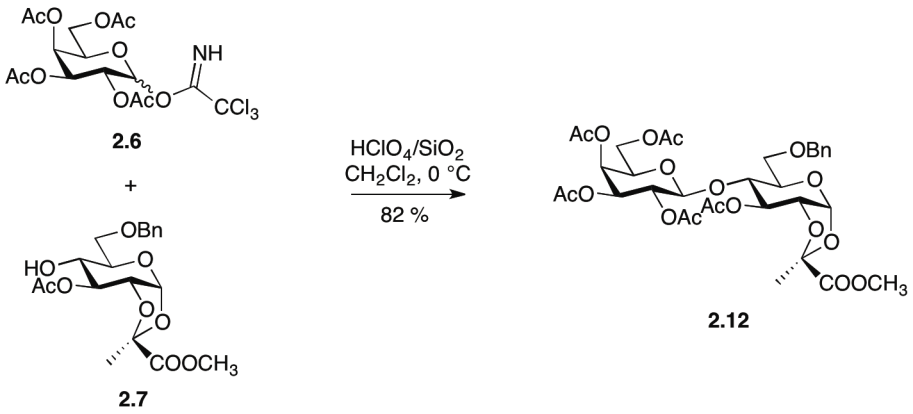

Scheme 2.14. Formation of disaccharide intermediate **2.12**.

Formation of the disaccharide **2.12** was accomplished by glycosylation of the known trichloroacetimidate donor **2.6**[201] with the glucosyl acceptor **2.7** in the presence of perchloric acid ($HClO_4$) adsorbed on silica.[202,203] This method was found to be advantageous versus other more traditional activators due to its highly

efficient reactions, mild reaction conditions and ease of use. The formation of **2.12** as the β isomer was achieved in 82 % exclusively.

Installation of the linker was performed as in Scheme 2.15. The removal on the sole benzyl ether group at C-6 was performed *via* hydrogenation to provide **2.13** in 71 % yield. Treatment of the free hydroxyl group in **2.13** with 4-nitrophenyl chloroformate **2.16** under basic conditions gave the carbonate species **2.14** in 95 % yield. Subsequent reaction of the carbonate **2.14** with the amine **2.17** in the presence of triethylamine (Et_3N) gave the linker addition product **2.15** in 92 % yield. Lastly, global deprotection of the intermediate **2.15** was done by treatment with sodium methoxide (CH_3ONa) in methanol (CH_3OH) to remove all the acetyl protecting groups, followed by treatment with water to convert the methyl ester to the corresponding carboxylic acid to provide **2.5** in 94 % yield.

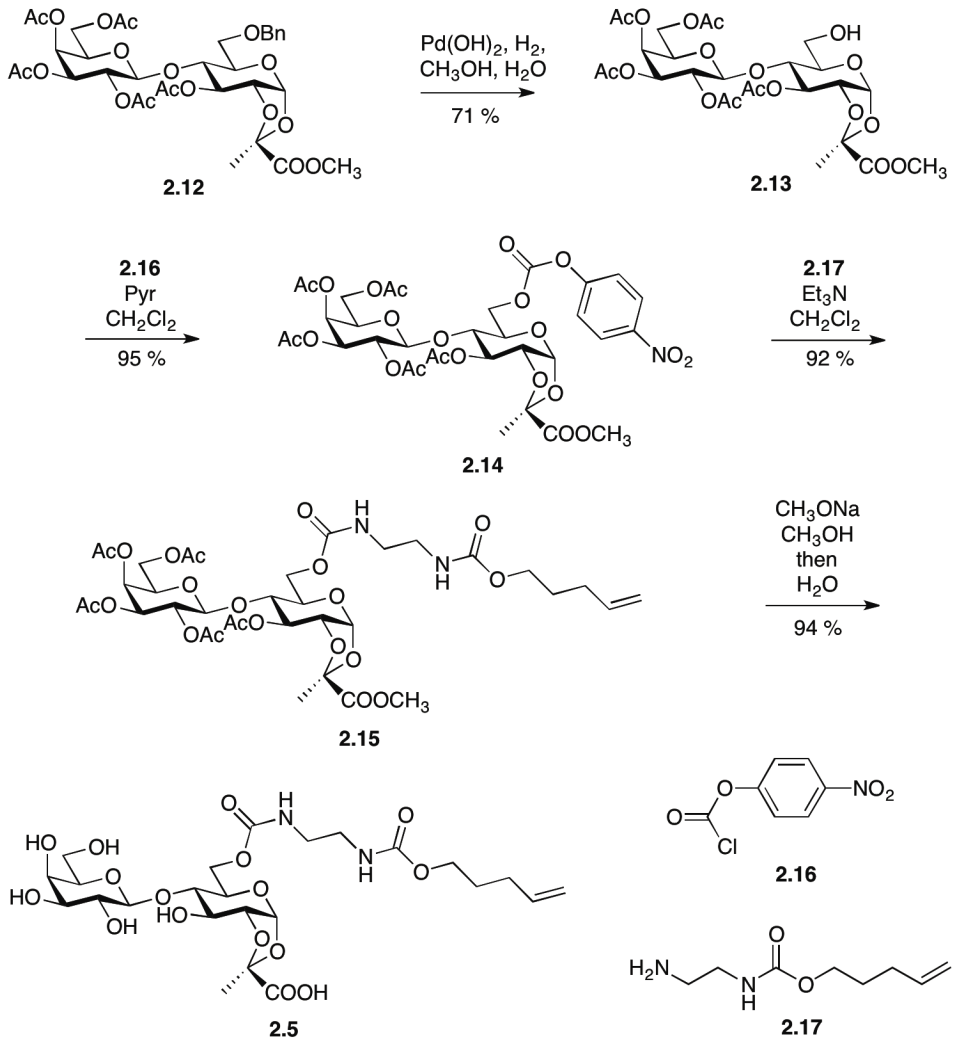

Scheme 2.15. Incorporation of linker moiety towards (*S*)-PolyBAIT **2.1** and formation of glycosyl acceptor **2.5**.

At this stage, the synthesis from compound **2.3** to compound **2.1** was completed by Dr. Eugenia Paszkiewicz in the Bundle group [Scheme 2.16].

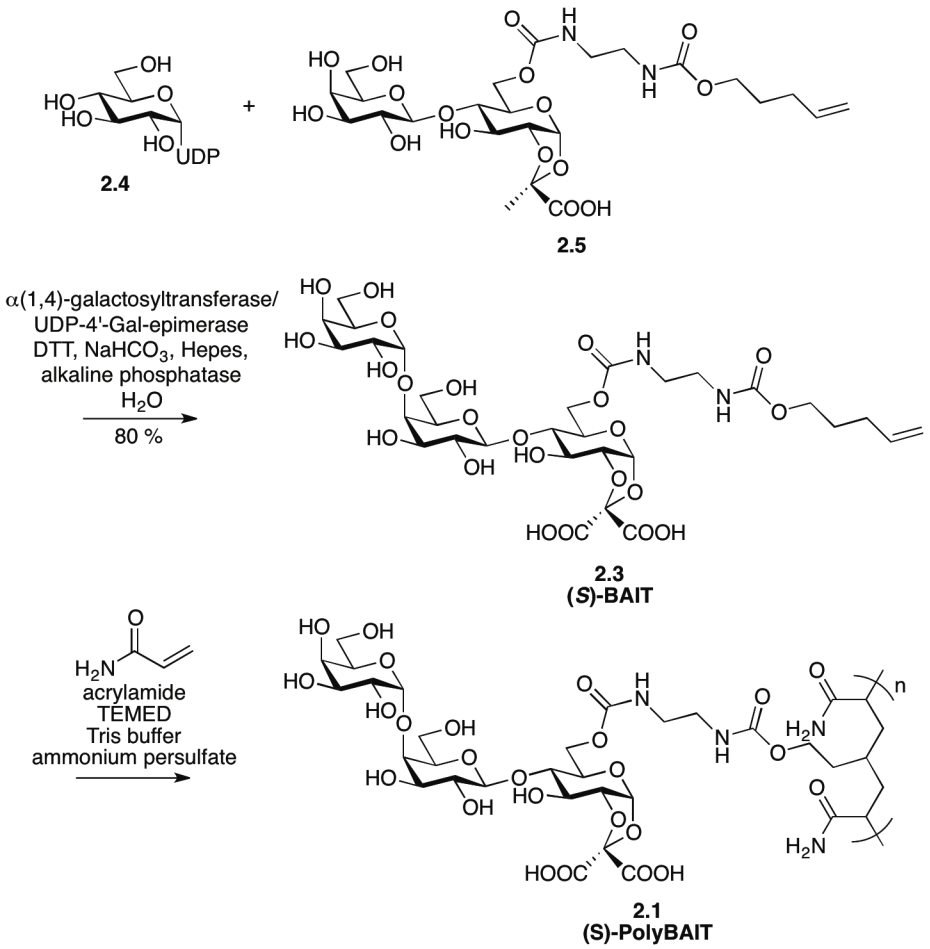

Scheme 2.16. Final steps towards the synthesis of (*S*)-PolyBAIT **2.1**.

The formation of the α(1→4) linkage was achieved *via* the coupling of UDP-glucose **2.4** and **2.5** using the fusion enzyme α(1→4)-galactosyltranferase/4'-Gal-epimerase to give **2.3** in 80% yield.[197] Subsequent copolymerization of the alkene on the linker of **2.3** with acrylamide in the presence of tetramethylethylenediamine (TEMED) provided the final compound (*S*)-PolyBAIT **2.1**.

2.2.2. The synthesis of (*R*)-PolyBAIT.

As with (*S*)-PolyBAIT, the synthesis of its inactive isomer (*R*)-PolyBAIT, **2.2** could be achieved in a similar manner to **2.1** [Scheme 2.17]. Rather than building the trisaccharide framework from monosaccharide building blocks, this approach would investigate if the synthesis could be achieved starting from lactose and thus eliminate a potentially unnecessary glycosylation. Once again, the use of the fusion enzyme α(1→4)-galactosyltranferase/4'-Gal-epimerase could be used for the formation of the trisaccharide backbone in **2.2**. As the 6-OH of glucose is required for the addition of the linker, it would be necessary to synthesize an orthogonally protected disaccharide such as **2.20,** which would allow for the selective addition of the linker. As such, introducing a *tert*-butyldiphenylsilyl (TBDPS) ether on the 6-OH would allow for its selective removal *via* the use of hydrogen fluoride. As with (*S*)-BAIT, installation of the pyruvate moiety could be achieved *via* the formation of a cyanoethylidene as described by Kotchetkov and coworkers.

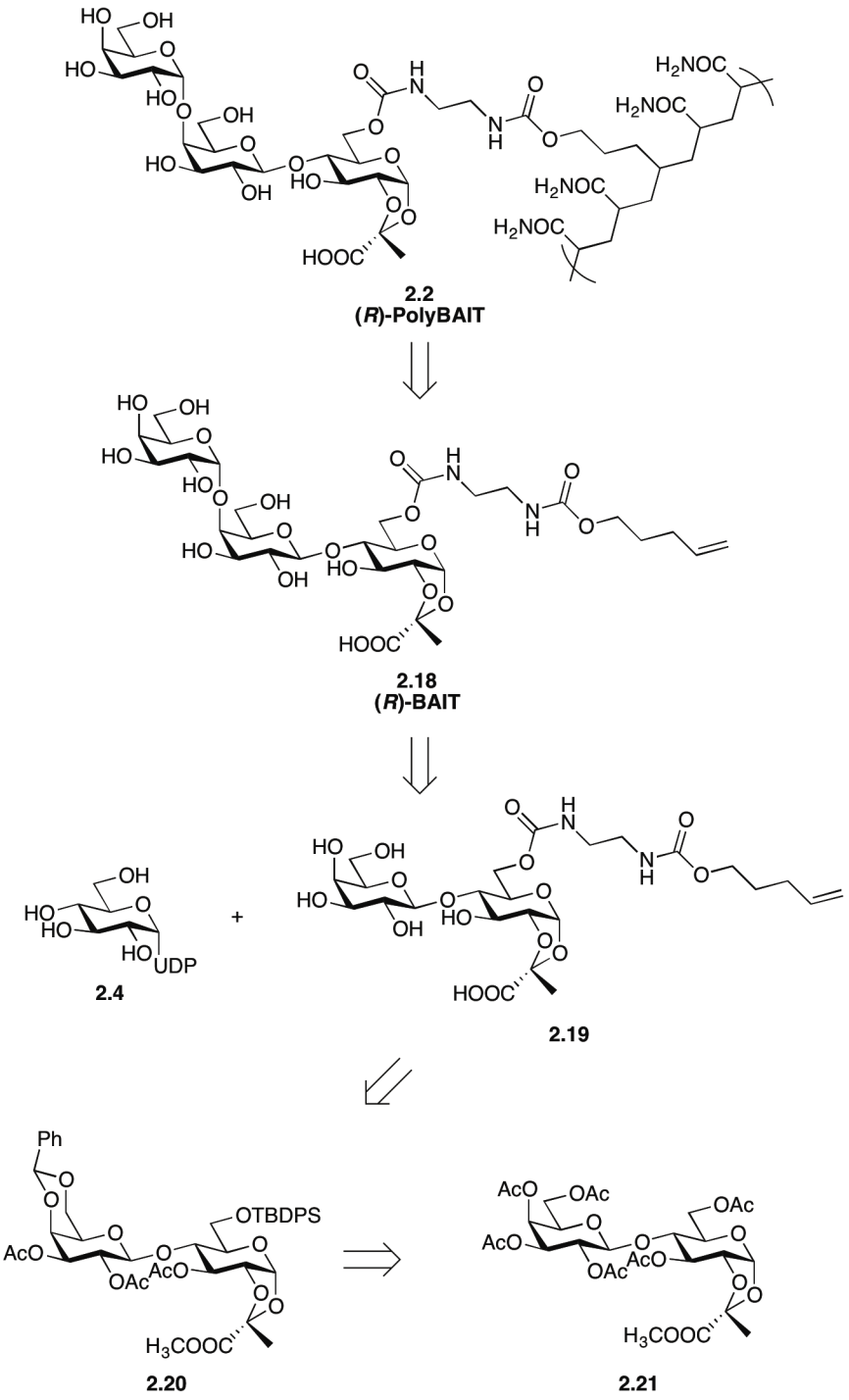

Scheme 2.17. Retrosynthetic analysis of synthetic target (*R*)-PolyBAIT, **2.2**.

The installation of the pyruvate moiety was achieved *via* the cyanoethylidene reaction on the lactosyl bromide **2.22** [Scheme 2.18]. In the

present case, the *endo*-CN derivative was desired over the *exo*-CN isomer to provide the lactosyl cyanoethylidene **2.23** in 26 % yield. This intermediate was treated with CH_3ONa in CH_3OH to a) remove the acetyl groups on the structure and, b) form a cyano imidate derivative, which upon treatment with glacial CH_3COOH converts the imidate to the desired methyl ester. Subsequent global acetylation provided the product **2.21** in 97 % yield without any need for purification. Treatment of **2.21** with CH_3ONa and CH_3OH yielded **2.24** in 75% yield.

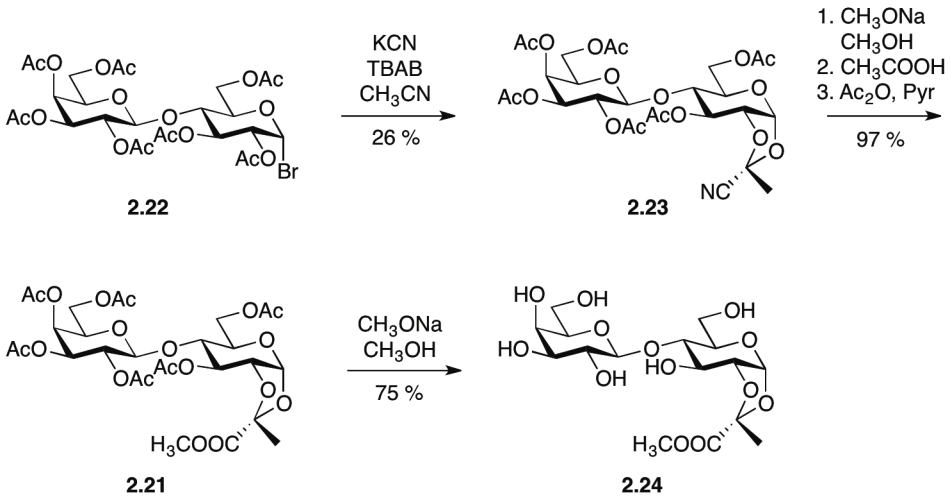

Scheme 2.18. Synthesis of intermediate **2.24**.

The deprotected sugar **2.17** was treated with α,α-dimethoxytoluene under catalytic acidic conditions to provide the benzylidene derivative **2.25** in 74 % yield. The addition of the benzylidene moiety was required to occupy the 6'-OH of galactose to allow for the selective protection of the 6-OH in glucose in the subsequent step.

The derivative **2.25** was selectively protected at the 6-OH position *via* the slow drop-wise addition of *tert*-butyldiphenylsilyl chloride (TBDPSCl) under basic conditions and subsequent global acetylation with Ac_2O and Pyr gave **2.20** in 48 % yield over two steps.[204]

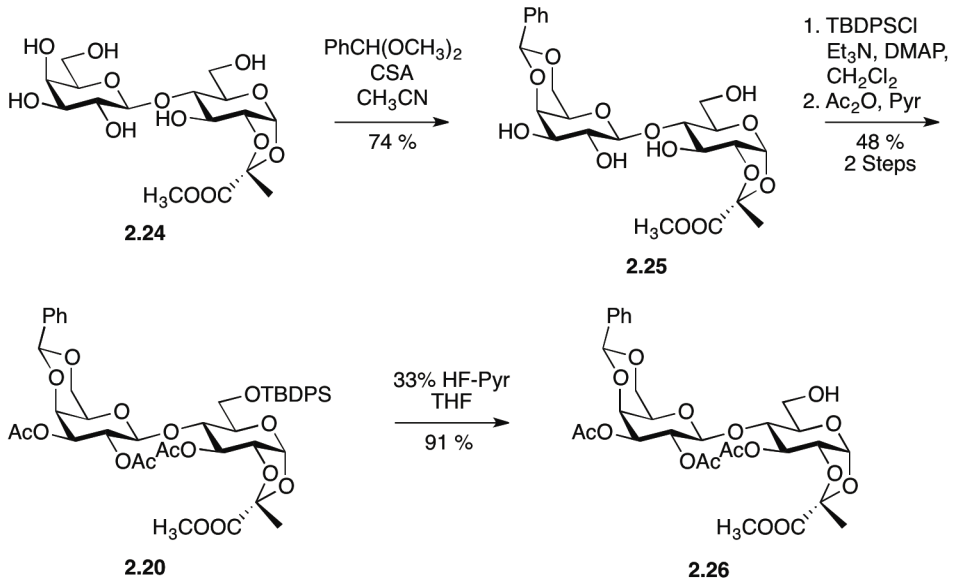

Scheme 2.19. Synthesis of disaccharide derivative **2.26**.

The low yield of the reaction was thought to be due to the addition of TBDPSCl to the 3'-OH of lactose to create the di-*O*-TBDPS ether derivative of lactose as thin layer chromatography (TLC) analysis showed the production of two independent products when chromatographed, but this product was not isolated or characterized. In order to facilitate the addition of the linker, the 6-OTBDPS group was selectively removed using 33% hydrogen-fluoride in pyridine (HF-Pyr) to give **2.26** in 91 % yield.[205]

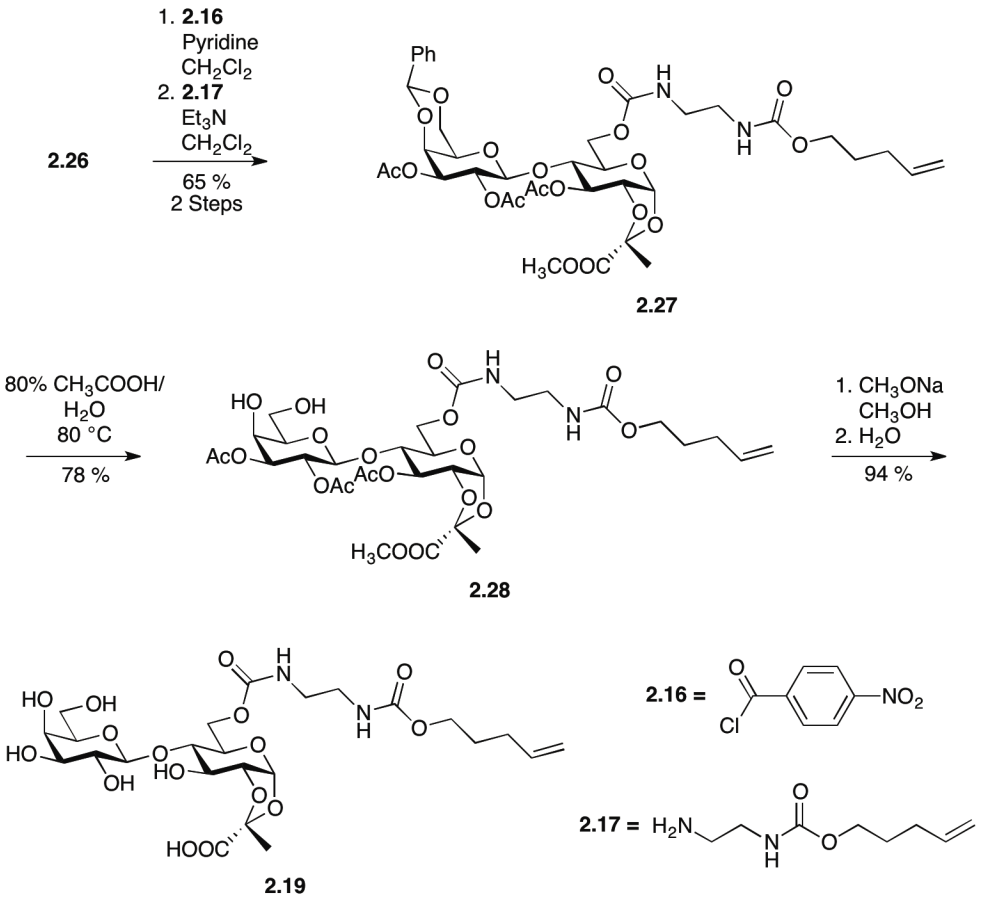

Scheme 2.20. The addition of the linker and preparation of glycosylation precursor **2.19**.

The addition of the linker was done *via* a two-step procedure. First, 4-nitrophenyl chloroformate **2.16** was added to **2.26** under mildly basic conditions to form an intermediate 6-*O*-*p*-nitrophenyl carbonate *in situ*, which was subsequently displaced by the addition of the amine **2.17** in the presence of Et_3N to form **2.27** in 65 % yield over two steps. The benzylidene acetal of **2.27** was removed by treatment with 80 % CH_3COOH in water at 80 °C to provide the diol **2.28** in 78 % yield. Treatment of the partially acetylated intermediate **2.28** with sodium CH_3ONa in CH_3OH, facilitated the removal of the remaining acetyl groups. Once complete, the solution was concentrated to dryness and treated with

water to convert the methyl ester to a carboxylic acid to give **2.19** in 94 % yield over two steps.

At this stage of the synthesis, the synthesis from compound **2.18** to compound **2.2** was completed by Dr. Eugenia Paszkiewicz of the Bundle group.

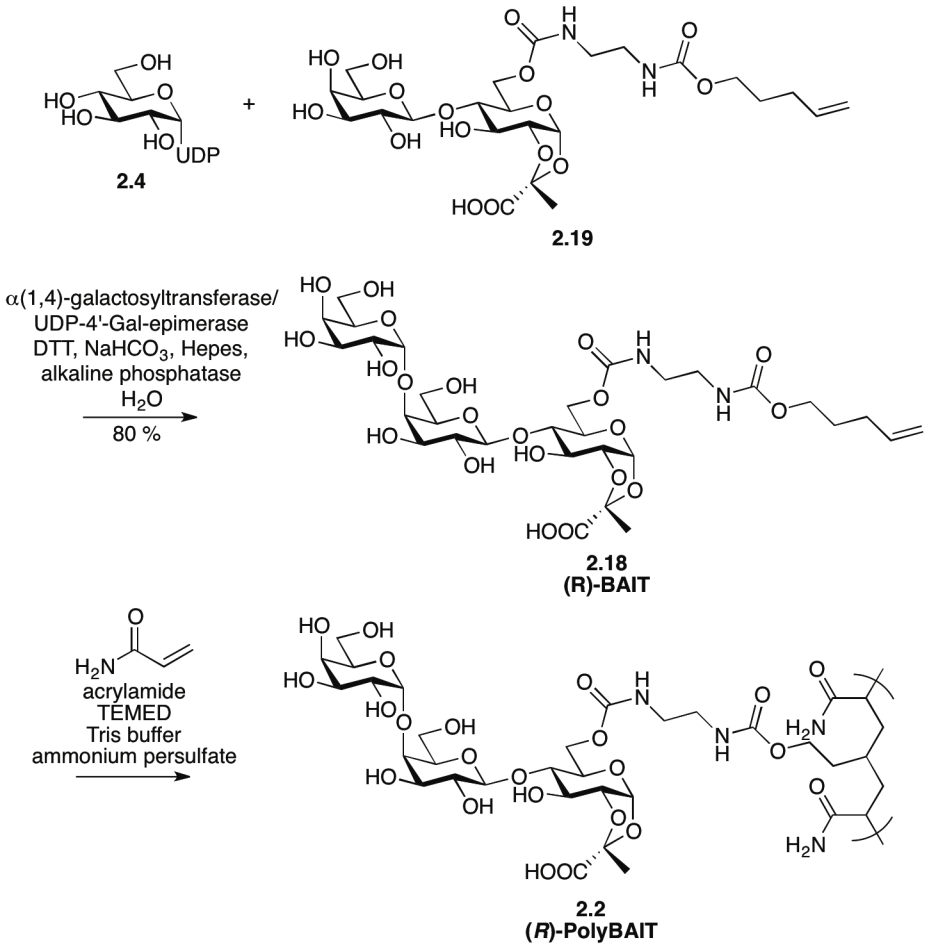

Scheme 2.21. Formation of the trisaccharide **2.18** and the subsequent polymerization of (*R*)-BAIT **2.18** to form (*R*)-PolyBAIT **2.2**.

The addition of the terminal galactose moiety was achieved *via* the use of the fusion enzyme α(1,4)-Galactosyltransferase/UDP-4'-Gal-epimerase with

UDP-glucose **2.4** and the disaccharide acceptor **2.19** to give the trisaccharide intermediate **2.18** in one step and in 80 % yield. With the trisaccharide **2.18** completed, the final step in the preparation of (*R*)-PolyBAIT was the co-polymerization of the terminal alkene of **2.18** with acrylamide in the presence of TEMED to provide the final product (*R*)-PolyBAIT **2.2**.

With both (*S*)- and (*R*)-PolyBAITs completed, the biological evaluation of the inhibitors was assed in vitro and in vivo.

2.2.3. *In vitro* analysis of (*S*)-PolyBAIT

In order to test the ability of (*S*)-PolyBAIT to bind Stx1 and HuSAP towards the formation of a heterobifunctional supramolecular complex and inhibition of Stx1, an *in vitro* ELISA assay was performed [Figure 2.15a] (Ms. J. Sadowska – Bundle group) as well as a Vero cell cytotoxicity neutralization assay [Figure 2.15b] (performed by collaborators in the Armstrong group, University of Calgary). The ELISA measured the ability of (*S*)-PolyBAIT to inhibit Stx1 binding to P^k-coated ELISA microtitre plates in the presence of HuSAP.

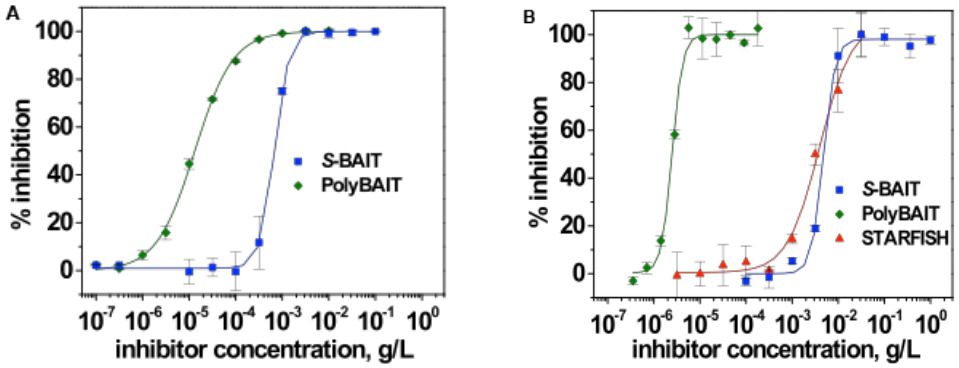

Figure 2.9. ELISA results for (*S*)-PolyBAIT. (a) (*S*)-BAIT versus (*S*)-PolyBAIT. (*S*)-PolyBAIT showed a greater sensitivity against Stx1 and was more potent at lower concentrations. (b) Vero call cytotoxicity neutralization assay, (*S*)-PolyBAIT was approximately four-orders of magnitude stronger than the previously investigated Starfish.

In the presence of HuSAP, the polyacrylamide copolymer (*S*)-PolyBAIT demonstrated high activity (IC_{50} = 6 ng/ml) in a solid-phase Stx1-binding inhibition assay. In contrast, the copolymer (*R*)-PolyBAIT the inactive isomer of (*S*)-PolyBAIT showed no inhibitory activity even at concentrations as high as 1 mg/ml. It is important to note that each isomer showed comparable activity with respect to each protein, but only the (*S*)-isomer showed synergy with HuSAP thereby confirming the importance of the optimal orientation of the binding moieties to allow for supramolecular complex formation. *In vitro* Vero cell cytotoxicity neutralization assay of (*S*)-PolyBAIT showed good inhibitory activity (IC_{50} = 8 ng/ml), which was comparable to that measured in ELISA.

In a parallel investigation,[206] a series of polymer-based ligands were synthesized to display the distributed P^k trisaccharide and cyclic pyruvate as a

polymer expressing two independently bound head groups (polymer **A**, Figure 2.16), or the prearranged heterobifunctional P^k-CP ligands as a distinct entity on the polymer (polymer **B**, Figure 2.17).

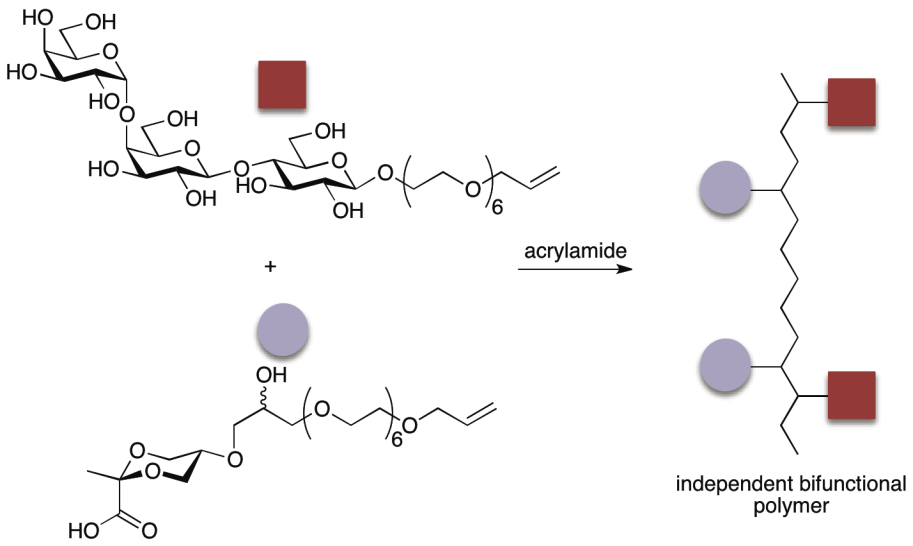

Figure 2.10. Polymer **A** expressing P^k and CP as two independently bound head groups.

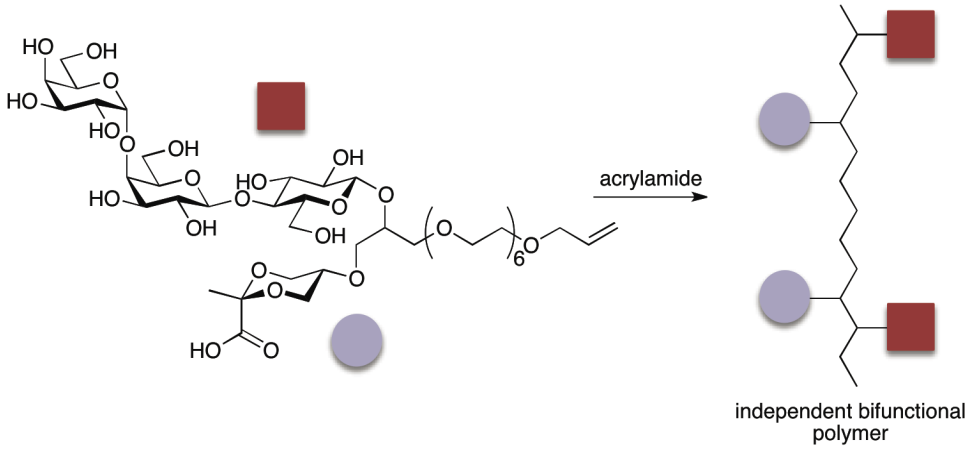

Figure 2.11. Polymer **B** expressing P^k and CP as a distinct entity.

Solid phase binding inhibition assays were done [Figure 2.18] and the results showed that the pre-organized polymer **B** showed a 6000-fold increase in

inhibitory activity of Stx1 in the presence of HuSAP versus without. In the latter case, the P^k trisaccharide epitope is able to inhibit Stx1 binding to immobilized P^k antigen but far less efficiently.

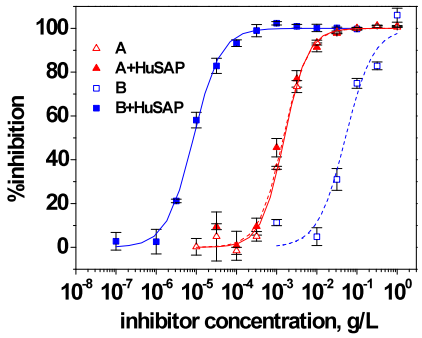

Figure 2.12. Solid-phase binding inhibition data for polymers **A** and **B**.

The polymer **A** however, did not show any HuSAP dependent inhibitory activity. The polymer **B** was designed to be able to bind to the five Ca^{2+}-dependent binding sites of HuSAP while at the same time binding to the five most occupied binding sites of Stx1 (Site 2). This effect resulted in an increase in inhibitory activity by a factor of 300 when in the presence of HuSAP and thus it can be concluded that the formation of a ternary complex is necessary for activity enhancement.[206]

2.2.4. *In vivo* analysis of (*S*)-PolyBAIT

The ability of (*S*)-PolyBAIT to inhibit shigatoxemia *in vivo* was assessed by using HuSAP expressing transgenic mice (C57BL/6-Tg(APSC)1lmeg). Biological studies were performed by George Mulvey and Dr. Glen Armstrong of the University of Calgary.

Two protocols for the *in vivo* analysis of (*S*)-PolyBAIT were developed using HuSAP expressing transgenic (HuSAP-tg) mice at a representative physiological concentration. In the first protocol, HuSAP-tg mice were intravenously treated with a lethal dose of Stx1 (LD_{100} 20 ng/g mouse body weight), premixed with (*S*)-PolyBAIT, (*S*)-BAIT or (*R*)-PolyBAIT. The results showed that only the (*S*)-PolyBAIT/Stx1 treated tg mice were protected from Stx1 poisoning [Figure 2.13] at a concentration of 3.15 μg/g mouse. Those HuSAP-tg mice treated with either (*S*)-BAIT, (*R)*-PolyBAIT or saline (negative control) all showed signs of shigatoxemia within 72 – 110 hours and the mice were subsequently euthanized. The inability of (*R*)-PolyBAIT to inhibit Stx1 infection, once again proves the importance of the correct orientation of the ligands to promote the formation of a supramolecular complex.

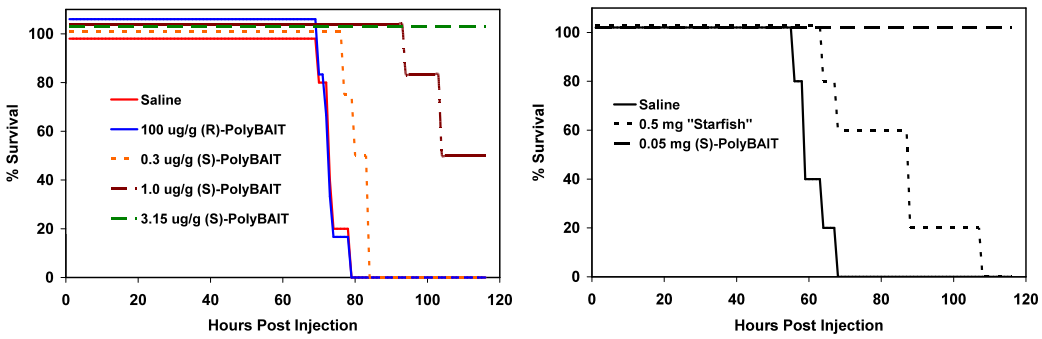

Figure 2.13. *In vivo* assay results for (*S*)- and (*R*)-PolyBAITs.

As a measure of comparison, the ability of (*S*)-PolyBAIT to inhibit Stx1 poisoning was compared to that of the decavalent Starfish ligand. At its maximum possible dose, Starfish was found to be completely ineffective. Consequently, it can be assumed that a peripheral rather than a radial topology is desired for the formation of an Stx1-Ligand-HuSAP complex [Figure 2.14].

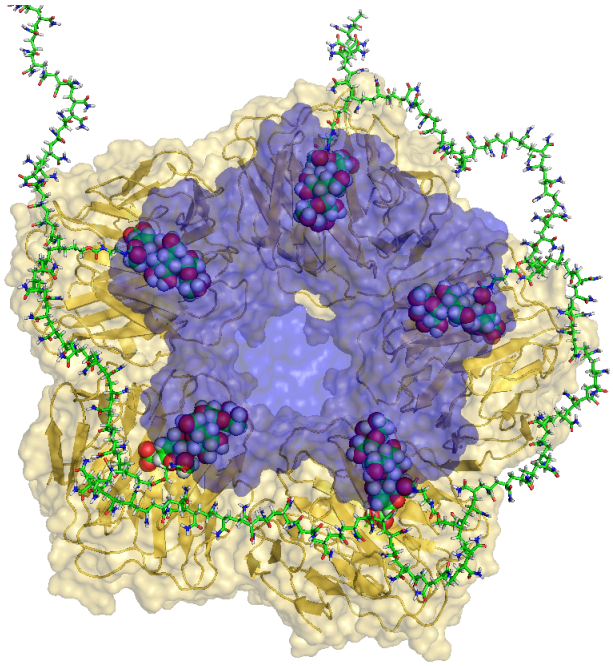

Figure 2.14. A graphical model of (*S*)-PolyBAIT binding to Stx1-B_5 and HuSAP to form a supramolecular complex. The image highlights the use of a peripheral topology for complex formation. Stx1-B_5 is colored in blue and HuSAP is colored in yellow.

In the second protocol, HuSAP-tg mice were treated with a lethal dose of Stx1 subcutaneously in their backs. Injection of the toxin was immediately followed by a single intravenous injection of (*S*)-PolyBAIT. The experiment was designed to mimic a more realistic clinical situation whereby the toxin slowly enters the blood from the intestine and is distributed to its target organs *via* the circulation. Once again, all HuSAP-tg treated with (*S*)-PolyBAIT were protected against Stx1 infection at as low as 1 μg/g mouse.

In addition to protection studies, a biodistribution experiment was done to assess the final location of the Stx1-(*S*)-PolyBAIT-HuSAP complex [Figure 2.15]. Using ^{125}I labeled Stx1, it was found that (*S*)-PolyBAIT redirected Stx1 from the

kidney to the liver for cellular metabolisis. Therefore in addition to preventing Stx1 from binding to Gb_3 receptors in the kidney, (*S*)-PolyBAIT and HuSAP redirected the toxin away from its target organ to the more resilient liver. By redirecting the toxin complex to the liver, it will be incorporated into the reticuloendothelial system (RES) where it may be catabolically disposed of.

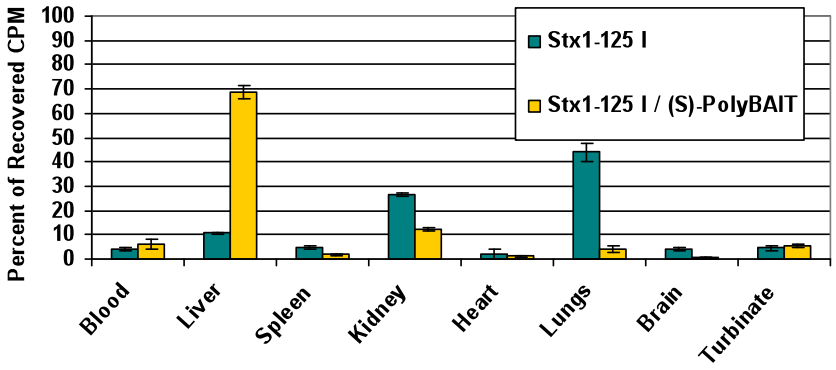

Figure 2.15. Biodistribution of Stx1-^{125}I in HuSAP tg mice. The results indicate that (*S*)-PolyBAIT diverts the toxin away from the target organ kidneys to the liver. Possibly due to the size of the supramolecular complex formed between Stx1, HuSAP and (*S*)-PolyBAIT.

The protective effect of (*S)*-PolyBAIT can be attributed to three factors:

1. Persistence of the polymer bound ligand in circulation and the prolonged bioavailability as compared to (*S*)-BAIT.
2. Promotion of the formation of a stable Stx1-(*S*)-PolyBAIT-HuSAP complex.
3. Redirection of Stx1 complexes to the liver RES for catabolic disposal

2.3. Conclusions

In this chapter it has been shown that pre-organized heterobifunctional ligands displayed on a polymeric scaffold can increase the activity of binding to the Stx1 target protein. The efficacy and increase in binding avidity is due to two overlying factors, a combination of the multivalency and supramolecular effects. It has been shown that the use of a template protein with suitable heterobifunctional ligand can bind to and inhibit a target protein *in vivo*. This approach may yield new insights into the development of new toxin proteins. In the specific case, the heterobifunctional ligand (S)-PolyBAIT bound to and inhibited Stx1 *in vivo* after the formation of a supramolecular complex with HuSAP. The formation of the complex resulted in mice survival and the redirection of the toxin away from the target organ kidneys to the liver.

Chapter 3

Investigating the Nature of Binding to Shiga toxin 2

3.1. Introduction

In this chapter the analysis of Stx2 binding site specificity will be investigated. The synthesis and evaluation of an Stx2 selective ligand will be explored. The synthesis of an Stx2 specific monovalent ligand will be discussed and its mode of binding to Stx2 will be investigated using saturation transfer difference (STD) NMR. The development of bovine serum albumin (BSA), Stx2 specific glycoconjugates and a respective Gb_3-BSA glycoconjugate will be described. Lastly, the synthesis of an Stx2 specific ligand for determination of the first X-Ray crystallographic structure of Stx2 with a bound carbohydrate ligand will be covered.

3.2. The Recent Discovery of an Stx2 Specific Ligand

As mentioned in Chapter 1, the natural ligand for Stx1 is Gb_3 however no other specific ligand has been discovered to be the natural ligand for Stx2. It has therefore been a long-standing assumption, that due to the similarities between Stx1 and Stx2, Gb_3 is also the naturally occurring ligand for Stx2.

In a previous study, Gamage *et al.* of the Weiss group,[207] showed that *O*-polysaccharides on a number of lipopolysaccharides isolated from harmless *E.*

coli bacterial serotypes, specifically neutralized Stx2 but not Stx1 infection. Of the serotypes explored, the structure of one had been previously solved corresponding to the LPS of *E. coli* O117 [Figure 3.1]. A comparison of Gb_3 and the LPS derived from O117 show remarkable structural similarities. Both structures are comprised of a terminal α-(1→4)-digalactose component. However, the LPS from O117 possesses two 2-acetamido-2-deoxy-galactopyranosyl moieties.

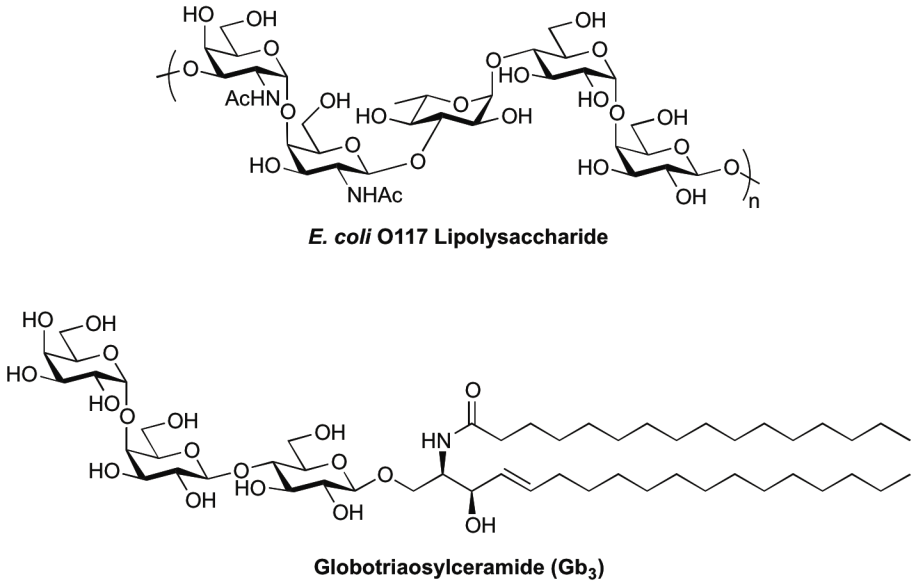

Figure 3.1. The structures of *E. coli* O117 LPS and globotriaosylceramide. (Top) *E. coli* O117 LPS containing two terminal 2-acetamido-2-deoxy galactose moieties that possessed the ability to neutralize Stx2 but not Stx1 poisoning. (Bottom) The structure of globotriaosylceramide (Gb_3).

As an extension of the previous work, Kale *et al.*,[147] with the Weiss group synthesized and tested a series of biotinylated glycoconjugates to distinguish between Stx variants [Figure 3.2]. The various synthetic targets included a series

of P^k trisaccharide derivatives with varying linker lengths. P^k trisaccharide derivatives included a disaccharide α-D-GalNAc*p*-(1→4)-β-D-GalNAc*p*-(linker) glycoconjugate derived from the structure of *E. coli* O117 LPS (GC-1), P^k trisaccharide (GC-2a, GC-2b) and lastly, P^k trisaccharide with the terminal galactose moiety replaced with a terminal 2-acetamido-2-deoxy-galactopyranosyl residue (GC-3a, GC-3b).

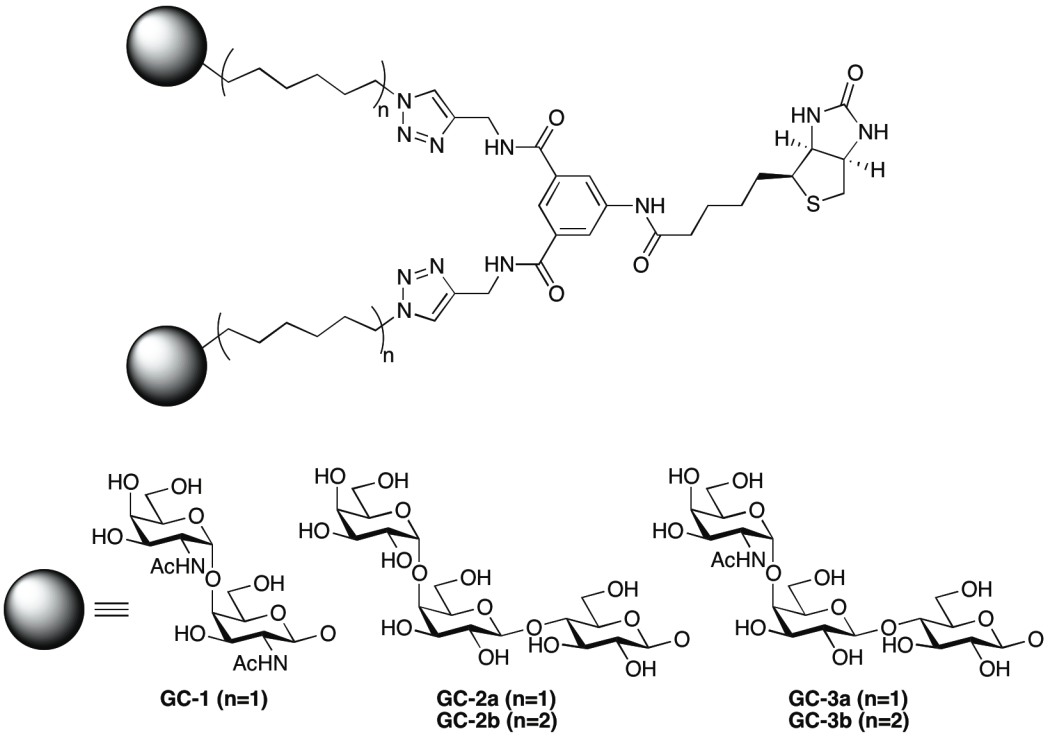

Figure 3.2. Structures of glycoconjugates GC-1, GC-2a, GC-2b, GC-3a and GC-3b. Reproduced from Kale *et al.*[147]

The authors tested the ability of the glycoconjugates to bind to and interact with Stx1 and Stx2 using ELISA. The experiments were performed by adding the biotinylated glycoconjugates to streptavidin-coated plates, coating the surface of the plates with the various Gb_3 analogues to assess their ability to bind to either

Stx1 or Stx2. Their results indicated that Stx2 bound to di- and mono-*N*-acetyl substituted galactosamines GC-1 and GC-3a whereas Stx1 failed to bind either. In addition, the trisaccharide GC-3a appeared to be a better substrate for Stx2 than the disaccharide GC-1. Interestingly, GC-2a was found to bind to Stx1 only and not Stx2. Compounds with longer linkers (n=2) were found to have decreased sensitivity and selectivity; GC-2a bound to Stx1 with greater affinity than GC-2b and GC-3b bound to both Stx1 and Stx2 and with less affinity than GC-3a.

These results provided by Gamage *et al*.[207] and Kale *et al*.[147] suggest that a P^k trisaccharide derivative modified with a 2-acetamido-2-galactopyranosyl moiety at the non-reducing end would allow for an interesting platform to investigate the nature of binding to Stx2.

As a result, the synthesis of a modified methyl glycoside of P^k trisaccharide was performed. The target, Methyl-P^kNAc, **3.1**, incorporates a 2-acetamido-2-deoxy galactose moiety at the non reducing terminus for selective Stx2 binding. In parallel the known methyl glycoside of P^k trisaccharide (Methyl-P^k), **3.2**, was synthesized according to literature procedures.[208] To investigate the nature of ligand binding to Stx2, STD NMR was performed.[209]

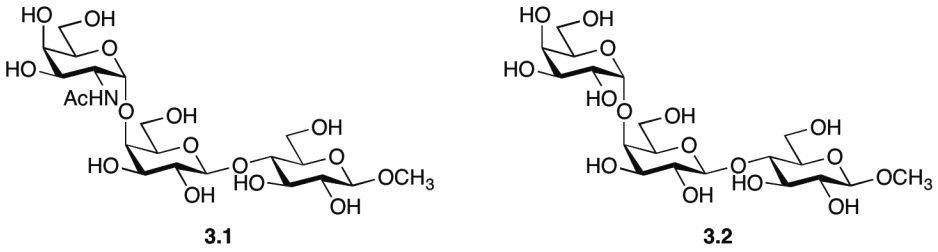

Figure 3.3. Structures of synthetic target Methyl-P^{k}NAc **3.1** and its counterpart Methyl-P^k **3.2**.

3.2.1. The Syntheses of Methyl-P^{k}NAc 3.1

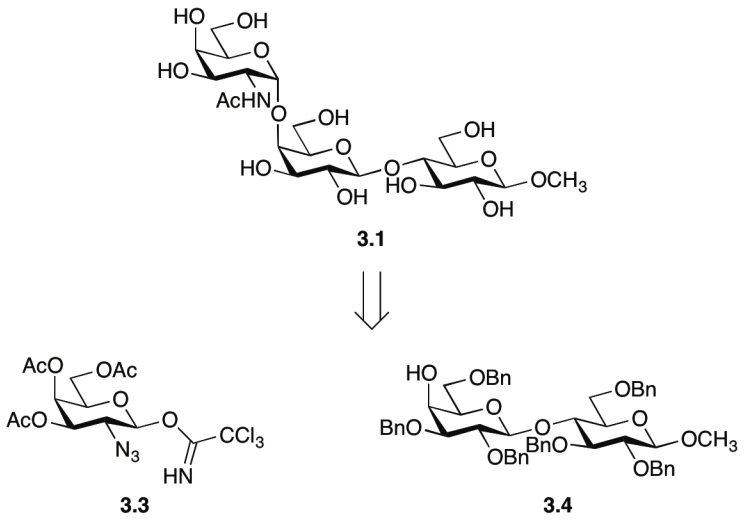

Scheme 3.1. Retrosynthetic analysis of Methyl-P^{k}NAc trisaccharide **3.1**.

The synthesis of **3.1** could be achieved *via* the glycosylation between the known trichloroacetimidate **3.3**[210] and the glycosyl acceptor **3.4**. The intermediate **3.4** can be obtained from lactose *via* a series of protection/deprotection manipulations.

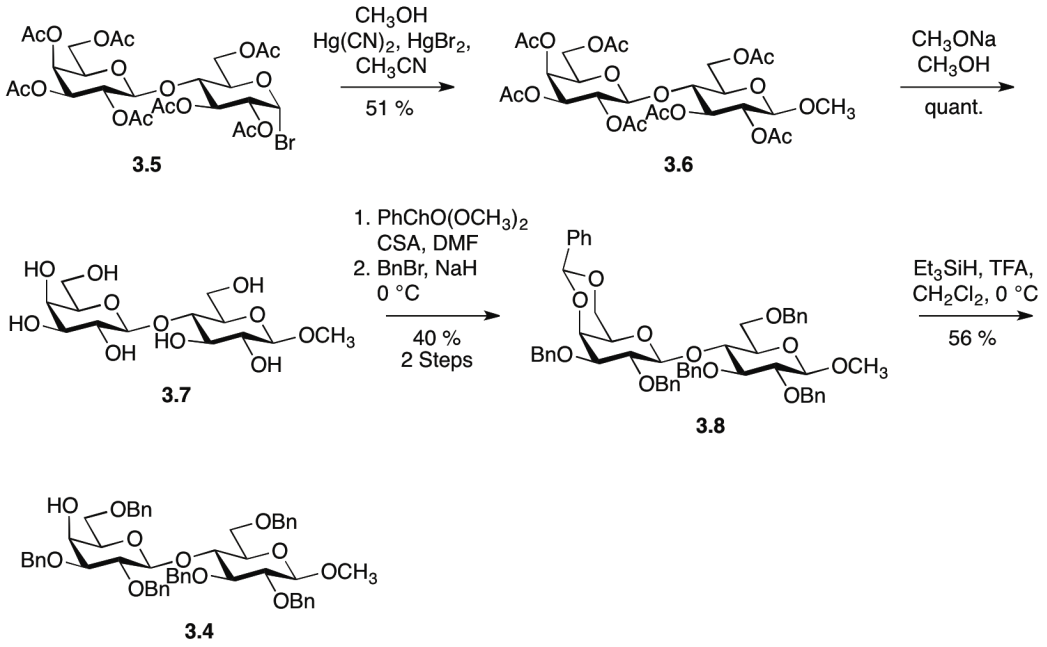

Scheme 3.2. The synthesis of glycosyl acceptor **3.4**.

The formation of the peracetylated methyl lactoside **3.6** was achieved by a Helferich glycosylation procedure involving the lactosyl bromide donor **3.5** and CH_3OH as the acceptor.[211] The reaction was performed using $Hg(CN)_2$ and $HgBr_2$ in CH_3CN to form **3.6** in 51% yield predominantly as the β-anomer. Global deprotection of **3.6** was done using CH_3ONa in CH_3OH to provide the methyl lactoside **3.7** in quantitative yield. Installation of the benzylidene moiety of **3.8** was accomplished by treating **3.7** with α,α-dimethoxytoluene in the presence of CSA in DMF.[199] Subsequent treatment of the benzylidene intermediate with BnBr and NaH, benzylated the remaining hydroxyls to provide intermediate **3.8** in 40 % yield over two steps. The selective cleavage of the benzylidene acetal was accomplished using Et_3SiH and TFA in CH_2Cl_2 to provide the 4-OH, 6-OBn product **3.4** in 56 % yield.[212]

The formation of the protected trisaccharide **3.9** was accomplished as in Scheme 3.3.

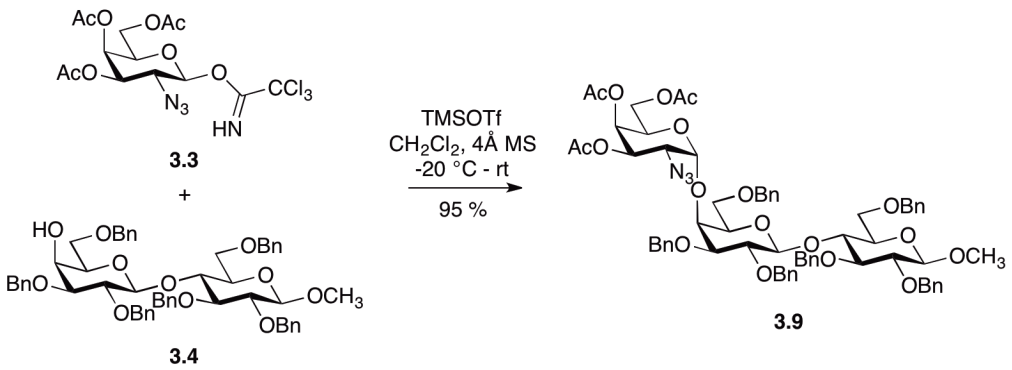

Scheme 3.3. Glycosylation reaction between the trichloroacetimidate donor **3.3** and glycosyl acceptor **3.4**.

The trisaccharide **3.9** was synthesized by the glycosylation reaction between glycosyl acceptor **3.4** and the known trichloroacetimidate donor **3.3**.[210,213] The reaction was performed using TMSOTf as the lewis acid activator in CH_2Cl_2 in the presence of 4Å molecular sieves at -20 ºC warming to room temperature. The trisaccharide intermediate **3.9** was synthesized in 95 % yield and exclusively as the α-anomer.

The final steps towards the preparation of **3.1** are given in Scheme 3.4. The azide of **3.9** was reduced to the corresponding amine using H_2S gas in a solvent mixture of Pyr:water:Et_3N (10:1:0.3).[214] Subsequent acetylation of the amine was done by treatment with Ac_2O and Pyr to give the 2-acetamido intermediate **3.10** in 85 % yield over two steps.

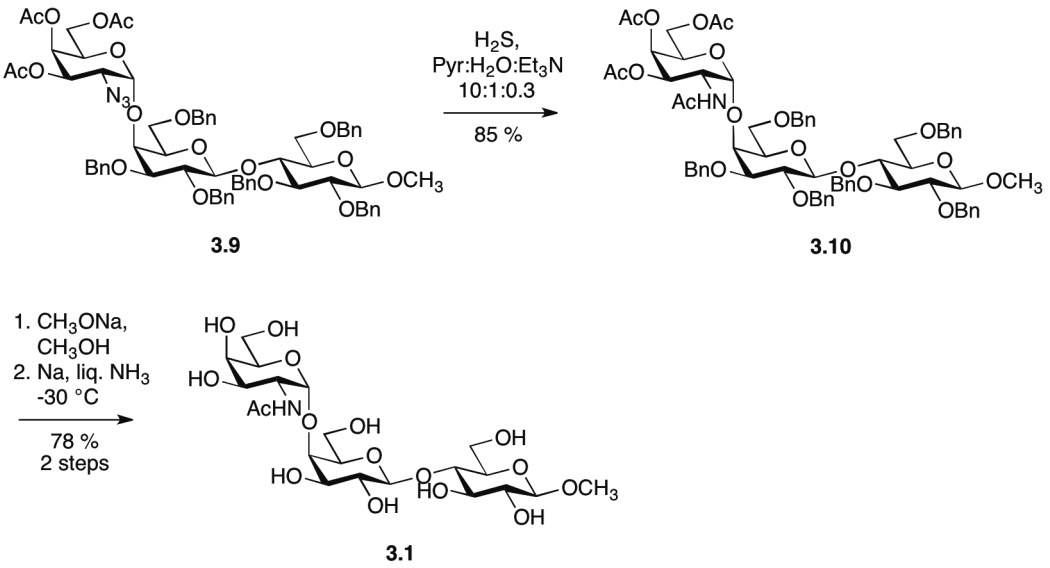

Scheme 3.4. Global deprotection and completion of the synthesis of Methyl-P^{k}NAc **3.1**.

Lastly, global deprotection of **3.10** was achieved *via* a two-step procedure. The acetyl protecting groups were removed by treatment of **3.10** with CH_3ONa in CH_3OH. Subsequent removal of the benzyl ethers was done by Birch reduction using Na in liquid NH_3 to provide the target compound **3.1** in 78 % yield over two steps.[215,216]

The synthesis of the known Methyl-P^k **3.2** was accomplished *via* previously published procedures.[208]

3.2.2. Saturation Transfer Difference NMR spectroscopy

STD NMR spectroscopy was developed by Mayer and Meyer in 1999,[217] and has to date been used to great effectiveness in studying protein-ligand interactions. STD NMR is most often used to study and characterize carbohydrate ligands and their interaction with a respective protein. A typical STD NMR

experiment involves the combination of protein and its ligand and the acquisition of an "on resonance" NMR spectrum as well as an "off-resonance" spectrum. An "on-resonance" spectrum is obtained by the selective irradiation of the protein at least 700 MHz away from the closest ligand signal. Magnetization on the protein will be transferred to the bound ligand by saturation transfer and the degree of ligand saturation depends on the residence time of the ligand within the protein-binding pocket and its proximity to the protein hydrogen atoms. Dissociation of the ligand from the protein into solution provides for the acquisition of resonance signals from the ligand. Of these proton signals, those protons that interact with the protein directly, do so through an intermolecular transfer nuclear Overhauser effect (trNOE) and a decrease in signal intensity is observed. An "off-resonance" spectrum is obtained by irradiation at value far from any signal, ligand or protein. The spectrum recorded yields a normal NMR spectrum of the mixture. The formation of an STD NMR spectrum results from the subtraction of the "on-resonance" spectrum from the "off-resonance" spectrum in which only the protons on the ligand that interact with the protein are visible. All signals that arise from protons that do not show any binding activity are cancelled.[209,217] The effect is depicted graphically in Figure 3.4.

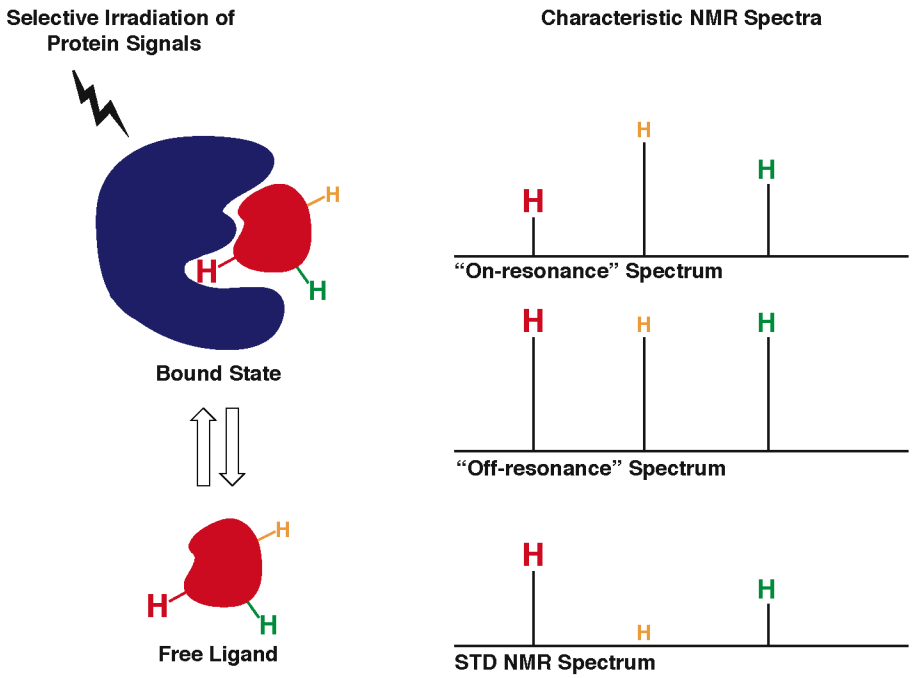

Figure 3.4. Graphical representation of the principle of saturation transfer difference (STD) NMR spectroscopy. The "on-resonance" spectrum is obtained by selectively irradiating the protein. In addition to saturation of the protein, any bound ligands also become saturated. Upon disassociation into solution the saturated ligand provides a spectrum. Protons in close proximity to the protein and potentially involved in the binding event (red and green H's) provide weaker intensity peaks compared to those protons not closely associated to the protein (yellow H). Subtraction of the "on-resonance" spectrum from the "off resonance" spectrum provides the STD NMR spectrum. The relative intensities of peaks in the STD NMR spectrum provide insights as to the specific protons involved in protein binding.

STD NMR analysis of both compounds, **3.1** and **3.2**, was performed by a former Bundle group postdoctoral fellow Dr. Margaret Johnson and the STD NMR spectra are presented below [Figures 3.5 and 3.6].

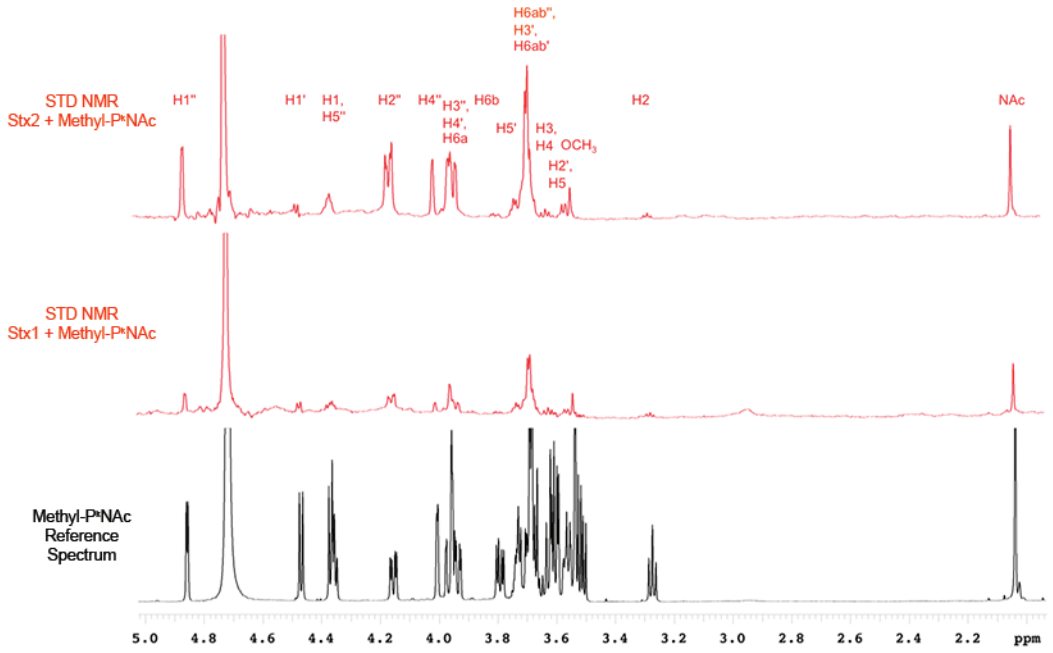

Figure 3.5. ^{1}H STD NMR spectra for Methyl-P^{k}NAc **3.1** with Stx2 and Stx1.

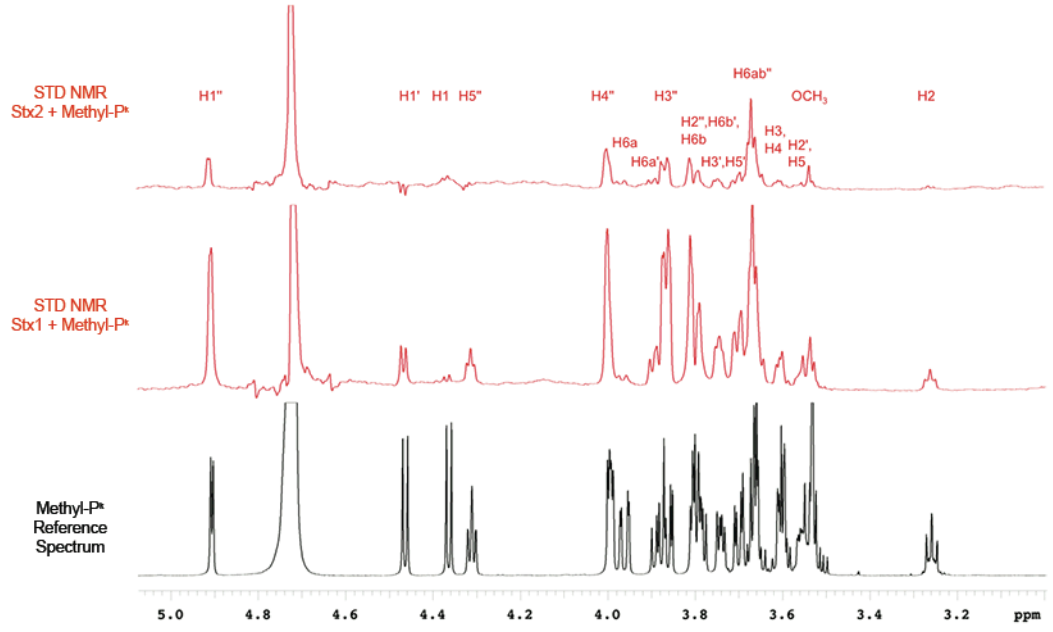

Figure 3.6. ^{1}H STD NMR spectra for Methyl-P^{k} **3.2** with Stx2 and Stx1.

The analysis of the spectra is displayed as a table of STD intensities. Using the intensity of H-1" as a reference (100 %) the relative ratios of the remaining protons in the spectrum provide the intensities of the remaining protons in the spectra [Table 3.1 and Table 3.2].

Methyl-P^{k}NAc	Proton	Stx1	Stx2
Gal"	H-1"	100	100
	H-2"	150	200
	H-4"	48	76
	NHAc	68	34
Gal'	H-1'	57	14
	H-5'	55	35
Glc	H-2	35	12
	H-2, H-4	28	9
	H-6b	20	8
	OCH_3	25	8
	H-3", H-4", H-6a	84	80
	H-5", H-1	35	22
	H-6ab", H-3', H-6ab'	95	67
	H-2', H-5	55	23

Table 3.1. Table of STD NMR intensities (% relative to H-1") of Methyl-P^{k}NAc **3.1** binding to Shiga toxins Stx1 and Stx2.

The enhancement strengths for the interaction of Methyl-P^{k}NAc with Stx1 and Stx2 in Table 3.1 follow the general trend of GalNAc" > Gal' > Glc for both Stx1 and Stx2. GalNAc H-2" is more strongly enhanced when interacting with Stx2 than Stx1. The Glc moiety in Methyl-P^{k}NAc interacts with Stx1 more so than with Stx2.

Methyl-P^k	Proton	Stx1	Stx2
Gal"	H-1"	100	100
	H-3"	140	113
	H-4"	67	90
	H-5"	30	4
	H-6ab"	70	150
	H-1'	28	0
	H-3'	80	64
	H-5'	43	54
	H-6a'	51	50
	H-1	4	23
	H-2	24	23
	H-3, H-4	11	21
	H-6a	8	29
	OCH_3	5	15
	H-2", H-6b', H-6b	62	64
	H-2', H-5	16	20

Table 3.2. Table of STD NMR intensities (% relative to H-1") of Methyl-P^k **3.2** binding to Shiga toxins Stx1 and Stx2.

The enhancement strengths for the interaction of Methyl-P^k **3.2** with Stx1 and Stx2 in Table 3.1 follow the same general trend as **3.1**, Gal" > Gal' > Glc for both Stx1 and Stx2. Considering both sets of data, the overall enhancement patterns are the same for both ligands and both toxins. This would suggest that Methyl-P^kNAc binding to Stx2 occurs in the same, if not a very similar, mode as Methyl-P^k to Stx1. In addition, other specific protons seem to differ in their relative enhancements. Gal H-1 of Methyl-P^kNAc **3.1** is more strongly enhanced when interacting with Stx1 and Stx2 than the corresponding Gal H-1 of Methyl-P^k **3.2**. Lastly, an observable difference in Stx1 and Stx2 binding is seen when comparing Glc enhancements; they are stronger in Stx2 for Methyl-P^k and in Stx1 for Methyl-P^kNAc. Lastly, the *N*-acetyl moiety of Methyl-P^kNAc interacts more

strongly with Stx1 than Stx2 and based on these data does not contribute greatly to the binding of Methyl-P^kNAc to Stx2.

A possible disadvantage of using STD NMR spectroscopy for the analysis of ligand binding to a protein is that signal overlap complicates its analysis.[209] Only discreet signals that arise from a singular proton or group of equivalent protons may be used for analysis. This is due to overlapping signals giving rise to what would appear to be STD effects however are simply peaks due to additive effects of signals overlapping. In addition, the binding location of the ligand cannot be conclusively deduced from the spectra as both Stx1 and Stx2 have multiple binding sites. From the results the percent saturation of the ligand protons involved in protein binding are calculated and presented [Figure 3.7].

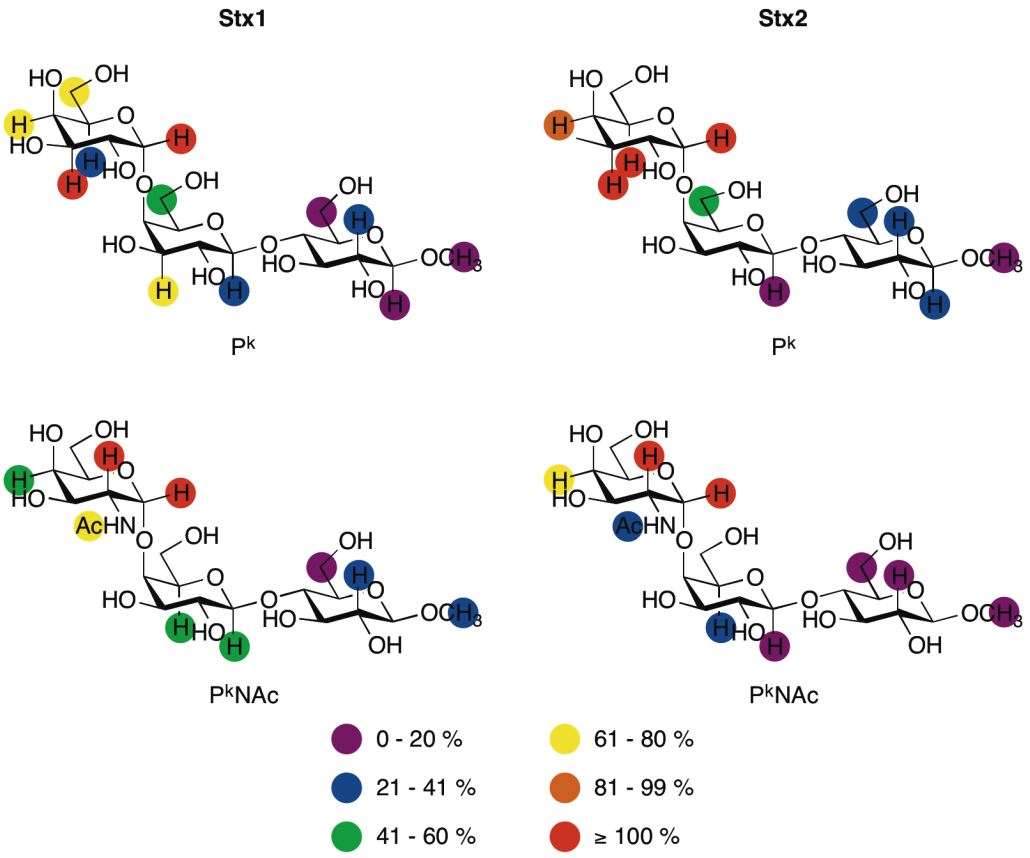

Figure 3.7. Summary of STD NMR signal enhancements.

3.2.3. Determination of Methyl-P^{k}NAc Binding Constant

In collaboration with Dr. John Klassen and coworkers at the University of Alberta, the analysis of the binding affinity constant, K_a of Methyl-P^{k}NAc **3.1** was determined.

Using a technique pioneered by the Klassen group, nanoelectrospray (nanoES) Fourier-transform ion cyclotron resonance mass spectrometry (FT-ICT-MS)[218] it is possible to observe oligosaccharide-protein complexes in the gas-phase with dissociation complexes in the millimolar range.

Previous investigations have shown that binding affinity of a Methyl-P^k trisaccharide for Stx1 is approximately K_a = 3.6 x 10^2 M^{-1} (360 M^{-1}) and for Stx2 is K_a = 2.5 x 10^2 M^{-1} (250 M^{-1}).[136] In addition, these investigations found that binding to Stx2 occurred primarily in site 2 and to a lesser extent site 1, therefore site 2 is the primary binding site. Analysis of Methyl-P^kNAc **3.1** binding to Stx2 provided a binding affinity of K_a = 4.5 x 10^2 M^{-1} (450 M^{-1}). As a consequence, Methyl-P^kNAc, **3.1**, binds to Stx2 with almost double the affinity of Methyl-P^k. The stronger binding affinity provides a rationale for the further development and investigation of Stx2 specific 2-acetamido-2-deoxy-galactopyranosyl modified ligands.

3.3. The Synthesis and Development of an Stx2 Specific ELISA

Based on the earlier observations of Kale *et al.*[147] and our initial STD NMR studies the development of an Stx2 specific ELISA assay was undertaken. Two glycoconjugates were envisioned to be necessary for its development and study [Figure 3.8]. The first, P^kNAc-BSA or **3.11**, is a P^kNAc trisaccharide derivative conjugated to BSA through the use of a squarate ester moiety for selective binding to Stx2. The second, P^k-BSA or **3.12**, is a P^k trisaccharide derivative also conjugated to BSA through a squarate ester. The synthesis of **3.11** and **3.12** will be discussed followed by some preliminary ELISA results.

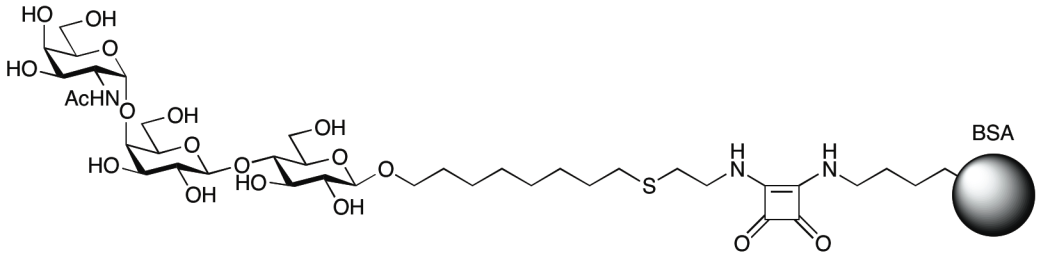

3.11
P^{k}NAc-BSA Glycoconjugate

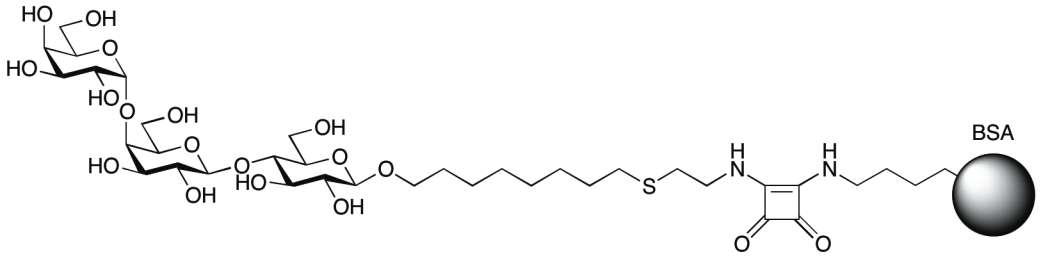

3.12
P^{k}-BSA Glycoconjugate

Figure 3.8. Structures of BSA glycoconjugates P^{k}NAc-BSA **3.11** and P^{k}-BSA **3.12**.

3.3.1. The Synthesis of P^{k}NAc-BSA 3.11

The synthesis of P^{k}NAc-BSA **3.11** can be accomplished as in Scheme 3.5.

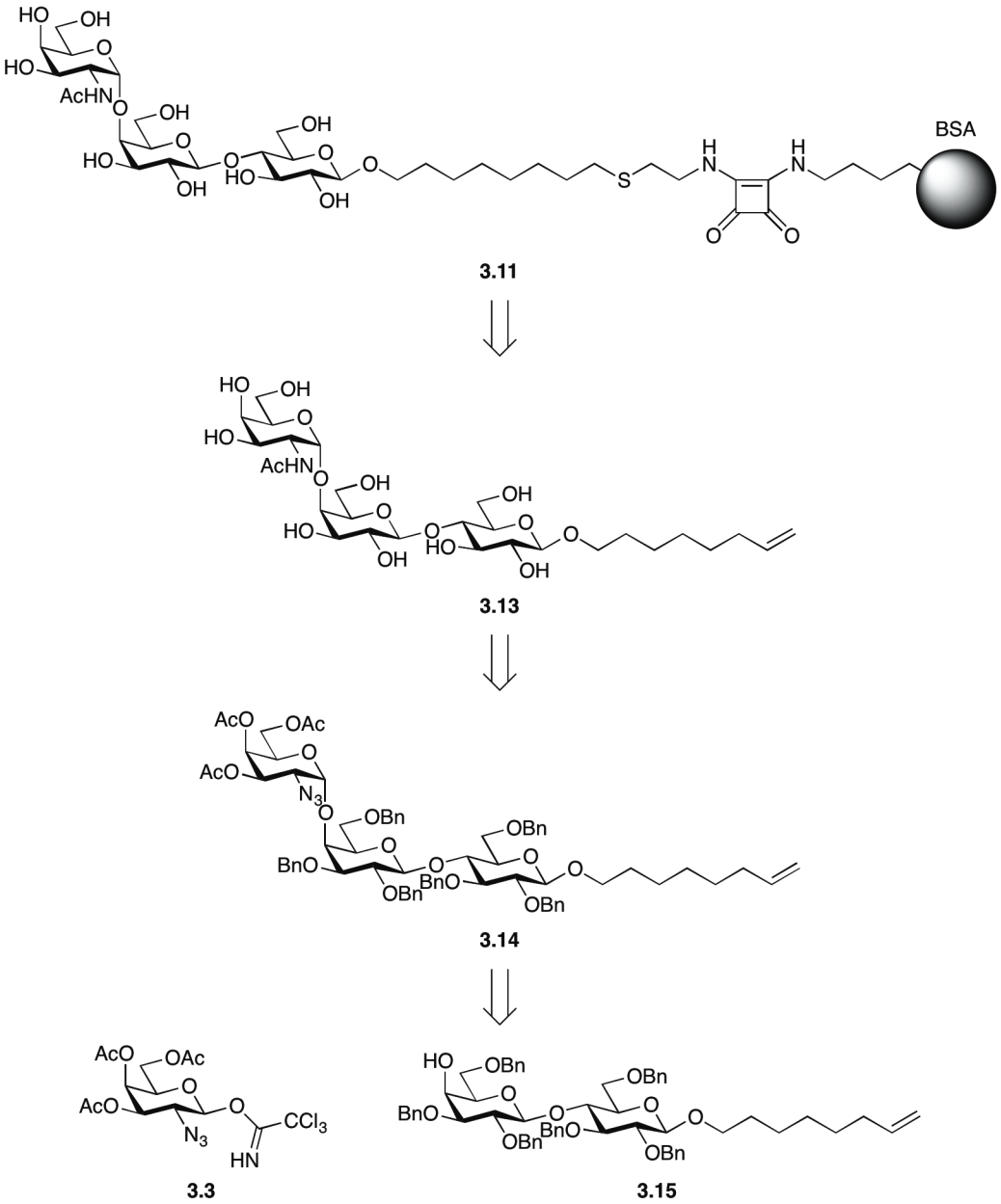

Scheme 3.5. Retrosynthetic analysis of P^{k}NAc-BSA **3.11**.

The synthesis of **3.11** can be accomplished *via* the elaboration of the linker and subsequent conjugation to BSA through the use of a squarate group. The fully

deprotected compound **3.13** can be readily obtained from intermediate **3.14** *via* the reduction and acetylation of the azido moiety followed by a series of deprotection steps. The formation of the trisaccharide **3.14** can be achieved *via* the $\alpha(1\rightarrow4)$ glycosylation between the known trichloroacetimidate donor **3.3** and the glycosyl acceptor **3.15**. Lastly, **3.15** can be readily obtained from lactose *via* a series of protection/deprotection manipulations.

The synthesis of glycosyl acceptor **3.15** is described in Scheme 3.6. Peracetylated lactose was treated with 7-Octen-1-ol in the presence of the lewis acid, $BF_3 \bullet OEt_2$ in CH_2Cl_2 to provide the β-glycosylation product **3.16** in 45 % yield.[219,220] Global deprotection of the acetyl protecting groups in **3.16** was done by treatment with CH_3ONa in CH_3OH to give 7-Octenyl lactoside **3.17** in 93 % yield. Installation of the benzylidene acetal of **3.18** was done by treatment of **3.17** with α,α-dimethoxytoluene in the presence of CSA in CH_3CN followed by the addition of BnBr under basic conditions to benzylate the remaining hydroxyl groups to form **3.18** in 68 % yield over two steps.[199] Lastly, the selective reduction of the benzylidene acetal was accomplished by the treatment of **3.18** with Et_3SiH in the presence of TFA to form the 4'-OH, 6'-OBn product **3.15** in 72 % yield.[212]

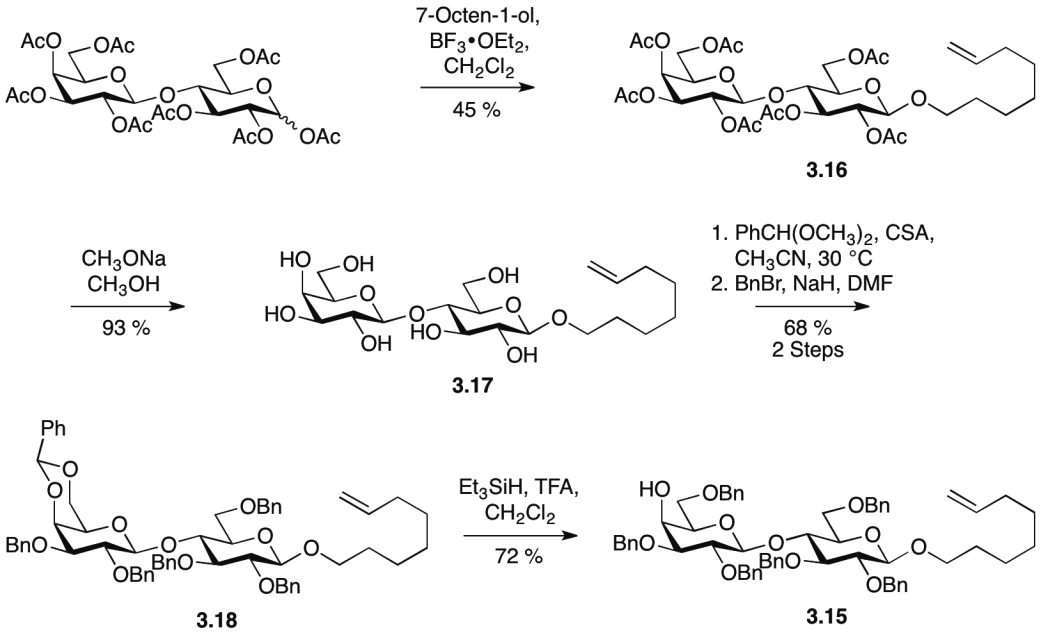

Scheme 3.6. Synthesis of glycosyl acceptor **3.15**.

The formation of the trisaccharide was accomplished by the α(1→4) glycosylation reaction between the trichloroacetimidate donor **3.3** and glycosyl acceptor **3.15** [Scheme 3.7]. Combination of the acceptor and donor in Et_2O and activation with TMSOTf, resulted in the formation of product **3.14** in 91 % yield, exclusively as the α product.

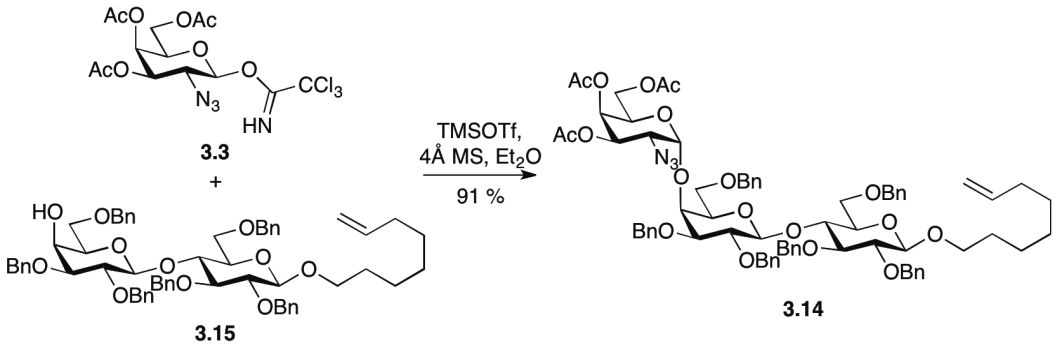

Scheme 3.7. Formation of trisaccharide **3.14**.

The azide of **3.14** was reduced to the corresponding amine using H_2S gas in a solvent mixture of Pyr:water:Et_3N (10:1:0.3) and the amine was subsequently acetylated by treatment with Ac_2O and Pyr to give **3.19** in 74 % yield over two steps [Scheme 3.8].[214] Global deprotection of **3.19** was initiated by the removal of all acetyl protecting groups on the terminal GalNAc moiety using CH_3ONa in CH_3OH to provide **3.20** in 89 % yield. The removal of the remaining benzyl ether protecting groups was achieved *via* Birch reduction using Na in liquid NH_3 while adding **3.20** in a small amount of a THF/CH_3OH solvent mixture at -78 °C. While a Birch reduction could be used in one step for the removal of both types of protecting groups, it was found to be ineffective due to the poor solubility of **3.19** in liquid NH_3. The removal of the acetyl protecting groups was found to be necessary to effectively remove the benzyl ether protecting groups in the subsequent step. As a consequence, the fully deprotected trisaccharide **3.13** was obtained in an uncalculated yield due to the presence of large amounts of salts in the sample. The intermediate **3.13** was therefore carried forward in the synthesis directly [Scheme 3.9].

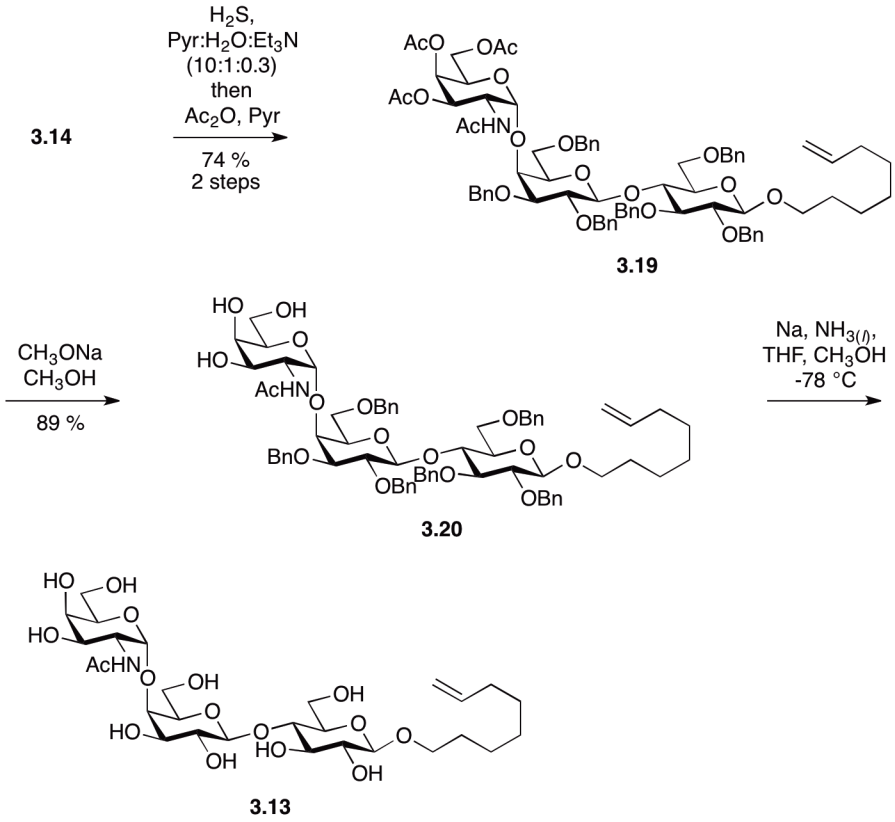

Scheme 3.8. Reduction of azide moiety and global deprotection towards trisaccharide **3.13**.

To conclude the synthesis of P^{k}NAc-BSA, the terminal olefin of the octenyl linker was elaborated to allow for protein conjugation [Scheme 3.9]. Reaction of **3.13** with cysteamine-hydrochloride in water under ultraviolet (UV)-irradiation[221] and subsequent treatment with dibutoxy-3-cyclobutene-1,2-dione under basic conditions afforded the squarate derivative **3.21** in 89 % yield over two steps, ready for conjugation to BSA.[222] The squarate intermediate **3.21** was combined with BSA in a boronate buffer solution to maintain basic (pH 9) reaction conditions and resulted in the formation of the P^{k}NAc-BSA glycoconjugate **3.11**. The units of incorporation of the trisaccharide on the protein were calculated using matrix assisted laser desorption ionization time of flight

(MALDI-TOF) mass spectrometry by comparing the overall mass of conjugated versus non-conjugated protein. The final compound P^{k}NAc-BSA **3.11** was synthesized with 25 units of trisaccharide incorporated onto the surface of the protein.

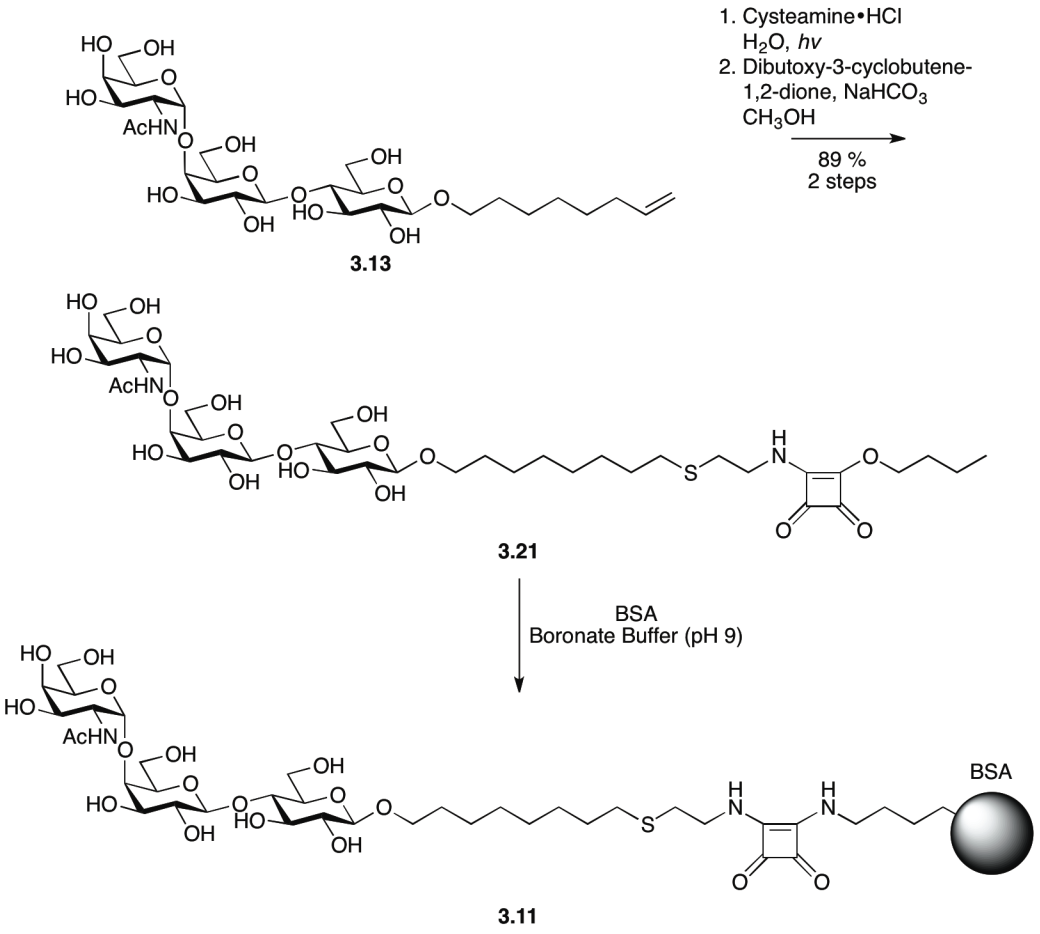

Scheme 3.9. Linker elaboration and protein conjugation for the synthesis of P^{k}NAc-BSA.

3.3.2. The Synthesis of P^k-BSA 3.12

The synthesis of the Stx1 specific Pk-BSA glycoconjugate **3.12** was started with the common intermediate **3.17** from the previous synthesis [Scheme 3.10]. The formation of the trisaccharide framework could be achieved in a

simpler fashion than P^{k}NAc-BSA through the use of the fusion enzyme α(1→4)-galactosyltranferase/UDP-4'-Gal epimerase[208] as was used in the syntheses of (*S*)- and (*R*)-PolyBAIT (Chapter 2). Therefore, the intermediate **3.17** was combined with UDP-Glc in the presence of the fusion enzyme to afford the trisaccharide **3.22** in 92 % yield.

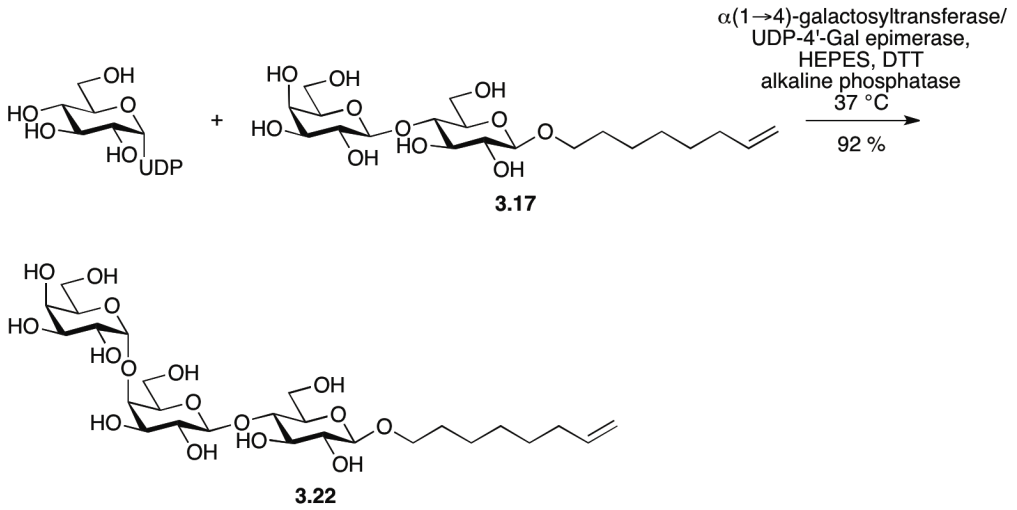

Scheme 3.10. Chemo-enzymatic synthesis of P^k trisaccharide octenyl glycoside **3.22**.

The synthesis of P^k-BSA **3.12** was completed as in Scheme 3.11. The linker of the fully deprotected trisaccharide **3.22** was elaborated by treatment with cysteamine-hydrochloride in water under UV-irradiation.[221] Subsequent reaction of the intermediate amine generated in the previous step with dibutoxy-3-cyclobutene-1,2-dione under basic conditions gave the squarate intermediate **3.23** in 61 % yield over two steps.[222] Lastly, conjugation to BSA was performed by reaction of the squarate **3.23** with BSA in a boronate buffer solution to provide the P^k-BSA glycoconjugate **3.12**. Units of incorporation were calculated using

MADLI-TOF mass spectrometry and the glycoconjugate was found to include 26 units of trisaccharide per BSA.

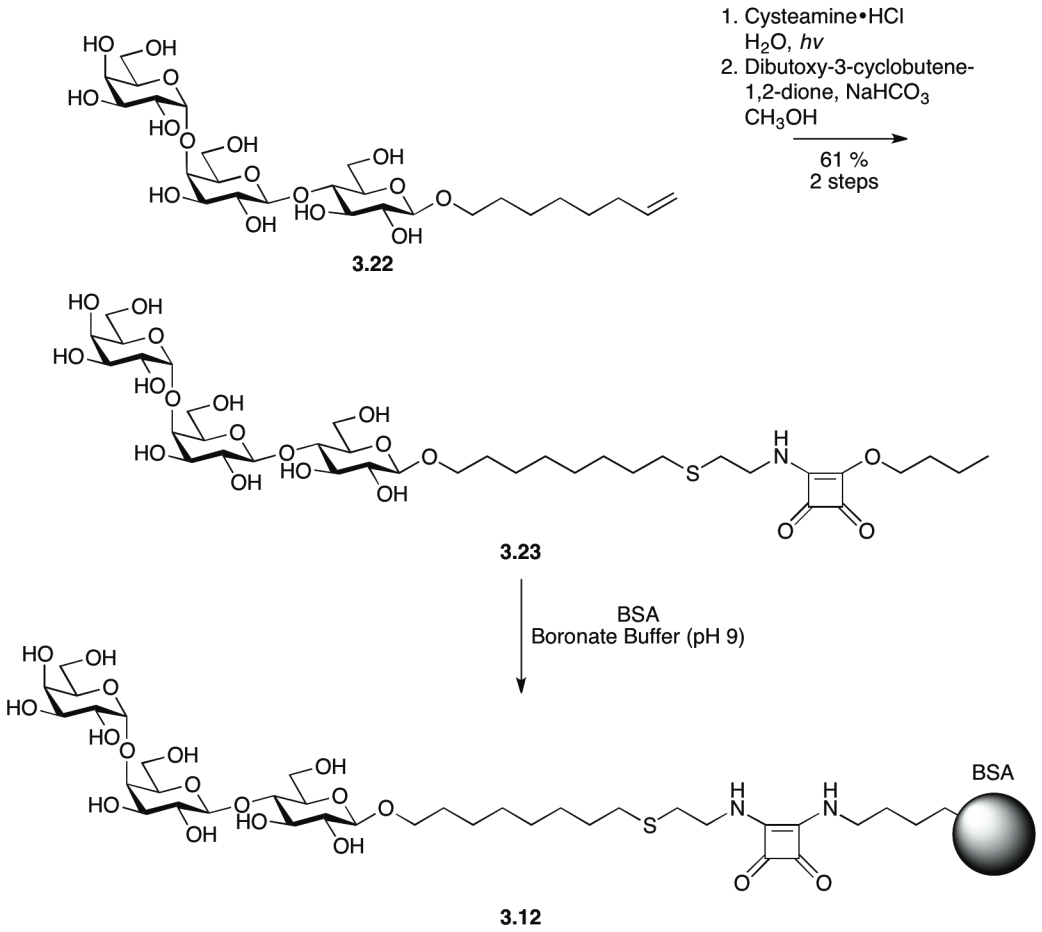

Scheme 3.11. Linker elaboration and protein conjugation for the synthesis of P^k-BSA **3.12**.

3.3.3. ELISA Analysis of Stx Binding

With the two BSA-glycoconjugates synthesized the specificity of Stx1 and Stx2 binding to P^k and P^kNAc ligands was assessed *via* ELISA. The wells of 96-well microtitre plates were coated with either P^kNAc-BSA **3.11** or P^k-BSA **3.12** and varying concentrations of either Stx1 or Stx2 were added to the wells. The

results show that P^kNAc-BSA binds with higher avidity to Stx2 than Stx1 and conversely, P^k-BSA was found to bind Stx1 with higher avidity than to Stx2 [Figure 3.9]. The graph data is expressed in terms of EC_{50}, which is defined as the half-minimal effective concentration for binding.

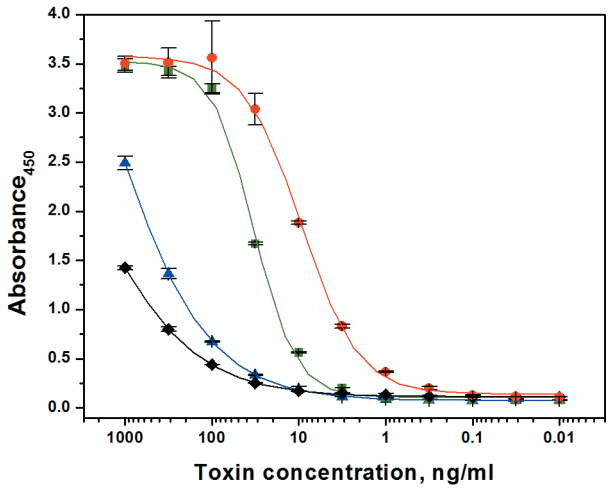

Figure 3.9. Solid-phase binding of Stx1 and Stx2 to microtitre plates coated with glycoconjugates **3.11** or **3.12**. ● :P^kNAc-BSA **3.11** vs. Stx2 (EC_{50} = 9 ng/ml); ▲:P^kNAc-BSA **3.11** vs. Stx1 (EC_{50} = 1660 ng/ml); ◆ :P^k-BSA **3.12** vs. Stx2 (EC_{50} = 2480 ng/ml); ■ :P^k-BSA **3.12** vs. Stx1 (EC_{50} = 33 ng/ml). Error bars represent standard deviations for triplicates.

In addition, attempts to perform competitive inhibition assays with trisaccharides **3.1** and **3.2** failed to register any inhibition of Stx1 or Stx2 binding to the corresponding glycoconjugates on the plate. This was most likely due to the weaker innate affinity of the monovalent ligands to either Stx1 or Stx2, compared to the multivalent interaction on the plate surface.

3.4. Crystal Structure of Stx2 with a Bound Ligand

The previous results in this chapter show that P^kNAc binds preferentially to Stx2 over Stx1 and with greater selectivity than P^k trisaccharide. Our STD NMR results suggest that the relative conformation of P^kNAc binding to Stx2 may be similar to that of P^k binding to Stx1 however these data are not conclusive. There exists the potential that a variety of trisaccharide orientations and conformations may provide the same, if not very similar results obtained from STD NMR analysis. As a consequence we strove to produce a co-crystal structure of Stx2 with a modified P^kNAc derivative to assess the nature of its binding. Two potential synthetic targets were identified for co-crystallization with Stx2. The first is the methyl glycoside of P^kNAc, **3.1**, and the second is a disaccharide derivative of P^kNAc, methyl 2-acetamido-2-deoxy-α-D-galactopyranosyl-(1→4)-β-D-galactopyranoside, **3.24**, [Figure 3.10].

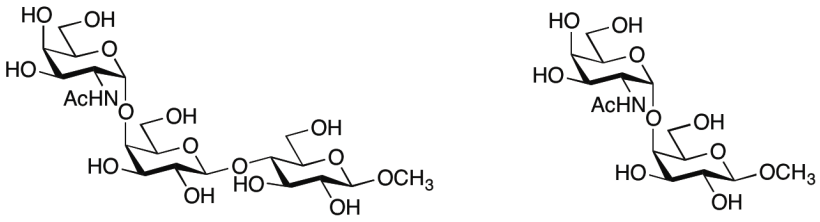

Figure 3.10. Synthetic targets for co-crystallization with Stx2: methyl P^kNAc **3.1** and the methyl 2-acetamido-galabiose derivative of P^kNAc, **3.14**.

3.4.1. The Synthesis of 2-acetamido-2-deoxy-α-D-galactopyranosyl-(1→4)-β-D-galactopyranoside 3.24

The synthesis of disaccharide **3.24** could be synthesized *via* the retrosynthetic scheme, scheme 3.12.

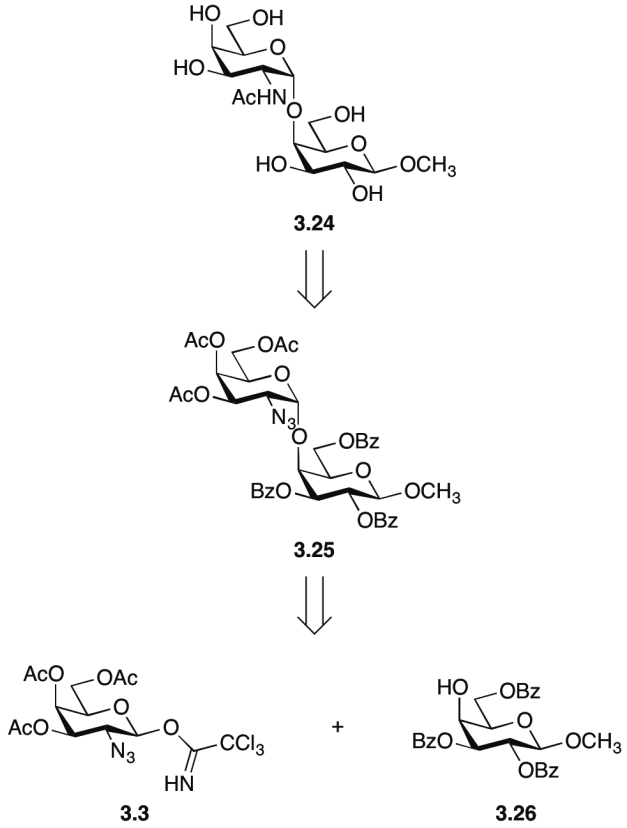

Scheme 3.12. Retrosynthetic scheme for the synthesis of the P^k-like disaccharide derivative **3.24**.

The disaccharide **3.24** can be synthesized from the corresponding, fully protected disaccharide **3.25**, *via* firstly reducing and subsequently acetylating the azido moiety and secondly *via* a series of deprotection manipulations. The disaccharide **3.25** can be synthesized *via* the α(1→4) glycosylation between the

known glycosyl trichloroacetimidate **3.3** and the glycosyl acceptor **3.26**. The glycosyl acceptor **3.26** is obtainable from the commercially available galactose.

The synthesis of the glycosyl donor **3.26** was started with the commercially available β-methyl glycoside of galactose **3.27** [Scheme 3.13]. Installation of the benzylidene moiety was done by reacting **3.27** with α,α-dimethoxytoluene in the presence of CSA in CH_3CN at 30 °C and subsequent treatment with benzoyl chloride (BzCl) and Pyr gave the fully protected galactoside **3.28** in 87 % yield over two steps.[199] Next, the benzylidene was removed *via* acid hydrolysis using 80 % CH_3COOH in water and heating at 80 °C to give the diol **3.29** in 89 % yield.[223] Lastly, the 6-OH was selectively protected by adding one equivalent of BzCl in Pyr at 0 °C to provide the acceptor **3.26** in 71 % yield.[224]

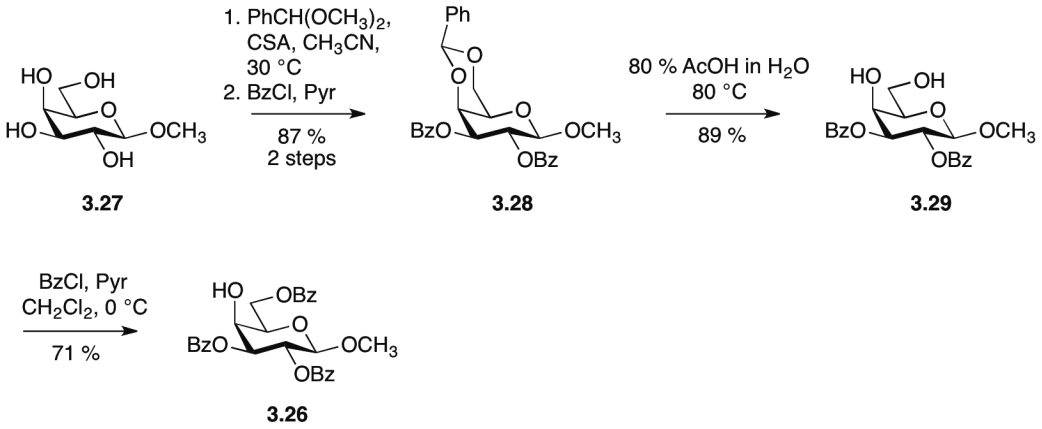

Scheme 3.13. The synthesis of glycosyl acceptor **3.26**.

Construction of the disaccharide was achieved *via* the α(1→4) glycosylation between trichloroacetimidate donor **3.3** and the glycosyl acceptor **3.26** [Scheme 3.14]. The glycosylation reaction was done using TMSOTf as the activator under anhydrous conditions in Et_2O to provide the disaccharide **3.25** in 48 % yield as an inseparable mixture of isomers (6:1, α:β).

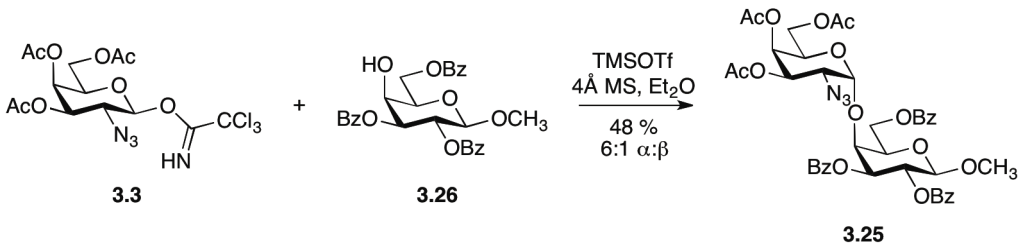

Scheme 3.14. Synthesis of disaccharide **3.25**.

As the glycosylation reaction yielded an inseparable mixture of isomers, a small amount was carried forward in the proposed scheme to determine if a later step in the synthesis would allow for resolution. Therefore, reduction of the azide in **3.25** was performed using $Pd(OH)_2$ on carbon in CH_3OH and the resulting amine was acetylated using Ac_2O in Pyr [Scheme 3.15].[225] After purification and isolation of the primary spot identified by TLC, only the α-product was obtained. The 2-acetamido intermediate **3.30** was obtained in 72 % yield over two steps. Lastly, global deprotection of **3.30** was performed using CH_3ONa in CH_3OH to give the desired **3.24** in 89 % yield.

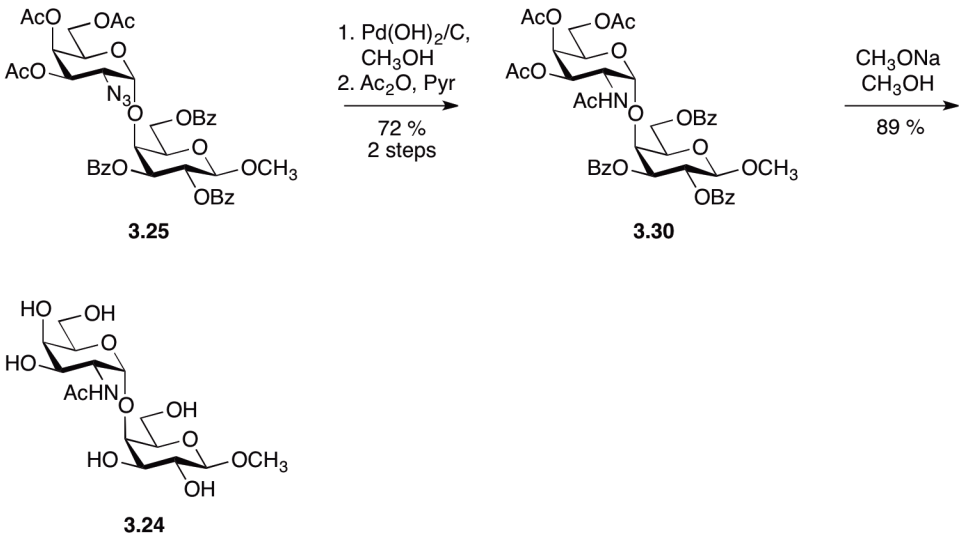

Scheme 3.15. Completion of disaccharide **3.24**.

3.4.2. The Crystal Structure of Stx2 with Bound Ligand

Stx2 was co-crystallized with P^kNAc disaccharide methyl glycoside **3.24** [Figure 3.11] and the structure of the complex was determined by X-ray crystallography [Chapter 6, Table 6.1] in collaboration with Dr. Michael James and Dr. Jiang Yin at the University of Alberta. Based on previous work, both in the literature and stated in this chapter, site 2 is the primary binding site in Stx2.[79,130,136,218]

The structure of the Stx2-**3.24** complex aligned very well to that of the *apo* Stx2 (PDB entry 1R4P)[146] holotoxin with an r.m.s.d. of 0.4 Å over 624 C^{α} atoms. Two molecules of **3.24** were found to bind to two distinct sites in Stx2 in the asymmetric unit [Figure 3.11 and Figure 3.12b]. For the residues making contacts with **3.24** (distance < 4 Å), the r.m.s.d. is 0.1 and 0.2 Å for sites 1 and 2, respectively. This suggests that little conformational change in Stx2 is required

for the binding of disaccharide **3.24**. Similar conclusions could be drawn from the structures of the *apo* (PDB codes 1C48, 1CQF, 1DM0)[77] and P^k-MCO-bound Stx1 (PDB code 1BOS) solved by Ling *et al*.[78] (MCO: *O*-methoxycarbonyl octane), which is hardly surprising given the high sequence identity between the protein sequences of the two families of AB_5 toxins.

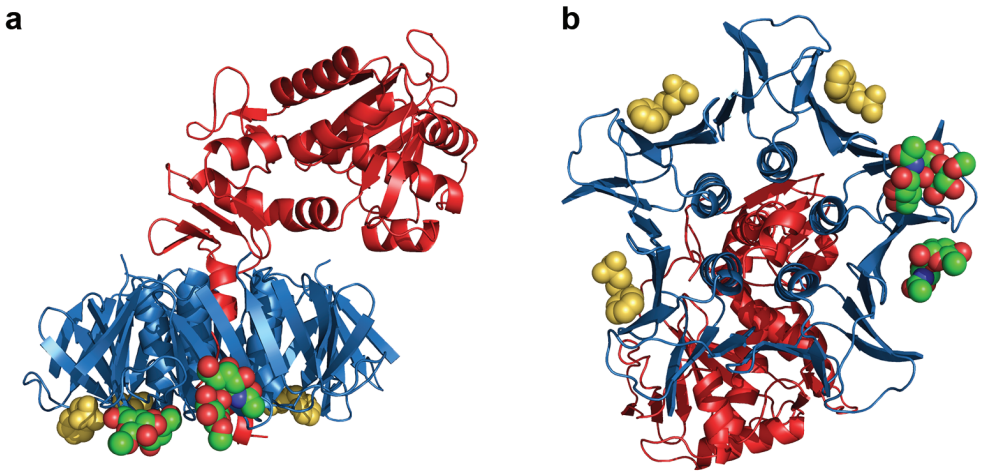

Figure 3.11. Stx2-**3.24** crystal structure. (a) and (b): Side and bottom profiles of the newly acquired Stx2-**3.24** crystal structure. The A subunit is colored red and the B5 pentameric subunit is colored blue. The carbon, oxygen and nitrogen atoms of **3.24** are colored green, red, and blue respectively. The three molecules of PPS (3-(1-pyridinio)-1-propanesulfonate) are colored yellow.

The $Stx1B_5$-P^k-MCO complex shows there exist three distinct carbohydrate-binding pockets per B protomer of the B_5 pentamer: site 1 is formed within each protomer, whereas sites 2 and 3 involve residues from two adjacent protomers [Figure 3.12a]. Although the binding sites are lined with identical or similar amino acid residues in Stx1 and Stx2, compound **3.24** in the Stx2-**3.24**

complex occupied only two of the fifteen potential sugar-binding sites [Figure 3.11b].

The lack of carbohydrate binding to the remaining sites could be attributed to a variety of reasons: (a) steric hindrance from the C-terminus of the A subunit of the holotoxin protruding from the central hole in the B_5 pentamer; (b) presence of another small ligand used as a crystallization additive; (c) conformational changes in key residues forming the binding site (Trp33); and (d) crystal packing [Chapter 6, Table 6.2].

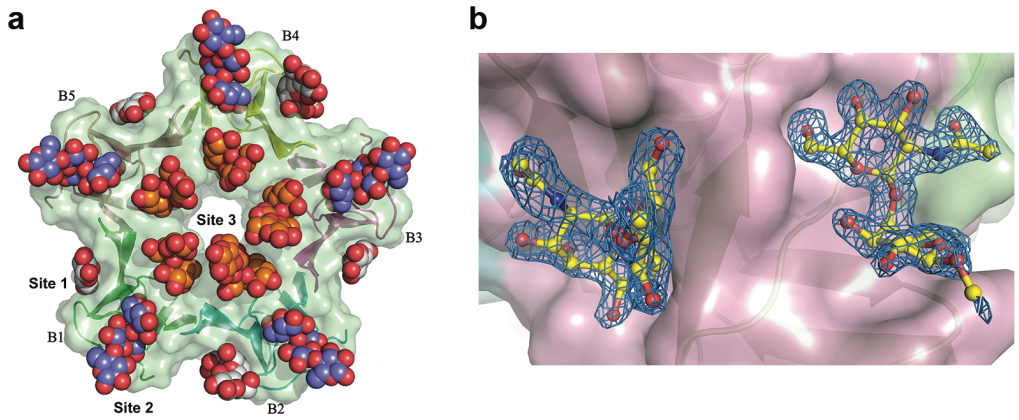

Figure 3.12. Binding sites of Stx1 and the Stx2-**3.24** complex. (a) The Stx1B_5-P^k-MCO complex. The five B subunits are named B1 through B5. The bound carbohydrates are shown as spheres with oxygen and nitrogen atoms colored red and blue, respectively; the carbon atoms of the carbohydrate ligands bound in sites 1, 2 and 3 are colored in grey, slate, and gold, respectively. (b) The contoured electron density surrounding the bound disaccharide methyl glycoside **3.24** in sites 1 (left) and 2 (right) of Stx2. Neighboring B subunits are shown in different colors and the oxygen, nitrogen and carbon atoms of **3.24** are colored red, blue and yellow, respectively. Figures provided by Dr. Jiang Yin, University of Alberta.

Binding of carbohydrate ligands to site 2 in Stx2 involves more polar and van der Waals contacts than those occurring between P^k-MCO and Stx1 and those occurring between compound **3.24** and Stx2 at site 1. Site 2 consists of residues Trp29, Ser31, Arg32, Ser53, Ser54, Thr55, Gly61, Phe62, Ala63 of B5 and Glu15 from the neighboring B1 subunit. The binding modes of compound **3.24** and P^k-MCO in site 2 are similar and the two small molecule ligands are virtually superimposable in the structurally aligned Stx2 and Stx1 [Figure 3.13]. Arg32, that forms bifurcated H-bonds with O3 and the acetyl oxygen of GalNAc, adopts very similar conformations in the Stx1-P^k-MCO and Stx2-**3.24** complexes. However, in contrast to site 1, there are significant differences between the site 2 of Stx1 and Stx2 in addition to the substitution of Phe30 by Trp29. The residues in Stx1 that are equivalent to Glu15, Ser31, Ser54 and Thr55 in Stx2 are Asp16, Asn32, Asn55, and Ala56, respectively. The change from Glu15 (Stx2) to Asp16 (Stx1) seems most relevant.

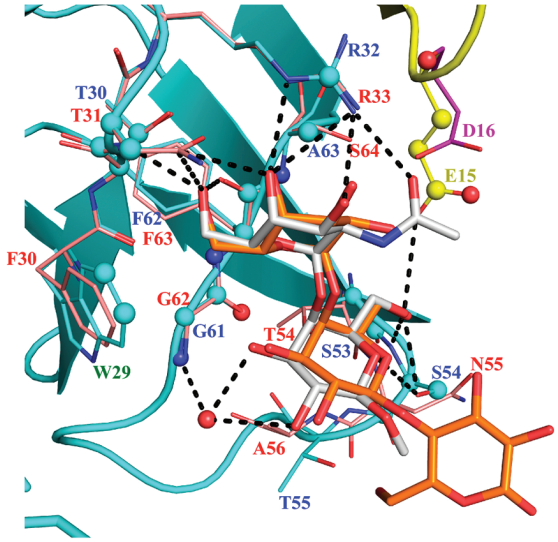

Figure 3.13. Interactions between Stx2 and **3.24** at site 2. A solvent molecule bridging the interactions between Gal and Gly61 in Stx2-**3.24** complex is shown as a red sphere. Those atoms in Stx2 within van der Waals contact distance (4 Å) from the disaccharide ligand **3.24** are shown as spheres. The aligned complexes of Stx2-**3.24** and $Stx1B_5$-P^k-MCO (r.m.s.d. 0.5 Å over 292 C^α atoms) are distinguished by the carbon atoms colored in cyan and salmon in one B subunit and in yellow and purple in the adjacent B subunit, respectively. The bound carbohydrate ligands (thick sticks), the interacting protein residues (thin sticks). Grey and orange colored carbon atoms distinguish compound **3.24** and P^k-MCO, respectively. The solvent molecules bridging the interactions between Stx2 and **3.24** are shown as red spheres. Hydrogen bonds are depicted in black dashed lines for the Stx2-**3.24** complexes, respectively. Figure provided by Dr. Jiang Yin, University of Alberta.

In the $Stx1B_5$-P^k-MCO complex, the side chain carboxylate $O^{\delta 1}$ oxygen of Asp16 accepts a 2.8 Å H-bond from O2 of Gal; its location would most likely lead to a destabilizing short contact (1.5 Å) with the carbonyl oxygen if the 2-substituent is present as an *N*-acetyl function. A stereo view of binding is presented in Figure 3.14. On the other hand, the side chain of Glu15 in the Stx2-**3.24** complex points away from the bound GalNAc moiety and forms a weak H-

bond (3.4 Å) with O6 of Gal, that in turn forms an H-bond (2.8 Å) with the O^{γ} of Ser54; both of these interactions have no counterparts in the $Stx1B_5$-P^k-MCO complex.

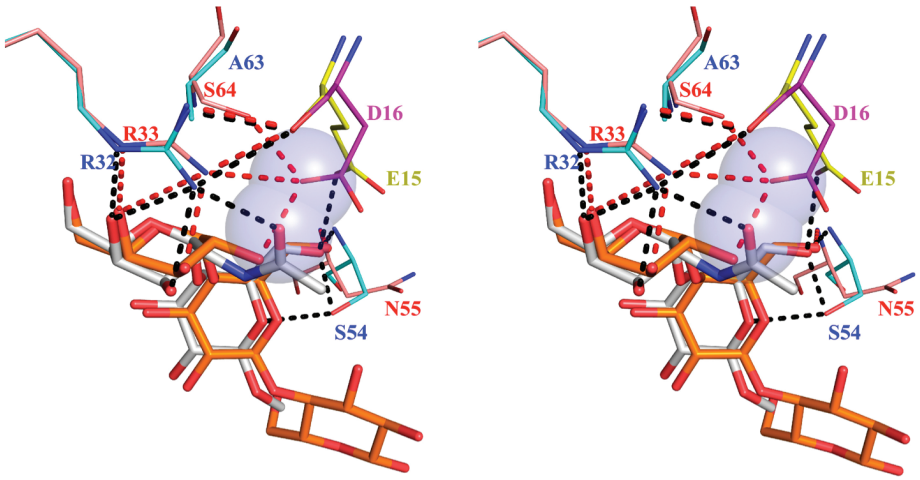

Figure 3.14. A stereogram of the NAc-specificity determinant in site 2 of Stx2. The Stx2-**3.24** and $Stx1B_5$-P^k-MCO complexes are colored as described in Figure 3.13. The semi-transparent spheres show the van der Waals radii of the two oxygen atoms in short contact in a hypothetical $Stx1B_5$-P^k-NAc complex at site 2

The major difference in the conformation of these two acidic residues lies in the placement of their side chains: the χ1 torsion angle of Glu15 (Stx2a) adopts a *gauche* (-) conformation (-76 °) and the equivalent angle for Asp16 (Stx1) adopts a *trans* conformation (-172 °). If the side chain of Asp16 (Stx1) were to take on a *gauche* (-) conformation as observed for that of Stx2 Glu15, its side chain carboxylate would fall short of making contact with the 6-OH of Gal in a bound P^kNAc-like ligand. It is interesting to note that the respective conformations of these two residues are preserved in all presently available

crystal structures of Stx1 and Stx2 toxins with either ligand-bound or unoccupied site 2. In particular, Asp16 of Stx1 is "locked" in the observed conformation through its interactions with Ser64 and Arg33; the main chain carbonyl of Asp16 accepts two H-bonds from the guanidino group of Arg33, and O of Ser64 donates an H-bond to O^{γ} of Asp16 that receives another H-bond from Arg33. The residue in Stx2 equivalent to Ser64 in Stx1 is Ala63, thus only the H-bonds between $O^{\delta 1}$ of Glu15 and the guanidino group of Arg33 are conserved between Stx1 and Stx2.

Another residue in site 2, Ser31 in Stx2 vs. Asn32 in Stx1, may also play a role in the preferential binding of carbohydrate ligands by these two Shiga toxins. Flagler *et al.* showed that point mutations N32S in Stx1 and S31N in Stx2, residues that share the same approximate location in the binding sites, resulted in a reversal of selectivity: P^{k}NAc showed preferential binding to the mutated Stx1, whereas P^{k} preferentially bound to mutated Stx2.[226] However, the proposition that steric hindrance between an asparagine residue at this position and GalNAc might prevent the binding of P^{k}NAc to site 2 alone, is not convincingly supported by this newly acquired structural data. Furthermore, Stx2e, a Shiga toxin causing edema in pigs, has a preference for GalNAc albeit possessing an asparagine at the equivalent position.[63] In site 2 of Stx2, Ser31 is situated across the binding pocket for GalNAc opposing Glu15; a similar orientation between Asn32 and Asp16 is observed in the binding pocket for Gal in site 2 of Stx1. Because GalNAc has a larger molcular size than Gal, the distances between amino acid residues at positions 31 and 15 in Stx2 (and those at 32 and 16 in Stx1) may serve to regulate

the substrate specificity for Shiga toxins. Taken together, this indicates that residues Glu15 and Ser31 of Stx2, and likewise, residues Asp16 and Asn32 of Stx1, may collectively determine ligand specificity in site 2.

Binding site 1 in Stx2 consists of residues Lys12, Asn14, Asp16, Thr18, Thr20, Glu27, Trp29, and Gly59, all of which are conserved in Stx1 except for Trp29, which is substituted by Phe30. The interactions between disaccharide **3.24** and the residues constituting Stx2 site 1 are similar to those observed between P^k-MCO and $Stx1B_5$; GalNAc is bound at the "bottom" of site 1 and Gal packs against the aromatic rings of Trp29 or Phe30 [Figure 3.15].

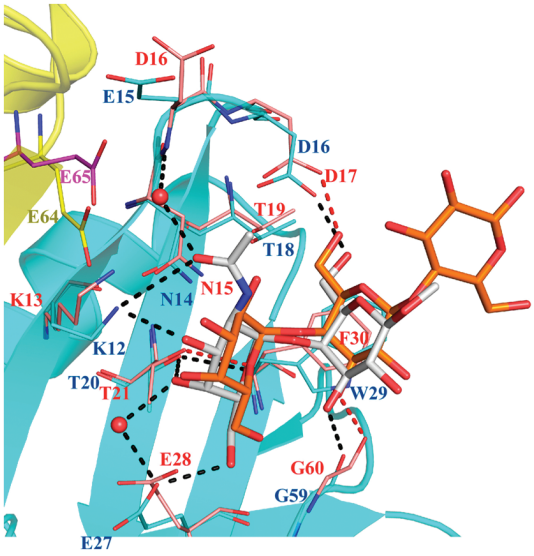

Figure 3.15. Interactions between Stx2 and **3.24** at site 1. The Stx2-**3.24** and $Stx1B_5$-P^k-MCO complexes are colored as described in Figure 3.13. Figure provided by Dr. Jiang Yin, University of Alberta.

The carbonyl oxygen of the *N*-acetyl moiety of compound **3.24** receives a weak H-bond from the ε-amino group of Lys12 and is also involved in a solvent-

bridged polar interaction with the backbone amide nitrogen of Glu15. Compound **3.24** makes more contacts with the residues of site 1 of Stx2 (51 interactions within 4 Å) than those between the corresponding disaccharide in P^k-MCO and Stx1 (37 interactions within 4 Å), however, this may not directly translate into differences in binding affinity as the strengths of these interactions have not been taken into account. Altogether, site 1 may not contribute significantly to the different affinities of Stx1 and Stx2 towards P^k and P^kNAc.

3.5. Conclusions

In this chapter, the design and synthesis of an Stx2 specific ligand, Methyl-P^kNAc **3.1** was described. To further understand the nature of binding to Stx2 proteins, STD NMR was performed using Methyl-P^kNAc **3.1** and Methyl-P^k **3.2** and of the NMR spectra suggests that the binding of ligands to Stx2 occurs in a similar fashion to binding to Stx1. In addition, the monovalent binding affinity of Methyl-P^kNAc **3.1** to Stx2 was determined to be K_a = 4.5 x 10^2 M^{-1} in collaboration with Dr. John Klassen of the University of Alberta.

The design and synthesis of two BSA-glycoconjugates was described, P^kNAc-BSA, **3.11** and P^k-BSA, **3.12**. Their ability to bind Stx2 was investigated using ELISA. The results show that there is a preference for Stx2 to bind P^kNAc-BSA over P^k-BSA and for Stx1 to bind P^k-BSA preferentially over P^kNAc-BSA.

Lastly, an X-ray crystal structure of Stx2 was obtained with a bound disaccharide ligand **3.24** in collaboration with Dr. Jiang Yin and Dr. Michael James at the University of Alberta. Analysis of the structure showed good agreement with previously solved structures of Stx2. The bound ligand **3.24** was found in two binding sites of the toxin, one ligand was in site 2 and the other in site 1. From the structure, it would appear that site 2 is the primary binding site of Stx2 as the number of contacts formed between the ligand and protein is greater is site 2 than site 1. The addition of the *N*-acetyl moiety to the ligand introduces more hydrogen bond interactions to Arg32 potentially contributing to the greater affinity of 2-acetamido derivatives of P^k trisaccharide to Stx2. Structural analysis also showed that Glu15 may confer selectivity in P^kNAc binding to Stx2. The conformation of the Glu15 side chain allows for a hydrogen bond to O6 of Gal which in turn also interacts with Ser54. Both of these interactions are unique to Stx2 and are not found in Stx1.

Chapter 4

Multivalent Heterobifunctional Ligands for the Sequestering of Stx2

4.1. Introduction

Shiga toxins produced by the bacterium *E. coli* O157:H7 cause hemolytic uremic syndrome. Stx2 has been found to be the predominant toxin responsible for the development of HUS,[227] therapeutic strategies that target Stx2 specifically may be beneficial in preventing or ameliorating the disease. In earlier chapters, examples were given of previous attempts to develop Stx1 and Stx2 inhibitors, specifically inhibitors of toxin binding Gb_3 on the cell surface (Chapter 2). However, all of the examples represent P^k trisaccharide from Gb_3 being presented in various multivalent formats. A disadvantage of this approach is the even weaker affinity of P^k trisaccharide towards Stx2 when compared to the already very low affinity of Stx1 (Chapter 3).

The BAIT/PolyBAIT approach that allowed us to neutralize Stx1 by creating an Stx1-HuSAP supramolecular complex held together by heterobifunctional ligands, is crucially dependent on HuSAP interacting preferentially with the heterobifunctional ligand.[135,206] Unfortunately, the Armstrong group has shown that HuSAP interacts with Stx2 in the absence of

BAIT-type ligands.[228] Consequently the *in vitro* and *in vivo* testing of any Stx2 preferred ligands becomes impossible. However, Armstrong and coworkers were able to show that HuSAP-tg mice could be rendered susceptible to Stx2 if the mice were treated with LPS.[229] The role of LPS in HUS pathogenesis has not, as yet, been clearly established. However previous studies have suggested that LPS increases the lethal effects of Stx2 by inducing a pro-inflammatory response, observable in renal tissue.[229] As a consequence of these results, the development of an Stx2 specific ligand may offer a solution to the lack of activity displayed by the Stx1 specific (*S*)-PolyBAIT **2.1**. In this chapter, the syntheses of Stx2 specific ligands, PolyBAIT-P^{k}NAc and PolyBAIT-*di*NAc will be discussed. The *in vitro* and *in vivo* analysis of PolyBAIT-P^{k}NAc will also be presented.

4.2. Synthetic Target

Based on the work of Kale *et al.*[147] and earlier investigations done by the Bundle group (Chapter 3), we hypothesized that incorporation of a terminal 2-acetamido-2-deoxy galactose moiety into an (*S*)-PolyBAIT-type derivative, could provide the means to sequester Stx2 specifically [Figure 4.1]. This ligand, coined PolyBAIT-P^{k}NAc **4.1**, incorporates the necessary P^{k}NAc trisaccharide component for binding to Stx2, as well as the cyclic pyruvate acetal required for binding to HuSAP.

In addition, much like in (*S*)-PolyBAIT (Chapter 2), the incorporation of a suitable linker that would allow for conjugation to a polymeric scaffold. The

description of the synthesis has been previously published and has been modified in the following sections.[230]

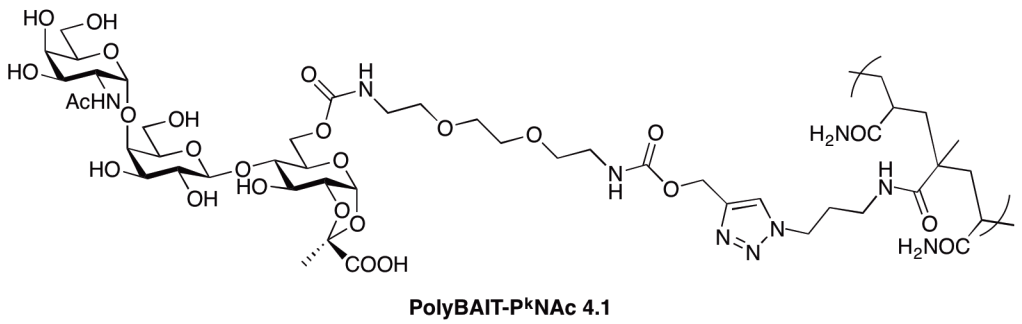

Figure 4.1. Structure of PolyBAIT-P^{k}NAc, **4.1**.

4.2.1. Retrosynthetic Analysis of PolyBAIT-P^{k}NAc 4.1

A retrosynthetic analysis of **4.1** requires the incorporation of four essential components [Scheme 4.1]; a linker **4.5** that allows for conjugation to a polymeric scaffold and three monosaccharide building blocks, **3.3**, **4.6**, and **2.7**.

The synthesis of **4.1** may be accomplished *via* a Cu-catalyzed [3+2]-Huisgen cycloaddition[231,232] reaction between BAIT-P^{k}NAc, **4.2** and the previously synthesized poly[acrylamide-co-(3-azidopropylmethacrylamide)][233] **4.3**. The monomeric BAIT-P^{k}NAc **4.2** can be synthesized *via* coupling of the amine linker **4.5** and a P^k trisaccharide derivative obtainable from **4.4**. The P^k trisaccharide derivative **4.4** can be made *via* the glycosylation between thioglycoside donor **4.6** and the previously synthesized acceptor **2.7**, which after glycosylation with trichloroacetimidate donor **3.3** provides the P^k trisaccharide derivative **4.4**. In contrast to the synthesis of (*S*)-PolyBAIT **2.1**, the synthesis of

PolyBAIT-P^{k}NAc could not be achieved *via* the use of enzymes to form the α(1→4) glycosidic linkage. As a consequence, careful chemical consideration was taken into account to provide protecting groups that would be orthogonal and easily removed when necessary.

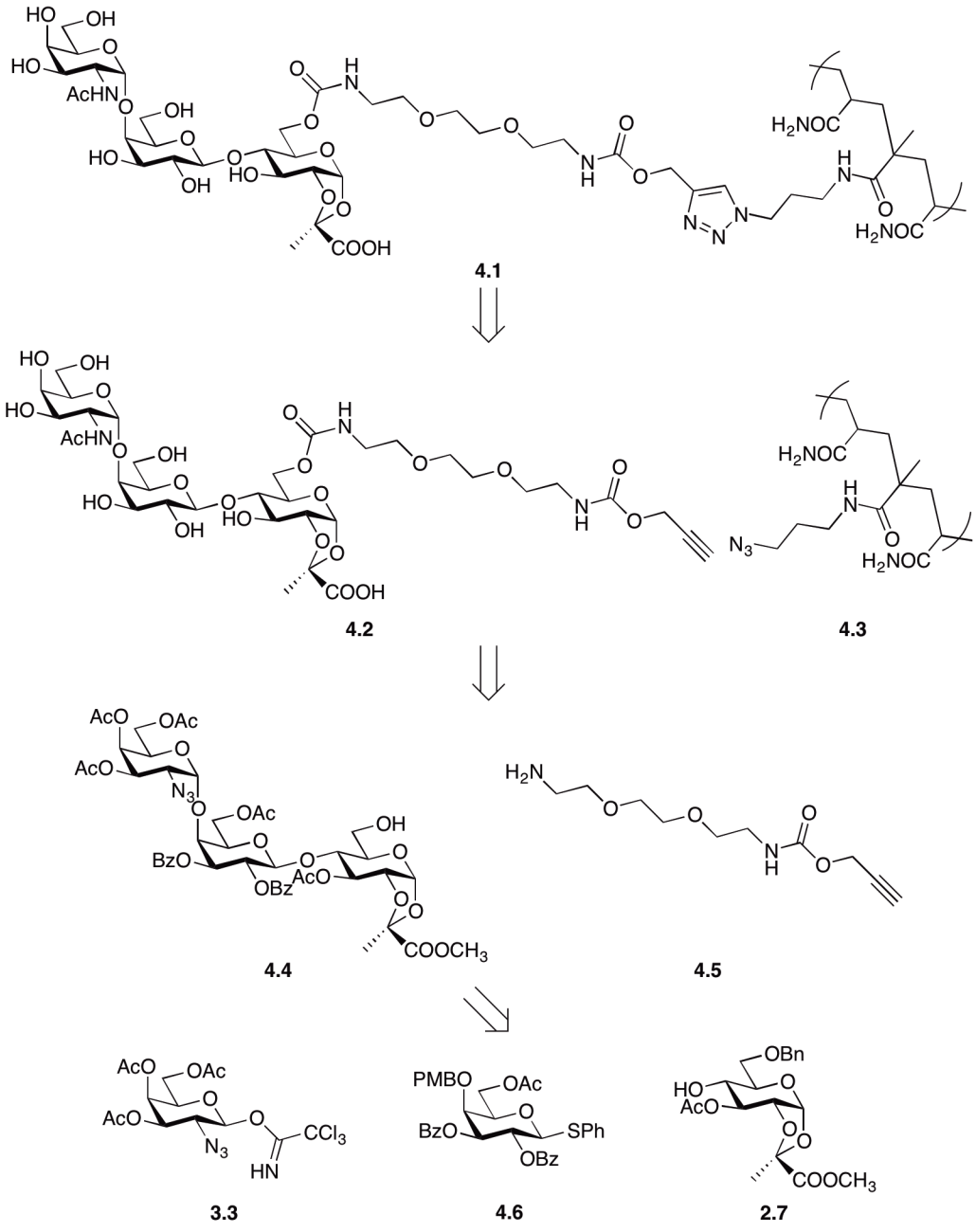

Scheme 4.1. A retrosynthetic analysis of PolyBAIT-P^{k}NAc **4.1**.

4.2.2. Synthesis of PolyBAIT-P^{k}NAc 4.1

The synthesis of the acceptor **2.7** was previously described in Chapter 2 [Scheme 2.13].

The synthesis of the thiophenyl galactoside donor **4.6** was achieved through the synthesis of the known thiogalactoside **4.8** from the peracetylated derivative **4.7** using CH_3ONa in CH_3OH to give **4.8** in 97% yield [Scheme 4.2].[234] The deprotected galactoside **4.8** was treated with the dimethyl acetal of *p*-anisaldehyde and CSA to provide a *para*-methoxybenzylidene intermediate which was subsequently treated with BzCl in Pyr to provide the intermediate **4.9** in 88 % over two steps.[199] The *para*-methoxybenzylidene acetal of **4.9** was regioselectively opened using borane tetrahydrofuran complex (BH_3•THF) and TMSOTf to provide the 6-OH, 4-*O*-*p*-methoxybenzyl intermediate which was subsequently acetylated to provide **4.6** in 84 % yield over two steps.[235]

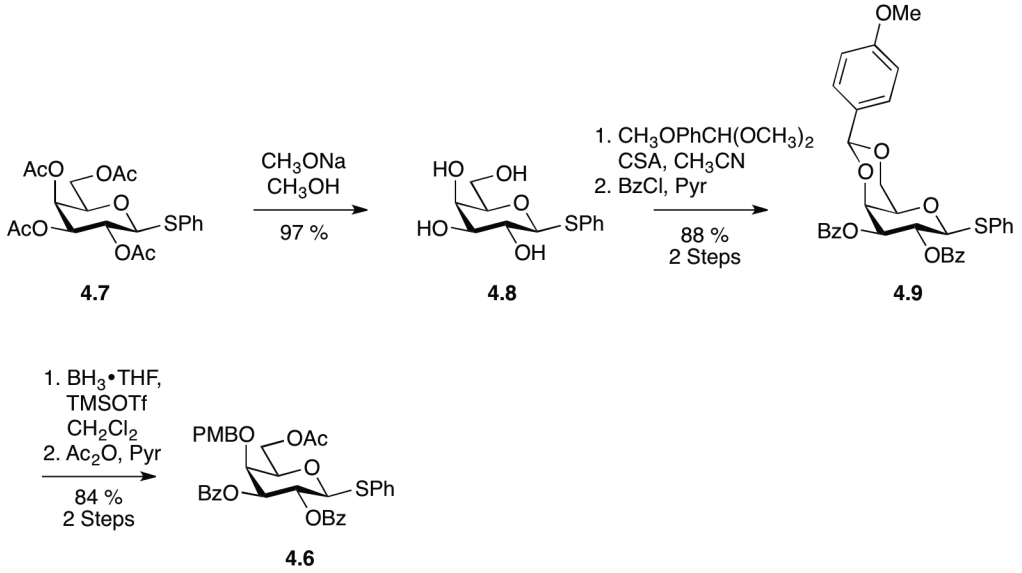

Scheme 4.2. The synthesis of thioglycoside donor **4.6**.

The synthesis of the disaccharide acceptor was accomplished by glycosidation of thiophenyl donor **4.6** and the glucosyl acceptor **2.7** using NIS and AgOTf at -20 °C to give the lactosyl derivative β-product **4.10** selectively in 90 % yield [Scheme 4.3]. The selective deprotection of the 4'-OPMB ether was done by addition of one equivalent of TfOH at -20 °C to give the lactosyl 4'-OH acceptor **4.11** in 81 % yield.

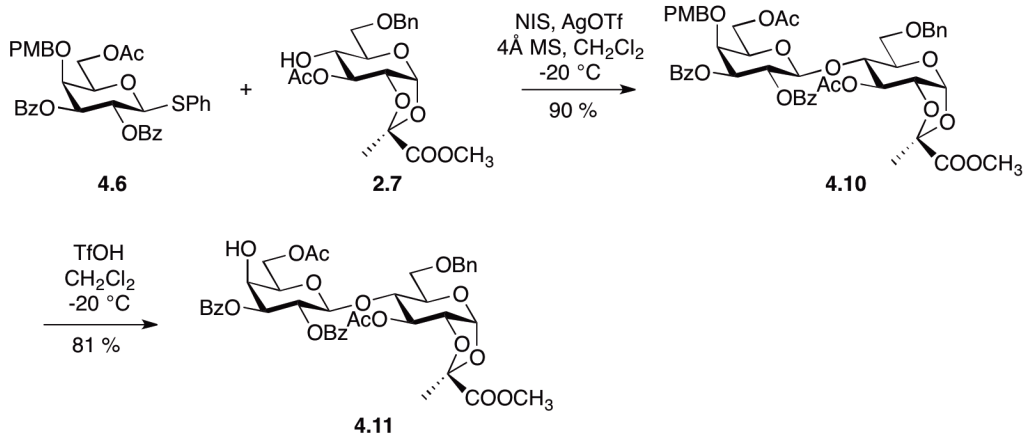

Scheme 4.3. The synthesis of lactosyl acceptor **4.11**.

Glycosylation of acceptor **4.11** with known trichloroacetimidate donor **3.3**[210] was performed using TMSOTf in Et_2O at room temperature to provide the trisaccharide **4.4** in a modest 48 % yield [Scheme 4.4]. Decomposition of the donor was observable before the formation of the glycosidic linkage and often resulted in no yield of the product. This problem was circumvented by the slow drop-wise addition of donor to a mixture of acceptor and activator.[213]

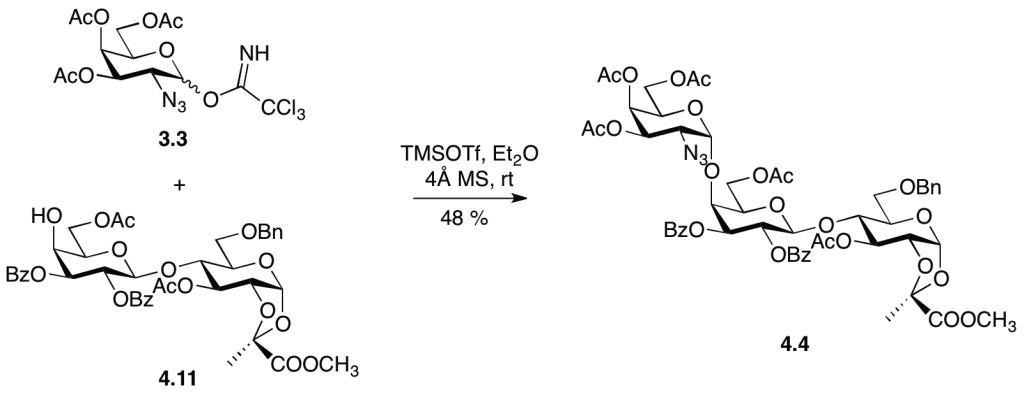

Scheme 4.4. Glycosylation reaction to form trisaccharide intermediate **4.4**.

To prepare the ligand for linker incorporation, the azide of **4.4** was reduced using dithiothreitol (DTT) in a solvent mixture of CH_3CN and Et_3N (6:1) [Scheme 4.5].[236] Subsequent addition of Ac_2O and Pyr to acetylate the intermediate amine provided the 2-acetamido-2-deoxy intermediate **4.12** in 87 % yield over two steps.

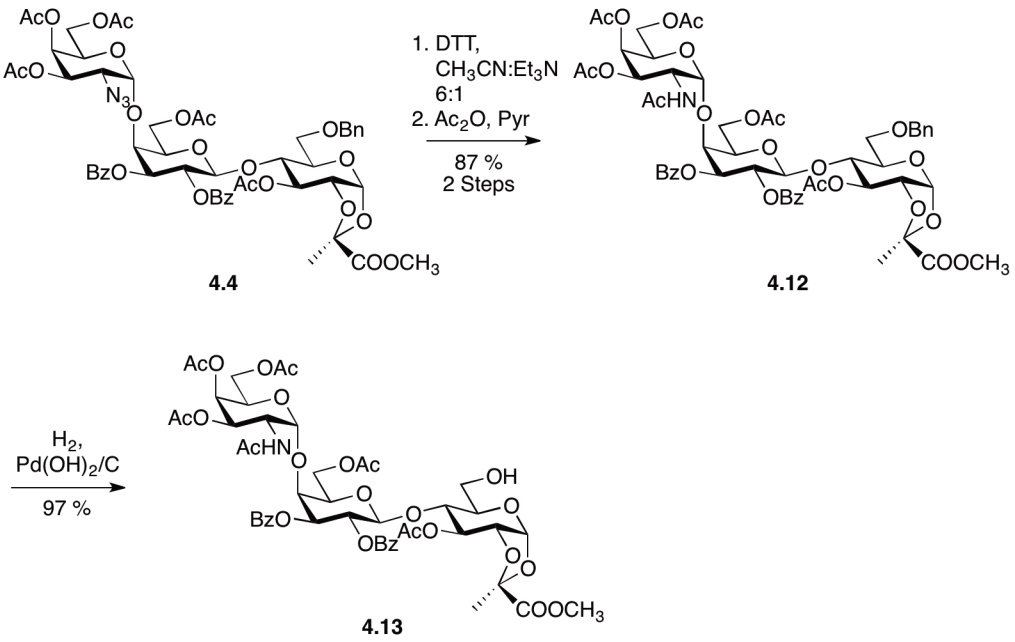

Scheme 4.5. The synthesis of pre-linker addition intermediate **4.13** from glycosylation product **4.4**.

Installation of the linker moiety was achieved by the reaction of the 6-OH of **4.13** with 4-nitrophenyl chloroformate **4.16** in the presence of Pyr to make the 4-nitrophenyl carbonate **4.14** in 99 % yield [Scheme 4.6]. Subsequent treatment of **4.14** with amine **4.5** under basic conditions gave **4.15** in 95 % yield. Global deprotection of **4.15** was achieved through the use of one equivalent of 1M CH_3ONa in CH_3OH to remove acyl protecting groups. Subsequent treatment with water, converted the methyl ester of the cyclic pyruvate moiety to the carboxylic acid to form **4.2** in 88 % yield.

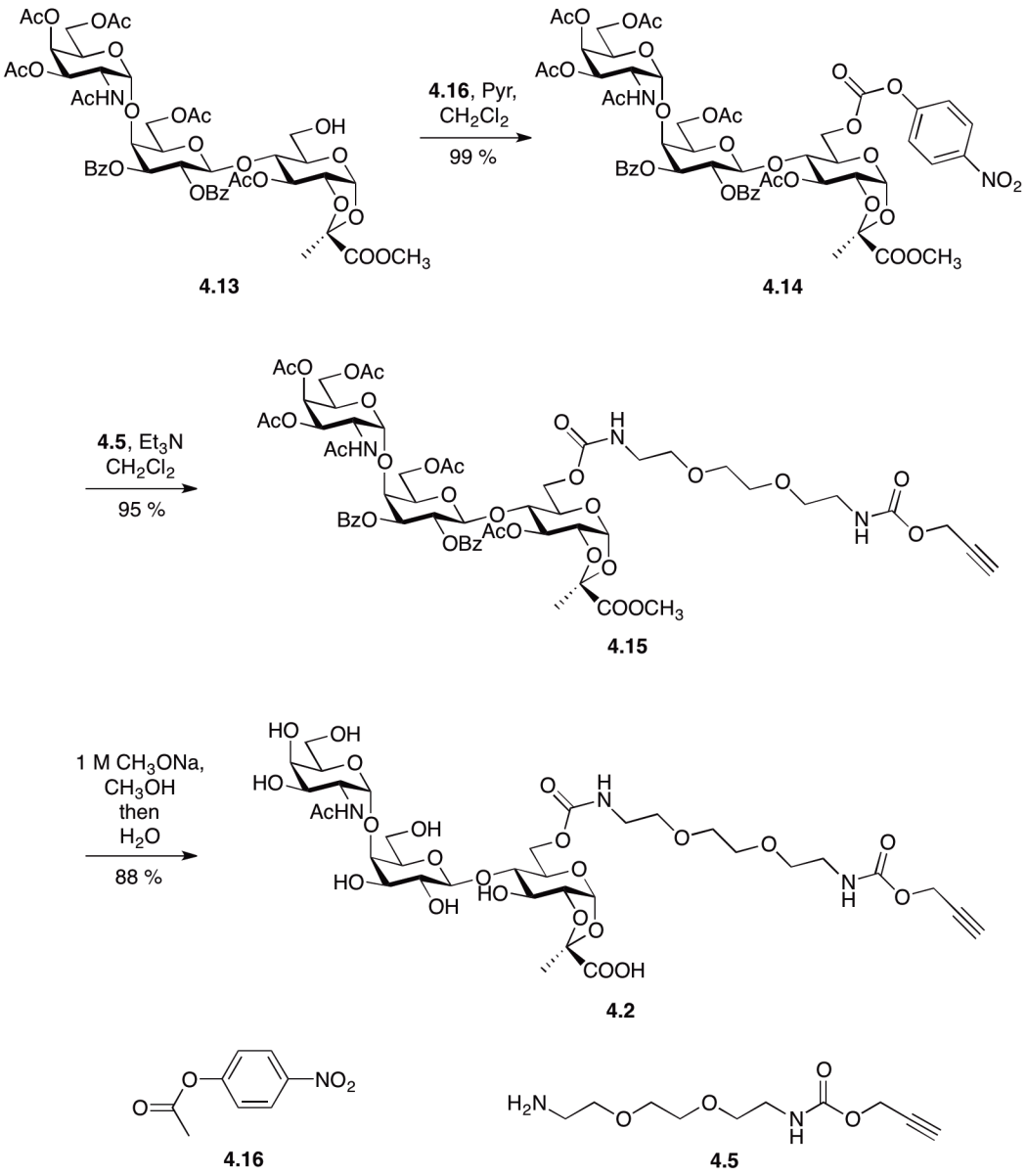

Scheme 4.6. Linker addition to intermediate **4.13** and subsequent global deprotection for the synthesis of BAIT-P^{k}NAc **4.2**.

Lastly, intermediate **4.2** or BAIT-P^{k}NAc was conjugated to the previously synthesized poly[acrylamide-co-(3-azidopropylmethacrylamide)],[233] **4.3** *via* a Cu-catalyzed [3+2]-Huisgen cycloaddition strategy to provide the desired PolyBAIT-P^{k}NAc **4.1** [Scheme 4.7].[231,232]

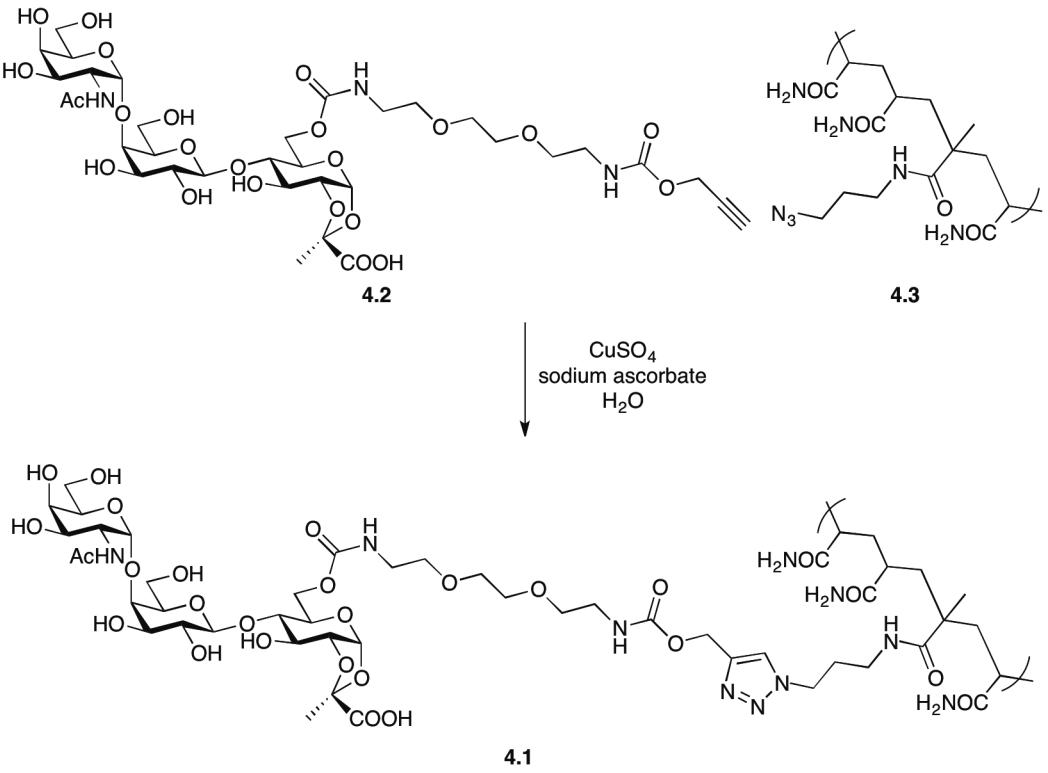

Scheme 4.7. Conjugation of BAIT-P^{k}NAc **4.2** to a polyacrylamide backbone to form PolyBAIT-P^{k}NAc **4.1**.

4.2.3. *In vitro* evaluation of PolyBAIT-P^{k}NAc 4.1

With the final compound **4.1** in hand, efforts were undertaken to evaluate its potential to bind to and inhibit Stx2 *in vitro*.

The first strategy employed to investigate the ability of PolyBAIT-P^{k}NAc to bind Stx2 was performed *via* ELISA analysis. Employing the use of the P^{k}NAc-BSA glycoconjugate synthesized in chapter 3, a preliminary competitive binding assay was performed. The protocol initially used, was adopted from previous studies for (*S*)-PolyBAIT.[135,206] P^{k}NAc-BSA was used to coat the plates and a pre-mixed solution of Stx2 and HuSAP was added to the wells. Following

which, varying concentrations of PolyBAIT-P^{k}NAc was added to the wells. Unfortunately, no results were obtained utilizing this procedure. Further literature investigations provided a rationale as to why this protocol was unsuitable for Stx2 investigation. Kimura *et al.*[237] previously discovered that HuSAP is a potent binder to Stx2 and therefore pre-mixing HuSAP and Stx2 formed a HuSAP-Stx2 complex to which PolyBAIT-P^{k}NAc could not compete for binding. The interaction between HuSAP and Stx2 was once thought to be a potential treatment strategy for Stx2 infection, however it failed to protect mice challenged with a lethal dose of Stx2 *in vivo*.[228]

As a consequence of this finding, an investigation of the binding potential of HuSAP to Stx2 and PolyBAIT-P^{k}NAc's potential inhibition of this process was done. Two experiments were performed. The first experiment used P^{k}NAc-BSA coated plates and measured the ability of HuSAP to bind to Stx2 without PolyBAIT-P^{k}NAc present. In the second experiment, P^{k}NAc-BSA was used to coat the plates; and varying concentrations of PolyBAIT-P^{k}NAc was premixed with variable concentrations of HuSAP and added to the wells. After which, Stx2 was added and the ability of HuSAP to bind Stx2 was assessed. Considering the first procedure [Figure 4.2a], HuSAP was able to bind to Stx2 with an observed IC_{50} of 94 ng/ml. In the second procedure, the inhibitory activity of HuSAP in the presence of PolyBAIT-P^{k}NAc gave an observed IC_{50} of 364 ng/ml [Figure 4.2b].

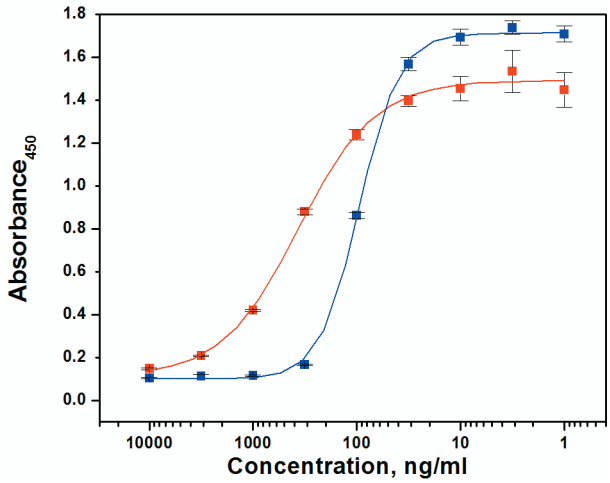

Figure 4.2. Solid-phase binding inhibition assay results. Blue: HuSAP vs. Stx2 binding assay. Red: HuSAP vs. Stx2 competitive binding assay with a fixed concentration of PolyBAIT-P^{k}NAc.

This data suggests that the introduction of PolyBAIT-P^{k}NAc **4.1** interferes with and inhibits the interaction of HuSAP with Stx2. A comparison of the relative IC_{50}'s shows that the introduction of PolyBAIT-P^{k}NAc **4.1** reduces HuSAP's ability to bind Stx2 by a factor of four. As a result, the analysis of the heterobifunctional ligand PolyBAIT-P^{k}NAc is not possible using ELISA as establishing its inhibitory potential cannot be distinguished from the naturally occuring Stx2-HuSAP interaction. However, it is important to note that these results are not indicative of PolyBAIT-P^{k}NAc's ability to induce supramolecular complex formation and as such other methods need to be investigated.

PolyBAIT-P^{k}NAc **4.1** was next tested *in vitro* utilizing Stx sensitive Vero cells but unfortunately, these results were once again complicated by the Stx2-HuSAP interaction and failed to provide results.

4.2.4. *In vivo* analysis of PolyBAIT-P^{k}NAc 4.1

Based on the work done by Griener *et al*. it was hypothesized that HuSAP-tg mice pre-exposed to LPS may still benefit from treatment with PolyBAIT-P^{k}NAc.[229] Consequently, PolyBAIT-P^{k}NAc **4.1** was tested in a modified HuSAP-tg mouse model of disease that ablated the Stx2-HuSAP interaction. HuSAP-tg mice pre-exposed to lipopolysaccharide (LPS) are no longer protected against the toxicity of Stx2 [Figure 4.3]. Introduction of an Stx2 specific ligand, PolyBAIT-P^{k}NAc established a dose dependent inhibition by selectively binding to Stx2. HuSAP-tg mice (C57BL/6-Tg(APSC)1Imeg) treated I.P. with a lethal dose of Stx2 (225 pg/g mouse) combined with *E. coli* O55 LPS (300 ng/g mouse) were immediately given increasing intravenous concentrations of (*S*)-PolyBAIT **2.1** or PolyBAIT-P^{k}NAc **4.1**.

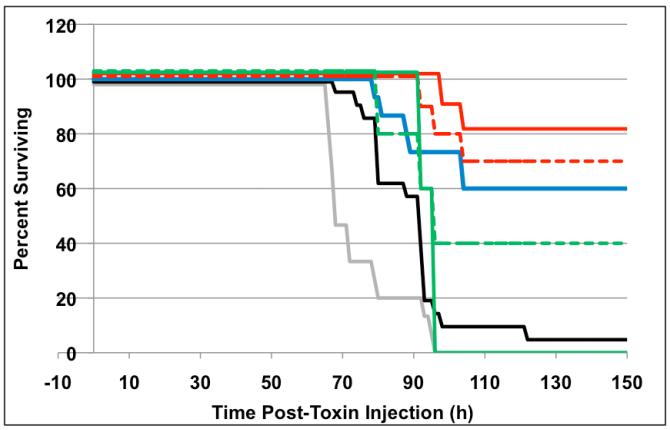

Figure 4.3. Survival graph for *in vivo* mouse model of disease after challenge with a lethal dose of Stx2.

——— :Wild-type mice, Stx2 and O55 LPS, N=15;

——— :Stx2, O55 LPS and HuSAP, N=21;

——— :Stx2, O55 LPS, HuSAP and (*S*)-PolyBAIT **2.1** (100 mg/g), N=15;

——— :Stx2, O55 LPS, HuSAP and PolyBAIT-P^{k}NAc **4.1** (100 mg/g), N=11;

- - - - : Stx2, O55 LPS, HuSAP and PolyBAIT-P^{k}NAc **4.1** (31.5 mg/g), N=10;

- - - - : Stx2, O55 LPS, HuSAP and PolyBAIT-P^{k}NAc **4.1** (10 mg/g), N=5;

——— : Stx2, O55 LPS, HuSAP and PolyBAIT-P^{k}NAc **4.1** (3.15 mg/g), N=5.

N represents the number of HuSAP trangenic mice used for each set of experiments.

Non-transgenic mice and HuSAP-tg mice pre-treated with Stx2 and LPS, but not (*S*)-PolyBAIT **2.1** or PolyBAIT-P^{k}NAc **4.1**, succumbed to infection within 100 hr post injection. Mice treated with (*S*)-PolyBAIT showed modest signs of protection albeit with approximately 60% of mice surviving over the course of the experiment. In contrast, HuSAP-tg mice receiving PolyBAIT-P^{k}NAc **4.1** at two concentrations (100 mg/g or 31.5 mg/g mouse) showed over 80% survival over 150 hr. The difference in protection between (*S*)-PolyBAIT **2.1** and PolyBAIT-P^{k}NAc **4.1** can be attributed to selective binding of PolyBAIT-P^{k}NAc to Stx2. The lowest effective concentration of PolyBAIT-P^{k}NAc was 31.5 mg/g mouse. In previous studies it was shown that (*S*)-PolyBAIT **2.1** protects HuSAP-tg mice

against Stx1 at concentrations approximately ten fold lower (3.15 mg/g mouse) but treatment with (*S*)-PolyBAIT **2.1** at a concentration as high as 100 mg/g mouse afforded only modest protection against Stx2 infection.[206]

It is highly unlikely the protective effect of PolyBAIT-P^{k}NAc **4.1** in LPS-sensitized HuSAP transgenic mice is indirectly related to anti-inflammatory activity induced by pre-treatment with LPS other than its ability to form supramolecular complexes involving HuSAP and Stx2. This is because the analogous (*S*)-PolyBAIT **2.1** protects HuSAP transgenic mice from Stx1-mediated Shigatoxemia in the absence of inflammation. This is only possible due to the ability of (*S*)-PolyBAIT to coordinate the formation of supramolecular complexes involving HuSAP and Stx1 because HuSAP does not bind to and neutralize Stx1 *in vitro* or *in vivo.*[206]

The ability of **4.1** to protect HuSAP-tg mice after a lethal dose of Stx2 establishes that P^{k}NAc modified Gb_3 analogs may potentially be lead compounds for the development of more active inhibitors of Stx2. This represents the first report of an effective inhibitor, based on structural evidence, for the clinically more relevant toxin (Stx2) involved in *E. coli* O157:H7-mediated HUS.

When considering potential strategies for the implementation of PolyBAIT-P^{k}NAc **4.1** as a therapeutic agent, it can be observed that the therapeutic potential of PolyBAIT-P^{k}NAc in preventing HUS from developing in

E. coli O157:H7-infected subjects may be quite limited after these individuals present in the Emergency Room with HC. This is not to say, however, that administration of PolyBAIT-P^{k}NAc **4.1** or another suitable compound to these patients would not ameliorate the spectrum of HUS symptoms thereby shortening time-to-recovery and possibly the long-term sequelae of the condition.

Moreover, it is well established that, due to the low infectious dose, person-to-person spread of the infection is quite common in sporadic occurrences of *E. coli* O157:H7 or other EHEC serotypes.[238] It is not unreasonable to suggest, that a prophylactic application, such as that evaluated in the LPS-sensitized HuSAP-tg mouse experiments presented here, to individuals at risk for developing the infection could be beneficial, especially in large outbreak situations like the 2011 *E. coli* outbreak O104:H4 in Germany.[239,240]

4.3. 2nd Generation Ligand for Stx2

Based upon the previously acquired crystal structure of the disaccharide **3.24** and Stx2 complex, the synthesis of a disaccharide based heterobifunctional ligand was performed. Crystal structure and STD NMR analysis suggests that the glucose moiety of P^k trisaccharide derivatives does not play an important role in binding. Therefore, the synthesis of PolyBAIT-*di*NAc **4.17** was hypothesized to be another potential inhibitor of Stx2 [Figure 4.4].

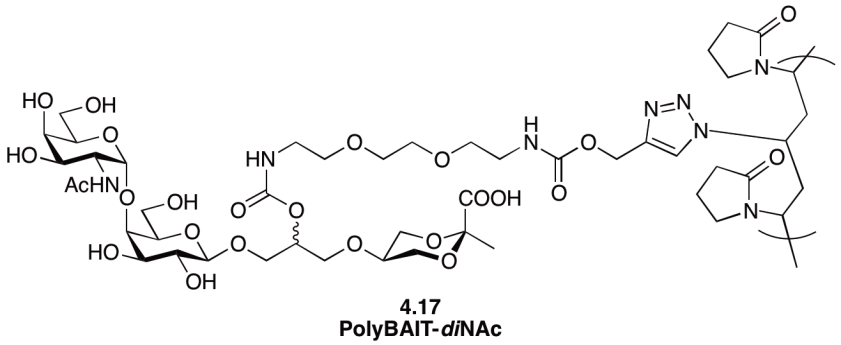

Figure 4.4. Structure of PolyBAIT-*di*NAc **4.17**.

4.3.1. The synthesis of PolyBAIT-*di*NAc 4.17

A retrosynthetic analysis of **4.17** is presented in Scheme 4.8.

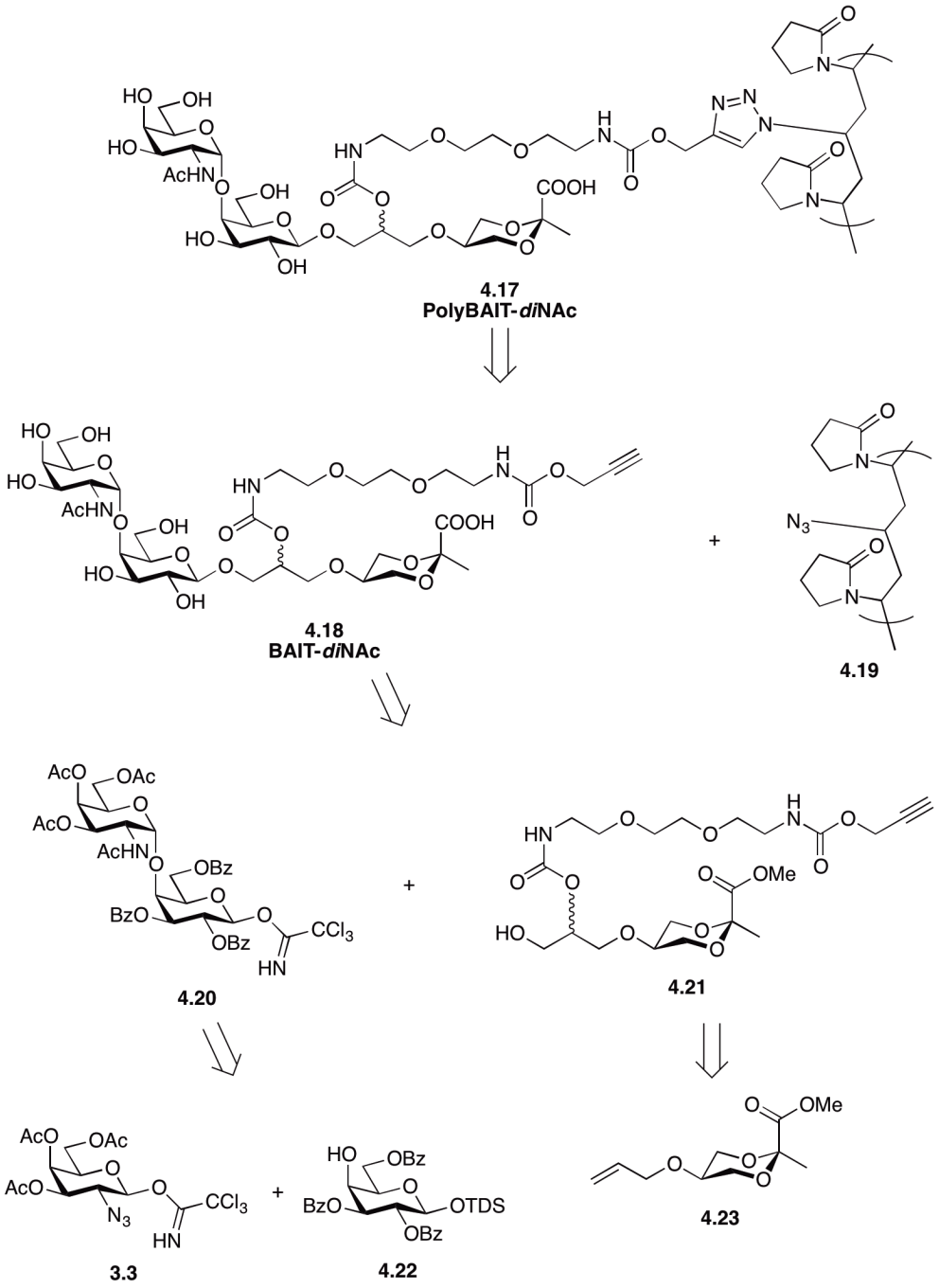

Scheme 4.8. Retrosynthetic analysis of PolyBAIT-*di*NAc **4.17**.

The synthesis of **4.17** can be achieved *via* the coupling of a suitable monomeric ligand **4.18** with an azido povidone polymer *via* a Cu-catalyzed [3+2]-Huisgen cycloaddition. The synthesis of the monomeric heterobifunctional ligand

4.18 can be accomplished *via* the convergent synthesis of a disaccharide trichloroacetimidate donor **4.20** and the linker modified glycosyl acceptor **4.21**. The disaccharide **4.20** can be synthesized from two monosaccharide building blocks, the 2-azido-2-deoxy-galactopyranosyl trichloroacetimidate **3.3** and a suitably protected galactosyl acceptor **4.22**. Lastly, the synthesis of **4.21** is obtainable from the simple methyl ester **4.23**.

The synthesis of intermediate **4.23** was achieved by reaction of the bicyclic lactone **4.24**[241] with 40% dimethyl amide under aqueous conditions and subsequent treatment with AllBr and NaH provided the dimethyl amide **4.25** in 37 % yield over two steps.[242] Treatment of **4.25** with sodium hydroxide facilitated the conversion of the dimethyl amide to the corresponding carboxylic acid, which after treatment with $SOCl_2$ formed the methyl ester **4.23** in 46 % yield over two steps.

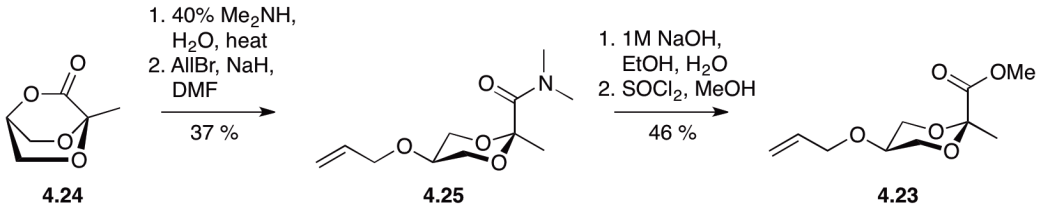

Scheme 4.9. The synthesis of intermediate **4.23**.

The cyclic methyl ester **4.23** was treated with OsO_4 and NMO in acetone and water to dihydroxylate the allyl olefin and the diol intermediate **4.26** was synthesized in 97 % yield.[243] Subsequent treatment of the primary hydroxyl group of **4.26** with TBDPSCl and Et_3N selectively silylated the primary hydroxyl group

to provide **4.27** in 73 % yield.[204] Introduction of the linker moiety was done as in the previous synthesis of PolyBAIT-P^{k}NAc, the secondary hydroxyl of **4.27** was treated with 4-nitrophenyl chloroformate **4.16** under basic conditions. Subsequently the addition of the propargylated amine **4.5** resulted in the formation of **4.28** in 93% yield over two steps. Lastly, the removal of the TBDPS silyl ether was accomplished *via* the addition of HF-Pyr to **4.28** to provide the glycosyl acceptor **4.21** in 83 % yield.[205]

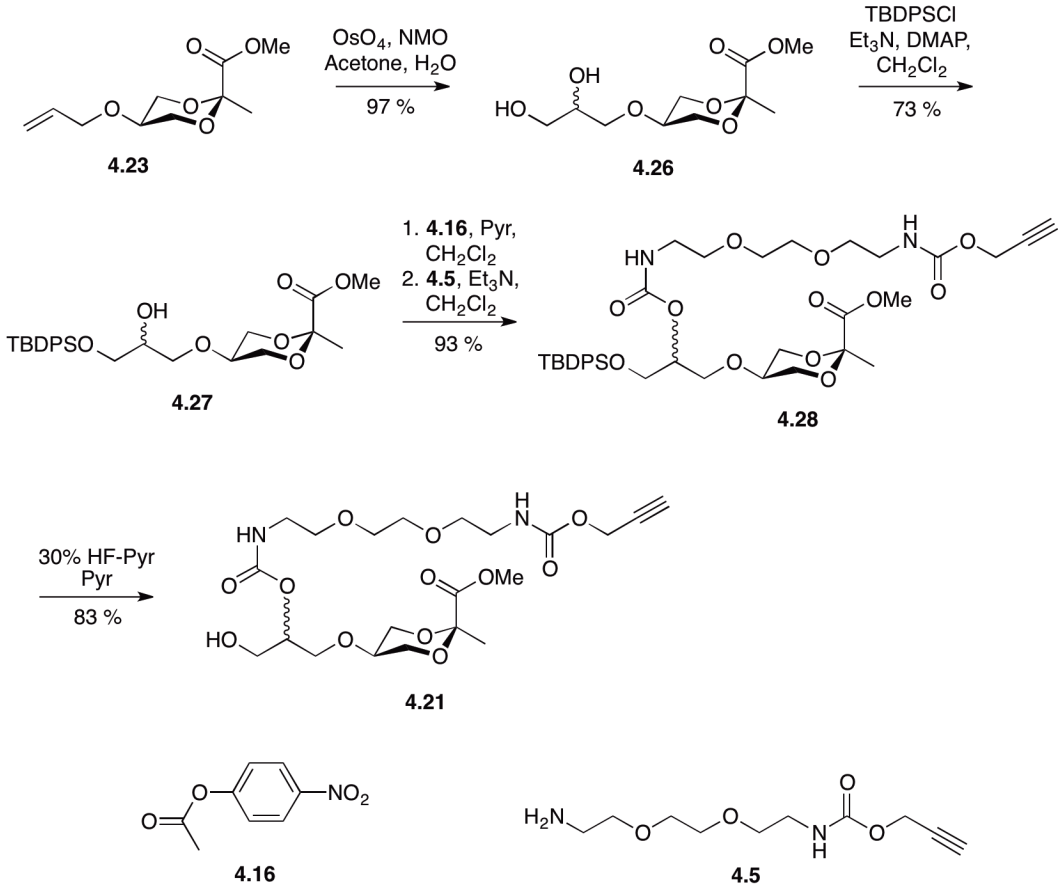

Scheme 4.10. The synthesis of aglycon **4.21**.

The synthesis of the disaccharide donor was initiated *via* the synthesis of the acceptor **4.22** [Scheme 4.11]. Protection of the anomeric hydroxyl as a (dimethyl)thexylsilyl (TDS) ether was achieved by treatment of **4.19** with TDSCl and imidazole to provide exclusively the β product **4.3**0 in 95 % yield.[244] The removal of the acetyl protecting groups on **4.30** was accomplished by reaction with CH_3ONa in CH_3OH at -20 °C.[244] The low temperatures were found to be necessary and in accordance with previously established methods to avoid the migration of the TDS ether to the 2-OH position. Subsequent workup of the deacetylation reaction and treatment with α,α-dimethoxytoluene and CSA resulted in benzylidene formation.[199] Lastly, the addition of BzCl and Pyr resulted in the benzoylation of 2- and 3-OH providing the intermediate **4.31** in 76 % yield over three steps. Removal of the benzylidene acetal of **4.31** was removed by reaction with 80 % CH_3COOH under reflux to provide **4.32** in 64 % yield.

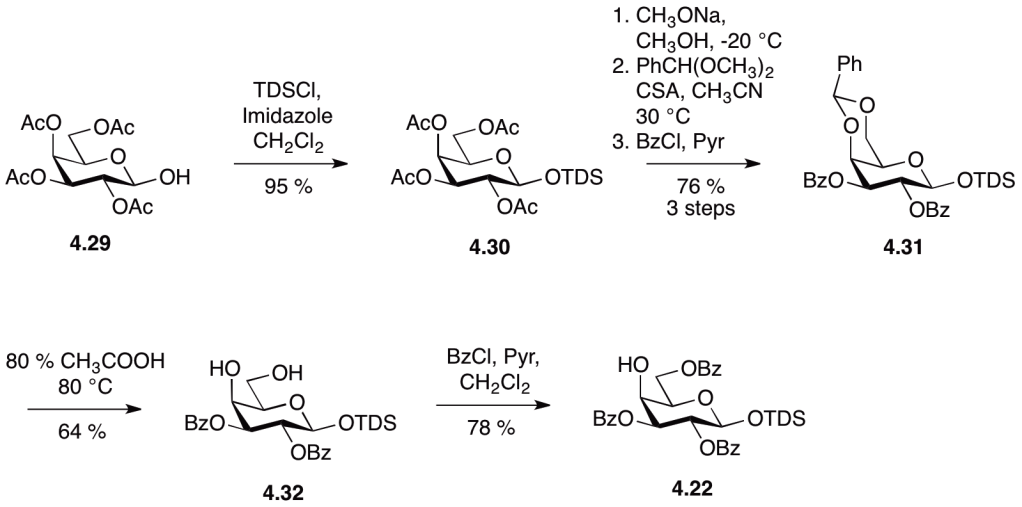

Scheme 4.11. The synthesis of glycosyl acceptor **4.22**.

The selective protection of the 6-OH of **4.32** was done by treatment with one equivalent of BzCl in the presence of Pyr to provide **4.22** in 78 % yield.

The glycosylation between acceptor **4.22** and the 2-azido-2-deoxy-galactopyranosyl donor **3.3** was performed by activation of a mixture of both **4.22** and **3.3** with TMSOTf at -20 °C in CH_2Cl_2 [Scheme 4.12]. The disaccharide **4.33** was synthesized exclusively as the α-product in 97 % yield.

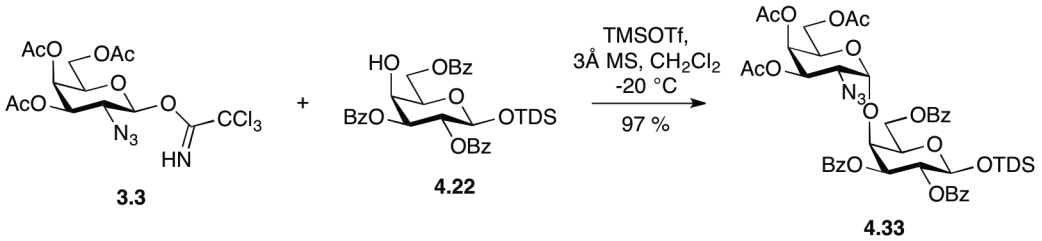

Scheme 4.12. Glycosylation reaction between donor **3.3** and acceptor **4.22** to form disaccharide **4.33**.

Following the glycosylation reaction, the disaccharide was further elaborated before coupling to the linker moiety **4.21**. The azide of **4.33** was reduced using DTT in a solvent mixture of CH_3CN:Et_3N (6:1) and the intermediate amine subsequently acetylated to created the 2-acetamido-2-deoxy disaccharide intermediate **4.34** in 86 % yield [Scheme 4.13].[236] The anomeric TDS ether was removed by treatment of **4.34** with 33 % HF-Pyr in THF to provide the free sugar **4.35** in 71 % yield as a mixture of isomers (3:1, α:β).[205] Lastly, the disaccharide donor **4.20** was formed by treatment of the free sugar

4.35 with Cl_3CCN and K_2CO_3 to form the trichloroacetimidate donor **4.20** in 81 % yield as a mixture of isomers (1.5:1, α:β).

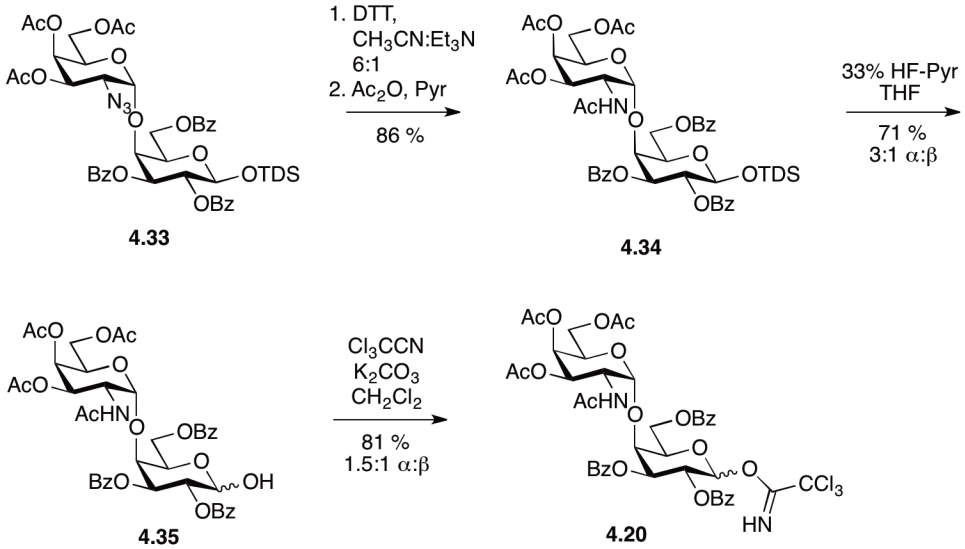

Scheme 4.13. The synthesis of disaccharide trichloroacetimidate donor **4.20**.

The convergence of disaccharide donor **4.20** and the linker moiety acceptor **4.21** [Scheme 4.14] was performed by combining the donor **4.20** and the acceptor **4.21** with 3Å molecular sieves and cooling the solution to -20 °C. TMSOTf was used as the activator and the reaction proceeded to provide the intermediate **4.36** in 87 % yield as the β-product and as an inseparable mixture of isomers (*R*:*S*, 1:1). Subsequent global deprotection of the glycosylation product **4.36** was achieved *via* the addition of one equivalent of 1 M CH_3ONa in anhydrous CH_3OH to remove the acyl protecting groups. Once transesterification was complete and the methanol removed, a small amount of water was added to the reaction flask to facilitate the conversion of the methyl ester of the pyruvate to

the corresponding carboxylic acid to provide the monomeric BAIT-*di*NAc **4.18** intermediate in 97 % yield.

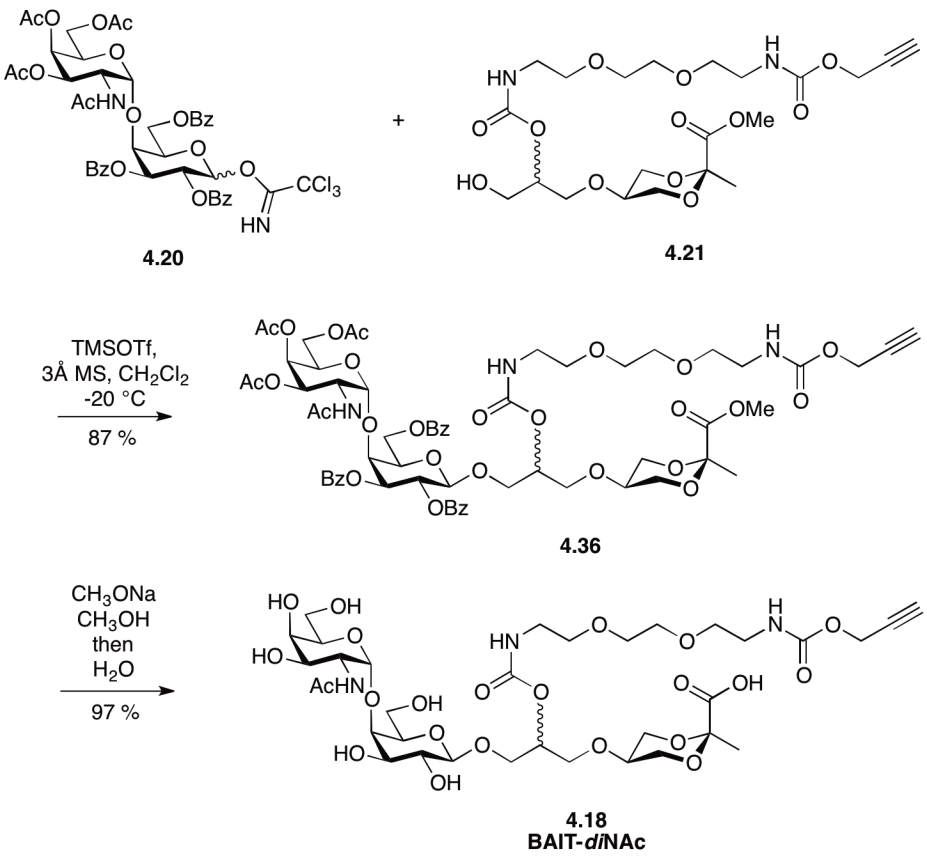

Scheme 4.14. Convergent glycosylation between disaccharide donor **4.20** aglycon **4.21**and subsequent global deprotection to provide BAIT-*di*NAc **4.18**.

Lastly, the monomeric **4.18** was conjugated to an azide-modified povidone synthesized in the Bundle group[245] [Scheme 4.15] *via* a Cu-catalyzed [3+2]-Huisgen cycloaddition reaction using $CuSO_4$ as the catalyst.[231,232] After purification the final compound PolyBAIT-*di*NAc **4.17** was synthesized in 84 % yield and with 6.7 % incorporation of the ligand onto the polymer.

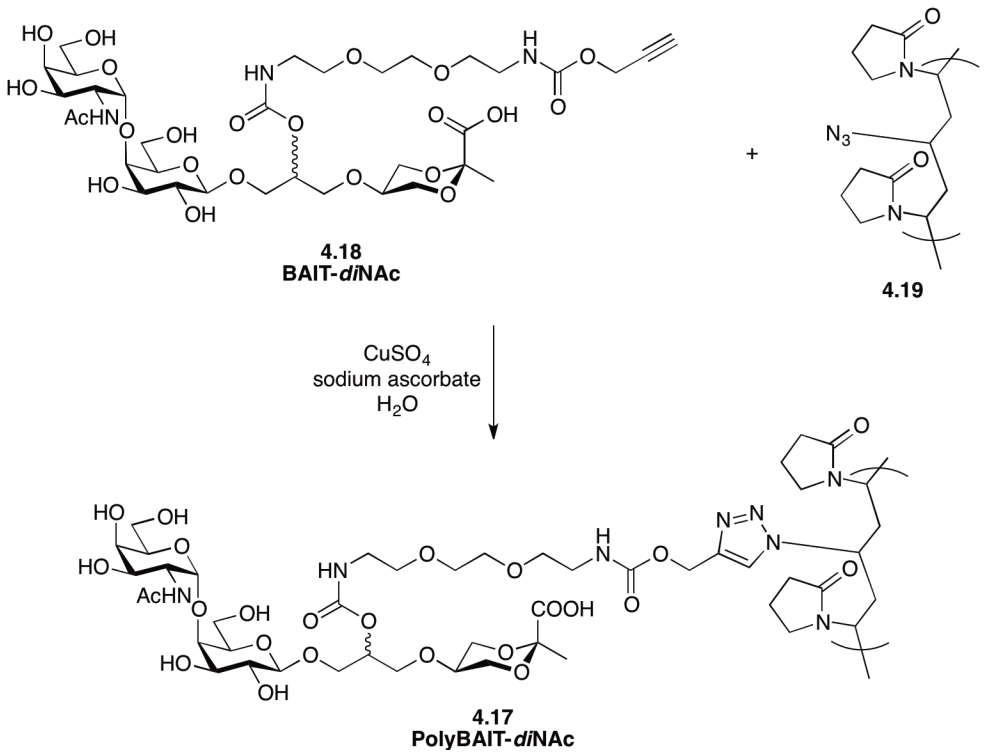

Scheme 4.15. The synthesis of PolyBAIT-diNAc 4**.17** *via* a Cu catalyzed [3+2]-Huisgen cycloaddition reaction.

Biological evaluation of the PolyBAIT-*di*NAc compound **4.17** is currently underway in collaboration with Dr. Glen Armstrong at the University of Calgary.

4.4. Conclusions

The syntheses of the multivalent heterobifunctional ligands, PolyBAIT-P^{k}NAc **4.1** and PolyBAIT-*di*NAc **4.17** were performed. Evaluation of this polymeric inhibitor of Stx2a binding to Vero cells *in vitro* is masked by a documented interaction of HuSAP with Stx2. HuSAP binds to and neutralizes Stx2 in the absence of glycan ligands and, based on the observation that HuSAP transgenic mice were completely resistant to Stx2. In the presence of LPS the interference of HuSAP with protection studies is ablated and this allowed

PolyBAIT-P^{k}NAc **4.1** to be evaluated *in vivo*. HuSAP-tg mice pre-exposed to LPS after challenge with a lethal amount of Stx2a were significantly protected from the lethal effect of Stx2 at concentrations of **4.1** as low as 31.5 mg/g mouse.

Chapter 5

Conclusions and Future Directions

The research presented in this thesis focuses on gaining a better understanding of binding events to Shiga toxins produced by *Escherichia coli* O157:H7. In addition, the syntheses and biological evaluation of both Stx1 specific and Stx2 specific multivalent heterobifunctional ligands, to sequester the toxins and prevent Shigatoxemia were performed.

The synthesis of (S)-PolyBAIT **2.1** and its inactive isomer (R)-PolyBAIT **2.2** were performed linearly and subsequently copolymerized with acrylamide. The $\alpha(1\rightarrow4)$ glycosidic linkage was formed using the fusion enzyme $\alpha(1,4)$-galactosyltranferase/4'-Gal-epimerase which allowed for a simple and direct method for the trisaccharide formation. *In vitro* analysis of (S)-PolyBAIT **2.1** displayed high activity in a solid-phase Stx1-binding inhibition assay and showed comparable activity in a Vero cell cytotoxicity assay. *In vivo* analysis of **2.1** in HuSAP-tg mice showed complete protection after exposure to lethal amounts of Stx1. Tissue analysis of these mice provided insight into the possible mechanism of action of **2.1**, whereby the Stx1-**2.1**-HuSAP supramolecular complex was diverted from the kidneys to the liver.

To better understand the nature of binding to the clinically more relevant Stx2, a 2-acetamido-2-deoxy galactosyl derivative of P^k trisaccharide was made coined Methyl-P^kNAc **3.1**, where the terminal α-Gal residue of P^k trisaccharide was replaced with a 2-acetamido-2-deoxy galactosyl residue at the non-reducing end. STD NMR analysis of the binding of **3.1** to Stx2 was performed and showed that P^kNAc bound to Stx2 in the same relative conformation as P^k trisaccharide to Stx1. The selectivity of P^kNAc-analogs to Stx2 was determined by synthesizing two BSA-glycoconjugates: P^kNAc-BSA **3.11** and P^k-BSA **3.12**. Solid-phase binding assays were performed and determined that **3.11** bound Stx2 approximately 275-times stronger than P^k-BSA **3.12**. To gain more insight into the nature of P^kNAc binding to Stx2 a crystal structure of Stx2 with a bound disaccharide **3.24** (Methyl 2'-acetamido-2'-deoxy galabiose) was acquired. The ligand was found to occupy sites 1 and 2 of the toxin and the conformations of the disaccharides aligned very well to those of a previously solved crystal structure of a Gb_3 analog bound by Stx1. Analysis of the binding sites provides evidence that site 2 is also the primary binding site for Stx2 because it displays more polar and van der Waals contacts than site 1. In addition, a unique interaction between Glu15 and O6 of the reducing end galactose would suggest a possible reason for Stx2 selectivity as this interaction is not possible in Stx1 (Glu15 (Stx2) = Asp16 (Stx1)). The introduction of the *N*-acetyl moiety in Stx2 ligands introduces more hydrogen bond interactions to Arg32 (Stx2), potentially contributing to the selectivity of 2-acetamido derivatives of P^k trisaccharide to Stx2.

Based on the information provided from the crystal structure as well as STD NMR, the synthesis of an Stx2 specific multivalent heterobifunctional ligand PolyBAIT-P^{k}NAc **4.1**, was performed. *In vitro* analysis of 4.1 proved to be difficult due to a naturally occurring binding phenomenon between Stx2 and HuSAP with which 4.1 competes. However, *in vivo* analysis in LPS-presensitized HuSAP-tg mice showed that 4.1 protects mice against Stx2 induced shigatoxemia with approximately 80 % survival and with greater selectivity than the Stx1 specific (*S*)-PolyBAIT.

The crystal structure of Stx2 with the bound disaccharide ligand **3.24**, also suggests possible modifications that could enhance binding. It is proposed that the elaboration of the *N*-acetyl moiety in P^{k}NAc derivatives, would allow for the development of a new and potentially better class of univalent or multivalent inhibitors. The crystal structure suggests that the introduction of more diversity at this position would not interfere with the conformation of disaccharide binding and could lead to new potential interactions to improve binding affinity or avidity. This approach could involve the construction and investigation of a dynamic library of potential appendages *via* computational means to provide a hit with which to elaborate new inhibitors. The potential discovery of a good binder that does not require supramolecular complex formation to HuSAP to function would provide additional benefits as the investigation of Stx2 specific heterobifunctional ligands is complicated by the naturally occurring HuSAP-Stx2 interaction. An

effective inhibitor of Stx2 that does not require complex formation would contribute to the development of a practical, potentially therapeutic inhibitor.[245]

Chapter 6

Experimental Section

6.1. General Methods

All chemical reagents obtained were of analytical grade and used as obtained from commercial sources unless otherwise indicated. All solvents used in water-sensitive reactions were purified by passage through columns of alumina and copper under nitrogen atmosphere except for methanol, which was distilled prior to use over sodium hydride and collected as needed. Unless otherwise stated, all reactions were performed at room temperature and under argon atmosphere. Molecular sieves were dried in an oven maintaining an internal temperature of 350 °C to ensure dryness and were allowed to cool under vacuum or under argon atmosphere at room temperature. Reactions were monitored by analytical TLC on Silica gel60-F_{254} (E. Merck). Plates were visualized under UV light and/or by treatment with either 5% sulfuric acid in ethanol, potassium permanganate solution, ninhydrin solution, or molybdate solution followed by charring. All solvents were removed by rotary evaporation at <40 ºC unless otherwise stated. Flash column chromatography was performed using silica gel (230-400 mesh, Silicycle, Montreal) at flow rates between 6 and 18.5 ml min^{-1}. ^{1}H NMR spectra were recorded at 500, 600, or 700 MHz. Chemical shifts are reported in ppm (δ) and were referenced to internal residual protonated solvent signals or to external

acetone in the case of D_2O (0.1% external acetone @ 2.225 ppm). ^{13}C NMR spectra were recorded at 125 MHz and chemicals shifts are referenced to internal $CDCl_3$ (77.23 ppm) or external acetone (31.07 ppm). Electrospray ionization High-resolution mass spectra (ESI HRMS) were obtained on a Micromass Zabspec TOF-mass spectrometer by analytical services in the department (U of A). Optical rotations were determined with a Perkin-Elmer model 241 polarimeter at room temperature using the sodium D-line and are reported in deg ml g^{-1} dm^{-1}. Percent incorporation of ligands onto BSA proteins was calculated *via* MADLI-TOF mass spectrometry comparing conjugated against un-conjugated masses. High Performance Liquid Chromatography (HPLC) purifications were performed on an X-Bridge reverse phase column with the indicated solvent systems. Fourier transform infrared spectrometry was performed on a Thermo Scientific Nicolet 8700 FTIR spectrometer and Nicolet Continuum FTIR microscope. Combustion analysis was performed on a CE Thermo EA11808 CHNS-O elemental analyzer.

6.2. Chapter 2 Experimental

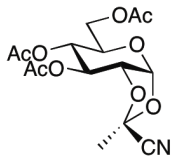

2.9

3,4,6-Tri-*O*-acetyl-1,2-*O*-[(*S*)-1-(cyano)ethylidene]-α-D-glucopyranoside (2.9):

2,3,4,6-Tetra-O-acetyl-α,β-D-glucosyl bromide **2.8** (19.9 g, 0.0485 mol) was combined with ground up KCN (15.8 g 0.242 mol) and TBAB (5.10 g, 0.0242 mol) in a round bottom flask to which dry CH_3CN (120 ml) was added. The vessel was placed under argon atmosphere and the reaction proceeded at room temperature for three days. The reaction turned a dark brown color, indicating a completed reaction. Reaction completion was confirmed using ^1H NMR spectroscopy, which showed no remaining anomeric proton signal for the bromide. The reaction mixture was then filtered through Celite® and concentrated to dryness. The crude reaction mixture was then purified by flash column chromatography on silica gel (2:1, hexanes-ethyl acetate). The fractions were collected and found to contain both *exo* and *endo* products. The *exo* product was re-crystallized from ethyl acetate-hexanes and provided the pure *exo* product **2.9** (7.26 g, 42 %) as a white needle solid; R_f 0.52 (1:1, hexanes-ethyl acetate); $[\alpha]_D$ +12.9 ^{o}(*c* 1.01, $CHCl_3$); ^1H NMR (500 MHz, $CDCl_3$) δ 5.80 (d, 1 H, $J_{1,2}$ 5.1 Hz, H-1), 5.21 (vt, 1 H, $J_{2,3}$ 2.8 Hz, $J_{3,4}$ 2.8 Hz, H-3), 4.91 (ddd, 1 H, $J_{2,4}$ 0.8 Hz, $J_{2,4}$ 2.6 Hz, $J_{4,5}$ 9.6 Hz, H-4), 4.39 (ddd, 1 H, $J_{2,4}$ 0.9 Hz, $J_{2,3}$ 2.9 Hz, $J_{1,2}$ 5.2 Hz, H-2), 4.20 (m, 1 H, H-6a), 4.19 (m, 1 H, H-6b), 3.90 (ddd, 1 H, $J_{5,6a}$ 4.3 Hz, $J_{5,6b}$ 4.3 Hz,

$J_{4,5}$ 9.3 Hz, H-5), 2.14 (s, 3 H, CH_3C(O)O), 2.09 (s, 3 H, CH_3C(O)O), 2.09 (s, 3 H, CH_3C(O)O), 1.92 (s, 3 H, CH_3); ^{13}C NMR (125 MHz, $CDCl_3$) δ 170.6 (CH_3C(O)O), 169.5 (CH_3C(O)O), 168.9 (CH_3C(O)O), 116.4 (C≡N), 98.8 (quaternary C *pyruvate*), 97.4 (C-1), 74.2 (C-2), 69.3 (C-3), 67.8 (C-4), 67.3 (C-5), 62.8 (C-6), 24.3 (-CH_3), 20.7 (CH$_3$C(O)O); ESI HRMS: calcd. for $C_{15}H_{19}NO_{19}Na$ 380.0952. Found 380.0947; Anal. calcd for $C_{15}H_{19}NO_{19}$: C, 50.42; H, 5.36; N, 3.92. Found: C, 50.59; H, 5.33; N, 3.93.

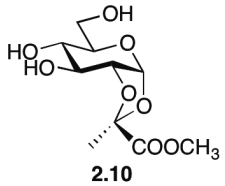

2.10

1,2-*O*-[(*S*)-1-(Methoxycarbonyl)ethylidene]-α-D-glucopyranoside (2.10):

The cyanoethylidene **2.9** (6.56 g, 18.4 mmol) was dissolved in anhydrous CH_3OH (60 ml). The flask was placed under argon atmosphere following which Na metal (0.200 g) was added and allowed to dissolve. The reaction proceeded for two days at which point TLC analysis (20%, methanol-dichloromethane) showed no remaining starting material. CH_3COOH (40 ml) was added and the reaction proceeded overnight. The reaction mixture was subsequently co-evaporated with toluene. Once dry, the solid was dissolved in methanol, and adsorbed onto silica gel and purified by flash column chromatography (5%, methanol-dichloromethane) to give the product **2.10** (3.48 g, 72 %) as a white solid; $[\alpha]_D$+34.5 ^{o}(*c* 1.10, CH_3OH); ^{1}H NMR (500 MHz, D_2O) δ 5.77 (d, 1 H, $J_{1,2}$ 4.9 Hz, H-1), 4.27 (ddd, 1 H, $J_{2,4}$ 0.8 Hz, $J_{2,3}$ 2.2 Hz , $J_{1,2}$ 5.0 Hz, H-2), 3.99 (vt, 1 H,

$J_{2,3}$ 4.0 Hz , $J_{3,4}$ 4.0 Hz, H-3), 3.85 (m, 1 H, H-6a), 3.80 (s, 3 H, COOCH_3), 3.72 (m, 2 H, H-5, H-6b), 3.58 (ddd, 1 H, $J_{2,4}$ 0.7 Hz, $J_{3,4}$ 3.9 Hz , $J_{4,5}$ 9.1 Hz, H-4), 1.72 (s, 3 H, -CH_3); ^{13}C-NMR (125 MHz, $CDCl_3$): δ 172.2 (*C*(O)OCH_3), 105.7 (quaternary C *pyruvate*), 98.6 (C-1), 76.9 (C-2), 73.7 (C-5), 72.4 (C-3), 69.0 (C-4), 62.2 (C-6), 54.3 (C(O)O*C*H_3), 22.2 (-*C*H_3); ESI HRMS Calcd. for $C_{10}H_{16}O_8Na$ 287.0737. Found 287.0733.

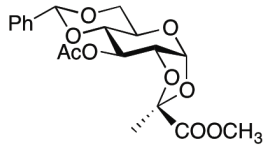

2.11

3-*O*-Acetyl-4,6-*O*-benzylidene-1,2-*O*-[(*S*)-1-(methoxycarbonyl)ethylidene]-α-D-glucopyranoside (2.11):

The glucoside **2.10** (2.58 g, 9.76 mmol) was dissolved in anhydrous CH_3CN (30 ml). $PhCH(OCH_3)_2$ (1.97 ml, 13.6 mmol) was then added followed by a catalytic amount of CSA (20 mg). The reaction was done at reduced pressure at 30 ºC to remove CH_3OH generated during reaction. After 2.5 hours, TLC analysis (5%, methanol-dichloromethane) showed the reaction to be complete. The reaction was quenched with five drops of Et_3N and concentrated. The crude benzylidene product was dissolved in Pyr (50 ml) and Ac_2O (50 ml) and the reaction proceeded overnight under argon atmosphere after which TLC analysis (2:1, hexanes-ethyl acetate) showed maximum product formation. The mixture was co-evaporated with toluene and purified by flash column chromatography on silica gel (3:1 → 1:1, hexanes-ethyl acetate) to provide the product **2.11** (3.18 g, 83 %) as a white solid; R_f 0.56 (1:1, hexanes-ethyl acetate); $[a]_D$ +27.1^o (*c* 1.02,

$CHCl_3$); ^{1}H NMR (500 MHz, $CDCl_3$) δ 7.47 (m, 2H, ArH), 7.37 (m, 3H, ArH), 5.84 (d, 1 H, $J_{1,2}$ 5.1 Hz, H-1), 5.53 (s, 1 H, *benzylidene* C-*H*), 5.24 (dd, 1 H, $J_{2,3}$ 3.5 Hz, $J_{3,4}$ 3.5 Hz, H-3), 4.41 (dd, 1 H, $J_{5,6a}$ 5.2 Hz, $J_{6a,6b}$ 10.6 Hz, H-6a), 4.33 (dd, 1 H, $J_{2,3}$ 3.4 Hz, $J_{1,2}$ 5.1 Hz, H-2), 3.94 (ddd, $J_{5,6a}$ 5.3 Hz, $J_{4,5}$ 9.8 Hz, H-5), 3.77 (s, 3 H, C*H*$_3$OC(O)), 3.72 (m, 2 H, H-4, H-6b), 2.12 (s, 3 H, C*H*$_3$C(O)O), 1.76 (s, 3 H, CH_3); ^{13}C-NMR (125 MHz, $CDCl_3$): δ 169.8 (CH_3*C*(O)O), 169.5 (*C*(O)OCH_3), 136.8 (Ar), 129.2 (Ar), 128.3 (Ar), 126.1 (Ar), 104.0 (quaternary C *pyruvate*), 101.6 (*benzylidene C*-H), 98.8 (C-1), 77.7 (C-4), 77.2 (C-2), 73.1 (C-3), 68.8 (C-6), 62.3 (C-5), 52.7 (C(O)O*C*H_3), 22.4 (*C*H_3C(O)O), 20.9 (-CH_3); ESI HRMS calcd. for $C_{19}H_{22}O_9Na$ 417.1156. Found 417.1154; Anal. Calcd. for $C_{19}H_{22}O_9$: C, 57.86; H, 5.62; O, 36.51. Found: C, 58.01; H, 5.77.

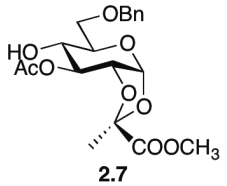

2.7

3-*O*-Acetyl-6-*O*-benzyl-1,2-*O*-[(*S*)-1-(methoxycarbonyl)ethylidene]-α-D-glucopyranoside (2.7):

The benzylidene **2.11** (3.89 g, 9.88 mmol) was dissolved in dry CH_2Cl_2 (20 ml) and the reaction vessel placed under argon atmosphere. Et_3SiH (16 ml, 98.8 mmol) was added and the mixture cooled to 0 °C using an ice-water bath. TFA (7.6 ml, 98.8 mmol) was added and the reaction proceeded at 0°C. After one hour, TLC analysis (15%, ethyl acetate-toluene) showed no remaining starting material. The reaction mixture was diluted with dichloromethane and transferred

to a separatory funnel where the organic layer was washed with saturated aqueous sodium bicarbonate, distilled water and saturated aqueous sodium chloride. The organic layer was dried over anhydrous sodium sulfate, filtered and concentrated to dryness. The crude product was purified by flash column chromatography on silica gel (15% → 30%, ethyl acetate-toluene) to provide the product **2.7** (3.35 g, 85 %) as a white solid; R_f 0.18 (15%, ethyl acetate-toluene); $[a]_D$ +12.9 ^{o}(*c* 1.03, $CHCl_3$); ^{1}H NMR (500 MHz, $CDCl_3$) δ 7.35-7.26 (m, 5 H, ArH), 5.81 (d, 1 H, $J_{1,2}$ 5.1 Hz, H-1), 5.03 (vt, 1 H, $J_{2,3}$ 3.4 Hz, $J_{3,4}$ 3.4 Hz, H-3), 4.62 (d, 1 H, J_{gem} 12.2 Hz, PhCH_2O), 4.57 (d, 1 H, J_{gem} 12.1 Hz, PhCH_2O), 4.38 (ddd, 1 H, $J_{2,4}$ 0.8 Hz, $J_{2,3}$ 3.1 Hz, $J_{1,2}$ 5.1 Hz, H-2), 3.83 (m, 1 H, H-5), 3.76 (m, 4 H, H-4, CH_3OC(O)), 3.71 (m, 2 H, H-6a, H-6b), 2.83 (bs, 1 H, O-H), 2.09 (s, 3 H, CH_3C(O)O), 1.77 (s, 3 H, CH_3); ^{13}C-NMR (125 MHz, $CDCl_3$): δ 170.7 (CH_3C(O)O), 169.4 (C(O)OCH_3), 137.7 (Ar), 128.4 (Ar), 127.8 (Ar), 104.9 (quaternary C pyruvate), 98.1 (C-1), 74.8, 74.5 (C-2, C-3), 73.7 (PhCH_2O), 70.2 (C-5), 69.6 (C-6), 69.2 (C-4), 52.7 (C(O)OCH_3), 21.7 (CH_3C(O)O), 20.9 (-CH_3 pyruvate); ESI HRMS calcd. for $C_{19}H_{24}O_9Na$ 419.1313. Found 419.1311; Anal. Calcd. for $C_{19}H_{24}O_9$: C, 57.57; H, 6.10; O, 36.33. Found: C, 57.29; H, 6.45.

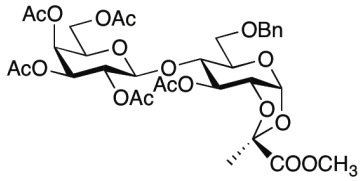

2.12

2,3,4,6-Tetra-*O*-acetyl-β-D-galactopyranosyl-(1→4)-3-*O*-Acetyl-6-*O*-benzyl-1,2-*O*-[(*S*)-1-(methoxycarbonyl)ethylidene]-α-D-glucopyranoside (2.12):

The galactosyl donor **2.6** (3.99 g, 8.10 mmol) and glucosyl acceptor **2.7** (2.14 g, 5.40 mmol) were combined and dissolved in anhydrous CH_2Cl_2 (30 ml). After 30 minutes, the contents were cooled to 0 °C and $HClO_4$ on silica (1.09 g, 0.405 mmol, 5 % per mol of donor) was added. The reaction proceeded at 0 °C under argon atmosphere for two hours until TLC analysis (1:1, hexanes-ethyl acetate) showed the reaction to be complete. The crude reaction mixture was washed with saturated aqueous sodium bicarbonate, distilled water and saturated aqueous sodium chloride. The organic layer was dried of anhydrous sodium sulfate, filtered and concentrated. The crude product was purified by flash column chromatography on silica gel (2:1, hexanes-ethyl acetate) to give the product **2.12** (3.21 g, 82 %) as a white foam; R_f 0.25 (1:1, hexanes-ethyl acetate); $[a]_D$ +4.0 ^{o}(*c* 2.6, $CHCl_3$); ^{1}H NMR (600 MHz, $CDCl_3$) δ 7.40-7.30 (m, 5 H, ArH), 5.80 (d, 1 H, $J_{1,2}$ 5.2 Hz, H-1), 5.44 (dd, 1 H, $J_{2,3}$ 2.2 Hz, $J_{3,4}$ 2.7 Hz, H-3), 5.34 (dd, 1 H, $J_{3',4'}$ 3.5 Hz, $J_{4',5'}$ 1.0 Hz, H-4'), 5.12 (dd, 1 H, $J_{2',3'}$ 7.9 Hz, $J_{3',4'}$ 10.4 Hz, H-2'), 4.92 (dd, 1 H, $J_{3',4'}$ 3.5 Hz, $J_{2',3'}$ 10.4 Hz, H-3'), 4.70 (d, 1 H, J_{gem} 12.2 Hz, PhCH_2O), 4.50 (d, 1 H, J_{gem} 12.2 Hz, PhCH_2O), 4.43 (d, 1 H, $J_{1',2'}$ 8.0 Hz, H-1'), 4.32 (m, 1 H, $J_{2,4}$ 0.99Hz, $J_{2,3}$ 2.8 Hz, $J_{1,2}$ 5.2 Hz, H-2), 4.13-4.09 (m, 2 H, H-6a', H-6b'), 3.87-3.78 (m, 3 H, H-4, H-5, H-5'), 3.76 (s, 3 H, C(O)OCH_3), 3.67 (dd, 1 H, $J_{5,6a}$

2.2 Hz, $J_{6a,6b}$ 10.9 Hz, H-6a), 3.59 (dd, 1 H, $J_{5,6b}$ 3.4 Hz, $J_{6a,6b}$ 10.9 Hz, H-6b), 2.16 (s, 3 H, CH_3C(O)O), 2.08 (s, 3 H, CH_3C(O)O), 2.03 (s, 3 H, CH_3C(O)O), 1.97 (s, 3 H, CH_3C(O)O), 1.92 (s, 3 H, CH_3C(O)O), 1.73 (s, 3 H, CH_3); ^{13}C-NMR (150 MHz, $CDCl_3$): δ 170.4 (CH_3*C*(O)O), 170.3 (CH_3*C*(O)O), 170.1 (*C*(O)OCH_3), 169.4 (CH_3*C*(O)O), 169.1 (CH_3*C*(O)O), 169.0 (CH_3*C*(O)O), 137.8 (Ar), 128.5 (Ar), 127.96 (Ar), 105.4 (quaternary C *pyruvate*), 102.1 (C-1'), 98.1 (C-1), 76.1, 74.1, 73.6 (Ph*C*H_2O), 70.8, 70.6, 70.4, 68.9, 68.8, 68.3 (C-6'), 66.9, 61.0 (C-6), 52.6 (C(O)O*C*H_3), 21.3 (*C*H_3C(O)O), 20.9 (*C*H_3C(O)O), 20.69 (*C*H_3C(O)O), 20.65 (*C*H_3C(O)O), 20.62 (*C*H_3C(O)O), 20.5 (-CH_3). ESI HRMS calcd $C_{33}H_{42}O_{18}Na$ for 749.22634. Found 749.22665.; Anal. Calcd for $C_{33}H_{42}O_{18}$: C, 54.54; H, 5.83. Found: C, 54.23; H, 5.73.

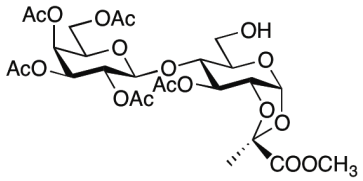

2.13

2,3,4,6-Tetra-*O*-acetyl-β-D-galactopyranosyl-(1→4)-3-*O*-Acetyl-1,2-*O*-[(*S*)-1-(methoxycarbonyl)ethylidene]-α-D-glucopyranoside (2.13):

To a solution of **2.12** (1.6 g, 2.2 mmol) in CH_3OH (10 ml), a drop of water and $Pd(OH)_2$ (30 mg) were added. After two hours of stirring under H_2 atmosphere the mixture was filtered *via* Millipore® membrane filter, concentrated and purified by flash column chromatography on silica gel (1:1, acetone-hexanes) to give **2.13** (1.0 g, 71%) as a white foam; R_f 0.12 (1:1, hexanes-ethyl acetate); $[\alpha]_D$ +8 ^{o}(*c* 1.2, $CHCl_3$); ^{1}H NMR (600 MHz, $CDCl_3$) δ 5.76 (d, 1 H, $J_{1,2}$ 5.2 Hz,

H-1), 5.51 (dd, 1 H, $J_{2,3}$ 2.3 Hz, $J_{3,4}$ 2.3 Hz, H-3), 5.38 (dd, 1 H, $J_{3',4'}$ 3.5 Hz, $J_{4',5'}$ 0.9 Hz, H-4'), 5.18 (dd, 1 H, $J_{2',3'}$ 8.0 Hz, $J_{3',4'}$ 10.4 Hz, H-2'), 5.01 (dd, 1 H, $J_{3',4'}$ 3.7 Hz, $J_{2',3'}$ 10.4 Hz, H-3'), 4.64 (d, 1 H, $J_{1',2'}$ 7.9 Hz, H-1'), 4.33 (ddd, 1 H, $J_{2,4}$ 1.1 Hz, $J_{2,3}$ 2.9 Hz, $J_{1,2}$ 5.2 Hz, H-2), 4.14-4.10 (m, 2 H, H-6a', H-6b'), 3.93 (td, 1 H, $J_{4',5'}$ 0.9 Hz, $J_{5',6a'}$ 6.7 Hz, $J_{5',6b'}$ 6.7 Hz, H-5'), 3.85-3.82 (m, 2 H, H-4, H-6a), 3.76 (s, 3 H, C(O)OCH_3), 3.75 (m, 1 H, H-5), 3.61 (dd, 1 H, $J_{5,6b}$ 3.8 Hz, $J_{6a,6b}$ 12.0 Hz, H-6b), 2.16 (s, 3 H, CH_3C(O)O), 2.09 (s, 3 H, CH_3C(O)O), 2.06 (s, 3 H, CH_3C(O)O), 2.03 (s, 3 H, CH_3C(O)O), 1.98 (s, 3 H, CH_3C(O)O), 1.74 (s, 3 H, pyruvate, CH_3). ^{13}C-NMR (150 MHz, $CDCl_3$) δ 170.4 (CH_3C(O)O), 170.3 (CH_3C(O)O), 170.1 (C(O)OCH_3), 169.3 (CH_3C(O)O), 169.1 (CH_3C(O)O), 105.5 (quaternary C *pyruvate*), 102.3 (C-1'), 97.8 (C-1), 76.5, 74.4, 70.9, 70.8. 70.4, 69.1, 68.9, 66.89, 61.80 (C-6'), 61.1 (C-6), 52.7 (C(O)OCH$_3$), 21.3 (C(O)OCH$_3$), 20.9 (C(O)OCH$_3$), 20.7 (C(O)OCH$_3$), 20.6 (C(O)OCH$_3$), 20.5 (-CH_3); ESI HRMS calcd for $C_{26}H_{36}O_{18}Na$ 659.17939. Found 659.17920.; Anal. Calc'd for $C_{26}H_{36}O_{18}$: C, 49.06; H, 5.70. Found: C, 49.12; H, 5.70.

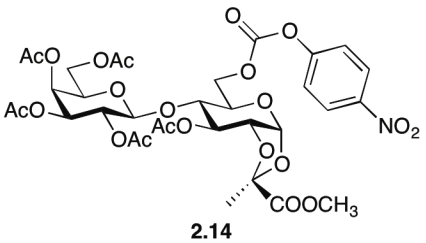

2.14

2,3,4,6-Tetra-*O*-acetyl-β-D-galactopyranosyl-(1→4)-3-*O*-Acetyl-6-*O*-(4-nitrophenoyl)-1,2-*O*-[(*S*)-1-(methoxycarbonyl)ethylidene]-α-D-glucopyranoside (2.14):

To a solution of **2.13** (1 g, 1.57 mmol) and 4-nitrophenyl chloroformate **2.16** (380 mg, 1.88 mmol) in dry CH_2Cl_2 (10 ml), Pyr (0.2 ml) was added. The reaction proceeded at room temperature until TLC analysis (1:1, hexanes-ethyl acetate) showed complete conversion after five minutes. Water (0.2 ml) was added and the mixture was concentrated to dryness and purified by flash column chromatography on silica gel (1:1, hexanes-ethyl acetate) to give **2.14** (1.2 g, 95 %); R_f 0.32 (1:1, hexanes-ethyl acetate); $[\alpha]_D$ +0.7 ^{o}(*c* 1, $CHCl_3$); ^{1}H NMR (600 MHz, $CDCl_3$) δ 8.31-8.28 (m, 2 H, ArH), 7.42-7.39 (m, 2 H, ArH), 5.80 (d, 1 H, $J_{1,2}$ 5.1 Hz, H-1), 5.55 (dd, 1 H, $J_{2,3}$ 1.6 Hz, $J_{3,4}$ 2.5 Hz, H-3), 5.39 (dd, 1 H, $J_{3',4'}$ 3.5 Hz, $J_{4',5'}$ 1.1 Hz, H-4'), 5.21 (dd, 1 H, $J_{2',3'}$ 8.0 Hz, $J_{3',4'}$ 10.4 Hz, H-2'), 5.04 (dd, 1 H, $J_{3',4'}$ 3.5 Hz, $J_{2',3'}$ 10.4 Hz, H-3'), 4.70 (d, 1 H, $J_{1',2'}$ 7.9 Hz, H-1'), 4.51 (dd, 1 H, $J_{5,6a}$ 2.3 Hz, $J_{6a,6b}$ 11.7 Hz, H-6a), 4.39 (m, 1 H, H-2), 4.51 (dd, 1 H, $J_{5,6b}$ 5.7 Hz, $J_{6a,6b}$ 11.7 Hz, H-6b), 4.17 (dd, 1 H, $J_{5,6a'}$ 6.5 Hz, $J_{6a',6b'}$ 11.3 Hz, H-6a'), 4.07 (m, 1 H, H-5), 3.93 (td, 1 H, $J_{4',5'}$ 1.1 Hz, $J_{5',6a'}$ 6.6 Hz, $J_{5',6b'}$ 6.6 Hz, H-5'), 3.78 (m, 4 H, H-4, C(O)OCH_3), 2.17 (s, 3 H, CH_3C(O)O), 2.12 (s, 3 H, CH_3C(O)O), 2.07 (s, 3 H, CH_3C(O)O), 2.05 (s, 3 H, CH_3C(O)O), 1.98 (s, 3 H, CH_3C(O)O), 1.78 (s,

3 H, pyruvate, CH_3); ^{13}C NMR (150 MHz, $CDCl_3$) δ 170.4 ($CH_3C(O)O$), 170.2 ($CH_3C(O)O$), 170.1 ($C(O)OCH_3$), 169.4 ($CH_3C(O)O$), 169.1 ($CH_3C(O)O$), 169.0 ($CH_3C(O)O$), 155.3 (*C*-O of Ph), 152.2 (-O*C*(O)OPhNO_2), 145.5 (*C*-NO_2 of Ph), 125.4 (Ar), 121.7 (Ar), 105.7 (quaternary *C*, pyruvate), 101.7 (C-1'), 97.7 (C-1), 77.3, 74.2, 71.0, 70.8, 69.7, 68.9, 67.8 (C-6), 66.9, 66.6, 61.2 (C-6'), 52.8 (C(O)O*C*H_3), 21.2 (*C*H_3C(O)O), 20.8 (*C*H_3C(O)O), 20.7 (*C*H_3C(O)O), 20.67 (*C*H_3C(O)O), 20.64 (*C*H_3C(O)O), 20.5 (-CH_3); ESI HRMS calcd for $C_{33}H_{39}NO_{22}Na$ 824.18559. Found 824.18573.; Anal. Calcd for $C_{33}H_{39}NO_{22}$: C, 49.44; H, 4.90; N, 1.75. Found: C, 49.64; H, 4.88; N, 2.07.

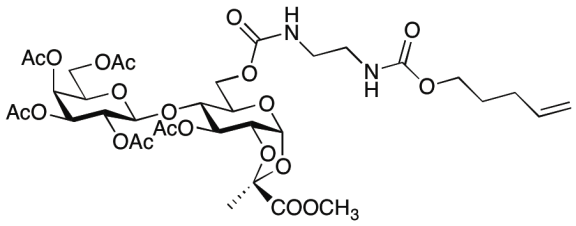

2.15

2,3,4,6-Tetra-*O*-acetyl-β-D-galactopyranosyl-(1→4)-3-*O*-Acetyl-6-*O*-(2,5-diaza-7-oxa-6-oxo-dodec-11-enoyl)-1,2-*O*-[(*S*)-1-(methoxycarbonyl)ethylidene]-α-D-glucopyranoside (2.15):

The nitrophenyl carbonate **2.14** (1.49 g, 1.87 mmol) was dissolved in anhydrous CH_2Cl_2 to which the amine **2.17** (1.30 g, 7.48 mmol) was added, followed by Et_3N (1.8 ml). The reaction proceeded at room temperature for 30 minutes until TLC analysis (1:2, acetone-hexanes) indicated completion of the reaction. The mixture was concentrated and the residue was purified by flash column chromatography on silica gel (1:2, acetone-hexanes) to give **2.15** (1.44 g,

92 %); R_f 0.18 (1:2, acetone-hexanes); $[\alpha]_D$+0.8 ^{o}(*c* 1, $CHCl_3$); ^{1}H NMR (600 MHz, $CDCl_3$) δ 5.84-5.76 (m, 1 H, -C*H*=CH_2), 5.76 (d, 1 H, $J_{1,2}$ 5.2 Hz, H-1), 5.53 (dd, 1 H, $J_{2,3}$ 1.4 Hz, $J_{3,4}$ 2.3 Hz, H-3), 5.38 (dd, 1 H, $J_{3',4'}$ 3.5 Hz, $J_{4',5'}$ 0.9 Hz, H-4'), 5.23 (broad s, 1 H, N-H), 5.18 (dd, 1 H, $J_{2',3'}$ 8.2 Hz, $J_{3',4'}$ 10.4 Hz, H-2'), 5.08-4.97 (m, 4 H, H-3', N-H, -CH=CH_2), 4.63 (d, 1 H, $J_{1',2'}$ 8.0 Hz, H-1'), 4.35 (m, 1 H, H-2), 4.22 (dd, 1 H, $J_{5,6a}$ 2.0 Hz, $J_{6a,6b}$ 11.6 Hz, H-6a), 4.18-4.09 (m, 3 H, H-6b, H-6a', H-6b'), 4.07 (m, 2 H, -CH_2-), 3.95 (td, 1 H, $J_{4',5'}$ 1.0 Hz, $J_{5',6a'}$ 7.3 Hz, $J_{5',6b'}$ 7.3 Hz, H-5'), 3.90 (m, 1 H, H-5), 3.77 (s, 3 H, C(O)OCH_3), 3.64 (m, 1 H, H-4), 3.32 (bs, 4 H, -NHCH_2CH_2NH-), 2.17 (s, 3 H, CH_3C(O)O), 2.10 (s, 3 H, CH_3C(O)O), 2.08 (s, 3 H, CH_3C(O)O), 2.03 (s, 3 H, CH_3C(O)O), 1.98 (s, 3 H, CH_3C(O)O), 2.14-2.10 (m, 2 H, -CH_2-), 1.75 (s, 3 H, -CH_3), 1.74-1.68 (m, 2 H, -CH_2-); ^{13}C NMR (150 MHz, $CDCl_3$): δ 170.4 (CH_3*C*(O)O), 170.3 (CH_3*C*(O)O), 170.1 (*C*(O)OCH_3), 169.5 (CH_3*C*(O)O), 169.3 (CH_3*C*(O)O), 169.0 (CH_3*C*(O)O), 157.0 (-O*C*(O)NH-), 156.3 (-NH*C*(O)O-), 137.5 (-*C*H=CH_2), 115.2 (-CH=*C*H_2), 105.6 (quaternary C *pyruvate*), 102.4 (C-1'), 97.7 (C-1), 77.3, 73.9, 70.9, 70.8, 69.8, 68.9, 67.2, 66.9, 64.5 (-*C*H_2-), 64.1 (-*C*H_2-), 61.9 (-*C*H_2-), 52.7 (C(O)O*C*H_3), 41.3 (-*C*H_2-), 41.1 (-*C*H_2-), 30.0 (-*C*H_2-), 28.2 (-*C*H_2-), 21.2 (*C*H_3C(O)O), 20.9 (*C*H_3C(O)O), 20.7 (*C*H_3C(O)O), 20.6 (*C*H_3C(O)O), 20.5 (-CH_3); ESI HRMS calcd for $C_{35}H_{50}N_2O_{21}Na$ 857.27983. Found 857.27929.; Anal. Calcd for $C_{35}H_{50}N_2O_{21}$: C, 50.36; H, 6.04, N, 3.36. Found: C, 50.37; H, 6.15; N, 3.35.

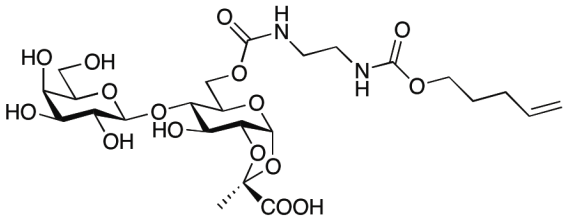

2.5

β-D-Galactopyranosyl-(1→4)-6-*O*-(2,5-diaza-7-oxa-6-oxo-dodec-11-enoyl)-1,2-*O*-[(*S*)-1-(carboxy)ethylidene]-α-D-glucopyranoside (2.5):

The fully acylated intermediate **2.15** (0.53 g, 0.63 mmol) was dissolved in anhydrous CH_3OH (3.5 ml) and CH_3ONa (1 M, 0.64 ml) was added. The mixture was stirred at room temperature for two hours then concentrated and the resulting solid was dissolved in water (3 ml). After 1 h the hydrolysis of the methyl ester was complete. The solution was neutralized with CH_3COOH, concentrated and used directly in the next step. A small sample was purified by HPLC chromatography on C-18 in water-methanol containing 1 % CH_3COOH; $[\alpha]_D$+19 ^{o}(*c* 1, H_2O); ^{1}H NMR (600 MHz, D_2O) δ 5.90 (m,1 H, -C*H*=CH_2), 5.62 (d, 1 H, $J_{1,2}$ 4.9 Hz, H-1), 5.10-5.01 (m, 2 H, -CH=CH_2), 4.44 (d, 1 H, $J_{1',2'}$ 7.8 Hz, H-1'), 4.41-4.34 (m, 2 H, H-3, H-6a), 4.23 (dd, 1 H, $J_{5,6b}$ 5.3 Hz, $J_{6a,6b}$ 12.0 Hz, H-6b), 4.18 (m, 1 H, H-2), 4.08-4.01 (m, 3 H, H-5, -OCH_2-), 3.92 (d, 1 H, $J_{3',4'}$ 3.4 Hz, H-4'), 3.83-3.74 (m, 3 H, H-4, H-6a', H-6b'), 3.69 (m, 1 H, H-5'), 3.64 (dd, 1 H, $J_{2',3'}$ 9.9 Hz, H-3'), 3.55 (m, 1 H, H-2'), 3.24 (s, 4 H, -NHCH_2-), 2.12 (m, 2 H, -CH_2-), 1.72 (m, 2 H, -CH_2-), 1.64 (s, 3 H, -CH_3); ^{13}C NMR (150 MHz, $CDCl_3$) δ 181.3 (C=O), 159.2 (C=O), 158.4 (C=O), 138.9 (-*C*H=CH_2), 115.3 (-CH=*C*H_2), 107.4 (quaternary C *pyruvate*), 105.2 (C-1'), 96.7 (C-1), 78.5, 75.6, 75.4, 72.8, 71.0, 69.5, 68.9, 68.5, 65.3 (-*C*H_2-), 64.3 (-*C*H_2-), 61.3 (-*C*H_2-), 40.6 (-CH_2-), 40.4 (-

CH_2-), 29.7 (-*C*H_2-), 27.8 (-*C*H_2-), 21.8 (-*C*H_3); ESI HRMS calcd for $C_{24}H_{37}N_2O_{16}$ 609.21376. Found 609.21365.; Anal. Calcd for $C_{24}H_{38}N_2O_{16}$: C, 47.21; H, 6.27; N, 4.59. Found: C, 46.67; H, 6.23; N, 4.57.

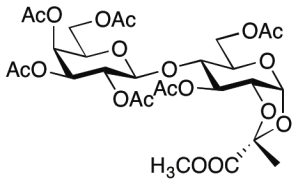

2.21

2,3,4,6-Tetra-*O*-acetyl-β-D-galactopyranosyl-(1→4)-3,6-di-*O*-acetyl-1,2-*O*-[(*R*)-1-(methoxycarbonyl)ethylidene]-α-D-glucopyranose (2.21):

To a solution of 2,3,4,6-tetra-*O*-acetyl-β-D-galactopyranosyl-(1→4)-3,6-di-*O*-acetyl-1,2-*O*-[(*R*)-1-(cyano)ethylidene]-α-D-glucopyranose **2.23** (2.56 g, 3.97 mmol) in dry CH_3OH (120 ml), was added CH_3ONa (1 N, 3 ml). The mixture was stirred overnight until TLC analysis (1:1, hexanes-ethyl acetate) indicated maximum product formation. CH_3COOH (150 ml) was added to convert the imidate intermediate into the methyl ester. ^1H NMR spectroscopy was used to determine the completion of product formation *via* analysis of anomeric protons. The mixture was concentrated to dryness and a 1:1 mixture of Ac_2O:Pyr (20 ml) was added. The reaction progress was monitored by TLC analysis (1:1, hexanes-ethyl acetate) and was found to be complete. The mixture was concentrated and co-evaporated with toluene (3 x 20 ml) to remove pyridine. The residue was dissolved in ethyl acetate, washed with saturated aqueous sodium bicarbonate, saturated aqueous sodium chloride, filtered and concentrated to give **2.21** (2.607 g, 97 %) without the need for purification; R_f 0.16 (1:1, hexanes-ethyl acetate);

$[\alpha]_D$ +16 ^{o}(*c* 0.9, $CHCl_3$); ^{1}H NMR (600 MHz, $CDCl_3$): δ 5.63 (d, 1 H, $J_{1,2}$ 4.7 Hz, H-1), 5.52 (t, 1 H, $J_{2,3}$ 3.2 Hz, $J_{3,4}$ 3.2 Hz, H-3), 5.38 (dd, 1 H, $J_{3',4'}$ 3.4 Hz, $J_{4',5'}$ 0.9 Hz, H-4'), 5.18 (dd, 1 H, $J_{2',3'}$ 10.3 Hz, $J_{1',2'}$ 7.9 Hz, H-2'), 5.00 (dd, 1 H, H-3'), 4.65 (d, 1 H, H-1'), 4.34 (dd, 1 H, $J_{6a,6b}$ 11.9 Hz, $J_{5,6a}$ 2.1 Hz, H-6a), 4.29 (ddd, 1 H, $J_{4,5}$ 9.7 Hz, $J_{5,6b}$ 5.2 Hz, H-5), 4.24 (t, 1 H, H-2), 4.16-4.08 (m, 3 H, H-6a', H-6b', H-6b,), 3.99 (td, 1H, $J_{5',6a'}$ 7.3 Hz, $J_{5',6a'}$ 7.3 Hz, H-5'), 3.85 (s, 3 H, -OCH_3), 3.71 (dd, 1 H, H-4), 2.16 (s, 3 H, C*H*$_3$C(O)O), 2.12 (s, 3 H, C*H*$_3$C(O)O), 2.11 (s, 3 H, C*H*$_3$C(O)O), 2.07 (s, 3 H, C*H*$_3$C(O)O), 2.04 (s, 3 H, C*H*$_3$C(O)O), 1.97 (s, 3 H, C*H*$_3$C(O)O), 1.55 (s, 3 H, -C*H*$_3$). ^{13}C-NMR (125 MHz, $CDCl_3$): δ 170.6 (CH_3*C*(O)O), 170.3 (CH_3*C*(O)O), 170.2 (CH_3*C*(O)O), 170.1 (CH_3*C*(O)O), 169.3 (CH_3*C*(O)O), 169.1 (CH_3*C*(O)O), 168.5 (*C*(O)OCH_3), 106.1 (quaternary C *pyruvate*), 101.4 (C-1'), 96.8 (C-1), 76.6, 74.2, 71.0, 70.6, 70.5, 68.8, 67.5, 66.8, 63.2, 60.9 (C-6, C-6'), 53.1 (C(O)O*C*H_3), 22.8 (*C*H_3C(O)O), 20.9 (*C*H_3C(O)O), 20.8 (*C*H_3C(O)O), 20.7 (*C*H_3C(O)O), 20.66 (*C*H_3C(O)O), 20.63 (*C*H_3C(O)O), 20.5 (-*C*H_3); ESI HRMS: calcd. for $C_{28}H_{38}O_{19}Na$ 701.18995. Found 701.18995; Anal. calcd for $C_{28}H_{38}O_{19}$: C, 49.56; H, 5.64. Found: C, 49.73; H, 5.70.

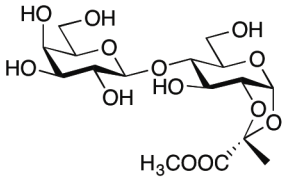

2.24

β-D-Galactopyranosyl-(1→4)-1,2-*O*-[(*R*)-1-(methoxycarbonyl)ethylidene]-α-D-glucopyranose (2.24):

To a solution of **2.21** (2.56 g, 3.77 mmol) in anhydrous CH_3OH (60 ml) CH_3ONa (1N, 3 ml) was added. The reaction was allowed to proceed at room temperature overnight until completion as indicated by TLC (20%, methanol-dichloromethane). The reaction mixture was neutralized using Dowex 50W (H^+) resin to pH 7, filtered and concentrated. The crude product was purified by flash column chromatography on silica gel (20%, methanol-dichloromethane) to give **2.24** (1.198 g, 75 %) as a clear syrup; R_f 0.18 (20%, methanol-dichloromethane); $[\alpha]_D$ +55 ^{o}(*c* 1, H_2O); ^{1}H NMR (600 MHz, D_2O) δ: 5.80 (d, 1 H, $J_{1,2}$ 4.8 Hz, H-1), 4.45 (d, 1 H, $J_{1',2'}$ 7.8 Hz, H-1'), 4.40 (t, 1 H, $J_{2,3}$ 4.8 Hz, H-2), 4.12 (t, 1 H, $J_{3,4}$ 5.2 Hz, H-3), 3.92 (d, 1 H, $J_{3',4'}$ 3.4 Hz, H-4'), 3.87-3.81 (m, 4 H, H-6a, C(O)OCH_3), 3.82–3.69 (m, 6 H, H-4, H-5, H-6b, H-5', H-6a', H-6b',), 3.65 (dd, 1 H, $J_{2',3'}$ 10.0 Hz, $J_{3',4'}$ 3.5 Hz, H-3'), 3.54 (dd, 1 H, $J_{1'2'}$ 7.8 Hz, $J_{2',3'}$ 9.9 Hz, H-2'); ^{13}C NMR (125 MHz, D_2O): δ 171.7 (*C*(O)OCH_3), 106.2 (quaternary C *pyruvate*), 104.6 (C-1'), 98.1 (C-1), 77.6, 77.5, 75.9, 73.2 (C-3'), 72.8 (C-2'), 71.6, 71.2 (C-3), 69.3 (C-4'), 61.78, 61.14 (C-6, C-6'), 54.3 (C(O)O*C*H_3), 23.5 (-*C*H_3); ESI HRMS: calcd. for $C_{16}H_{26}O_{13}Na$ 449.12656. Found 449.12663; Anal. calcd for $C_{16}H_{26}O_{13}$•0.5H_2O: C, 44.14; H, 6.25. Found: C, 44.35; H, 6.23.

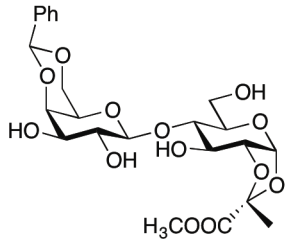

2.25

4,6-*O*-Benzylidene-β-D-galactopyranosyl-(1→4)-1,2-*O*-[(*R*)-1-(methoxycarbonyl)ethylidene]-α-D-glucopyranose (2.25):

To a solution of **2.24** (1.198 g, 2.81 mmol) in dry CH_3CN (60 ml), $PhCH(OCH_3)_2$ (464 μl, 3.09 mmol) and CSA (50 mg) were added. The reaction proceeded for two hours until TLC analysis (20%, methanol-dichloromethane) showed reaction to be complete. The reaction mixture was neutralized with a small amount of Et_3N, concentrated and purified by flash column chromatography on silica gel (5 %, methanol-dichloromethane) to give **2.25** (1.068 g, 74%); R_f 0.61 (20 %, methanol-dichloromethane); $[\alpha]_D$ +46 ^{o}(*c* 0.8, $CHCl_3$); ^{1}H NMR (500 MHz, CD_3OD) δ: 7.54 (m, 2 H, ArH), 7.35 (m, 3 H, ArH), 5.67 (d, 1 H, $J_{1,2}$ 4.9 Hz, H-1), 5.62 (s, 1 H, *benzylidene* C-*H*), 4.49 (d, 1 H, $J_{1',2'}$ 7.3 Hz, H-1'), 4.21 (m, 2 H, H-4', H-6a'), 4.15 (m, 2 H, H-6b', H-2), 4.00 (dd, 1 H, $J_{2,3}$ 5.6 Hz, $J_{3,4}$ 7.8 Hz, H-3), 3.94 (dd, 1 H, $J_{5,6a}$ 3.5 Hz, $J_{6a,6b}$ 12.1 Hz, H-6a), 3.88 (ddd, 1 H, $J_{5,6b}$ 2.4 Hz, $J_{4,5}$ 9.7 Hz, H-5), 3.81 (dd, 1 H, $J_{5,6b}$ 2.4 Hz, $J_{6a,6b}$ 12.2 Hz, H-6b), 3.77 (s, 3 H, C(O)OC*H*$_3$), 3.69-3.64 (m, 4 H, H-2', H-3', H-4), 3.62 (m, 1 H, H-5'), 1.53 (s, 3 H, CH_3); ^{13}C-NMR (125 MHz, CD_3OD): δ 171.7 (*C*(O)OCH_3), 139.5 (Ar), 129.9 (Ar), 129.1 (Ar), 127.5 (Ar), 105.8 (quaternary C *pyruvate*), 105.1 (C-1'), 102.3 (*benzylidene C*-H), 99.7 (C-1), 80.1 (C-2), 78.5, 77.4 (C-4'), 73.7, 73.6, 73.5 (C-3, C-5), 71.9, 70.26 (C-6'), 68.3 (C-5'), 61.66 (C-6), 53.26 (C(O)O*C*H_3), 24.29 (-

CH_3); ESI HRMS: calcd. for $C_{23}H_{30}O_{13}Na$ 537.15786. Found 537.15801; Anal. calcd for $C_{23}H_{30}O_{13}\bullet 0.5H_2O$: C, 52.77; H, 5.97. Found: C, 52.72; H, 5.89.

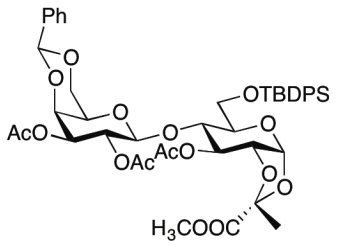

2.20

2,3-Di-*O*-acetyl-4,6-*O*-benzylidene-β-D-galactopyranosyl-(1→4)-3-*O*-acetyl-6-*O*-(*tert*-butyldiphenylsilyl)-1,2-*O*-[(*R*)-1-(methoxycarbonyl)ethylidene]-α-D-glucopyranose (2.20):

To a solution of **2.25** (994 mg, 1.93 mmol) in dry CH_2Cl_2 (30 ml), Et_3N (323 μl, 2.32 mmol) and DMAP (10 mg, 0.0772 mmol) were added. TBDPSCl (500 μl, 2.32 mmol) was added drop-wise over four hours. After 12 hours another one equivalent of TBDPSCl (400 μl) was added and the reaction proceeded for another 24 hours with occasional heating. Subsequent TLC analysis (10%, methanol-dichloromethane) showed the reaction to be complete. A 1:1 mixture of Ac_2O:Pyr (80 ml) was added the reaction proceeded until TLC analysis (1:1, hexanes-ethyl acetate) showed the reaction to be complete. The mixture was concentrated to dryness, co-evaporating with toluene (3 x 20 ml) and the crude product was purified by flash column chromatography on silica gel (1:1, hexanes:ethyl acetate) to give **2.20** (817 mg, 48 %) as a white foam; R_f 0.59 (1:1, hexanes-ethyl acetate); $[\alpha]_D$ +69 ^{o}(*c* 1.6, $CHCl_3$); ^{1}H NMR (500 MHz, $CDCl_3$) δ: 7.74-7.71 (m, 4 H, ArH), 7.49-7.36 (m, 11 H, ArH), 5.74 (d, 1 H, $J_{1,2}$ 4.9 Hz, H-

1), 5.46 (s, 1 H, *benzylidene* C-H), 5.34 (dd, 1 H, $J_{2,3}$ 6.2 Hz, $J_{3,4}$ 8.4 Hz, H-3), 5.24 (dd, 1 H, $J_{1',2'}$ 8.1 Hz, $J_{2',3'}$ 10.4 Hz, H-2'), 4.82 (dd, 1 H, $J_{3',4'}$ 3.7 Hz, $J_{2',3'}$ 10.3 Hz, H-3'), 4.79 (d, 1 H, $J_{1',2'}$ 8.6 Hz, H-1'), 4.32-4.27 (m, 3 H, H-4', H-6a', H-2), 4.07 (t, 1 H, $J_{4,5}$ 8.4, H-4), 4.03-3.96 (m, 4 H, H-6b', H-5, H-6a, H-6b), 3.86 (s, 3 H, C(O)OCH_3), 3.32 (m, 1 H, H-5'), 2.09 (s, 3 H, CH_3C(O)O), 2.07 (s, 3 H, CH_3C(O)O), 2.05 (s, 3 H, CH_3C(O)O), 1.83 (s, 3 H, CH_3), 1.09 (s, 9 H, *t*-Bu); ^{13}C-NMR (125 MHz, $CDCl_3$) δ 170.6 (*C*(O)OCH_3), 169.9 (CH_3*C*(O)O), 169.5 (CH_3*C*(O)O), 168.5 (CH_3*C*(O)O), 137.4 (Ar), 135.8 (Ar), 135.4 (Ar), 133.5 (Ar), 132.4 (Ar), 129.8 (Ar), 129.7 (Ar), 128.9 (Ar), 128.1 (Ar), 127.7 (Ar), 127.6 (Ar), 126.3 (Ar), 104.5 (quaternary C *pyruvate*) , 101.1 (*benzylidene C*-H), 100.2 (C-1'), 98.5 (C-1), 76.0 (C-2), 73.2 (C-4'), 72.8 (C-4), 72.3, 72.2 (C-5, C-3'), 71.7 (C-3), 68.9 (C-2'), 68.6 (C-6'), 66.1 (C-5), 61.4 (C-6), 52.9 (C(O)O*C*H_3), 26.8 (*t*Bu-CH_3), 23.9 (-*C*H_3), 20.9 (*C*H_3C(O)O), 20.8 (*C*H_3C(O)O), 20.5 (*C*H_3C(O)O), 19.4 (C of *t*-Bu); ESI HRMS: calcd. for $C_{45}H_{54}SiO_{16}Na$ 901.30734. Found 901.30795; Anal. calcd for $C_{45}H_{54}SiO_{16}$: C, 61.49; H, 6.19. Found: C, 61.48; H, 6.34.

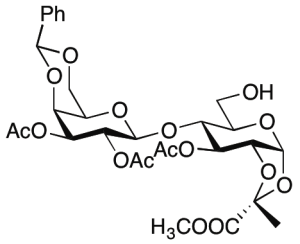

2.26

2,3-Di-*O*-acetyl-4,6-*O*-benzylidene-β-D-galactopyranosyl-(1→4)-3-*O*-acetyl-1,2-*O*-[(*R*)-1-(methoxycarbonyl)ethylidene]-α-D-glucopyranose (2.26):

To a solution of **2.20** (763 mg, 0.87 mmol) in dry THF (10 ml) in a polypropylene container was added 33 % HF-Pyr (60 μl, 1.74 mmol) at room temperature. The reaction was monitored by TLC analysis (1:1, acetone-hexane) for 2 hours and showed no progress. Another eight equivalents of HF-Pyr (240 μl) were added and the reaction proceeded overnight until TLC analysis showed the reaction to be complete. The mixture was transferred to a separatory funnel and washed with saturated aqueous sodium bicarbonate, distilled water and saturated aqueous sodium chloride. The organic layer was dried over anhydrous sodium sulfate, filtered and concentrated. The crude product was purified by flash column chromatography on silica gel (40 %, acetone-hexanes) to give **2.26** (505 mg, 91%); R_f 0.38 (1:1, acetone-hexanes); $[\alpha]_D$ +73 ^{o}(*c* 2.2, $CHCl_3$); ^{1}H NMR (500 MHz, $CDCl_3$) δ 7.49 (m, 2 H, ArH), 7.38 (m, 3 H, ArH), 5.66 (d, 1 H, $J_{1,2}$ 4.9 Hz, H-1), 5.48 (s, 1 H, *benzylidene* C-*H*), 5.39 (dd, 1 H, $J_{2,3}$ 4.9 Hz, $J_{3,4}$ 6.2 Hz, H-3), 5.31 (dd, 1 H, $J_{1',2'}$ 7.9 Hz, $J_{2',3'}$ 10.4 Hz, H-2'), 4.95 (dd, 1 H, $J_{3',4'}$ 3.7 Hz, $J_{2',3'}$ 10.4 Hz, H-3'), 4.71 (d, 1 H, $J_{1',2'}$ 8.1 Hz, H-1'), 4.34 (d, 1 H, $J_{3',4'}$ 3.6 Hz, H-4'), 4.29 (dd, 1 H, $J_{6a',5'}$ 1.5 Hz, $J_{6a',6b'}$ 12.4 Hz, H-6a'), 4.25 (t, 1 H, $J_{1,2}$ 4.8 Hz, $J_{2,3}$ 4.8 Hz, H-2), 4.08-4.03 (m, 2 H, H-6b', H-5), 3.92-3.88 (m, 2 H, H-4, H-6a),

3.87 (s, 3 H, C(O)OCH_3), 3.82-3.75 (m, 1 H, H-6b), 3.55 (m, 1 H, H-5'), 2.09 (s, 3 H, CH_3C(O)O), 2.07 (s, 3 H, CH_3C(O)O), 2.06 (s, 3 H, CH_3C(O)O), 1.57 (s, 3 H, -CH_3); ^{13}C NMR (125 MHz, $CDCl_3$) δ 170.8 (*C*(O)OCH$_3$), 169.7 (CH$_3$*C*(O)O), 169.1 (CH$_3$*C*(O)O), 169.0 (CH$_3$*C*(O)O), 137.5 (Ar), 129.1 (Ar), 128.2 (Ar), 126.4 (Ar), 105.2 (quaternary C *pyruvate*), 101.2 (*benzylidene C*-H), 100.7 (C-1'), 97.8 (C-1), 75.6 (C-2), 73.9 (C-4), 73.3 (C-4'), 72.2 (C-3'), 71.6 (C-3), 71.1 (C-5), 68.9 (C-2'), 68.7 (C-6'), 66.4 (C-5'), 60.8 (C-6), 53.1 (C(O)O*C*H$_3$), 23.5 (-CH$_3$), 20.9 (*C*H$_3$C(O)O), 20.9 (*C*H$_3$C(O)O), 20.8 (*C*H$_3$C(O)O); ESI HRMS: calcd. for $C_{29}H_{36}O_{16}Na$ 663.18956. Found 663.18945.

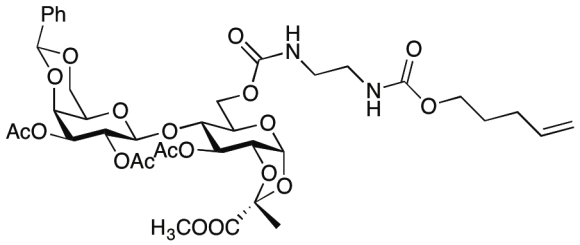

2.27

2,3-Di-*O*-acetyl-4,6-*O*-benzylidene-β-D-galactopyranosyl-(1→4)-3-*O*-acetyl-6-*O*-(2,5-diaza-7-oxa-6-oxo-dodec-11-enoyl)-1,2-*O*-[(*R*)-1-(methoxycarbonyl)ethylidene]-α-D-glucopyranose (2.27):

Alcohol **2.26** (427 mg, 0.67 mmol) was combined with *p*-nitrophenyl chloroformate **2.16** (161 mg, 0.804) and dissolved in dry CH_2Cl_2 (10 ml). Pyr (0.1 ml) was added and the reaction monitored by TLC (1:1, hexanes-ethyl acetate). After 10 minutes the reaction was shown to be complete. The reaction mixture was concentrated with no heating after which the residue was again dissolved in a minimum of CH_2Cl_2 and the 4-nitra-6-oxa-5-oxo-dec-10-en-1-

amine **2.17** (0.460 g, 2.67 mmol) was added followed by Et_3N (0.64 ml). The reaction proceeded for one hour at room temperature until TLC analysis (1:1, acetone-toluene) found the reaction to be complete. The mixture was concentrated to dryness and the crude product purified by flash column chromatography on silica gel (1:3 → 1:1, acetone-toluene) to give **2.27** (378 mg, 65 %); R_f 0.46 (1:1, acetone-toluene); $[\alpha]_D$ +50 ^{o}(*c* 1, $CHCl_3$); ^{1}H NMR (500 MHz, $CDCl_3$) δ 7.51-7.49 (m, 2 H, ArH), 7.40-7.34 (m, 3 H, ArH), 5.81 (ddt, J_{trans} 16.9 Hz, J_{cis} 10.3 Hz, $J_{CH,CH2}$ 6.6 Hz, -CH_2CH=CH_2), 5.63 (d, 1 H, $J_{1,2}$ 4.8 Hz, H-1), 5.49-5.46 (m, 2 H, *benzylidene* C-*H*, H-3), 5.31 (dd, 1 H, $J_{1',2'}$ 8.2 Hz, $J_{2',3'}$ 10.2 Hz, H-2'), 5.23 (broad s, 1 H, NH), 5.14 (broad s, 1 H, N-H), 5.06-4.98 (m, 2 H, CH=CH_2), 4.94 (dd, 1 H, $J_{3',4'}$ 3.6 Hz, H-3'), 4.63 (d, 1 H, $J_{1',2'}$ 8.0 Hz, H-1'), 4.38 (broad d, 1 H, H-6a), 4.34 (d, 1 H, H-4'), 4.30 (dd, 1 H, $J_{6a',5'}$ 1.3 Hz, $J_{6a',6b'}$ 12.1 Hz, H-6a'), 4.26-4.22 (m, 2 H, H-2, H-5), 4.18 (dd, 1 H, $J_{5,6b}$ 5.4 Hz, $J_{6a,6b}$ 11.6 Hz, H-6b), 4.08-4.03 (m, 3 H, H-6b', -C(O)CH_2O-), 3.86 (s, 3 H, C(O)OCH_3), 3.72 (dd, 1 H, $J_{3,4}$ 6.2 Hz, $J_{4,5}$ 10.6Hz, H-4), 3.58 (m, 1 H, H-5'), 3.33-3.23 (m, 4 H, -HNCH_2CH_2NH-), 2.14-2.10 (m, 2 H, -CH_2-), 2.09 (s, 3 H, CH_3C(O)O), 2.08 (s, 3 H, CH_3C(O)O), 2.05 (s, 3 H, CH_3C(O)O), 1.74-1.69 (m, 2 H, -*C*H_2-), 1.55 (s, 3 H, -*C*H_3); ^{13}C NMR (125 MHz, $CDCl_3$) δ 170.8 (*C*(O)OCH_3), 169.5 (*C*H_3C(O)O), 169.2 (*C*H_3C(O)O), 168.9 (*C*H_3C(O)O), 157.1 (-HNC(O)O-), 156.3 (-HNC(O)O-), 137.6 (-*C*H=CH_2), 137.5 (Ar), 129.1 (Ar), 128.2 (Ar), 126.4 (Ar), 115.2 (CH=*C*H_2), 105.6 (quaternary C *pyruvate*), 101.12 (*benzylidene C*-H, C-1'), 97.4 (C-1), 75.6 (C-4), 75.0 (C-2), 73.3 (C-4'), 72.1 (C-3'), 71.1 (C-3), 69.0 (C-2'), 68.8 (C-5), 68.69 (C-6'), 66.4 (C-5'), 64.5 (C-6), 63.6 (-CH_2-), 53.1 (C(O)O*C*H_3),

41.4 (-*C*H_2-), 41.0 (-*C*H_2-), 29.9 (-*C*H_2-), 28.2 (-*C*H_2-), 23.3 (-*C*H_3), 20.9 (C*H*$_3$C(O)O), 20.8 (C*H*$_3$C(O)O), 20.7 (C*H*$_3$C(O)O); ESI HRMS: calcd. for $C_{38}H_{50}N_2O_{19}Na$ 861.29000. Found 861.29070; Anal. calcd for $C_{38}H_{50}N_2O_{19}$: C, 54.41; H, 6.01; N, 3.26. Found: C, 54.62; H, 6.13; N, 3.25.

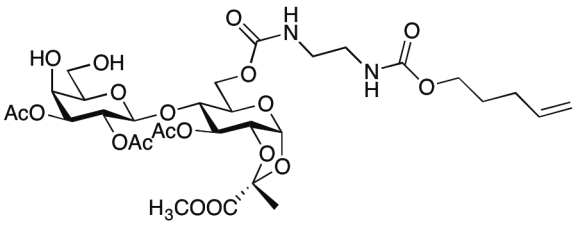

2.28

2,3-Di-*O*-acetyl-β-D-galactopyranosyl-(1→4)-3-*O*-acetyl-6-*O*-(2,5-diaza-7-oxa-6-oxo-dodec-11-enoyl)-1,2-*O*-[(*R*)-1-(methoxycarbonyl)ethylidene]-α-D-glucopyranose (2.28):

Intermediate **2.27** (337 mg, 0.402 mmol) was dissolved in 80 % CH_3COOH-water (25 ml) and heated to 80 °C for one hour until reaction was shown to be complete by TLC (1:1, acetone-toluene). The mixture was co-evaporated with toluene and a small amount of water to dryness. The crude product was purified by flash column chromatography on silica gel (1:1, acetone-toluene) to give **2.28** (235 mg, 78 %); R_f 0.31 (1:1, acetone-toluene); $[\alpha]_D$ +18 ^{o}(*c* 1.2, $CHCl_3$); ^{1}H NMR (500 MHz, $CDCl_3$) δ 5.80 (m, 1 H, -C*H*=CH_2), 5.66 (d, 1 H, $J_{1,2}$ 4.8 Hz, H-1), 5.60 (broad s, 1 H, H-3), 5.34 (broad s, 1 H, NH), 5.28 (dd, 1 H, $J_{1',2'}$ 8.0 Hz, $J_{2',3'}$ 10.3 Hz, H-2'), 5.22 (m, 1 H, NH), 5.06-4.97 (m, 2 H, -CH=C*H*$_2$), 4.92 (dd, 1 H, $J_{3',4'}$ 3.1 Hz, H-3'), 4.63 (d, 1 H, H-1'), 4.39 (broad d, 1 H, H-6a), 4.24 (m, 1 H, H-2), 4.20-4.14 (m, 1 H, H-5), 4.11-4.04 (m, 2 H, H-6b,

H-4'), 3.98-3.92 (m, 1 H, H-6a'), 3.85 (s, 3 H, OCH_3), 3.80-3.75 (m, 1 H, H-6b'), 3.66-3.60 (m, 2 H, H-4, 6'-OH), 3.34-3.36 (m, 5 H, H-5', -CH_2NH-), 3.15 (broad s, 1 H, 4'-OH), 2.14-2.10 (m, 2 H, CH_2), 2.12 (s, 3 H, C*H*$_3$C(O)O), 2.08 (s, 3 H, C*H*$_3$C(O)O), 2.07 (s, 3 H, C*H*$_3$C(O)O), 1.74-1.69 (m, 2 H, CH_2), 1.54 (s, 3 H, CH_3). ^{13}C-NMR (125 MHz, $CDCl_3$) δ 170.30 (CH_3*C*(O)O), 169.91 (CH_3*C*(O)O), 169.59 (CH_3*C*(O)O), 168.45 (C(O)OCH_3), 157.08 (-HNC(O)O-), 156.42 (-HNC(O)O-), 137.57 (-*C*H=CH_2), 115.18 (-CH=*C*H_2), 106.50 (quaternary C pyruvate), 101.70 (C-1'), 96.82 (C-1), 76.16, 74.78, 73.57, 73.42, 70.28, 69.17, 68.58, 68.25, 64.44 (-*C*H_2-), 64.24 (-*C*H_2-), 62.90 (-*C*H_2-), 53.13 (C(O)O*C*H_3), 41.24 (-*C*H_2-), 40.91 (-*C*H_2-), 29.96 (-*C*H_2-), 28.20 (-*C*H_2-), 22.82 (CH_3C(O)O), 20.97 (CH_3), 20.84 (CH_3), 20.63 (-*C*H_3); ESI HRMS: calcd. for $C_{31}H_{46}N_2O_{19}Na$ 773.25870. Found 773.25846.; Anal. calcd for $C_{31}H_{46}N_2O_{19}$: C, 49.60; H, 6.18; N, 3.73. Found: C, 49.52; H, 6.41; N, 3.44.

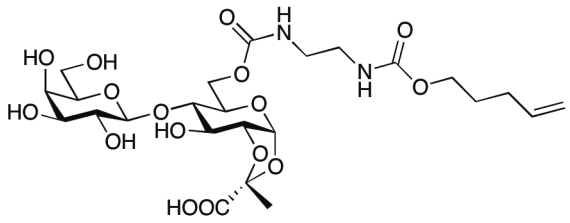

2.19

β-D-Galactopyranosyl-(1→4)-6-*O*-(2,5-diaza-7-oxa-6-oxo-dodec-11-enoyl)-1,2-*O*-[(*R*)-1-(carboxy)ethylidene]-α-D-glucopyranose (2.19):

To a solution of **2.28** (212 mg, 0.282 mmol) in dry CH_3OH (10 ml) CH_3ONa (1.13 ml, 0.564 mmol) was added and allowed to react overnight at room temperature. Subsequent TLC analysis (20%, methanol-dichloromethane)

showed the reaction to be complete. The mixture was concentrated to dryness after which water (10 ml) was added to convert methyl ester into carboxylic acid. After 2 hours analysis of TLC showed hydrolysis to be complete. The mixture was neutralized with Dowex 50W (H^+) resin, filtered, concentrated and freeze dried to give **2.19** (162 mg, 94 % yield); $[\alpha]_D$+27 ^{o}(*c* 0.8 H_2O); ^{1}H NMR (600 MHz, D_2O) δ 5.90 (m, 1 H, -C*H*=CH_2), 5.70 (d, 1 H, $J_{1,2}$ 4.7 Hz, H-1), 5.11-5.01 (m, 2 H, -CH=C*H*$_2$), 4.40 (d, 1 H, $J_{1',2'}$ 7.8 Hz, H-1'), 4.38-4.35 (m, 2 H, H-2, H-6a), 4.25 (dd, 1 H, $J_{5,6b}$ 4.8 Hz, $J_{6a,6b}$ 12.1 Hz, H-6b), 4.19 (t, 1 H, $J_{3,4}$ 6.3 Hz, $J_{2,3}$ 6.3 Hz, H-3), 4.10-4.05 (m, 2 H, -OCH_2-), 4.02-3.98 (m, 1 H, H-5), 3.91 (d, 1 H, $J_{3',4'}$ 3.4 Hz, H-4'), 3.80 (dd, 1 H, $J_{5',6a'}$ 8.1 Hz, $J_{6a',6b'}$ 11.7 Hz, H-6a'), 3.77-3.74 (m, 1 H, H-4), 3.74 (dd, 1 H, $J_{5',6b'}$ 4.1 Hz, $J_{6a',6b'}$ 11.8 Hz, H-6b'), 3.68 (dd, 1 H, $J_{5',6b'}$ 3.9 Hz, $J_{5',6a'}$ 8.1 Hz, H-5'), 3.62 (dd, 1 H, $J_{3',4'}$ 3.3 Hz, $J_{2',3'}$ 9.9 Hz, H-3'), 3.53 (dd, 1 H, $J_{1',2'}$ 7.8 Hz, $J_{2',3'}$ 9.7 Hz, H-2'), 3.24 (s, 4 H, -HNCH_2CH_2NH-), 2.18-2.10 (m, 2 H, -C*H*$_2$-), 1.78-1.70 (m, 2 H, -C*H*$_2$-), 1.54 (s, 3 H, -C*H*$_3$); ^{13}C-NMR ($CDCl_3$): δ 176.9 (*C*(O)OH), 159.8 (-HN*C*(O)O-), 158.9 (-HN*C*(O)O-), 139.5 (-*C*H=CH_2), 115.8 (-CH=*C*H_2), 108.6 (quaternary C *pyruvate*), 104.9 (C-1'), 97.5 (C-1), 78.4, 77.0, 76.2, 73.4, 71.7, 71.2, 70.1, 69.5, 65.9 (-*C*H_2-), 64.5 (-*C*H_2-), 62.0 (-*C*H_2-), 41.1 (-*C*H_2-), 30.3 (-*C*H_2-), 30.2 (-*C*H_2-), 24.1 (-*C*H_3). ESI HRMS: calcd. for $C_{24}H_{38}N_2O_{16}Na$ 633.21136. Found 633.21194.

6.3. Chapter 3 Experimental

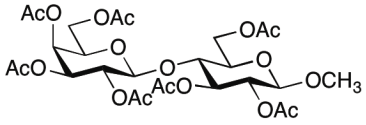

3.6

Methyl 2,3,4,5-tetra-*O*-acetyl-β-D-galactopyranosyl-(1→4)-2,3,6-tri-*O*-acetyl-β-D-glucopyranoside (3.6):

To a flame dried round bottom flask was added anhydrous CH_3CN (20 ml), $Hg(CN)_2$ (4.29 g. 0.017 mol) and $HgBr_2$ (0.56 g, 1.55 mmol). The acceptor, CH_3OH (6.3 ml, 0.155 mol) was then added and the reaction stirred at room temperature and under argon atmosphere. The glycosyl bromide donor **3.5** (10.81 g, 0.016 mol) was dissolved in anhydrous CH_3CN (20 ml) and placed in an addition funnel. The bromide was added slowly to the stirring solution and the reaction proceeded at room temperature for 4.5 hours at which point TLC analysis (1:1, hexanes-ethyl acetate) showed the reaction to be complete. The organic layer was washed with saturated aqueous potassium bromide, saturated aqueous sodium bicarbonate, distilled water and saturated aqueous sodium chloride. The crude product was purified by flask column chromatography on silica gel (3:1 → 1:1, hexanes-ethyl acetate) to give **3.6** (5.11g, 51 %) as a white flakey foam; R_f 0.17 (1:1, hexanes-ethyl acetate); $[\alpha]_D$ -14.2 °(*c* 1.01, $CHCl_3$); ^{1}H NMR (500 MHz, $CDCl_3$) δ 5.35 (dd, 1 H, $J_{4',5'}$ 1.1 Hz, $J_{3',4'}$ 3.5 Hz, H-4'), 5.20 (vt, 1 H, $J_{3,4}$ 9.2 Hz, $J_{2,3}$ 9.3 Hz, H-3), 5.11 (dd, 1 H, $J_{1',2'}$ 7.9 Hz, $J_{2',3'}$ 10.5 Hz H-2'), 4.95 (dd, 1 H, $J_{3',4'}$ 3.5 Hz, $J_{2',3'}$ 10.4 Hz, H-3'), 4.88 (dd, 1 H, $J_{1,2}$ 7.9 Hz, $J_{2,3}$ 9.4 Hz, H-2), 4.50 (dd, 1 H, $J_{5,6a}$ 2.2 Hz, $J_{6a,6b}$ 11.9 Hz, H-6a), 4.49 (d, 1 H, $J_{1',2'}$ 7.9 Hz, H-1'), 4.39 (d, 1 H, $J_{1,2}$ 7.9 Hz, H-1), 4.15-4.06 (m, 3 H, H-6b, H-6a', H-6b'), 3.87 (ddd, 1 H, $J_{4',5'}$

1.2 Hz, H-5'), 3.81 (vt, 1 H, $J_{3,4}$ 9.1 Hz, $J_{4,5}$ 9.8 Hz, H-4), 3.61 (ddd, 1 H, $J_{4,5}$ 2.2 Hz, $J_{5,6b}$ 4.9 Hz, $J_{5,6a}$ 9.8 Hz H-5), 3.48 (s, 3 H, -OC*H*$_3$), 2.15 (s, 3 H, C*H*$_3$C(O)O), 2.12 (s, 3 H, C*H*$_3$C(O)O), 2.06 (s, 3 H, C*H*$_3$C(O)O), 2.05 (s, 3 H, C*H*$_3$C(O)O), 2.04 (s, 3 H, C*H*$_3$C(O)O), 1.96 (s, 3 H, C*H*$_3$C(O)O); ^{13}C NMR (125 MHz, $CDCl_3$) δ 170.4 (C*H*$_3$C(O)O), 170.1 (C*H*$_3$C(O)O), 170.0 (C*H*$_3$C(O)O), 169.7 (C*H*$_3$C(O)O), 169.6 (C*H*$_3$C(O)O), 169.1 (C*H*$_3$C(O)O), 101.4 (C-1), 101.1 (C-1'), 76.3 (C-4), 72.9, 72.6 (C-3, C-5), 71.7, 70.9, 70.7 (C-2, C-3', C-5'), 69.1 (C-2'), 66.6 (C-4'), 61.9, 60.8 (C-6, C-6'), 56.9 (-O*C*H$_3$), 20.8 (*C*H$_3$C(O)O), 20.8 (*C*H$_3$C(O)O), 20.7 (*C*H$_3$C(O)O), 20.6 (*C*H$_3$C(O)O), 20.5 (*C*H$_3$C(O)O); ESI HRMS Calcd for $C_{27}H_{38}O_{18}Na$ 673.1950. Found 673.1953. Calcd for $C_{27}H_{38}O_{18}$: C, 49.85; H, 5.89. Found: C, 49.92; H, 5.98.

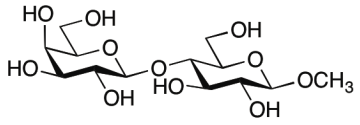

3.7

Methyl β-D-galactopyranosyl-(1→4)-β-D-glucopyranoside (3.7):

The acetylated lactoside **3.6** (4.76 g, 7.32 mmol) was dissolved in anhydrous CH_3OH (20 ml). A catalytic amount of Na metal was added and the reaction proceeded at room temperature for 30 minutes until TLC analysis (50%, methanol-dichloromethane) showed the reaction to be complete. The reaction mixture was concentrated to dryness and the remaining residue dissolved in distilled water. The reaction was quenched the Amberlite IR$^+$ 120 ion exchange resin (H^+) until pH was shown to be acidic. The mixture was filtered and concentrated while co-evaporating with anhydrous ethanol to remove water and

the product crashed out to give the product as a white flakey solid **3.7** in quantitative yield which was used directly in the next step without purification; R_f 0.33 (50 %, methanol-dichloromethane); $[\alpha]_D$ +3.82 °(*c* 1.00, H_2O); ^1H NMR (500 MHz, $CDCl_3$) δ 4.43 (d, 1 H, $J_{1',2'}$ 7.8 Hz, H-1'), 4.39 (d, 1 H, $J_{1,2}$ 8.1 Hz, H-1), 3.97 (dd, 1 H, $J_{5,6a}$ 2.1 Hz, $J_{6a,6b}$ 12.3 Hz, H-6a), 3.91 (d, 1 H, $J_{3',4'}$ 3.2 Hz, H-4'), 3.80–3.69 (m, 4 H, H-4, H-6b, H-6a', H-6b'), 3.65–3.61 (m, 3 H, H-3, H-3', H-5'), 3.58 (m, 1 H, H-5), 3.55 (s, 3 H, -OC*H*$_3$), 3.52 (dd, 1 H, $J_{1',2'}$ 7.9 Hz, $J_{2',3'}$ 9.9 Hz, H-2'), 3.29 (m, 1 H, H-2); ^{13}C NMR (125 MHz, $CDCl_3$) δ 103.9, 103.8 (C-1, C-1'), 79.3, 76.2, 75.6, 75.3, 73.7, 73.4 (C-3, C-4, C-5, C-2', C-3', C-5'), 71.8 (C-2), 69.4 (C-4'), 61.9, 60.9 (C-6, C-6'), 58.1 (O*C*H$_3$); ESI HRMS Calcd for $C_{15}H_{24}O_{11}Na$ 379.1211. Found 379.1210. Calcd for $C_{15}H_{24}O_{11}\bullet 0.5H_2O$: C, 42.74; H, 6.90. Found: C, 42.91; H, 6.93.

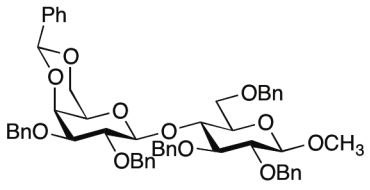

3.8

Methyl 2,3-di-*O*-benzyl-4,6-*O*-benzylidene-β-D-galactopyranosyl-(1→4)-2,3,6-tri-*O*-benzyl-β-D-glucopyranoside (3.8):

The lactoside **3.7** (0.52 g, 1.46 mmol) was dissolved in dry DMF (15 ml) to which $PhCH(OCH_3)_2$ (0.23 ml, 1.46mmol) was added followed by a catalytic amount of CSA (20 mg). The reaction proceeded at room temperature for two hours until TLC analysis (30%, methanol-dichloromethane) showed the reaction to be complete. The reaction was cooled to 0°C in an ice-water bath and NaH

(0.59 g, 14.6 mmol) was added. BnBr (1.74 ml, 14.6 mmol) was added slowly and once complete the reaction proceeded at room temperature for six hours. TLC analysis (2:1, hexanes-ethyl acetate) then showed the reaction to be complete. The reaction mixture was diluted with dichloromethane and washed with distilled water and saturated aqueous sodium chloride and concentrated to dryness. The crude product was purified by flash column chromatography on silica gel (4:1 → 3:1, hexanes-ethyl acetate) to give the product **3.8** (0.527 g, 40 %) as a white sticky foam; R_f 0.17 (1:1, hexanes-ethyl acetate); $[\alpha]_D$ +19.4 °(*c* 1.13, $CHCl_3$); ^{1}H NMR (500 MHz, $CDCl_3$) δ 7.52 (m, 2 H, ArH), 7.46 (m, 2 H, ArH), 7.39-7.24 (m, 21 H, ArH), 7.20 (m, 5 H, ArH), 5.46 (s, 1 H, *benzylidene* C-H), 5.18 (d, 1 H, J_{gem} 10.6 Hz, PhCH_2O), 4.88 (d, 1 H, J_{gem} 10.9 Hz, PhCH_2O), 4.85 (d, 1 H, J_{gem} 11.3 Hz, PhCH_2O), 4.75 (m, 5 H, PhCH_2O), 4.56 (d, 1 H, J_{gem} 12.1 Hz, PhCH_2O), 4.46 (d, 1 H, $J_{1',2'}$ 7.9 Hz, H-1'), 4.34 (d, 1 H, J_{gem} 12.1 Hz, PhCH_2O), 4.31 (d, 1 H, $J_{1,2}$ 7.9 Hz, H-1), 4.21 (dd, 1 H, $J_{5',6a'}$ 1.2 Hz, $J_{6a',6b'}$ 12.4 Hz, H-6a'), 4.02 (dd, 1 H, $J_{4',5'}$ 0.6 Hz, $J_{4',5'}$ 3.7 Hz, H-4'), 3.99 (vt, 1 H, $J_{3,4}$ 9.3 Hz, $J_{4,5}$ 9.3 Hz, H-4), 3.89 (dd, 1 H, $J_{5,6a}$ 4.0 Hz, $J_{6a,6b}$ 10.9 Hz, H-6a), 3.84 (dd, 1 H, $J_{5',6b'}$ 1.7 Hz, $J_{6a',6b'}$ 12.4 Hz, H-6b'), 3.77 (dd, 1 H, $J_{1',2'}$ 7.9 Hz, $J_{2',3'}$ 9.6 Hz, H-2'), 3.73 (dd, 1 H, $J_{5,6b}$ 1.6 Hz, $J_{6a,6b}$ 11.1 Hz, H-6b), 3.63 (vt, 1 H, $J_{3,4}$ 9.0 Hz, $J_{2,3}$ 9.0 Hz, H-3), 3.57 (s, 3 H, -OCH_3), 3.43 (dd, 1 H, $J_{1,2}$ 7.9 Hz, $J_{2,3}$ 9.2 Hz, H-2), 3.38 (m, 2 H, $J_{5,6a}$ 4.0 Hz, $J_{5,6b}$ 1.7 Hz, $J_{4,5}$ 9.6 Hz, $J_{3',4'}$ 3.7 Hz, $J_{2',3'}$ 9.6 Hz, H-5, H-3'), 2.93 (m, 1 H, H-5'); ^{13}C NMR (125 MHz, $CDCl_3$) δ 138.9 (Ar), 138.8 (Ar), 138.7 (Ar), 138.6 (Ar), 138.4 (Ar), 138.1 (Ar), 128.8 (Ar), 128.6 (Ar), 128.4 (Ar), 128.3 (Ar), 128.2 (Ar), 128.0 (Ar), 127.9 (Ar), 127.7 (Ar), 127.6 (Ar), 127.5 (Ar), 127.5 (Ar), 127.4 (Ar),

127.3 (Ar), 127.2 (Ar), 126.6 (Ar), 104.7 (C-1), 102.8 (C-1'), 101.4 (*benzylidene* C-H), 82.9 (C-3), 81.9 (C-2), 79.7 (C-3'), 78.8 (C-2'), 77.6 (C-4), 75.7 (PhCH_2O), 75.3 (PhCH_2O), 75.1 (C-5), 74.9 (PhCH_2O), 73.7 (C-4'), 72.9 (PhCH_2O), 71.6 (PhCH_2O), 68.9, 68.3 (C-6, C-6'), 66.3 (C-5'), 57.1 (-OCH_3); ESI HRMS Calcd for $C_{55}H_{58}O_{11}Na$ 917.3871. Found 917.3870. Calcd for $C_{55}H_{58}O_{11}$: C, 73.81; H, 6.53; O, 19.66. Found: C, 74.07; H, 6.78.

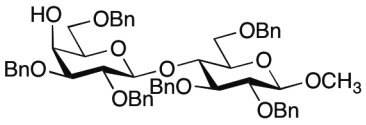

3.4

Methyl 2,3,6-tri-*O*-benzyl-β-D-galactopyranosyl-(1→4)-2,3,6-tri-*O*-benzyl-β-D-glucopyranoside (3.4):

The 4',6'-O-benzylidenyl starting material **3.8** (0.27 g, 0.30 mmol) was dissolved in anhydrous CH_2Cl_2 (8 ml) and cooled to 0°C. Et_3SiH (0.48 ml, 3.03 mmol) was added followed by the slow addition of TFA (0.23 ml, 3.03 mmol). The reaction proceeded at 0°C for 1.5 hours until TLC analysis (1:1, hexanes-ethyl acetate) showed the reaction to be complete. The reaction mixture was diluted with CH_2Cl_2 and washed with saturated aqueous sodium bicarbonate, distilled water and saturated aqueous sodium chloride. The organic layer was dried over anhydrous sodium sulfate, filtered and concentrated. The product was purified by flash column chromatography on silica gel (4:1 → 3:1, hexanes-ethyl acetate) to give the product **3.4** (0.15 g, 56 %) as an off white sticky foam; R_f 0.55 (2:1, hexanes-ethyl acetate); $[\alpha]_D$ +22.6 °(*c* 1.07, $CHCl_3$); ^{1}H NMR (500MHz, $CDCl_3$) δ 7.38 (m, 2 H, ArH), 7.35-7.19 (m, 28 H, ArH), 4.98 (d, 1 H, J_{gem} 10.9

Hz, PhCH_2O), 4.86 (d, 1 H, J_{gem} 10.9 Hz, J_{gem} 11.0 Hz, PhCH_2O), 4.77-4.70 (m, 5 H, J_{gem} 11.7 Hz, J_{gem} 11.0 Hz, J_{gem} 11.8 Hz, PhCH_2O), 4.66 (d, 1 H, J_{gem} 11.7 Hz, PhCH_2O), 4.56 (d, 1 H, J_{gem} 12.1 Hz, PhCH_2O), 4.46-4.38 (m, 4 H, $J_{1',2'}$ 7.6 Hz, J_{gem} 11.0 Hz, J_{gem} 11.8 Hz, J_{gem} 12.1 Hz, H-1'), 4.29 (d, 1 H, $J_{1,2}$ 7.8 Hz, H-1), 4.02 (m, 1 H, $J_{4',OH}$ 2.3 Hz, H-4'), 3.97 (dd, 1 H, $J_{3,4}$ 9.2 Hz, $J_{4,5}$ 9.4 Hz, H-4), 3.81 (dd, 1 H, $J_{5,6a}$ 4.3 Hz, $J_{6a,6b}$ 10.9 Hz, H-6a), 3.73 (dd, 1 H, $J_{5,6b}$ 1.7 Hz, $J_{6a,6b}$ 10.9 Hz, H-6b), 3.65 (dd, 1 H, $J_{5',6a'}$ 7.3 Hz, $J_{6a',6b'}$ 9.7 Hz, H-6a'), 3.60-3.55 (m, 5 H, $J_{1',2'}$ 7.9 Hz, $J_{2',3'}$ 9.3 Hz, $J_{2,3}$ 9.1 Hz, H-3, H-2', OCH_3), 3.47 (dd, 1 H, $J_{5'6b'}$ 5.2 Hz, $J_{6a'6b'}$ 9.6 Hz, H-6b'), 3.41-3.35 (m, 3 H, H-2, H-5, H-3'), 3.31 (m, 1 H, H-5'), 2.38 (d, 1 H, $J_{4',OH}$ 2.3 Hz, 4'O*H*); ^{13}C NMR (125MHz, $CDCl_3$) δ 139.1 (Ar), 138.7 (Ar), 138.6 (Ar), 138.3 (Ar), 138.2 (Ar), 137.9 (Ar), 128.5 (Ar), 128.4 (Ar), 128.3 (Ar), 128.0 (Ar), 127.9 (Ar), 127.8 (Ar), 127.6 (Ar), 127.5 (Ar), 127.4 (Ar), 127.2 (Ar), 104.7 (C-1), 102.5 (C-1'), 82.8 (C-3), 81.9, 81.1 (C-2, C-3'), 79.4 (C-2'), 76.6 (C-4), 75.3 (Ph*C*H_2O), 75.2 (Ph*C*H_2O), 75.1 (C-5), 74.9 (Ph*C*H_2O), 73.5 (Ph*C*H_2O), 73.1 (Ph*C*H_2O), 72.8 (C-5'), 72.0 (Ph*C*H_2O), 68.4, 68.3 (C-6, C-6'), 66.1 (C-4'), 57.0 (-O*C*H_3); ESI HRMS Calcd for $C_{55}H_{60}O_{11}Na$ 919.4028. Found 919.4021. Calcd for $C_{55}H_{60}O_{11}$: C, 73.64; H, 6.74. Found: C, 73.89; H, 6.91.

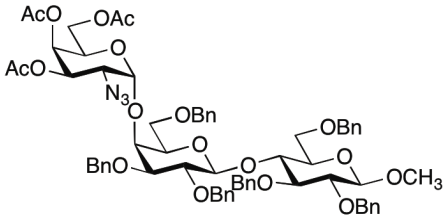

3.9

Methyl 3,4,6-tri-*O*-acetyl-2-azido-2-deoxy-α-D-glactopyranosyl-(1→4)-2,3,6-tri-*O*-benzyl-β-D-galactopyranosyl-(1→4)-2,3,6-tri-*O*-benzyl-β-D-glucopyranoside (3.9):

The acceptor **3.4** (0.14 g, 0.16 mmol) and the trichloroacetimidate donor **3.3** (0.12 g, 0.24 mmol) were combined in a flame-dried flask with pre-activated 4Å molecular sieves (30 mg). The starting materials were dissolved in dry CH_2Cl_2 (2 ml) and allowed to stir at room temperature under argon atmosphere for 45 minutes. The reaction vessel was cooled to -20 °C in a dry ice-acetone bath, and once cool TMSOTf (5.8 μL, 0.032 mmol) was added. The reaction proceeded at -20 °C for ten minutes and was removed from cooling and brought to room temperature. TLC analysis was done (2:1, hexanes-ethyl acetate) and the reaction was found to be complete. The reaction was quenched with Et_3N (1 drop), filtered through Celite and concentrated. The crude product was purified by flash column chromatography on silica gel (4:1 → 2:1, hexanes-ethyl acetate) to give the product **3.9** (0.14 g, 95 %) as a yellow syrup; R_f 0.33 (2:1, hexanes-ethyl acetate); $[\alpha]_D$ +59.0 ° (*c* 0.92, $CHCl_3$); ^{1}H NMR (500MHz, $CDCl_3$) δ 7.40-7.27 (m, 20 H, ArH), 7.26-7.20 (m, 10 H, ArH), 5.38 (dd, 1 H, $J_{4",5"}$ 1.4 Hz, $J_{3",4"}$ 3.2 Hz, H-4"), 4.31 (dd, 1 H, $J_{3",4"}$ 3.3 Hz, $J_{2",3"}$ 11.2 Hz, H-3"), 5.09 (d, 1 H, J_{gem} 11.0 Hz, PhCH_2O), 5.03 (d, 1 H, $J_{1",2"}$ 3.6 Hz, H-1"), 4.89 (d, 1 H, J_{gem} 11.0 Hz, PhCH_2O),

4.85 (m, 2 H, J_{gem} 11.3 Hz, J_{gem} 11.0 Hz, PhCH_2O), 4.74 (d, 1 H, J_{gem} 11.0 Hz, PhCH_2O), 4.69 (m, 3 H, PhCH_2O), 4.64 (ddd, 1 H, $J_{4",5"}$ 1.1 Hz, $J_{5",6b"}$ 5.3 Hz, $J_{5",6a"}$ 8.8 Hz, H-5"), 4.55 (d, 1 H, J_{gem} 12.1 Hz, PhCH_2O), 4.44 (d, 1 H, J_{gem} 11.9 Hz, PhCH_2O), 4.41 (d, 1 H, J_{gem} 12.1 Hz, PhCH_2O), 4.39 (d, 1 H, $J_{1',2'}$ 7.8 Hz, H-1'), 4.33 (d, 1 H, J_{gem} 12.1 Hz, PhCH_2O), 4.28 (d, 1 H, $J_{1,2}$ 7.8 Hz, H-1), 4.10 (d, 1 H, $J_{3',4'}$ 2.9 Hz, H-4'), 3.93 (dd, 1 H, $J_{5",6a"}$ 1.7 Hz, $J_{6a",6b"}$ 9.04 Hz, H-6a"), 3.92 (m, 1 H, $J_{3,4}$ 9.2 Hz, H-4), 3.87 (dd, 1 H, $J_{5,6a}$ 4.0 Hz, $J_{6a,6b}$ 10.9 Hz, H-6a), 3.83 (t, 1 H, $J_{6a',6b'}$ 9.5 Hz, H-6a'), 3.67 (m, 2 H, $J_{5,6b}$ 1.8 Hz, $J_{6a,6b}$ 10.7 Hz, $J_{1",2"}$ 3.6 Hz, $J_{2",3"}$ 11.1 Hz, H-6b, H-2"), 3.63 (dd, 1 H, $J_{1',2'}$ 7.7 Hz, $J_{2',3'}$ 9.9 Hz, H-2'), 3.57 (t, 1 H, $J_{2',3'}$ 9.0 Hz, $J_{3',4'}$ 9.0 Hz, H-3'), 3.55 (s, 3 H, OCH_3), 3.52 (dd, 1 H, $J_{5",6b"}$ 3.3 Hz, $J_{6a",6b"}$ 10.8 Hz, H-6b"), 3.42 (dd, 1 H, $J_{5',6b'}$ 5.3 Hz, $J_{6a',6b'}$ 9.2, H-6b'), 3.38 (dd, 1 H, $J_{1,2}$ 7.8 Hz, $J_{2,3}$ 9.2 Hz, H-2), 3.34 (ddd, 1 H, $J_{5,6b}$ 1.8 Hz, $J_{5,6a}$ 3.9 Hz, $J_{4,5}$ 9.8 Hz, H-5), 3.27 (dd, 1 H, $J_{5',6b'}$ 5.4 Hz, $J_{5',6a'}$ 9.7 Hz, H-5'), 3.25 (dd, 1 H, $J_{3',4'}$ 3.0 Hz, $J_{2',3'}$ 10.0 Hz, H-3'), 2.10 (s, 3 H, CH_3C(O)O), 1.99 (s, 3 H, CH_3C(O)O), 1.85 (s, 3 H, CH_3C(O)O); ^{13}C NMR (125MHz, $CDCl_3$) δ 170.1 (CH$_3$*C*(O)O), 170.0 (CH$_3$*C*(O)O), 169.7 (CH$_3$*C*(O)O), 139.4 (Ar), 138.7 (Ar), 138.5 (Ar), 138.4 (Ar), 138.0 (Ar), 137.7 (Ar), 128.5 (Ar), 128.4 (Ar), 128.3 (Ar), 128.2(2) (Ar), 128.2(1) (Ar), 128.0 (Ar), 127.9(8) (Ar), 128.9(4) (Ar), 127.8(5) (Ar), 127.8(2) (Ar), 127.7 (Ar), 127.6 (Ar), 127.5 (Ar), 127.4 (Ar), 127.3 (Ar), 127.0 (Ar), 104.6 (C-1), 103.4 (C-1'), 98.2 (C-1"), 82.9 (C-3), 81.8 (C-2), 80.2 (C-3'), 79.3 (C-2'), 77.9 (C-4), 75.4 (Ph*C*H$_2$O), 75.2 (Ph*C*H$_2$O), 75.0 (C-5), 74.9 (Ph*C*H$_2$O), 73.3 (Ph*C*H$_2$O), 73.2 (C-4'), 73.1 (Ph*C*H$_2$O), 72.9 (Ph*C*H$_2$O), 72.4 (C-3'), 68.8 (C-3"), 68.1 (C-6), 67.3 (C-4"), 66.6 (C-6'), 66.1 (C-5"), 60.3 (C-6"), 58.2

(C-2"), 57.1 (O*C*H_3), 20.66 (*C*H_3C(O)O), 20.63 (*C*H_3C(O)O), 20.5 (*C*H_3C(O)O); ESI HRMS Calcd for $C_{67}H_{75}N_3O_{18}Na$ 1232.4938. Found 1232.4935.

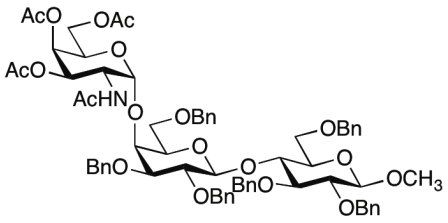

3.10

Methyl 2-Acetimido-3,4,6-tri-*O*-acetyl-2-deoxy-α-D-glactopyranosyl-(1→4)-3,6-tri-*O*-benzyl-β-D-galactopyranosyl-(1→4)-2,3,6-tri-*O*-benzyl-β-D-glucopyranoside (3.10):

The azide **3.9** (0.020 g, 16.52 μmol) was dissolved in a mixture of Pyr:water:Et_3N (10:1:0.3). H_2S gas was bubbled through the solution for one hour after which the addition of H_2S was ceased and the reaction proceeded overnight at room temperature. TLC analysis (1:1, hexanes-ethyl acetate) showed no remaining starting material and the contents of the flask diluted with toluene and concentrated to dryness while co-evaporating with toluene (3 x 10 ml). The crude amine intermediate was dissolved in pyridine (4 ml) and Ac_2O (4 ml) and the reaction proceeded overnight. TLC analysis (1:1, hexanes-ethyl acetate) was done and the reaction was found to be complete. The crude product was concentrated to dryness and purified by flash column chromatography on silica gel (30 % → 50 %, ethyl acetate-hexanes) to give the product **3.10** (0.017 g, 85 %) as an off white sticky foam; R_f 0.28 (1:1, hexanes-ethyl acetate); $[\alpha]_D$ +47.4 °(*c* 1.16, $CHCl_3$); ^{1}H NMR (500MHz, $CDCl_3$) δ 7.39-7.20 (m, 30 H, ArH), 5.63 (d, 1 H, $J_{NH,2"}$ 9.9 Hz,

N-H), 5.33 (m, 1 H, H-4''), 5.18 (dd, 1 H, $J_{3'',4''}$ 3.1 Hz, $J_{2'',3''}$ 11.5 Hz, H-3''), 5.08 (d, 1 H, $J_{1'',2''}$ 3.5 Hz, H-1''), 5.03 (d, 1 H, J_{gem} 12.5 Hz, PhCH_2O), 4.88 (d, 1 H, J_{gem} 11.4 Hz, PhCH_2O), 4.84 (d, 1 H, J_{gem} 11.1 Hz, PhCH_2O), 4.78 (m, 3 H, J_{gem} 11.2 Hz, J_{gem} 12.5 Hz, J_{gem} 12.5 Hz, PhCH_2O), 4.69 (d, 1 H, J_{gem} 12.4 Hz, PhCH_2O), 4.61 (m, 2 H, J_{gem} 11.2 Hz, PhCH_2O, H-5''), 4.56 (m, 2 H, J_{gem} 12.4 Hz, PhCH_2O, H-2''), 4.47 (d, 1 H, J_{gem} 11.8 Hz, PhCH_2O), 4.44 (d, 1 H, $J_{1',2'}$ 7.8 Hz, H-1'), 4.35 (d, 1 H, J_{gem} 12.1 Hz, PhCH_2O), 4.31 (d, 1 H, J_{gem} 11.8 Hz, PhCH_2O), 4.26 (d, 1 H, $J_{1,2}$ 7.7 Hz, H-1), 4.12 (d, 1 H, $J_{3',4'}$ 2.9 Hz, H-4'), 3.96 (m, 2 H, $J_{3,4}$ 3.1 Hz, H-4, H-6a''), 3.85 (dd, 1 H, $J_{5,6a}$ 4.0 Hz, $J_{6a,6b}$ 11.1 Hz, H-6a), 3.68 (dd, 1 H, $J_{5,6b}$ 1.6 Hz, $J_{6a,6b}$ 11.0 Hz, H-6b), 3.64 (dd, 1 H, $J_{1',2'}$ 7.8 Hz, $J_{2',3'}$ 9.9 Hz, H-2'), 3.61 (dd, 1 H, $J_{5'',6b''}$ 5.4 Hz, $J_{6a'',6b''}$ 10.8 Hz, H-6b''), 3.56 (dd, 1 H, $J_{2,3}$ 8.9 Hz, $J_{3,4}$ 8.9 Hz, H-3), 3.54 (s, 3 H, OCH_3), 3.47 (dd, 1 H, $J_{5',6a'}$ 5.9 Hz, $J_{6a',6b'}$ 9.2 Hz, H-6a'), 3.40 (m, 2 H, H-2, H-6b'), 3.32 (ddd, 1 H, $J_{5,6b}$ 1.7 Hz, $J_{5,6a}$ 3.7 Hz, $J_{4,5}$ 9.7 Hz, H-5), 3.25 (m, 2 H, $J_{3',4'}$ 3.0 Hz, $J_{2',3'}$ 9.8 Hz, $J_{5',6a'}$ 5.8 Hz, $J_{5',6b'}$ 10.5 Hz, H-3', H-5'), 2.11 (s, 3H, CH_3C(O)O), 1.99 (s, 3H, CH_3C(O)O), 1.86 (s, 3H, CH_3C(O)O), 1.42 (s, 3H, CH_3C(O)NH); ^{13}C NMR (125MHz, $CDCl_3$) δ 170.8 (CH$_3$*C*(O)O), 170.4 (CH$_3$*C*(O)O), 170.0 (CH$_3$*C*(O)O), 169.9 (CH$_3$*C*(O)NH), 139.3 (Ar), 138.5 (Ar), 138.3 (Ar), 137.9 (Ar), 137.3 (Ar), 128.6 (Ar), 128.4 (Ar), 128.3 (Ar), 128.0 (Ar), 127.9 (Ar), 127.8 (Ar), 127.6 (Ar), 127.5 (Ar), 127.3 (Ar), 126.9 (Ar), 104.6 (C-1), 103.2 (C-1'), 98.1 (C-1''), 81.9 (C-2, C-3), 80.3 (C-3'), 79.4 (C-2'), 75.2 (C-4, C-5'), 74.9 (C-5), 74.7 (Ph*C*H$_2$O), 73.9 (Ph*C*H$_2$O), 73.4 (Ph*C*H$_2$O), 73.1 (Ph*C*H$_2$O), 73.0 (Ph*C*H$_2$O), 72.6 (C-4'), 72.2 (C-3''), 68.2 (C-6), 67.1 (C-4''), 66.6 (C-6'), 66.4 (C-5''), 60.9 (C-6''), 57.0 (O*C*H$_3$), 47.7 (C-2''), 22.6

($CH_3C(O)NH$), 20.8 ($CH_3C(O)O$), 20.8 ($CH_3C(O)O$), 20.6 ($CH_3C(O)O$); ESI HRMS Calcd for $C_{69}H_{79}NO_{19}Na$ 1248.5139. Found 1248.5116. Calcd for $C_{69}H_{79}NO_{19}$: C, 67.58; H, 6.49; N, 1.14. Found: C, 67.28; H, 6.54; N, 1.24.

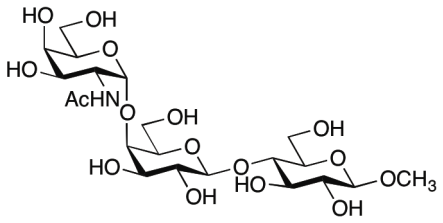

3.1

Methyl 2-acetimido-2-deoxy-α-D-galactopyranosyl-(1→4)-β-D-galactopyranosyl-(1→4)-β-D-glucopyranoside (3.1):

The protected trisaccharide **3.10** (0.066 g, 0.054 mmol) was dissolved in anhydrous CH_3OH (6 ml) and placed under argon atmosphere. A catalytic amount of Na metal was placed in the solvent and the reaction proceeded at room temperature for one hour at which point TLC analysis (10 %, methanol-dichloromethane) showed no remaining starting material. The reaction mixture was concentrated to dryness and the deacetylated trisaccharide intermediate was used directly in the next step. Liquid NH_3 was collected at -30 °C (10 ml) in a separate flask to which Na metal was added until a blue color persisted. The crude intermediate was dissolved in THF (3 ml) and added slowly to the stirring $Na/NH_{3(l)}$ solution. The reaction proceeded for 30 minutes at which point the reaction was neutralized by the addition of NH_4Cl until blue color disappeared. The $NH_{3(l)}$ was allowed to evaporate at room temperature and placed under high vacuum to ensure its removal. The crude residue was dissolved in D_2O, and

filtered through a Millipore cartridge (Millipore Millex-HV Hydrophylic PVDF 0.45μm) and the reaction checked progress checked by ^{1}H NMR spectroscopy and was found to be complete. The crude product was lyophilized and subsequently purified by Gel permeation chromatography on a Sephadex G-10 column and lyophilized to give the product **3.1** (0.0237 g, 78 %) as a white powder; $[\alpha]_D$ +102.7 °(*c* 0.59, $CHCl_3$); ^{1}H NMR (500MHz, $CDCl_3$) δ 4.90 (d, 1 H, $J_{1",2"}$ 3.9 Hz, H-1"), 4.51 (d, 1 H, $J_{1',2'}$ 7.7 Hz, H-1'), 4.40 (m, 2 H, $J_{1,2}$ 7.9 Hz, H-1, H-5"), 4.20 (dd, 1 H, $J_{1",2"}$ 3.9 Hz, $J_{2",3"}$ 11.2 Hz, H-2"), 4.05 (m, 1 H, $J_{3",4"}$ 3.1 Hz, H-4"), 4.01 (m, 2 H, H-6a, H-4'), 3.98 (dd, 1 H, $J_{3",4"}$ 3.3 Hz, $J_{2",3"}$ 11.5 Hz, H-2"), 3.83 (dd, 1 H, $J_{5,6b}$ 5.2 Hz, $J_{6a,6b}$ 12.2 Hz, H-6b), 3.77 (m, 1 H, H-5'), 3.73 (m, 5 H, H-3', H-6ab', H-6ab"), 3.66 (m, 2 H, H-3, H-4), 3.61 (m, 2 H, H-5, H-2'), 3.58 (s, 3 H, OC*H*$_3$), 3.32 (t, 1 H, $J_{1,2}$ 8.4 Hz, $J_{2,3}$ 8.4 Hz, H-2), 2.08 (s, 3 H, C*H*$_3$C(O)NH); ^{13}C NMR (125MHz, $CDCl_3$) δ 175.3 (CH_3C(O) NH), 104.1 (C-1), 103.9 (C-1'), 99.2 (C-1"), 79.4 (C-4), 77.4 (C-4'), 76.5 (C-5'), 75.7 (C-5), 75.3 (C-3), 73.7 (C-2), 72.9 (C-3'), 71.7 (C-2'), 71.6 (C-5"), 69.0 (C-4"), 68.0 (C-3"), 61.3, 61.3, 60.9 (C-6, C-6', C-6"), 58.0 (O*C*H$_3$), 50.9 (C-2"), 22.8 (*C*H$_3$C(O)NH); ESI HRMS Calcd for $C_{21}H_{37}NO_{16}Na$ 582.2005. Found 582.1997.

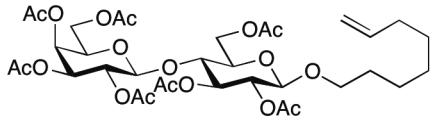

3.16

7-Octenyl 2,3,4,6-tetra-*O*-acetyl-β-D-galactopyranosyl-(1→4)-2,3,6-tri-O-acetyl-β-D-glucopyranoside (3.16):

Peracetylated lactose (10.5 g, 0.016 mol) was dissolved in anhydrous CH_2Cl_2 (60 ml) and placed under argon atmosphere. 7-Octen-1-ol (4.8 ml, 0.032 mol) was added to the solution followed by the drop wise addition of $BF_3 \bullet OEt_2$ (3.9 ml, 0.032 mol). The reaction proceeded at room temperature over night until TLC analysis (1:2, hexanes-ethyl acetate) showed no remaining starting material. The reaction was diluted with CH_2Cl_2 and washed with saturated aqueous sodium bicarbonate, distilled water and saturated aqueous sodium chloride. The organic layer was dried over anhydrous sodium sulfate, filtered and concentrated to dryness. The crude product was purified by flash column chromatography on silica gel (1:1, hexanes-ethyl acetate) to give the product **3.16** (5.39 g, 45 %) as a white foam; R_f 0.44 (1:1, hexanes-ethyl acetate); $[\alpha]_D$ -5.3 °(*c* 1.08, $CHCl_3$); ^1H NMR (500 MHz, $CDCl_3$) δ 5.78 (dddd, 1 H, J_1 6.7 Hz, J_2 6.7 Hz, J_3 10.3 Hz, J_4 16.9 Hz, -C*H*=CH_2), 5.34 (m, 1 H, $J_{4',5'}$ 0.8 Hz, $J_{3',4'}$ 3.3 Hz, H-4'), 5.18 (t, 1 H, $J_{2,3}$ 9.4 Hz, $J_{3,4}$ 9.4 Hz, H-3), 5.10 (dd, 1 H, $J_{1',2'}$ 7.9 Hz, $J_{2',3'}$ 10.4 Hz, H-2'), 4.99-4.91 (m, 3 H, $J_{3',4'}$ 3.5 Hz, $J_{2',3'}$ 10.5 Hz, H-3', -CH=CH_2), 4.87 (dd, 1 H, $J_{1,2}$ 7.8 Hz, $J_{2,3}$ 9.5 Hz, H-2), 4.48-4.43 (m, 3 H, $J_{1',2'}$ 7.9 Hz, $J_{1,2}$ 7.9 Hz, H-1, H-6a, H-1'), 4.14-4.05 (m, 3 H, H-6b, H-6a'b'), 3.86 (m, 1 H, H-5'), 3.80 (m, 2 H, H-4, -OCH_2-), 3.58 (ddd, 1 H, H-5), 3.44 (m, 1 H, -OCH_2-), 2.14 (s, 3 H, CH_3C(O)O), 2.10 (s, 3 H, CH_3C(O)O), 2.05 (s, 3 H, CH_3C(O)O), 2.04 (s, 6 H, CH_3C(O)O), 2.02 (m, 5 H,

C*H*$_3$C(O)O, -C*H*$_2$CH=CH$_2$), 1.96 (s, 3 H, C*H*$_3$C(O)O), 1.54 (m, 2 H, -OC*H*$_2$C*H*$_2$-), 1.32 (m, 6 H, -C*H*$_2$C*H*$_2$C*H*$_2$-); ^{13}C NMR (125 MHz, $CDCl_3$) δ 170.4 (CH3C(O)O), 170.1 (CH3C(O)O), 170.0 (CH$_3$*C*(O)O), 169.8 (CH$_3$*C*(O)O), 169.6 (CH$_3$*C*(O)O), 169.0 (CH$_3$*C*(O)O), 138.9 (-*C*H=CH$_2$), 114.3 (-CH=*C*H$_2$), 101.1 (C-1'), 100.6 (C-1), 76.3 (C-4) 72.9, 72.6 (C-3, C-5), 71.8 (C-2), 70.9, 70.7 (C-3', C-5'), 70.1 (-O*C*H$_2$-), 69.1 (C-2'), 66.6 (C-4'), 62.1 (C-6), 60.8 (C-6'), 33.7, 29.3, 28.2, 28.7, 25.6 (-CH$_2$-), 20.8 (*C*H$_3$C(O)O), 20.6 (*C*H$_3$C(O)O), 20.5 (*C*H$_3$C(O)O); ESI HRMS Calcd for $C_{34}H_{50}O_{18}Na$ 769.2889. Found 769.2879. Calcd for $C_{34}H_{50}O_{18}$: C, 54.69; H, 6.75. Found: C, 54.76; H, 6.78.

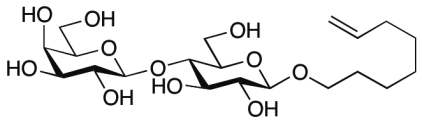

3.17

7-Octenyl β-D-galactopyranosyl-(1→4)-β-D-glucopyranoside (3.17):

The peracetylated lactoside **3.16** (2.45 g, 3.28 mmol) was dissolved in anhydrous CH_3OH (50 ml) and placed under argon atmosphere. A catalytic amount of Na metal was added and the reaction proceeded overnight. Subsequent TLC analysis (30%, methanol-dichloromethane) showed the reaction to be complete. The reaction mixture was neutralized using Amberlyst IR-120 ion exchange resin (H^+) and filtered. The crude reaction solution was concentrated to dryness and lyophilized to give the crude product **3.17** (1.38 g, 93 %) as a soft white solid; R_f 0.36 (30 %, methanol-dichloromethane); $[\alpha]_D$ +0.71 °(*c* 1.04, D_2O); ^{1}H NMR (500 MHz, D_2O) δ 6.00 (dddd, 1 H, J_1 6.6 Hz, J_2 6.6 Hz, J_3 10.3 Hz, J_4 16.9 Hz, -C*H*=CH$_2$), 5.13 (m, 1 H, -CH=C*H*$_2$), 5.05 (m, 1 H, -CH=C*H*$_2$),

4.55 (d, 1 H, $J_{1',2'}$ 7.8 Hz, H-1'), 4.52 (d, 1 H, $J_{1,2}$ 7.8 Hz, H-1), 4.05 (dd, 1 H, $J_{5,6a}$ 1.3 Hz, $J_{6a,6b}$ 12.3 Hz, H-6a), 3.99 (m, 2 H, $J_{3,4}$ 4.4 Hz, H-4, -OCH_2-), 3.88 (m, 2 H, H-6b, H-4'), 3.85-3.77 (m, 4 H, H-3, H-3', -OCH_2-), 3.66 (m, 1 H, H-5), 3.62 (dd, 1 H, J1,2 7.8 Hz, J2,3 9.9 Hz, H-2), 3.38 (m, 1 H, H-2'), 2.14 (m, 2 H, -CH_2CH=CH_2), 1.70 (m, 2 H, -OCH_2CH_2-), 1.45 (m, 6 H, -CH_2CH_2CH_2-); ^{13}C NMR (125 MHz, D_2O) δ 141.2 (-*C*H=CH_2), 114.9 (-CH=*C*H_2), 103.8 (C-1), 102.9 (C-1'), 79.3 (C-5') 76.2 (C-5'), 75.6 (C-5), 75.3 (C-3'), 73.7 (C-2'), 73.4 (C-3), 71.8 (C-2), 71.6 (-O*C*H_2), 69.4 (C-4), 61.9 (C-6'), 60.9 (C-6), 33.9, 29.5, 28.9, 28.9, 25.7 (-CH_2-); ESI HRMS Calcd for $C_{11}H_{36}O_{11}Na$ 475.2150. Found 475.2147.

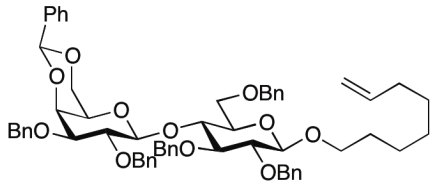

3.18

7-Octenyl 2,3-di-*O*-benzyl-4,6-*O*-benzylidene-β-D-galactopyranosyl-(1→4)-2,3,6-tri-*O*-benzyl–β-D-glucopyranoside (3.18):

The octenyl lactoside **3.17** (1.33 g, 2.94 mmol) was suspended in anhydrous CH_3CN (50 ml). $PhCH(OCH_3)_2$ (0.66 ml, 4.41 mmol) was added followed by a catalytic amount of CSA (100 mg). The reaction proceeded at 30 °C under mildly reduced pressure to remove CH_3OH formed during the reaction. The reaction proceeded for 2.5 hours until TLC analysis (10%, methanol-dichloromethane) showed no remaining starting material. The reaction was quenched with Et_3N and concentrated to dryness. The intermediate benzylidene

was dissolved in dry DMF (30 ml) and 60 % NaH in mineral oil dispersion (1.18 g, 29.4 mmol) was added. The reaction was stirred under argon atmosphere for 10 min after which BnBr (3.5 ml, 29.4 mmol) was added drop-wise. The reaction proceeded overnight and after 12 hours, TLC analysis (2:1, hexanes-ethyl acetate) showed the reaction to be complete. The contents were transferred to a separatory funnel and diluted with ethyl acetate. The organic layer was washed with saturated aqueous sodium chloride, distilled water and dried over anhydrous sodium sulfate. The crude product was purified by flash column chromatography on silica gel (3:1 hexanes-ethyl acetate) to provide the product **3.18** (1.98 g, 68 %) as a white foam; R_f 0.59 (2:1, hexanes-ethyl acetate); $[\alpha]_D$ +9.4 °(*c* 1.00, $CHCl_3$); ^{1}H NMR (500 MHz, $CDCl_3$) δ 7.52 (m, 2 H, ArH), 7.46 (m, 2 H, ArH), 7.36 (m, 5 H, ArH), 7.30 (m, 14 H, ArH), 7.20 (m, 9 H, ArH), 5.79 (dddd, 1 H, J_1 6.7 Hz, J_2 6.7 Hz, J_3 10.3 Hz, J_4 16.9 Hz, -C*H*=CH_2), 5.49 (s, 1 H, *benzylidene* C-*H*), 5.17 (d, 1 H, J_{gem} 10.7 Hz, PhCH_2O), 4.98 (m, 1 H, J_1 1.7 Hz, J_2 3.7 Hz, J_3 17.2 Hz, -CH=CH_2), 4.92 (m, 2 H, -CH=CH2), 4.84 (d, 1 H, J_{gem} 10.9 Hz, PhCH_2O), 4.78 (d, 1 H, J_{gem} 11.3 Hz, PhCH_2O), 4.74 (m, 2 H, J_{gem} 10.7 Hz, J_{gem} 10.9 Hz, PhCH_2O), 4.72 (bs, 2 H, PhCH_2O), 4.55 (d, 1 H, J_{gem} 12.2 Hz, PhCH_2O), 4.46 (d, 1 H, $J_{1',2'}$ 7.9 Hz, H-1'), 4.37 (d, 1 H, $J_{1,2}$ 7.9 Hz, H-1), 4.34 (d, 1 H, J_{gem} 12.1 Hz, PhCH_2O), 4.20 (dd, 1 H, $J_{5',6a'}$ 1.2 Hz, $J_{6a',6b'}$ 12.5 Hz, H-6a'), 4.02 (dd, 1 H, $J_{3',4'}$ 3.7 Hz, H-4'), 3.94 (m, 2 H, J_{gem} 9.3 Hz, H-4, -OC$H_2$$CH_2$-), 3.85 (m, 2 H, $J_{5,6a}$ 4.3 Hz, $J_{6a,6b}$ 10.9 Hz, $J_{5'6b'}$ 1.7 Hz, $J_{6a',6b'}$ 12.4 Hz, H-6a, H-6b'), 3. 76 (d, 2 H, $J_{1',2'}$ 7.9 Hz, $J_{2',3'}$ 9.6 Hz, H-2'), 3.72 (dd, 1 H, $J_{5,6b}$ 1.6 Hz, $J_{6a,6b}$ 10.9 Hz, H-6b), 3.62 (vt, 1 H, $J_{3,4}$ 9.1 Hz, $J_{2,3}$ 9.1 Hz, H-3), 3.51 (dt, 1 H, $J_{H,CH2}$ 6.9 Hz, J_{gem} 9.1 Hz, -

OC*H*$_2$CH$_2$-), 3.43 (dd, 1 H, $J_{1,2}$ 7.9 Hz, $J_{2,3}$ 9.2 Hz, H-2), 3.37 (m, 2 H, $J_{3',4'}$ 3.7 Hz, $J_{2',3'}$ 9.6 Hz, $J_{5,6b}$ 1.6 Hz, $J_{5,6a}$ 4.1 Hz, $J_{4,5}$ 9.9 Hz, H-5, H-3'), 2.93 (bs, 1 H, H-5'), 2.03 (m, 2 H, -C*H*$_2$CH=CH$_2$), 1.64 (m, 2 H, -C*H*$_2$CH=CH$_2$), 1.36 (m, 7/8H, -CH$_2$CH$_2$-); ^{13}C NMR (125 MHz, $CDCl_3$) δ 139.1 (-*C*H=CH$_2$), 139.0 (Ar), 138.9 (Ar), 138.7 (Ar), 138.6 (Ar), 138.4 (Ar), 138.1 (Ar), 128.8 (Ar), 128.5 (Ar), 128.34 (Ar), 128.30 (Ar), 128.2 (Ar), 128.1 (Ar), 128.0 (Ar), 127.7 (Ar), 127.6 (Ar), 127.5 (Ar), 127.4 (Ar), 127.3 (Ar), 127.2 (Ar), 126.6 (Ar), 114.2 (-CH=*C*H$_2$), 103.7 (C-1), 102.9 (C-1'), 101.3 (*benzylidene C*-H), 83.1 (C-3), 81.9 (C-2), 79.7 (C-3'), 78.8 (C-2'), 77.7 (C-4'), 75.7 (Ph*C*H$_2$O), 75.3 (Ph*C*H$_2$O), 75.1 (C-5), 74.9 (Ph*C*H$_2$O), 73.7 (C-4'), 72.9 (Ph*C*H$_2$O), 71.6 (Ph*C*H$_2$O), 70.0 (C-6), 68.9 (C-6'), 86.4 (-O*C*H$_2$CH$_2$-), 66.4 (C-5'), 33.7 (-CH$_2$-), 29.7 (-CH$_2$-), 28.9 (-CH$_2$-), 28.8 (-CH$_2$-), 26.0 (-CH$_2$-); ESI HRMS Calcd for $C_{62}H_{70}O_{11}Na$ 1013.4810. Found 1013.4806. Calcd for $C_{62}H_{70}O_{11}$: C, 75.13; H, 7.12. Found: C, 75.09; H, 7.49.

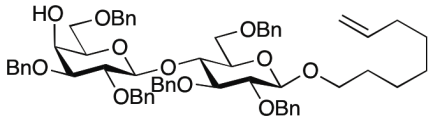

3.15

7-Octenyl 2,3,6-tri-*O*-benzyl-β-D-galactopyranosyl-(1→4)-2,3,6-tri-*O*-benzyl–β-D-glucopyranoside (3.15):

The benzylidene **3.18** (0.166 g, 0.169 mmol) was dissolved in anhydrous CH_2Cl_2 (5 ml) and the reaction vessel placed under argon atmosphere. Et_3SiH (0.27 ml, 1.68 mmol) was added and the reaction cooled to 0 °C while stirring in an ice-water bath. TFA (0.13 ml, 1.68 mmol) was added and the proceeded at 0

°C for 1.5 hours until TLC analysis (2:1, hexanes-ethyl acetate) showed the reaction to be complete. The reaction mixture was transferred to a separatory funnel and washed with saturated aqueous sodium bicarbonate, distilled water, and saturated aqueous sodium chloride. The organic layer was dried over anhydrous sodium sulfate, filtered and concentrated to dryness. The product was purified by flash column chromatography on silica (4:1, hexanes-ethyl acetate) to provide the product **3.15** (0.120 g, 72 %) as a white film; R_f 0.61 (2:1, hexanes-ethyl acetate); $[\alpha]_D$ +16.7 °(*c* 1.06, $CHCl_3$); ^{1}H NMR (500 MHz, $CDCl_3$) δ 7.38 (m, 2 H, ArH), 7.34-7.20 (m, 28 H, ArH), 5.79 (dddd, 1 H, J_1 6.7 Hz, J_2 6.7 Hz, J_3 10.3 Hz, J_4 16.9 Hz, -C*H*=CH_2), 4.98 (m, 2 H, J_{gem} 10.7 Hz, PhCH_2O, -CH=CH_2), 4.93 (m, 1 H, -CH=CH2), 4.89 (d, 1 H, J_{gem} 10.9 Hz, PhCH_2O), 4.76 (m, 3 H, PhCH_2O), 4.71 (m, 2 H, J_{gem} 11.6 Hz, J_{gem} 10.5 Hz, PhCH_2O), 4.66 (d, 1 H, J_{gem} 11.7 Hz, PhCH_2O), 4.55 (d, 1 H, J_{gem} 12.2 Hz, PhCH_2O), 4.44 (m, 2 H, $J_{1',2'}$ 7.8 Hz, J_{gem} 11.9 Hz, H-1', PhCH_2O), 4.39 (m, 2 H, J_{gem} 12.1 Hz, J_{gem} 12.0 Hz, PhCH_2O), 4.36 (d, 1 H, $J_{1,2}$ 7.8 Hz, H-1), 4.01 (m, 1 H, H-4'), 3.93 (m, 2 H, H-4, -OC$H_2$$CH_2$-), 3.79 (dd, 1 H, $J_{5,6a}$ 4.5 Hz, $J_{6a,6b}$ 10.9 Hz, H-6a), 3.72 (dd, 1 H, $J_{5,6b}$ 1.7 Hz, $J_{6a,6b}$ 10.9 Hz, H-6b), 3.65 (dd, 1 H, $J_{5',6a'}$ 7.2 Hz, $J_{6a',6b'}$ 9.6 Hz, H-6a'), 3.57 (m, 2 H, $J_{1',2'}$ 7.9 Hz, $J_{2',3'}$ 9.3 Hz, $J_{2,3}$ 8.9 Hz, $J_{3,4}$ 8.9 Hz, H-3, H-2'), 3.50 (m, 1 H, -OC$H_2$$CH_2$-), 3.47 (dd, 1 H, $J_{5',6b'}$ 5.1 Hz, $J_{6a',6b'}$ 9.6 Hz, H-6b'), 3.38 (m, 3 H, $J_{1,2}$ 7.8 Hz, $J_{2,3}$ 9.2 Hz, $J_{3',4'}$ 3.3 Hz, $J_{2',3'}$ 9.4 Hz, H-2, H-5, H-3'), 3.31 (m, 1 H, H-5'), 2.38 (d, 1 H, $J_{4',OH}$ 2.4 Hz, 4'-OH), 2.03 (m, 2 H, -OCH_2CH_2-), 1.64 (m, 2 H, -CH_2CH=CH_2), 1.36 (m, 6H, -CH_2CH_2-); ^{13}C NMR (125 MHz, $CDCl_3$) δ 139.2 (Ar), 139.0 (-*C*H_2=CH_2), 138.7 (Ar), 138.6 (Ar), 138.4 (Ar), 138.2 (Ar), 137.9

(Ar), 128.5 (Ar), 128.4 (Ar), 128.2 (Ar), 128.0 (Ar), 127.8 (Ar), 127.58 (Ar), 127.50 (Ar), 127.4 (Ar), 127.2 (Ar), 114.2 (-CH=*C*H_2), 103.6 (C-1), 102.5 (C-1'), 82.9 (C-3), 81.8 (C-2), 81.2 (C-3'), 79.4 (C-2'), 76.7 (C-4), 75.3 (Ph*C*H_2O), 75.2 (Ph*C*H_2O), 75.1 (C-5), 74.9 (Ph*C*H_2O), 73.5 (Ph*C*H_2O), 73.1 (Ph*C*H_2O), 72.8 (C-5'), 72.0 (Ph*C*H_2O), 69.9 (-O*C*H_2CH_2-), 68.4 (C-6), 68.3 (C-6'), 66.2 (C-4'), 33.7 (-*C*H_2CH=CH_2), 29.7 (-OCH_2*C*H_2-), 28.9 (-CH_2-), 28.8 (-CH_2-), 26.0 (-CH_2-); ESI HRMS Calcd for $C_{62}H_{72}O_{11}Na$ 1015.4967. Found 1015.4961. Calcd for $C_{62}H_{72}O_{11}$: C, 74.97; H, 7.31. Found: C, 74.97; H, 7.50.

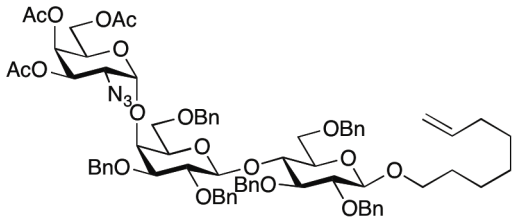

3.14

7-Octenyl 3,4,6-tri-*O*-acetyl-2-azido-2-deoxy-α-D-galactopyranosyl-(1→4)-2,3,6-tri-*O*-benzyl-β-D-galactopyranosyl-(1→4)-2,3,6-tri-*O*-benzyl–β-D-glucopyranoside (3.14):

The acceptor **3.15** (1.16 g, 1.17 mmol) and the 2-azido-2-deoxy-galactosyl trichloroacetimidate donor **3.3** (0.833 g, 1.75 mmol) were combined with pre-activated 4Å molecular sieves (1.0 g) and the contents dissolved in anhydrous Et_2O (10 ml). The contents were stirred under argon atmosphere for one hour to ensure dry conditions. TMSOTf (0.042 ml, 0.234 mmol) was added and the reaction proceeded at room temperature for 30 min until TLC analysis (2:1, hexanes-ethyl acetate) showed the reaction to be complete. The reaction was

neutralized with Et_3N (3 drops) and filtered through Celite. The filtrate was concentrated to dryness and subsequently purified by flash column chromatography on silica gel (10 %, ethyl acetate-toluene) to give the product **3.14** (1.395 g, 91 %) as a clear colorless syrup; R_f 0.48 (2:1, hexanes-ethyl acetate); $[\alpha]_D$ +62.7 °(*c* 0.53, $CHCl_3$); ^{1}H NMR (500 MHz, $CDCl_3$) δ 7.30 (m, 30 H, ArH), 5.82 (dddd, 1 H, J_1 6.7 Hz, J_2 6.7 Hz, J_3 10.3 Hz, J_4 16.9 Hz, -C*H*=CH_2), 5.40 (dd, 1 H, $J_{4'',5''}$ 1.4 Hz, $J_{3'',4''}$ 3.2 Hz, H-4''), 5.33 (dd, 1 H, $J_{3'',4''}$ 3.2 Hz, $J_{2'',3''}$ 11.2 Hz, H-3''), 5.11 (d, 1 H, J_{gem} 11.1 Hz, PhC*H*$_2$O), 5.05 (d, 1 H, $J_{1'',2''}$ 3.6 Hz, H-1''), 5.00 (m, 1 H, -CH=C*H*$_2$), 4.95 (m, 1 H, -CH=C*H*$_2$), 4.90 (m, 2 H, J_{gem} 11.4 Hz, J_{gem} 10.9 Hz, PhC*H*$_2$O), 4.86 (d, 1 H, J_{gem} 10.9 Hz, PhC*H*$_2$O), 4.75 (d, 1 H, J_{gem} 12.3 Hz, PhC*H*$_2$O), 4.71 (m, 3 H, J_{gem} 10.3 Hz, J_{gem} 11.1 Hz, PhC*H*$_2$O), 4.65 (ddd, 1 H, $J_{4'',5''}$ 1.0 Hz, H-5''), 4.56 (d, 1 H, J_{gem} 12.2 Hz, PhC*H*$_2$O), 4.46 (d, 1 H, J_{gem} 11.8 Hz, PhC*H*$_2$O), 4.42 (m, 2 H, J_{gem} 11.6 Hz, $J_{1',2'}$ 7.8 Hz, H-1', PhC*H*$_2$O), 4.36 (m, 2 H, J_{gem} 11.6 Hz, $J_{1,2}$ 7.6 Hz, H-1, PhC*H*$_2$O), 4.12 (d, 1 H, $J_{3',4'}$ 3.0 Hz, H-4'), 3.94 (m, 3 H, H-4, H-6a'', -OC*H*$_2$CH$_2$-), 3.87 (dd, 1 H, $J_{5,6a}$ 4.2 Hz, $J_{6a,6b}$ 6.2 Hz, H-6a), 3.84 (d, 1 H, $J_{6a',6b'}$ 9.6 Hz, H-6a'), 3.67 (m, 3 H, $J_{1',2'}$ 7.8 Hz, $J_{2',3'}$ 9.9 Hz, $J_{5,6b}$ 1.7 Hz, $J_{6a,6b}$ 10.9 Hz, $J_{1'',2''}$ 3.7 Hz, $J_{2'',3''}$ 11.2 Hz, H-6b, H-2', H-2''), 3.58 (vt, 1 H, $J_{2,3}$ 8.9 Hz, $J_{3,4}$ 8.9 Hz, H-3), 3.52 (m, 2 H, H-6b'', -OC*H*$_2$CH$_2$-), 3.43 (dd, 1 H, $J_{5',6b'}$ 5.3 Hz, $J_{6a',6b'}$ 9.2 Hz, H-6b'), 3.40 (dd, 1 H, $J_{1,2}$ 7.9 Hz, $J_{2,3}$ 9.2 Hz, H-2), 3.35 (ddd, 1 H, $J_{5,6b}$ 1.7 Hz, $J_{5,6a}$ 4.0 Hz, $J_{4,5}$ 9.8 Hz, H-5), 3.29 (m, 2 H, $J_{5',6b'}$ 5.3 Hz, $J_{5',6b'}$ 9.6 Hz, $J_{3',4'}$ 3.0 Hz, $J_{2',3'}$ 10.3 Hz, H-3', H-5'), 2.12 (s, 3 H, C*H*$_3$C(O)O), 2.05 (m, 2 H, -CH$_2$-), 2.01 (s, 3 H, C*H*$_3$C(O)O), 1.87 (s, 3 H, C*H*$_3$C(O)O), 1.66 (m, 2 H, -CH$_2$-), 1.38 (m, 6 H, -CH$_2$-); ^{13}C NMR

(125 MHz, $CDCl_3$) δ 170.0 (CH_3C(O)O), 169.7 (CH_3C(O)O), 139.5 (Ar), 139.0 (-CH=CH_2), 138.7 (Ar), 138.5 (Ar), 138.0 (Ar), 137.7 (Ar), 128.5 (Ar), 128.4 (Ar), 128.3 (Ar), 128.2 (Ar), 128.0 (Ar), 127.9 (Ar), 127.8 (Ar), 127.7 (Ar), 127.6 (Ar), 127.5 (Ar), 127.3 (Ar), 127.0 (Ar), 114.2 (-CH=CH$_2$), 103.6 (C-1), 103.4 (C-1'), 98.2 (C-1''), 83.0 (C-3), 81.8 (C-2), 79.4 (C-2'), 78.1 (C-4), 75.4 (PhCH$_2$O), 75.2 (PhCH$_2$O), 75.1 (C-5), 74.9 (PhCH$_2$O), 73.4 (PhCH$_2$O), 73.2 (C-4'), 73.1 (PhCH$_2$O), 72.9 (PhCH$_2$O), 72.4 (C-5'), 70.0 (-OCH$_2$CH$_2$-), 68.9 (C-3''), 68.2 (C-6), 67.3 (C-4''), 66.6 (C-6'), 66.1 (C-5''), 60.6 (C-6''), 58.2 (C-2''), 33.8 (-CH_2-), 29.7 (-CH_2-), 28.9 (-CH_2-), 28.6 (-CH_2-), 20.7 (CH$_3$C(O)O), 20.6 (CH$_3$C(O)O); ESI HRMS Calcd for $C_{74}H_{87}N_3O_{18}Na$ 1328.6877. Found 1328.5875. Calcd for $C_{74}H_{87}N_3O_{18}$: C, 68.03; H, 6.71; N, 3.22. Found: C, 67.94; H, 6.62; N, 3.57.

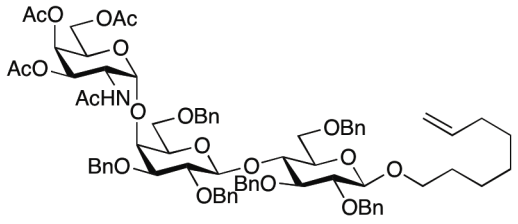

3.19

7-Octenyl 2-acetamido-3,4,6-tri-*O*-acetyl-2-deoxy-α-D-galactopyranosyl-(1→4)-2,3,6-tri-*O*-benzyl-β-D-galactopyranosyl-(1→4)-2,3,6-tri-*O*-benzyl–β-D-glucopyranoside (3.19):

The azide **3.14** (0.516 g, 0.395 mmol) was dissolved in a 5 ml mixture of Pyr:water:Et_3N (10:3:0.3). H_2S gas was bubbled through the stirring solution for one hour, after which the gas was removed and the reaction proceeded for an additional 3.5 hours. Subsequent TLC analysis (2:1, hexanes-ethyl acetate)

showed maximum product formation. The reaction mixture was concentrated to dryness and co-evaporated with toluene (3 x 5 ml). The resulting free amine was acetylated by dissolving the intermediate in a 1:1 mixture of Ac_2O:Pyr (5 ml) and the reaction proceeded for four hours. TLC analysis (1:1, hexanes-ethyl acetate) showed no remaining amine and the mixture was concentrated to dryness and co-evaporated with toluene (3 x 5 ml). The crude product was purified by flash column chromatography on silica gel (1:1, hexanes-ethyl acetate) to give the product **3.19** (0.385 g, 74 %) as an off-white foam; R_f 0.24 (1:1, hexanes-ethyl acetate); $[\alpha]_D$ +44.0 °(*c* 0.41, $CHCl_3$); ^{1}H NMR (500 MHz, $CDCl_3$) δ 7.29 (m, 30 H, ArH), 5.78 (dddd, 1 H, $J_{CH,CH2}$ 6.7 Hz, $J_{CH,CH2}$ 6.7 Hz, J_{cis} 10.2 Hz, J_{trans} 16.9 Hz, -C*H*=CH_2), 5.68 (d, 1 H, $J_{NH,2"}$ 9.7 Hz, N-H), 5.32 (m, 1 H, $J_{4",5"}$ 0.9 Hz, $J_{3",4"}$ 3.0 Hz, H-4"), 5.18 (dd, 1 H, $J_{3",4"}$ 3.2 Hz, $J_{2",3"}$ 11.5 Hz, H-3"), 5.06 (d, 1 H, $J_{1",2"}$ 3.7 Hz, H-1"), 4.99 (m, 2 H, J_{gem} 12.4 Hz, J_{trans} 17.1 Hz, PhCH_2O, -CH=CH_2), 4.92 (m, 1 H, J_{cis} 10.2 Hz, -CH=CH_2), 4.87 (dd, 2 H, J_{gem} 11.4 Hz, J_{gem} 10.9 Hz, PhCH_2O), 4.79 (m, 2 H, J_{gem} 12.4 Hz, PhCH_2O), 4.74 (d, 1 H, J_{gem} 12.4 Hz, PhCH_2O), 4.68 (d, 1 H, J_{gem} 12.4 Hz, PhCH_2O), 4.58 (m, 4 H, J_{gem} 10.9 Hz, J_{gem} 12.2 Hz, $J_{1",2"}$ 3.7 Hz, H-2", H-5", PhCH_2O), 4.44 (m, 2 H, J_{gem} 11.8 Hz, $J_{1',2'}$ 7.7 Hz, H-1', PhCH_2O), 4.33 (m, 2 H, J_{gem} 12.2 Hz, $J_{1,2}$ 7.8 Hz, H-1, PhCH_2O), 4.29 (d, 1 H, J_{gem} 11.8 Hz, PhCH_2O), 4.12 (d, 1 H, $J_{3',4'}$ 3.0 Hz, H-4'), 3.92 (m, 3 H, $J_{5",6a"}$ 8.9 Hz, $J_{6a",6b"}$ 10.9 Hz, H-4, H-6a", -OC$H_2$$CH_2$-), 3.83 (dd, 1 H, $J_{5,6a}$ 4.2 Hz, $J_{6a,6b}$ 10.9 Hz, H-6a), 3.67 (dd, 1 H, $J_{5,6b}$ 1.6 Hz, $J_{6a,6b}$ 10.9 Hz, H-6b), 3.61 (m, 2 H, $J_{1,2}$ 7.8 Hz, H-2', H-6b"), 3.55 (t, 1 H, $J_{2,3}$ 8.9 Hz, $J_{3,4}$ 8.9 Hz, H-3), 3.47 (m, 2 H, H-2, H-6b'), 3.30 (ddd, 1 H, $J_{5,6b}$ 1.6 Hz, $J_{5,6a}$ 3.8 Hz, $J_{5,6}$ 9.7 Hz, H-5), 3.25

(m, 2 H, H-3', H-5'), 2.10 (s, 3 H, C*H*$_3$C(O)O), 2.02 (m, 2 H, -CH_2-), 1.99 (s, 3 H, C*H*$_3$C(O)O), 1.85 (s, 3 H, C*H*$_3$C(O)O), 1.63 (m, 2 H, -CH_2-), 1.42 (s, 3 H, C*H*$_3$C(O)NH), 1.33 (s, 6 H, -CH_2-); ^{13}C NMR (125 MHz, $CDCl_3$) δ 170.8 (CH$_3$*C*(O)O), 170.4 (CH$_3$*C*(O)O), 170.0 (CH$_3$*C*(O)O), 169.9 (CH$_3$*C*(O)NH), 139.4 (Ar), 139.0 (Ar), 138.4 (Ar), 138.35 (Ar), 128.31 (Ar), 137.9 (Ar), 137.3 (Ar) 128.6 (-*C*H=CH$_2$), 128.4 (Ar), 128.3 (Ar), 128.0 (Ar), 127.84 (Ar), 127.80 (Ar), 127.6 (Ar), 127.3 (Ar), 126.9 (Ar), 114.2 (-CH=*C*H$_2$), 103.5, 103.2 (C-1, C-1'), 98.2 (C-1''), 82.0, 81.9 (C-2, C-3), 80.3 (C-3'), 79.4 (C-2'), 77.1 (C-4), 75.1 (PhC*H*$_2$O), 74.9 (C-5), 74.7 (PhC*H*$_2$O), 73.8 (PhC*H*$_2$O), 73.4 (PhC*H*$_2$O), 73.1 (PhC*H*$_2$O), 73.0 (PhC*H*$_2$O), 72.6 (H-5'), 72.2 (H-4'), 69.9 (-OC*H*$_2$CH$_2$-), 68.3 (C-6), 68.2 (C-3''), 67.0 (C-4''), 66.6 (C-6'), 66.3 (C-5''), 60.9 (C-6''), 47.7 (C-2''), 33.7 (-CH_2-), 29.7 (-CH_2-), 28.9 (-CH_2-), 28.8 (-CH_2-), 26.0 (-CH_2-), 22.6 (C*H*$_3$C(O)NH), 20.8 (C*H*$_3$C(O)O), 20.7 (C*H*$_3$C(O)O), 20.6 (C*H*$_3$C(O)O); ESI HRMS Calcd for $C_{76}H_{91}NO_{19}Na$ 1344.6078. Found 1344.6074. Calcd for $C_{76}H_{91}NO_{19}$: C, 69.02; H, 6.94; N, 1.06. Found: C, 69.20; H, 7.13; N, 1.06.

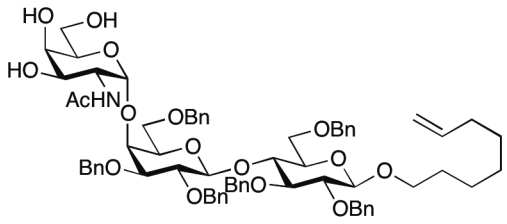

3.20

7-Octenyl 2-acetamido-2-deoxy-α-D-galactopyranosyl-(1→4)-2,3,6-tri-*O*-benzyl-β-D-galactopyranosyl-(1→4)-2,3,6-tri-*O*-benzyl–β-D-glucopyranoside (3.20):

The tri-*O*-acetylated trisaccharide **3.19** (0.385 g, 0.291 mmol) was dissolved in anhydrous CH_3OH (20 ml) and placed under argon atmosphere. A catalytic amount of Na metal was added and the reaction proceeded at room temperature for four hours until TLC analysis (10:1, dichloromethane-methanol) showed the reaction to be complete. The reaction was quenched with DOWEX H^+ ion-exchange resin until pH ~7. The resin was filtered off and the filtrate concentrated to dryness. The crude product was purified by flash column chromatography on silica gel (10:1 dichloromethane-methanol) to provide **3.20** (0.311 g, 89 %) as a clear colorless film; R_f 0.43 (10:1, dichloromethane-methanol); $[\alpha]_D$ +19.7 °(*c* 0.53, $CHCl_3$); ^{1}H NMR (600 MHz, $CDCl_3$) δ 7.37-7.22 (m, 30 H, ArH), 6.24 (d, 1 H, $J_{2",NH}$ 7.8 Hz, N-H), 5.80 (dddd, 1 H, $J_{CH,CH2}$ 6.6 Hz, $J_{CH,CH2}$ 6.6 Hz, J_{cis} 10.1 Hz, J_{trans} 16.9 Hz, -C*H*=CH_2), 4.98 (m, 2 H, J_{gem} 11.8 Hz, -CH=CH_2, PhCH_2O), 4.94 (m, 2 H, $J_{1",2"}$ 4.3 Hz, H-1", -CH=CH_2), 4.88 (d, 1 H, J_{gem} 10.9 Hz, PhCH_2O), 4.80 (m, 2 H, J_{gem} 11.4 Hz, J_{gem} 11.9 Hz, PhCH_2O), 4.75 (d, 1 H, J_{gem} 11.3 Hz, PhCH_2O), 4.70 (d, 1 H, J_{gem} 11.9 Hz, PhCH_2O), 4.66 (m, 2 H, J_{gem} 11.9 Hz, J_{gem} 10.9 Hz, PhCH_2O), 4.56 (d, 1 H, J_{gem} 12.1 Hz, PhCH_2O),

4.45 (d, 1 H, $J_{1',2'}$ 7.7 Hz, H-1'), 4.39 (s, 2 H, PhCH_2O), 4.36 (m, 2 H, $J_{1,2}$ 7.7 Hz, J_{gem} 9.7 Hz, H-1, PhCH_2O), 4.28 (bs, 1 H, OH), 4.21 (ddd, 1 H, $J_{1",2"}$ 3.8 Hz, $J_{2",NH}$ 7.8 Hz, $J_{2",3"}$ 10.9 Hz, H-2"), 4.11 (m, 1 H, H-5"), 4.02 (d, 1 H, $J_{3',4'}$ 2.8 Hz, H-4'), 3.92 (m, 3 H, H-4, H-4", -OCH_2CH_2-), 3.83 (dd, 1 H, $J_{5,6a}$ 4.2 Hz, $J_{6a,6b}$ 11.0 Hz, H-6a), 3.76 (dd, 1 H, $J_{3",4"}$ 2.4 Hz, $J_{2",3"}$ 10.4 Hz, H-3"), 3.70 (dd, 1 H, $J_{5,6b}$ 1.5 Hz, $J_{6a,6b}$ 10.9 Hz, H-6b), 3.57 (m, 4 H, H-3, H-2', -OCH_2CH_2-), 3.50 (dt, 1 H, J_{gem} 9.5 Hz, $J_{CH,CH2}$ 6.8 Hz, -OCH_2CH_2-), 3.41 (m, 3 H, H-2, H-6ab'), 3.34 (ddd, 1 H, $J_{5,6b}$ 1.6 Hz, $J_{5,6a}$ 3.9 Hz, $J_{4,5}$ 9.8 Hz, H-5), 3.25 (m, 2 H, H-3', H-5'), 3.19 (bs, 1 H, OH), 2.47 (bs, 1 H, OH), 2.03 (m, 2 H, -CH_2CH=CH_2), 1.64 (m, 2 H, -OCH$_2$CH_2-), 1.52 (s, 3 H, CH_3C(O)NH), 1.36 (m, 6 H, -CH_2-); ^{13}C NMR (125 MHz, $CDCl_3$) δ 173.1 (*C*H$_3$C(O)NH), 139.3 (Ar), 139.0 (-*C*H=CH$_2$), 138.44 (Ar), 138.40 (Ar), 138.3 (Ar), 137.8 (Ar), 136.9 (Ar), 128.6 (Ar), 128.5 (Ar), 128.3 (Ar), 128.2 (Ar), 128.1 (Ar). 127.9 (Ar), 127.8 (Ar), 127.6 (Ar), 127.5 (Ar), 127.3 (Ar), 127.0 (Ar), 114.2 (-CH=*C*H$_2$), 103.6 (C-1), 103.2 (C-1'), 98.4 (C-1"), 82.3 (C-2'), 81.7 (C-2), 80.8 (C-3'), 79.3 (C-3), 77.1 (C-4), 75.2 (Ph*C*H$_2$O), 74.9 (C-5), 74.8 (Ph*C*H$_2$O), 74.3 (Ph*C*H$_2$O), 73.7 (Ph*C*H$_2$O), 73.1 (Ph*C*H$_2$O), 73.0 (Ph*C*H$_2$O), 72.0 (C-4'), 71.1 (C-5'), 70.1 (C-3"), 70.0 (-O*C*H$_2$CH$_2$-), 69.5 (C-5"), 68.3 (C-6), 66.8 (C-6'), 63.4 (C-6"), 51.4 (C-2), 33.7 (-*C*H$_2$CH=CH$_2$), 29.7 (-OCH$_2$*C*H$_2$-), 28.9 (-CH$_2$-), 28.8 (-CH$_2$-), 26.0 (-CH$_2$-), 22.5 (*C*H$_3$C(O)NH); ESI HRMS Calcd for $C_{70}H_{85}NO_{16}Na$ 1218.5761. Found 1218.5759. Calcd for $C_{70}H_{85}NO_{16}$: C, 70.27; H, 7.16; N, 1.17. Found: C, 70.14; H, 7.15; N, 1.28.

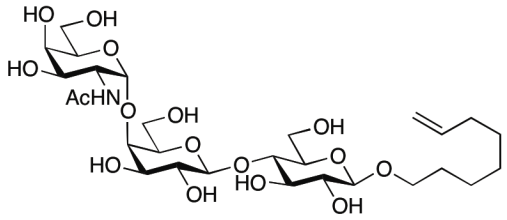

3.13

7-Octenyl 2-acetamido-2-deoxy-α-D-galactopyranosyl-(1→4)-β-D-galactopyranosyl-(1→4)-β-D-glucopyranoside (3.13):

Redistilled $NH_{3(l)}$ (15 ml) was collected in a flask cooled to -78 °C and treated with a small amount of Na until a blue color persisted. A solution of the benzylated trisaccharide **3.20** (0.058 g, 0.0485 mmol) in THF (2 ml) and CH_3OH (12 μL, 0.291 mmol) was added drop-wise and the solution stirred at -78 °C for one hour. The reaction was quenched by the addition of CH_3OH (4 ml) and the $NH_{3(l)}$ allowed to evaporate. The solution diluted with CH_3OH (20 ml) and neutralized with Amberlite IR 120 (H^+) ion exchange resin, filtered and concentrated to dryness. The crude product was filtered through two C18 SepPak cartridges in series (Waters Sep-Pak® Plus C18, 100 % H_2O then 100 % CH_3OH). The CH_3OH was removed under vacuum and the remaining residue was lyophilized to give the product **3.13**. A ^{1}H NMR spectrum of **3.13** was obtained and found to be of good purity and was used directly in the next step; R_f 0.76 (3:3:1:1, dichloromethane:methanol:water:acetic acid); $[\alpha]_D$ +92.0 °(*c* 0.64, H_2O); ^{1}H NMR (600 MHz, $CDCl_3$) δ 5.80 (dddd, 1 H, $J_{CH,CH2}$ 6.6 Hz, $J_{CH,CH2}$ 6.6 Hz, J_{cis} 10.3 Hz, J_{trans} 17.0 Hz, -C*H*=CH_2), 5.05 (m, 1 H, -CH=C*H*$_2$), 4.97 (m, 1 H, -CH=C*H*$_2$), 4.89 (d, 1 H, $J_{1",2"}$ 3.9 Hz, H-1"), 4.50 (d, 1 H, $J_{1',2'}$ 7.8 Hz, H-1'), 4.47 (d, 1 H, $J_{1,2}$ 8.1 Hz, H-1), 4.39 (t, 1 H, $J_{5",6ab"}$ 6.5 Hz, H-5"), 4.19 (dd, 1 H, $J_{1",2"}$

3.9 Hz, $J_{2''3''}$ 11.1 Hz, H-2''), 4.03 (bd, 1 H, $J_{3'',4''}$ 3.1 Hz, H-4''), 3.99-3.95 (m, 3 H, $J_{5,6a}$ 1.9 Hz, $J_{6a,6b}$ 12.7 Hz, $J_{3',4'}$ 3.2 Hz, $J_{2'',3''}$ 11.1 Hz, $J_{3'',4''}$ 3.1 Hz, H-6a, H-4', H-3''), 3.91 (dt, $J_{H,CH2}$ 6.8 Hz, J_{gem} 9.9 Hz, -OCH_2-), 3.81 (dd, 1 H, $J_{5,6b}$ 5.2 Hz, $J_{6a,6b}$ 12.3 Hz, H-6b), 3.76 (m, 1 H, H-5'), 3.72-3.68 (m, 5 H, $J_{2',3'}$ 10.2 Hz, $J_{3',4'}$ 12.3 Hz, H-3', H6ab', H-6ab''), 3.67 (m, 2 H, $J_{3,4}$ 8.9 Hz, H-4, -OCH_2-), 3.63 (t, 1 H, $J_{2,3}$ 8.8 Hz, H-3), 3.58 (m, 2 H, $J_{1',2'}$ 7.7 Hz, $J_{2',3'}$ 10.3 Hz, H-5, H-2'), 3.29 (t, 1 H, $J_{1,2}$ 8.4 Hz, H-2), 2.07 (s, 3 H, CH_3C(O)NH), 2.05 (m, 2 H, -CH_2CH=CH_2), 1.62 (m, 2 H, -OCH$_2$CH_2-), 1.36 (m, 6 H, -CH_2-); ^{13}C NMR (125 MHz, $CDCl_3$) δ 175.4 (CH_3C(O)NH), 141.3 (-CH=CH_2), 114.9 (-CH=CH$_2$), 104.2 (C-1'), 102.9 (C-1), 99.3 (C-1''), 79.6 (C-4), 77.6 (C-4'), 76.7 (C-5'), 75.8, 75.5 (C-3, C-5), 73.9 (C-2), 73.1 (C-3'), 71.8 (C-2'), 71.7 (C-5''), 71.6 (-OCH$_2$-), 69.2 (C-4''), 68.2 (C-3''), 61.5, 61.4 (C-6', C-6''), 61.1 (C-6), 51.1 (C-2''), 33.9 (-CH$_2$CH=CH_2), 29.7 (-OCH$_2C$H$_2$-), 28.9 (-CH_2-), 25.8 (-CH_2-), 22.9 (CH$_3$C(O)NH); ESI HRMS Calcd for $C_{70}H_{85}NO_{16}Na$ 1218.5761. Found 1218.5759.

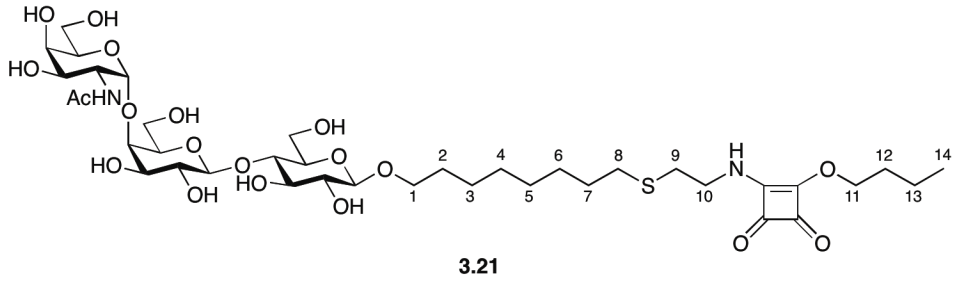

3.21

8-(2-(2-Butoxy-3,4-dioxocyclobut-1-enylamino)ethylthio)octyl 2-acetamido-2-deoxy-α-D-galactopyranosyl-(1→4)-β-D-galactopyranosyl-(1→4)-β-D-glucopyranoside (3.21):

The octenyl trisaccharide **3.13** (0.0323 g, 0.0492 mmol) was placed in a quartz tube to which cysteamine•HCl (0.0012 g, 0.0984 mmol) was added and the starting materials dissolved in degassed MilliQ water (0.5 ml) and the vessel placed under argon atmosphere. The reaction vessel was irradiated with a high intensity UV lamp for 30 minutes at which point TLC analysis (3:3:1:1, dichloromethane:methanol:water:acetic acid) was done and showed maximum product formation. Sodium bicarbonate (0.017 g, 0.197 mmol) was added until the pH of the solution was ~8. Dibutoxy-3-cyclobutene-1,2-dione (42 μl, 0.197 mmol) was added followed by CH_3OH (0.5 ml). The squarate addition proceeded at room temperature for 30 minutes until TLC analysis showed no remaining starting amine intermediate. The reaction was quenched with one drop CH_3COOH and concentrated to dryness. The crude product was purified by HPLC (100 % water/0.1 % acetonitrile → 100 % acetonitrile). The pure fractions were combined and lyophilized to provide the product **3.21** (0.0389 g, 89 %) as a white solid; R_f 0.76 (3:3:1:1, dichloromethane:methanol:water:acetic acid); $[\alpha]_D$ +56.9 °(*c* 0.89, H_2O); ^1H NMR (600 MHz, $CDCl_3$) δ 4.89 (d, 1 H, $J_{1'',2''}$ 3.9 Hz, H-

1"), 4.70 (m, 2 H, -OCH_2- [11]), 4.50 (d, 1 H, $J_{1',2'}$ 7.7 Hz, H-1'), 4.44 (d, 1 H, $J_{1,2}$ 7.8 Hz, H-1), 4.38 (t, 1 H, $J_{5",6ab"}$ 6.6 Hz, H-5"), 4.18 (dd, 1 H, $J_{1",2"}$ 3.9 Hz, $J_{2"3"}$ 11.3 Hz, H-2"), 4.03 (d, 1 H, $J_{3",4"}$ 2.8 Hz, H-4"), 3.99 (d, 1 H, $J_{3',4'}$ 2.3 Hz, H-4'), 3.98-3.94 (m, 2 H, H-3", H-6a), 3.88 (m, 1 H, -OCH_2CH$_2$- [1]), 3.82 (m, 2 H, H-6b, -CH_2NH- [10]), 3.76 (m, 1 H, H-3'), 3.75-3.54 (m, 11 H, H-3, H6ab', H-6ab", -OCH_2CH$_2$- [1], -SCH$_2$CH_2NH- [10], H-5', H-5, H-4, H-2'), 3.30 (t, 1 H, $J_{2,3}$ 8.5 Hz, H-2), 2.77 (m, 2 H, -SCH_2CH$_2$NH- [9]), 2.57 (m, 2 H, -CH_2SCH$_2$- [8]), 2.07 (s, 3 H, CH_3C(O)NH), 1.79 (m, 2 H, -OCH$_2$CH_2CH$_2$- [2]), 1.60 (m, 2 H, -OCH$_2$CH_2- [12]), 1.55 (m, 2 H, -CH_2CH$_2$S- [7]), 1.45 (m, 2 H, -CH_2CH$_3$ [13]), 1.32 (m, 8 H, -CH2- [3,4,5,6]), 0.94 (m, 3 H, -CH$_3$ [14]); ^{13}C NMR (150 MHz, CDCl$_3$) δ 189.8 (C *squarate*), 183.9 (C *squarate*), 177.9 (C *squarate*), 175.3 (CH$_3$*C*(O)NH), 174.1 (C *squarate*), 104.2 (C-1'), 103.1 (C-1), 99.3 (C-1"), 79.4 (C-4), 77.6 (C-4'), 76.6 (C-3'), 75.7 (C-3), 75.5 (C-5), 74.9 (-OCH$_2$-), 73.9 (-OCH$_2$-), 73.1, 71.8, 71.7 (C-2, C-2', C-5'), 71.4 (C-5"), 71.3 (-OCH2-), 69.1 (C-4"), 68.1 (C-3"), 61.4, 61.3, 61.1 (C-6, C-6', C-6"), 50.9 (C-2"), 45.1 (-CH$_2$-), 33.0 (-CH$_2$-), 32.6 (-CH$_2$-), 32.5 (-CH$_2$-), 32.4 (-CH$_2$-), 30.1 (-CH$_2$-), 30.0 (-CH$_2$-), 29.9 (-CH$_2$-), 29.8 (-CH$_2$-), 29.6 (-CH$_2$-), 29.5 (-CH$_2$-), 29.2 (-CH$_2$-), 29.1 (-CH$_2$-), 26.3 (-CH$_2$-), 22.9 (CH_3C(O)NH), 19.4 (-CH$_2$-), 19.2 (-CH$_2$-), 14.2 (-CH$_3$), 14.1 (-CH$_3$); ESI HRMS Calcd for $C_{38}H_{64}N_2O_{19}Na$ 907.3716. Found 907.3706.

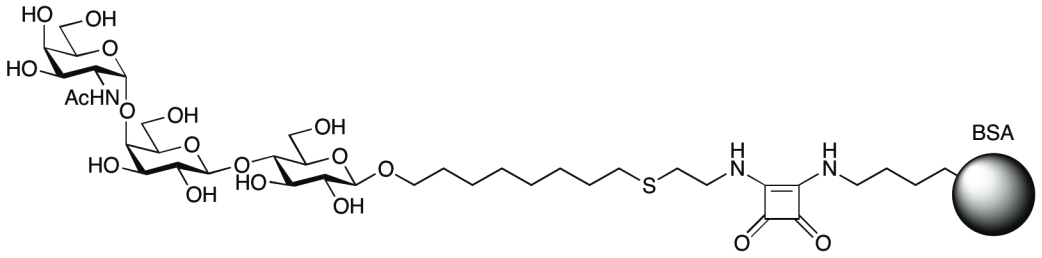

3.11

P^{k}NAc-BSA Conjugate (3.11):

BSA (29.56 mg, 0.448 μmol) was combined with **3.21** and dissolved in a pH 9 boronate buffer (1 ml). The tube was sealed and the reaction proceeded for 72 hours. Once complete the contents were placed in a dialysis bag and dialyzed over 2 days. As dialysis proceeded, the conjugate precipitated out of solution and was re-dissolved by the addition of one drop of NH_4OH. The product was extracted and lyophilized to give the conjugate **3.11** as a cotton-like solid. MALDI-TOF MS was done to assess degree of incorporation and was found to be 25 units of trisaccharide incorporated per BSA.

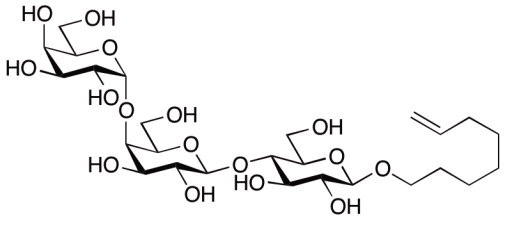

3.22

7-Octenyl α-D-galactopyranosyl-(1→4)-β-D-galactopyranosyl-(1→4)-β-D-glucopyranoside (3.22):

The lactoside **3.17** (0.514 g, 1.135 mmol) was dissolved in a 1.0 M HEPES buffer (17.1 ml) followed by the addition of a 64 mg/ml solution of DTT in water (18 mg/1.21 ml). Alkaline phosphatase (99.8 μl) was added followed by

the addition of UDP-Glc (1.04 g, 1.70 ml). The α(1→4)-galactosyltransferase/UDP-4'-Gal-epimerase fusion enzyme was added (2.14 ml) and the reaction proceeded at 37 ºC for 24 hours. A small amount of reaction solution was removed and filtered through a Sepak® C-18 cartridge and the reaction checked by ^{1}H NMR spectroscopy and found to be complete. The bulk reaction mixture was treated with Dowex® ion exchange resin (H^{+}) overnight and subsequently filtered. The crude mixture was flushed though a Sepak C-18 cartridge and the filtrate lyophilized to give the trisaccharide **3.22** (0.640 g, 92 %) as a white powder; R_f 0.86 (3:3:1:1, dichloromethane:methanol:water:acetic acid); $[\alpha]_D$ +47.5 °(*c* 0.79, H_2O); ^{1}H NMR (600 MHz, D_2O) δ 5.89 (ddt, 1 H, $J_{CH,CH2}$ 6.6 Hz, $J_{CH,CH(cis)}$ 10.2 Hz, $J_{CH,CH(trans)}$ 19.0 Hz, -C*H*=CH_2), 5.02 (m, 1 H, -CH=C*H*$_2$), 4.94 (m, 1 H, -CH=C*H*$_2$), 4.92 (d, 1 H, J1",2" 3.9 Hz, H-1"), 4.47 (d, 1 H, $J_{1',2'}$ 7.8 Hz, H-1'), 4.44 (d, 1 H, $J_{1,2}$ 8.0 Hz, H-1), 4.32 (m, 1 H, H-5"), 4.00 (m, 2 H, H-4, H-4"), 3.95 (dd, 1 H, H-6a'), 3.91-3.86 (m, 3 H, H-3", H-6, -OC*H*$_2$-), 3.82-3.74 (m, 4 H, H-6 (x3), H-2"), 3.72-3.58 (m, 6 H, -OC*H*$_2$-, H-3', H-3, H-5, H-5'), 3.56-3.53 (m, 2 H, H-2', H-4), 3.26 (m, 1 H, H-2), 2.03 (m, 2 H, -C*H*$_2$CH=CH_2), 1.59 (m, 2 H, -OCH$_2$C*H*$_2$-), 1.39-1.28 (m, 6 H, -C*H*$_2$C*H*$_2$C*H*$_2$-); ^{13}C NMR (150 MHz, D_2O) δ 140.4 (-*C*H=CH_2), 114.1 (-CH=*C*H_2), 103.3 (C-1'), 102.0 (C-1), 100.4 (C-1"), 78.8, 77.4, 75.5, 74.8, 74.6, 72.9, 72.2, 70.9, 70.8, 70.7 (-O*C*H_2), 69.2, 68.9, 68.6, 60.6, 60.4, 60.1, 33.0 (-*C*H_2CH=CH_2), 28.7 (-OCH$_2$*C*H_2-), 28.04 (-CH_2-), 28.02(-CH_2-), 24.9(-CH_2-); ESI HRMS Calcd for $C_{26}H_{46}O_{16}Na$ 637.2678. Found 637.2688.

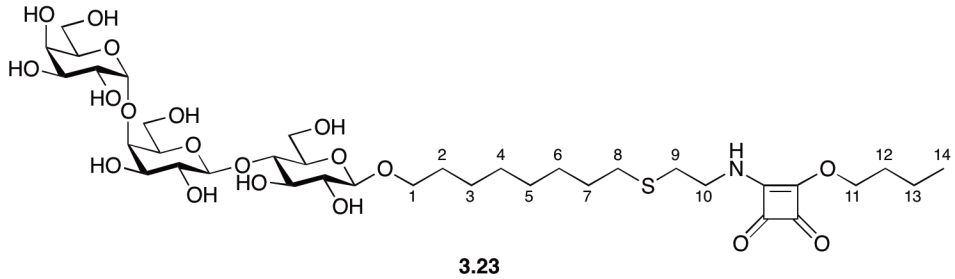

3.23

8-(2-(2-Butoxy-3,4-dioxocyclobut-1-enylamino)ethylthio)octyl α-D-galactopyranosyl-(1→4)-β-D-galactopyranosyl-(1→4)-β-D-glucopyranoside (3.23):

The octenyl trisaccharide **3.22** (0.112 g, 0.183 mmol) was placed in a quartz tube to which cysteamine•HCl (0.042 g, 0.365 mmol) was added and the starting materials dissolved in degassed MilliQ water (2.0 ml) and the vessel placed under argon atmosphere. The reaction vessel was irradiated with a high intensity UV lamp for 30 minutes at which point TLC analysis (3:3:1:1, dichloromethane:methanol:water:acetic acid) was done and still showed some remaining starting material. The vessel was irradiated once more for 30 minutes and subsequent TLC showed maximum product formation. A small portion of the amine intermediate was removed and used in the next step directly. The amine (0.0497 g, 0.0617 mmol) was dissolved in MilliQ H_2O (2 ml) and CH_3OH (1 ml). Dibutoxy-3-cyclobutene-1,2-dione (27 μl, 0.123 mmol) was added followed by Et_3N (17 μl, 0.123 mmol). The squarate addition proceeded at room temperature for 90 minutes until TLC analysis showed no remaining starting amine intermediate. The reaction was quenched with one drop of CH_3COOH and concentrated to dryness. The crude product was purified by HPLC (100 % water/0.1 % acetonitrile → 100 % acetonitrile) and the pure fractions were

combined and lyophilized to provide the product **3.23** (0.03183 g, 61 %) as a white solid; R_f 0.84 (3:3:1:1, dichloromethane:methanol:water:acetic acid); $[\alpha]_D$ +39.9 °(*c* 0.51, H_2O); ^{1}H NMR (600 MHz, $CDCl_3$) δ 4.94 (d, 1 H, $J_{1",2"}$ 4.0 Hz, H-1"), 4.73 (m, 2 H, -OC*H*$_2$- [11]), 4.51 (d, 1 H, $J_{1',2'}$ 7.7 Hz, H-1'), 4.44 (d, 1 H, $J_{1,2}$ 7.6 Hz, H-1), 4.35 (t, 1 H, $J_{5",6ab"}$ 6.6 Hz, H-5"), 4.03 (m, 2 H, H-4', H-4"), 3.97-3.87 (m, 4 H, H-4, H-3", H-6, -OC*H*$_2$- [1]), 3.86-3.77 (m, 5 H, H-2", H-6 (x3), -C*H*$_2$NH- [10]), 3.76-3.69 (m, 3 H, H-3', H-6ab"), 3.67-3.54 (m, 6 H, -OC*H*$_2$- [1], H-5', H-3, -C*H*$_2$NH- [10], H-2'), 3.29 (t, 1 H, $J_{2,3}$ 8.5 Hz, H-2), 2.77 (m, 2 H, -CH$_2$SC*H*$_2$CH$_2$NH- [9]), 2.57 (t, 2 H, -C*H*$_2$SCH$_2$- [8]), 1.78 (m, 2 H, -OCH$_2$C*H*$_2$- [12]), 1.58 (m, 4 H, -OCH$_2$C*H*$_2$- [2], -C*H*$_2$CH$_2$S- [7]), 1.50-1.40 (m, 2 H, -C*H*$_2$CH$_3$ [13]), 1.38-1.26 (m, 8 H, -CH$_2$- [3], [4], [5], [6]), 0.95 (m, 3 H, -CH$_2$C*H*$_3$ [14]); ^{13}C NMR (150 MHz, $CDCl_3$) δ 188.9 (C *squarate*), 183.0 (C *squarate*), 177.1 (C *squarate*), 173.2 (C *squarate*), 103.3 (C-1'), 102.2 (C-1), 100.4 (C-1"), 78.8. 77.5, 75.5, 74.8, 74.7, 74.6, 74.0, 73.93, 73.92, 73.91, 72.9, 72.3, 70.9, 70.8, 70.4, 69.1, 68.9, 68.6, 62.5, 60.6, 60.4, 60.2, 44.2 (-CH$_2$-), 32.2 (-CH$_2$-), 31.8 (-CH$_2$-), 31.7 (-CH$_2$-), 31.6 (-CH$_2$-), 31.56 (-CH$_2$-), 31.55 (-CH$_2$-), 29.3 (-CH$_2$-), 29.1 (-CH$_2$-), 28.9 (-CH$_2$-), 28.8 (-CH$_2$-), 28.4 (-CH$_2$-), 28.3 (-CH$_2$-), 25.4 (-CH$_2$-), 18.5 (-CH$_2$-), 18.3 (-CH$_2$-), 13.4 (-CH$_2$-), 13.3 (-CH$_3$); ESI HRMS Calcd for $C_{36}H_{61}NO_{19}SNa$ 866.3451. Found 866.3448. Calc'd for $C_{36}H_{61}O_{19}S$: C, 51.23; H, 7.29; N, 1.72; S, 3.80. Found: C, 51.04; H, 7.35; N, 1.72; S, 3.66.

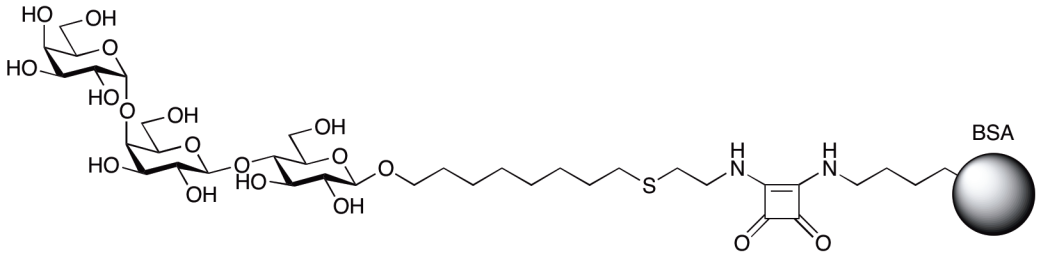

3.12

P^{k}-BSA Conjugate (3.12):

BSA (26.4 mg, 0.40 μmol) was combined with **3.23** and dissolved in a pH 9 Boronate buffer (1 ml). The tube was sealed and the reaction proceeded for 72 hours. Once complete the contents were placed in a dialysis bag and dialyzed over 2 days. As dialysis proceeded, the conjugate precipitated out of solution and was re-dissolved by the addition of one drop of NH4OH. The product was extracted and lyophilized to give the conjugate **3.12** as a cotton-like solid. MALDI-TOF MS was done to assess degree of incorporation and was found to be 26 units of trisaccharide incorporated per BSA.

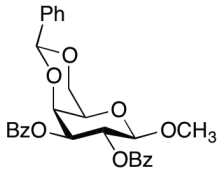

3.28

Methyl 2,3-di-*O*-benzoyl-4,6-*O*-benzylidenyl-β-D-galactopyranoside (3.28):

Methyl galactoside **3.27** (1.026 g, 5.28 mmol) was suspended in dry CH_3CN (20 ml). $PhCH(OCH_3)_2$ (0.95 ml, 6.34 mmol) was added followed by a catalytic amount of CSA (20 mg). The reaction proceeded at 30 °C under mildly reduced pressure to remove CH_3OH formed over the course of the reaction. After 1.5 hours, TLC analysis (10%, methanol-dichloromethane) showed maximum

product formation. The benzylidination was quenched by the addition of 3 drops of Et_3N and the mixture concentrated to dryness. The intermediate product was dissolved in Pyr (50 ml) and placed under argon atmosphere. BzCl (3.07 ml, 26.4 mmol) was added slowly and the reaction proceeded overnight at room temperature. TLC analysis (1:1, hexanes-ethyl acetate), showed the reaction to be complete. The reaction mixture was concentrated to dryness (co-evaporating with toluene 3 x 20 ml) and the crude product was purified by flash column chromatography on silica gel (2:1 → 1:1, hexanes-ethyl acetate) to provide the product **3.28** (2.27 g, 87 %) as a white foam; R_f 0.46 (1:1, hexanes-ethyl acetate); $[\alpha]_D$ 148.0 (*c* 1.05, $CHCl_3$); ^{1}H NMR (600 MHz, $CDCl_3$) δ 7.99 (m, 4 H, ArH), 7.53 (m, 2 H, ArH), 7.49 (m, 2 H, ArH), 7.37 (m, 7 H, ArH), 5.88 (dd, 1 H, $J_{1,2}$ 8.1 Hz, $J_{2,3}$ 10.5 Hz, H-2), 5.56 (s, 1 H, *benzylidene* C-*H*), 5.38 (dd, 1 H, $J_{3,4}$ 3.6 Hz, $J_{2,3}$ 10.4 Hz, H-3), 4.70 (d, 1 H, $J_{1,2}$ 8.1 Hz, H-1), 4.60 (d, 1 H, $J_{3,4}$ 3.6 Hz, H-4), 4.43 (dd, 1 H, $J_{5,6a}$ 1.3 Hz, $J_{6a,6b}$ 12.4 Hz, H-6a), 4.16 (dd, 1 H, $J_{5,6b}$ 1.6 Hz, $J_{6a,6b}$ 12.4 Hz, H-6b), 3.70 (bs, 1 H, H-5), 3.57 (s, 3 H, -OC*H*$_3$); ^{13}C NMR (150 MHz, $CDCl_3$) δ 166.2 (Ph*C*(O)O), 165.3 (Ph*C*(O)O), 137.5 (Ar), 133.4 (Ar), 133.1 (Ar), 129.9 (Ar), 129.8 (Ar), 129.7 (Ar), 129.1 (Ar), 128.9 (Ar), 128.4 (Ar), 128.3 (Ar), 128.1 (Ar), 126.3 (Ar), 101.9 (*benzylidene C*-H), 100.9 (C-1), 73.6 (C-4), 72.8 (C-3), 68.9(7) (C-2), 68.9(6) (C-6), 66.5 (C-5), 56.6 (O*C*H$_3$); ESI HRMS Calcd for $C_{28}H_{26}O_8Na$ 513.1520. Found 513.1510. Calc'd for $C_{28}H_{26}O_8$: C, 68.56; H, 5.34. Found: C, 68.23; H, 5.39.

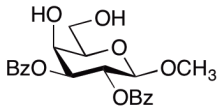

3.29

Methyl 2,3-di-*O*-benzoyl-β-D-galactopyranoside (3.29):

The benzylidenyl galactoside **3.28** (0.555 g, 1.13 mmol) was suspended in 80% CH_3COOH/water and heated to 80 ºC. The reaction was stirred for one hour until TLC analysis (10%, methanol-dichloromethane) showed the reaction to be complete. The reaction mixture was allowed to cool to room temperature and was transferred to a separatory funnel and diluted with CH_2Cl_2. The organic layer was washed with saturated aqueous sodium bicarbonate, distilled water saturated aqueous sodium chloride. The organic layer was dried over anhydrous sodium sulfate, filtered and concentrated to dryness. The crude product was purified by flash column chromatography on silica gel (1:1, hexanes-ethyl acetate) to give the product **3.29** (0.409 g, 89 %) as a white foam; R_f 0.20 (1:1, hexanes-ethyl acetate); $[\alpha]_D$ +96.9 (*c* 0.61, $CHCl_3$); ^{1}H NMR (600 MHz, $CDCl_3$) δ 7.97 (m, 4 H, ArH), 7.50 (m, 2 H, ArH), 7.36 (m, 4 H, ArH), 5.77 (dd, 1 H, $J_{1,2}$ 7.9 Hz, $J_{2,3}$ 10.4 Hz, H-2), 5.32 (dd, 1 H, $J_{3,4}$ 3.2 Hz, $J_{2,3}$ 10.4 Hz, H-3), 4.65 (d, 1 H, $J_{1,2}$ 7.9 Hz, H-1), 4.42 (d, 1 H, $J_{3,4}$ 2.3 Hz, H-4), 4.04 (dd, 1 H, $J_{5,6a}$ 5.8 Hz, $J_{6a,6b}$ 11.9 Hz, H-6a), 3.98 (dd, 1 H, $J_{5,6b}$ 4.5 Hz, $J_{6a,6b}$ 11.8 Hz, H-6b), 3.79 (m, 1 H, H-5), 3.55 (s, 3 H, -OC*H*$_3$); ^{13}C NMR (150 MHz, $CDCl_3$) δ 165.9 (Ph*C*(O)O), 165.5 (Ph*C*(O)O), 133.4 (Ar), 133.1 (Ar), 129.9 (Ar), 129.8 (Ar), 129.5 (Ar), 129.0 (Ar), 128.4 (Ar), 128.3 (Ar), 102.4 (C-1), 77.4 (C-3), 74.2 (C-5), 69.6 (C-2), 68.3 (C-4), 62.5 (C-6), 57.1 (O*C*H$_3$); ESI HRMS Calcd for $C_{21}H_{22}O_8Na$ 425.1207. Found 425.1204.

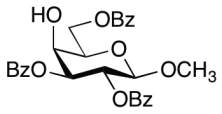

3.26

Methyl 2,3,6-tri-*O*-benzoyl-β-D-galactopyranoside (3.26):

The 4,6-diol galactoside **3.29** (0.369 g, 0.918 mmol) was placed under argon atmosphere and dissolved in dry CH_2Cl_2 (12 ml). The solution was cooled to 0 ºC in an ice-water bath and Pyr (0.148 ml, 1.84 mmol) was added. BzCl (0.117 ml, 1.01 mmol) was added slowly to the stirring solution. The reaction proceeded overnight, warming to room temperature. Subsequent TLC analysis (10%, ethyl acetate-toluene) showed maximum product formation and the reaction mixture concentrated to dryness. The crude product was purified by flash column chromatography on silica gel (10 %, ethyl acetate-toluene) to give the product **3.26** (0.329 g, 71 %) as a white foam; R_f 0.30 (10 %, ethyl acetate-toluene); $[\alpha]_D$ +54.5 (*c* 1.10, $CHCl_3$); ^{1}H NMR (500 MHz, $CDCl_3$) δ 8.05 (d, 2 H, ArH), 7.97 (d, 4 H, ArH), 7.58 (t, 1 H, ArH), 7.52 (t, 2 H, ArH), 7.45 (t, 2 H. ArH), 7.36 (m, 4 H, ArH), 5.77 (dd, 1 H, $J_{1,2}$ 7.9 Hz, $J_{2,3}$ 10.3 Hz, H-2), 5.37 (dd, 1 H, $J_{3,4}$ 3.2 Hz, $J_{2,3}$ 10.3 Hz, H-3), 4.71 (dd, 1 H, $J_{5,6a}$ 6.4 Hz, $J_{6a.6b}$ 11.4 Hz, H-6a), 4.66 (d, 1 H, $J_{1,2}$ 7.9 Hz, H-1), 4.62 (dd, 1 H, $J_{5,6b}$ 6.4 Hz, $J_{6a,6b}$ 11.4 Hz, H-6b), 4.36 (m, 1 H, H-4), 4.08 (t, 1 H, $J_{5,6a}$ 6.4 Hz, $J_{6,5b}$ 6.4 Hz, H-5), 3.54 (s, 3 H, -OC*H*$_3$), 2.62 (d, 1 H, $J_{4,OH}$ 5.0 Hz, 4-OH); ^{13}C NMR (125 MHz, $CDCl_3$) δ 166.4 (Ph*C*(O)O), 165.8 (Ph*C*(O)O), 165.4 (Ph*C*(O)O) 133.5 (Ar), 133.3 (Ar), 133.1 (Ar), 129.9 (Ar), 129.8 (Ar), 129.7 (Ar), 129.6 (Ar), 129.5 (Ar), 128.9 (Ar), 128.5 (Ar), 128.3 (Ar), 102.3 (C-1), 74.1 (C-3), 72.3 (C-4), 69.5 (C-2), 67.3 (C-5), 62.7

(C-6), 56.9 (O*C*H$_3$); ESI HRMS Calcd for $C_{28}H_{26}O_9Na$ 529.1469. Found 529.1467. Calcd for $C_{28}H_{26}O_9$: C, 66.40; H, 5.17. Found: C, 66.53; H, 5.19.

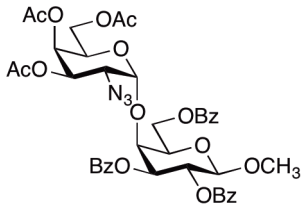

3.25

Methyl 3,4,6-tri-*O*-acetyl-2-azido-2-deoxy-α-D-galactopyranosyl-(1→4)-2,3,6-tri-*O*-benzoyl-β-D-galactopyranoside (3.25):

The acceptor **3.26** (0.291 g, 0.575 mmol) and trichloroacetimidate donor **3.3** (0.569 g, 1.15 mmol) were combined with pre-activated 4Å molecular sieves (200 mg) and the vessel placed under argon atmosphere. The starting materials were dissolved in anhydrous Et_2O (5 ml) and stirred over the sieves for one hour at room temperature. TMSOTf (16 μL, 0.086 mmol) was added and the reaction proceeded for 2 hours. TLC analysis (1:1, hexanes-ethyl acetate) was done and no remaining donor was observed. The reaction was quenched with Et_3N, filtered through Celite and concentrated to dryness. The crude product was purified by flash column chromatography on silica gel (3:1 → 1:1, hexanes-ethyl acetate) to provide the product **3.25** (0.225 g, 48 %) as an inseparable mixture of isomers (6:1 α:β) as a white foam; R_f 0.60 (1:1, hexanes-ethyl acetate); **For 3.25α:** ^{1}H NMR (500 MHz, $CDCl_3$) δ 8.06 (m, 2 H, ArH), 7.97-7.93 (m, 4 H, ArH), 7.59 (m, 1 H, ArH), 7.50-7.45 (m, 4 H, ArH), 7.37-7.34 (m, 4 H, ArH), 5.69 (dd, 1 H, $J_{1,2}$ 7.9 Hz, $J_{2,3}$ 10.6 Hz, H-2), 5.45 (m, 2 H, H-3', H-4'), 5.36 (dd, 1 H, $J_{3,4}$ 2.9 Hz, $J_{2,3}$ 10.6 Hz, H-3), 5.07 (d, 1 H, $J_{1',2'}$ 3.6 Hz, H-1'), 4.75 (d, 2 H, $J_{5,6ab}$ 6.9 Hz, H-6ab),

4.67 (d, 1 H, $J_{1,2}$ 7.8 Hz, H-1), 4.55 (m, 1 H, H-5'), 4.47 (d, 1 H, $J_{3,4}$ 2.9 Hz, H-4), 4.12 (t, 1 H, $J_{5,6ab}$ 6.9 Hz, H-5), 3.86 (m, 2 H, H-2', H-6a'), 3.56 (m, 4 H, $J_{5',6b'}$ 6.1 Hz, $J_{6a',6b'}$ 11.0 Hz, H-6b', OCH_3), 2.07 (s, 3 H, CH_3C(O)O), 2.06 (s, 3 H, CH_3C(O)O), 1.86 (s, 3 H, CH_3C(O)O); ^{13}C NMR (125 MHz, $CDCl_3$) δ 170.2 (CH_3C(O)O), 169.9 (CH_3C(O)O), 169.5 (CH_3C(O)O), 166.0 (Ph*C*(O)O), 165.1 (PH*C*(O)O), 133.6 (Ar), 133.4 (Ar), 133.1 (Ar), 129.9 (Ar), 129.8 (Ar), 129.7 (Ar), 129.6 (Ar), 129.4 (Ar), 128.7 (Ar), 128.6 (Ar), 128.5 (Ar), 128.3 (Ar), 102.3 (C-1), 99.2 (C-1'), 75.3 (C-4), 73.5 (C-3), 72.3 (C-5), 69.4 (C-2), 68.9 (C-3'), 67.4, 67.2 (C-4', C-5'), 62.2 (C-6), 60.6 (C-6'), 58.6 (C-2'), 56.9 (O*C*H_3), 20.6 (*C*H_3C(O)O), 20.57 (*C*H_3C(O)O), 20.51 (*C*H_3CO(O)O); **For 3.25β:** ^{1}H NMR (500 MHz, $CDCl_3$) δ 8.06 (m, 4 H, ArH), 7.53 (m, 1 H, ArH), 7.48 (m, 2 H, ArH), 7.40 (m, 2 H, ArH), 7.35 (m, 2 H, ArH), 7.24 (m, 1 H, ArH), 7.16 (m, 3 H, ArH), 5.87 (dd, 1 H, $J_{1,2}$ 7.9 Hz, $J_{2,3}$ 10.3 Hz, H-2), 5.46 (dd, 1 H, $J_{3,4}$ 3.2 Hz, $J_{2,3}$ 10.5 Hz, H-3), 5.22 (d, 1 H, $J_{3',4'}$ 3.4 Hz, H-4'), 4.73 (dd, 1 H, $J_{5,6a}$ 4.9 Hz, $J_{6a,6b}$ 11.7 Hz, H-6a), 4.67 (d, 1 H, $J_{1,2}$ 7.9 Hz, H-1), 4.59 (m, 2 H, H-6b, H-3'), 4.51 (d, 1 H, $J_{3,4}$ 3.1 Hz, H-4), 4.43 (d, 1 H, $J_{1',2'}$ 7.9 Hz, H-1'), 4.11 (m, 1 H, H-5), 4.01 (dd, 1 H, $J_{5',6ab'}$ 6.6 Hz, $J_{6a',6b'}$ 11.2 Hz, H-6a'), 3.93 (dd, 1 H, $J_{5',6b'}$ 6.6 Hz, $J_{6a',6b'}$ 11.2 Hz, H-6b'), 3.82 (dd, 1 H, $J_{1',2'}$ 7.9 Hz, $J_{2',3'}$ 10.8 Hz, H-2'), 3.63 (t, 1 H, $J_{5',6ab'}$ 6.6 Hz, H-5'), 3.54 (s, 3 H, -OCH_3), 2.14 (s, 3 H, CH_3C(O)O), 2.04 (s, 3 H, CH_3C(O)O), 1.93 (s, 3 H, CH_3C(O)O); ^{13}C NMR (125 MHz, $CDCl_3$) δ 170.2, 169.9, 169.5, 166.0, 165.1, 133.8, 133.2, 133.1, 129.8, 129.7, 129.5, 129.4, 129.0, 128.7, 128.68, 128.61, 128.2, 125.3, 102.4 (C-1'), 102.3 (C-1), 74.2, 73.6, 70.9, 70.7, 69.8, 66.1, 63.7, 61.1, 60.9, 56.9, 20.6, 20.57, 20.51; For **3.25α 3.25β** mixture:

ESI HRMS Calc'd for $C_{40}H_{41}N_3O_{16}Na$ 842.2379. Found 842.2374. Calc'd for $C_{40}H_{41}N_3O_{16}$: C, 58.61; H, 5.04; N, 5.13. Found: C, 58.91; H, 5.26; N, 4.86.

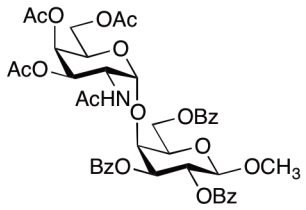

3.30

Methyl 2-acetamido-3,4,6-tri-*O*-acetyl-2-deoxy-α-D-galactopyranosyl-(1→4)-2,3,6-tri-*O*-benzoyl-β-D-galactopyranoside (3.30):

The azide **3.25** (0.101 g, 0.123 mmol) was combined with $Pd(OH)_2$ (0.036 g) and dissolved in CH_3OH (5 ml). The reaction vessel was placed under hydrogen atmosphere and the reaction proceeded overnight at room temperature. Subsequent TLC analysis (1:1, hexanes-ethyl acetate) was done and the reaction found to be complete. The contents were filtered through Celite and concentrated to dryness. The crude intermediate was dissolved in a 1:1 mixture of Ac_2O:Pyr (20 ml) and the reaction proceeded for 12 hours. Subsequent TLC analysis showed the reaction to be complete. The reaction mixture was concentrated to dryness, co-evaporating with toluene (3 x 10 ml). The crude product was purified by flash column chromatography on silica gel (1:2, hexanes-ethyl acetate) to give the product **3.30** (0.074 g, 72 %) was a white foam; R_f 0.29 (1:2, hexanes-ethyl acetate); $[\alpha]_D$ +111.8 (*c* 0.37, $CHCl_3$); ^{1}H NMR (500 MHz, $CDCl_3$) δ 8.07 (m, 2 H, ArH), 7.98 (m, 2 H, ArH), 7.95 (m, 2 H, ArH), 7.63 (m, 1 H, ArH), 7.51 (m, 4 H, ArH), 7.39 (m, 4 H, ArH), 6.24 (d, 1 H, $J_{NH,2'}$ 9.4 Hz, N-H), 5.75 (dd, 1 H, $J_{1,2}$ 7.5 Hz, $J_{2,3}$ 10.4 Hz, H-2), 5.41 (dd, 1 H, $J_{3,4}$ 3.1 Hz, $J_{2,3}$ 10.4 Hz, H-3), 5.34 (m, 2

H, H-3', H-4'), 5.19 (d, 1 H, $J_{1',2'}$ 3.7 Hz, H-1'), 4.85 (dd, 1 H, $J_{5,6a}$ 6.9 Hz, $J_{6a,6b}$ 11.3 Hz, H-6a), 4.70 (m, 2 H, H-1, H-2'), 4.52 (d, 1 H, $J_{3,4}$ 3.0 Hz, H-4), 4.42 (vt, 1 H, $J_{5',6ab'}$ 7.3 Hz, H-5'), 4.36 (dd, 1 H, $J_{5,6b}$ 7.1 Hz, $J_{6a,6b}$ 11.1 Hz, H-6b), 4.15 (t, 1 H, $J_{5,6ab}$ 7.1 Hz, H-5), 3.68 (dd, 1 H, $J_{5',6a'}$ 7.9 Hz, $J_{6a',6b'}$ 10.9 Hz, H-6a'), 3.58 (s, 3 H, -OCH_3), 3.36 (dd, 1 H, $J_{5',6b'}$ 6.3 Hz, $J_{6a',6b'}$ 11.0 Hz, H-6b'), 2.10 (s, 3H, CH_3C(O)O), 2.09 (s, 3 H, CH_3C(O)O), 2.05 (s, 3 H, CH_3C(O)NH), 1.78 (s, 3 H, CH_3C(O)O); ^{13}C NMR (125 MHz, $CDCl_3$) δ 170.7 (CH_3*C*(O)O), 170.6 (CH_3*C*(O)NH), 170.2 (CH_3*C*(O)O), 169.9 (CH_3C(O)O), 165.9 (Ph*C*(O)O), 165.8 (Ph*C*(O)O), 165.3 (PH*C*(O)O), 133.7 (Ar), 133.6 (Ar), 133.3 (Ar), 129.8 (Ar), 129.7 (Ar), 129.3 (Ar), 129.2 (Ar), 128.8 (Ar), 128.6 (Ar), 128.4 (Ar), 102.4 (C-1), 98.5 (C-1'), 73.0 (C-3), 72.5, 72.3 (C-4, C-5), 69.6 (C-2), 67.9, 67.0, 66.8 (C-3', C-4', C-5'), 61.5 (C-6), 60.7 (C-6'), 57.2 (O*C*H$_3$), 47.9 (C-2'), 23.3 (*C*H$_3$C(O)O), 20.8 (*C*H$_3$C(O)NH), 20.7 (*C*H$_3$C(O)O), 20.4 (*C*H$_3$CO(O)O); ESI HRMS Calc'd for $C_{42}H_{44}NO_{17}Na$ 858.2580. Found 858.2567. Calc'd for $C_{42}H_{44}NO_{17}$: C, 60.36; H, 5.43; N, 1.68. Found: C, 60.43; H, 5.54; N, 1.43.

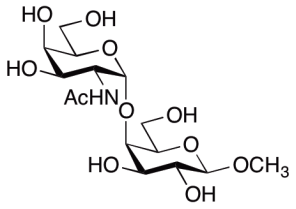

3.24

Methyl 2-acetamido-2-deoxy-α-D-galactopyranosyl-(1→4)-β-D-galactopyranoside (3.24):

The acylated disaccharide **3.30** (0.0542 g, 0.0649 mmol) was dissolved in anhydrous CH_3OH (10 ml) and placed under argon atmosphere. A small portion of Na metal was added to the stirring solution (10 mg) and the reaction allowed to proceed at room temperature overnight. Subsequent TLC analysis showed the reaction to be complete. The reaction was neutralized with Dowex H^+ ion exchange resin and filtered. The filtrate was concentrated to dryness. The crude product was purified by flash column chromatography on Iatrobeads® (20 %, methanol-dichloromethane). The pure fractions were collected and concentrated, dissolved in MilliQ water and lyophilized to provide the product **3.24** (0.02143 g, 83 %) was a white powder; R_f 0.20 (30 %, methanol-dichloromethane); $[\alpha]_D$ +143.7 (*c* 0.56, H_2O); ^{1}H NMR (600 MHz, CD_3OD) δ 4.91 (d, 1 H, $J_{1',2'}$ 3.8 Hz, H-1'), 4.41 (m, 1 H, H-5'), 4.34 (dd, 1 H, $J_{1',2'}$ 3.8 Hz, $J_{2',3'}$ 11.1 Hz, H-2'), 4.20 (d, 1 H, $J_{1,2}$ 7.5 Hz, H-1), 3.97 (d, 1 H, $J_{3,4}$ 2.9 Hz, H-4), 3.93 (d, 1 H, $J_{3',4'}$ 2.5 Hz, H-4'), 3.78 (dd, 2 H, $J_{3',4'}$ 3.2 Hz, $J_{2',3'}$ 11.2 Hz, H-3'), 3.71 (m, 3 H, H-6a, H-6ab'), 3.61 (m, 2 H, H-5, H-6b), 3.57 (s, 3 H, -OCH_3), 3.55 (dd, 1 H, $J_{3,4}$ 3.1 Hz, $J_{2,3}$ 10.0 Hz, H-3), 3.47 (dd, 1 H, $J_{1,2}$ 7.5 Hz, $J_{2,3}$ 10.1 Hz, H-2), 2.02 (s, 3 H, CH_3C(O)NH); ^{13}C NMR (125 MHz, CD_3OD) δ 173.9 (CH_3C(O)NH), 106.3 (C-1), 100.5 (C-1'), 77.6 (C-4), 76.6 (C-5), 74.5 (C-3), 72.7 (C-2), 72.2 (C-5'), 70.4

(C-4'), 69.7 (C-3'), 62.6 (C-6'), 60.8 (C-6), 57.8 (OCH_3), 51.6 (C-2'), 23.7 ($CH_3C(O)NH$); ESI HRMS Calcd for $C_{15}H_{27}NO_{11}Na$ 420.1476. Found 420.1469.

Data collection	
Space Group	P61
Cell dimensions	
a,b,c (Å)	146.25, 146.25, 60.31
α,β,γ (°)	90, 90, 120
wavelength (Å)	0.97949
resolution (Å)	50.0-1.56 (1.65-1.56) *
Rsym (%)	8.2 (97.8) *
I(σ(I))	8.8 (1.4) *
Completeness (%)	92.8 (89.9) *
Multiplicity	5.7 (2.9) *
Refinement	
resolution (Å)	40.0-1.56 (1.60-1.56) *
No. observed reflections	99448
Rwork/Rfree (%)	17.0/19.2
No. total atoms	5798
No. protein atoms	4971 (12.9)¥
No. ligand atoms	93 (35.8) ¥
No. water	734 (29.0) ¥
R.m.s. deviations	
Bond length (Å)	0.01
Bond angle (°)	0.99

Table 6.1. Structural data for Stx2-**3.24** complex. *, values in parentheses are for the highest-resolution shell. Data collected on a single crystal were used for structure determination. ¥, values in parentheses indicate the average value of temperature factors in $Å^2$.

	Stx1-P^{k}MCO	Stx2a-**2**
Site 1		
H-Bonds		Gal1NAc:O7-N:Glu15 (2.7, 2.9)[£]
		Gal1NAc:O7-N$^{\zeta}$:Lys12 (3.4)
		Gal1NAc:O3-N$^{\zeta}$:Lys12 (2.9)
		Gal1NAc:O4-O$^{\varepsilon 1}$:Glu27 (2.7, 2.6)
		Gal1NAc:O4-O$^{\gamma 1}$:Thr20 (2.9)
		Gal1NAc:O6-O$^{\varepsilon 1}$:Glu27 (2.9)
	Gal1:O5-O$^{\gamma 1}$:Thr21 (3.2)[¥]	Gal1NAc:O5-O$^{\gamma 1}$:Thr20 (3.1)
	Gal2:O6-O$^{\delta 2}$:Asp17 (2.5)	Gal2:O6-O$^{\delta 2}$:Asp16 (2.6)
	Gal2:O3-O:Gly60 (2.6)	Gal2:O3-O:Gly59 (2.8)
VDW[§]	37	51
Site 2		
H-bonds	Gal1:O2-O$^{\delta 1}$:Asp16 (2.8)	Gal1NAc:O7-N$^{\eta 2}$:Arg32 (3.1)
	Gal1:O3-N$^{\eta 2}$:Arg33 (2.8)	Gal1NAc:O3-N$^{\eta 2}$:Arg32 (3.2)
	Gal1:O4-O$^{\delta 1}$:Asn32 (2.7)	Gal1NAc:O4-O$^{\gamma}$:Ser31 (3.2)
	Gal1:O4-N$^{\varepsilon}$:Arg33 (3.0)	Gal1NAc:O4-N$^{\varepsilon}$:Arg32 (3.0)
	Gal1:O4-N$^{\eta 2}$:Arg33 (3.5)	Gal1NAc:O4-N$^{\eta 2}$:Arg32 (3.3)
	Gal1:O6-O$^{\delta 1}$:Asn32 (3.0)	Gal1NAc:O6-O$^{\gamma}$:Ser31 (3.3)
	Gal1:O6-N:Asn32 (3.1)	Gal1NAc:O6-N:Ser31 (2.9)
	Gal1:O6-O:Phe63 (2.9)	Gal1NAc:O6-O:Phe62 (2.7)
		Gal2:O2-N:Gly61 (3.2, 2.9)[¶]
		Gal2:O3-N:Gly61 (3.0, 2.9)[¶]
		Gal2:O5-O$^{\gamma}$:Ser54 (3.2)
		Gal2:O6-O$^{\gamma}$:Ser54 (2.8)
	Gal2:O6-N:Asn55 (3.2)	Gal2:O6-N:Ser54 (2.9)
		Gal2:O6-O$^{\varepsilon 2}$:Glu15 (3.3)
VDW	46	59

Table 6.2. Comparison of the interactions between carbohydrate ligands and Stx1 (PDB code, 1BOS) and Stx2.[§], Number of van der Waals contacts between the ligand and the toxin; [¥], distance in Å between the two atoms forming the hydrogen bond; [£], solvent-bridged interaction between the ligand and the toxin (the H-bond distance between residue1 and water, the H-bond distance between residue2 and water). ¶, these solvent-bridged interactions were also observed in Stx1-starfish complex (PDB code, 1QNU).

6.4. Chapter 4 Experimental

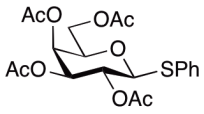

4.7

Phenyl 2,3,4,6-tetra-*O*-acetyl-1-thio-β-D-galactopyranoside (4.7):

α,β-Galactose pentaacetate (40.6 g, 0.104 mol) was dissolved in anhydrous CH_2Cl_2 (60 ml) and placed under argon atmosphere. PhSH (16.0 ml, 0.156 mol) was added and the solution was cooled to 0 °C in an ice-water bath while stirring. Once cool BF_3•OEt_2, (19.6 ml, 0.156 mol) was added and the reaction proceeded while warming to room temperature. After two hours TLC analysis (1:1, hexanes-ethyl acetate) showed maximum product formation. The reaction was quenched with Et_3N until neutral and the mixture was diluted with CH_2Cl_2 (20 ml) and concentrated to dryness. The crude product was purified by flash column chromatography on silica gel (2:1, hexanes-ethyl acetate) to obtain the product **4.7** (45.1 g, 98 %) as a white foam; R_f 0.40 (1:1, hexanes-ethyl acetate); $[a]_D$ +3.5 ^{o}(*c* 1.06, $CHCl_3$); ^{1}H NMR (500 MHz, $CDCl_3$) δ 7.52 (m, 2 H, ArH), 7.32 (m, 3 H, ArH), 5.42 (dd, 1 H, $J_{4,5}$ 1.0 Hz, $J_{3,4}$ 3.4 Hz, H-4), 5.24 (dd, 1 H, $J_{2,3}$ 9.9, $J_{1,2}$ 9.9 Hz, H-2), 5.06 (dd, 1 H, $J_{3,4}$ 3.3 Hz, $J_{2,3}$ 9.9 Hz, H-3), 4.72 (d, 1 H, $J_{1,2}$ 9.9 Hz, H-1), 4.20 (dd, 1 H, $J_{5,6a}$ 7.0 Hz, $J_{6a,6b}$ 11.3 Hz, H-6a), 4.12 (dd, 1 H, $J_{5,6b}$ 6.2 Hz, $J_{6a,6b}$ 11.4 Hz, H-6b), 3.94 (ddd, 1 H, $J_{4,5}$ 1.0, $J_{5,6b}$ 6.1 Hz, $J_{5,6a}$ 7.1 Hz, H-5), 2.12 (s, 3 H, C*H*$_3$C(O)O), 2.10 (s, 3 H, C*H*$_3$C(O)O), 2.05 (s, 3 H, C*H*$_3$C(O)O), 1.98 (s, 3 H, C*H*$_3$C(O)O); ^{13}C NMR (125 MHz, $CDCl_3$): δ 170.3 (C=O), 170.2 (C=O), 170.0 (C=O), 169.4 (C=O), 132.6 (Ar), 132.4 (Ar), 128.9

(Ar), 128.1 (C=O), 86.6 (C-1), 74.4 (C-5), 72.0 (C-3), 67.3, 67.2 (C-2, C-4), 61.6 (C-6), 20.8 (*C*H_3C(O)O), 20.6 (*C*H_3C(O)O), 20.5 (*C*H_3C(O)O); ESI HRMS calcd. for $C_{20}H_{24}O_9SNa$ 463.10332. Found 463.10322; Anal. Calcd. for $C_{20}H_{24}O_9S$: C, 54.54; H, 5.49; S, 7.28. Found: C, 54.38; H, 5.56; S, 7.29.

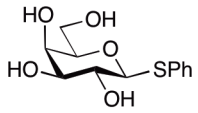

4.8

Phenyl 1-thio-β-D-galactopyranoside (4.8):

The acetylated thiogalactoside **4.7** (11.84 g, 26.9 mmol) was dissolved in anhydrous CH_3OH (60 ml) to which a catalytic amount of Na metal (0.045 g) was added. The reaction was allowed to proceed overnight at room temperature and under argon atmosphere. Subsequent TLC analysis (20 %, methanol-dichloromethane) showed no remaining starting material The reaction was neutralized with Dowex H^+ ion exchange resin, filtered and concentrated to dryness. The crude product was recrystallized from anhydrous ethanol and filtered to give the pure product **4.8** (7.10 g, 97 %) as a white solid; R_f 0.79 (20 %, methanol-dichloromethane); $[a]_D$ -51.6 ^{o}(*c* 1.00, CH_3OH); ^{1}H NMR (500 MHz, D_2O) δ 7.65 (m, 2 H, ArH), 7.47 (m, 3 H, ArH), 4.84 (d, 1 H, $J_{1,2}$ 13.2 Hz, H-1), 4.06 (d, 1 H, $J_{3,4}$ 3.2 Hz, H-4), 3.85-3.75 (m, 4 H, H-3, H-5, H-6ab), 3.70 (m, 1 H, H-2); ^{13}C NMR (125 MHz, D_2O): δ 133.7 (Ar), 132.1 (Ar), 130.3 (Ar), 128.8 (Ar), 89.0 (C-1), 79.9 (C-5), 74.9 (C-3), 70.2 (C-2), 69.7 (C-4), 61.9 (C-6); ESI HRMS calcd. for $C_{12}H_{16}O_5Na$ 295.0611. Found 295.0607; Anal. Calcd. for $C_{12}H_{16}O_5$: C, 52.93; H, 5.92; S, 11.77. Found: C, 52.67; H, 5.99; S, 11.76.

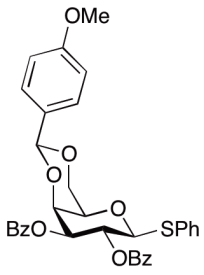

4.9

Phenyl 2,3-di-*O*-benzoyl-4,6-*O*-*p*-methoxybenzylidenyl-1-thio-β-D-galactopyranoside (4.9):

To a solution of dry Phenyl 1-thio-β-D-galactopyranoside **4.8** (5.43 g, 19.9 mmol) in anhydrous CH_3CN (50 ml), $CH_3OPhCH(OCH_3)_2$ (4.1 ml, 23.9 mmol) was added followed by a catalytic amount of CSA (100 mg). The reaction was done at reduced pressure at 30 °C to remove CH_3OH generated during reaction. After 1.5 hours, TLC analysis (10 %, methanol-dichloromethane) showed the reaction to be complete. The reaction was quenched with five drops of Et_3N and concentrated. The crude *para*-methoxybenzylidene product was dissolved in Pyr (50 ml) and BzCl (11.6 ml, 99.7 mmol) was added slowly and the reaction proceeded overnight. TLC analysis (2:1, hexanes-ethyl acetate) showed maximum product formation and no remaining starting material. The mixture was concentrated to dryness while co-evaporating with toluene (3 x 20 ml). The crude product was purified by flash column chromatography on silica gel (3:1 → 1:1, hexanes-ethyl acetate) to provide the product **4.9** (10.5 g, 88 %) as a white foam; R_f 0.71 (1:1, hexanes-ethyl acetate); $[a]_D$ +81.4 ^{o}(*c* 1, $CHCl_3$); ^{1}H NMR (500 MHz, $CDCl_3$) δ 7.97 (m, 2 H, ArH), 7.92 (m, 2 H, ArH), 7.62 (m, 2 H, ArH), 7.52 (m, 1 H, ArH), 7.46 (m, 1 H, ArH), 7.39 (m, 2 H, ArH), 7.31 (m, 7 H, ArH), 6.87 (m, 2 H, ArH), 5.80 (t, 1 H, $J_{1,2}$ 9.9 Hz, $J_{2,3}$ 9.9 Hz, H-2), 5.46 (s, 1 H, *benzylidene* C-

H), 5.35 (dd, 1 H, $J_{3,4}$ 3.4 Hz, $J_{3,2}$ 10.0 Hz, H-3), 4.96 (d, 1 H, $J_{1,2}$ 9.8 Hz, H-1), 4.57 (d, 1 H, $J_{3,4}$ 3.3 Hz, H-4), 4.43 (dd, 1 H, $J_{5,6a}$ 1.3 Hz, $J_{6a,6b}$ 12.3 Hz, H-6a), 4.08 (dd, 1 H, $J_{5,6b}$ 1.4 Hz , $J_{6a,6b}$ 12.3, H-6b), 3.82 (s, 3 H, C*H*$_3$OPh), 3.74 (s, 1 H, H-5); ^{13}C NMR (125 MHz, $CDCl_3$) δ 166.2 (*C*=O), 164.9 (*C*=O), 160.1 (Ar), 133.9 (Ar), 133.3 (Ar), 133.1 (Ar), 131.1 (Ar), 130.2 (Ar), 129.9 (Ar), 129.8 (Ar), 129.7 (Ar), 129.1 (Ar), 128.8 (Ar), 128.4 (Ar), 128.3 (Ar), 128.2 (Ar), 127.8 (Ar), 114.7 (Ar), 113.5 (Ar), 100.9 (*benzylidene C*-H), 85.3 (C-1), 74.1 (C-3), 73.7 (C-4), 69.9 (C-5), 69.1 (C-6), 67.1 (C-2), 55.3 (O*C*H$_3$); ESI HRMS Calcd. for $C_{34}H_{30}O_8SNH_4$ 616.2000. Found 616.1998; Anal. Calcd. for $C_{34}H_{30}O_8S$: C, 68.21; H, 5.05; S, 5.36. Found: C, 68.25; H, 5.28; S, 5.36.

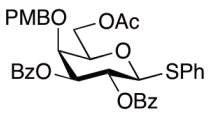

4.6

Phenyl 6-*O*-acetyl-2,3-di-*O*-benzoyl-4-*O*-*para*-methoxybenzyl-1-thio-β-D-galactopyranoside (4.6):

The *p*-methoxylbenzylidene acetal **4.9** (0.540 g, 0.902 mmol) was dissolved in dry CH_2Cl_2 (30 ml) to which 1.0M BH_3•THF (4.51 ml, 4.51 mmol) was added followed by TMSOTf (24 μl, 0.135 mmol). The reaction proceeded at room temperature for 1.5 hours at which point TLC (1:1, hexanes-ethyl acetate) showed no remaining starting material. The reaction was quenched with two drops of Et_3N followed by very slow addition of CH_3OH until bubbling ceased. The reaction mixture was then concentrated to dryness and subsequently dissolved in a 1:1 mixture of Ac_2O:Pyr (10 ml) and reacted overnight. TLC

analysis (1:1, hexanes-ethyl acetate) showed no remaining intermediate. The mixture was co-evaporated with toluene (3 x 20 ml) until dry. The crude product was purified by flash column chromatography on silica gel (3:1 → 2:1, hexanes-ethyl acetate) and recrystallized from ethyl acetate and hexanes to give the product **4.6** (0.486 g, 84 %) as a white powder; R_f 0.58 (1:1, hexanes-ethyl acetate); $[a]_D$ +66.7 ^{o}(*c* 1, $CHCl_3$); ^{1}H NMR (500 MHz, $CDCl_3$) δ 7.96 (m, 4 H, ArH), 7.51 (m, 4 H, ArH), 7.38 (m, 4 H, ArH), 7.26 (m, 3 H, ArH), 7.13 (m, 2 H, ArH), 6.76 (m, 2 H, ArH), 5.87 (vt, 1 H, $J_{1,2}$ 10.0 Hz, $J_{2,3}$ 10.0 Hz, H-2), 5.34 (dd, 1 H, $J_{3,4}$ 2.9 Hz, $J_{2,3}$ 10.0 Hz, H-3), 4.91 (d, 1 H, $J_{1,2}$ 10.0 Hz, H-1), 4.68 (d, 1 H, J_{gem} 11.4 Hz, CH_3OPhCH_2O), 4.46 (d, 1 H, J_{gem} 11.4 Hz, OCH_2PhOCH_3), 4.35 (dd, 1 H, $J_{5,6a}$ 6.8 Hz, $J_{6a,6b}$ 11.3 Hz, H-6a), 4.16 (d, 1 H, $J_{3,4}$ 2.8 Hz, H-4), 4.11 (dd, 1 H, $J_{5,6b}$ 6.2 Hz, $J_{6a,6b}$ 11.3 Hz, H-6b), 3.91 (m, 1 H, H-5), 3.76 (s, 3 H, OCH_2PhOCH_3), 2.03 (s, 3 H, $CH_3C(O)O$); ^{13}C NMR (125 MHz, $CDCl_3$) δ 170.4 (C=O), 165.9 (C=O), 165.2 (C=O), 159.3 (ArC-O), 133.5 (Ar), 133.2 (Ar), 132.8 (Ar), 132.5 (Ar), 129.9 (Ar), 129.8 (Ar), 129.5 (Ar), 129.4 (Ar), 128.9 (Ar), 128.8 (Ar), 128.5 (Ar), 128.4 (Ar), 127.9 (Ar), 113.8 (Ar), 86.7 (C-1), 76.1 (C-5), 75.9 (C-3), 74.3 (CH_3OPhCH_2O), 72.9 (C-4), 68.3 (C-2), 62.7 (C-6), 55.2 (CH_3OPhCH_2O), 20.8 ($CH_3C(O)O$); ESI HRMS Calcd. for $C_{36}H_{34}O_9SNa$ 665.1816. Found 665.1806; Anal. Calcd. for $C_{36}H_{34}O_9S$: C, 67.27; H, 5.33; S, 4.99. Found: C, 67.37; H, 5.33; S, 4.78.

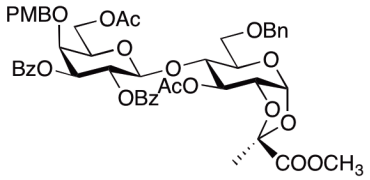

4.10

6-*O*-Acetyl-2,3-di-*O*-benzoyl-4-*O*-*para*-methoxybenzyl-β-D-galactopyranosyl-(1→4)-3-*O*-acetyl-6-*O*-benzyl-1,2-*O*-[(*S*)-1-(methoxycarbonyl)ethylidene]-α-D-glucopyranoside (4.10):

The acceptor **2.7** (0.518 g, 1.31 mmol) and donor **4.6** (1.26 g, 1.96 mmol) were combined with pre-activated 4Å molecular sieves (0.500 g) and dissolved in anhydrous CH_2Cl_2 (25 ml). The mixture was stirred for one hour at room temperature and under argon atmosphere. The contents were cooled to -20 °C after which the reaction was activated by the addition of NIS (0.209 g, 1.57 mmol) and AgOTf (0.050 g, 0.196 mmol). Reaction progress was monitored by TLC analysis (1:1, hexanes-ethyl acetate) and after one hour the reaction was found to be complete. The reaction was quenched by the addition of Et_3N (1 drop) and the mixture was diluted with CH_2Cl_2. This mixture was filtered through Celite and subsequently washed with saturated aqueous sodium bicarbonate, saturated aqueous sodium thiosulfate, distilled water and saturated aqueous sodium chloride. The organic layer was dried over anhydrous sodium sulfate, filtered and concentrated to dryness. The crude product was purified by flash column chromatography on silica gel (1:1, hexanes-ethyl acetate) to give the product **4.10** (1.09 g, 90 %) as a white foam; R_f 0.38 (1:1, hexanes-ethyl acetate); $[a]_D$ +23.9 ^{o}(*c* 1.08, $CHCl_3$); ^{1}H NMR (500 MHz, $CDCl_3$) δ 7.96 (m, 2 H, ArH), 7.89 (m, 2 H, ArH), 7.50 (m, 2 H, ArH), 7.35 (m, 7 H, ArH), 7.19 (m, 2 H, ArH),

7.15 (m, 2 H, ArH), 6.75 (m, 2 H, ArH), 5.77 (m, 2 H, $J_{1,2}$ 4.9 Hz, $J_{1',2'}$ 7.9 Hz, $J_{2',3'}$ 10.4 Hz, H-1, H-2'), 5.52 (vt, 1 H, $J_{2,3}$ 2.5 Hz, $J_{3,4}$ 2.5 Hz, H-3), 5.22 (dd, 1 H, $J_{3',4'}$ 3.1 Hz, $J_{2',3'}$ 10.5 Hz, H-3'), 4.65 (m, 2 H, J_{gem} 11.3 Hz, $J_{1',2'}$ 7.9 Hz, CH_3OPhCH_2O, H-1'), 4.45 (d, 1 H, J_{gem} 11.5 Hz, CH_3OPhCH_2O), 4.36 (d, 1H, J_{gem} 12.2 Hz, $PhCH_2O$), 4.31 (ddd, 1 H, $J_{2,4}$ 1.0 Hz, $J_{2,3}$ 2.9 Hz, $J_{1,2}$ 5.2 Hz, H-2), 4.27 (dd, 1 H, $J_{5',6a'}$ 5.9 Hz, $J_{6a',6b'}$ 11.0 Hz, H-6a'), 4.15 (d, 1 H, J_{gem} 12.2 Hz, $PhCH_2O$), 4.11 (m, 2 H, H-4', H-6b'), 3.89 (m, 1 H, H-4), 3.82 (m, 1 H, H-5'), 3.74 (s, 3 H, CH_3OPhCH_2O), 3.74 (s, 3 H, $C(O)OCH_3$), 3.70 (m, 1 H, H-5), 3.39 (m, 2 H, $J_{5,6a}$ 2.3 Hz, $J_{6a,6b}$ 10.9 Hz, $J_{5,6b}$ 3.5 Hz, $J_{6a,6b}$ 10.9 Hz, H-6a, H-6b), 2.07 (s, 3 H, $CH_3C(O)O$), 2.01 (s, 3 H, $CH_3C(O)O$), 1.67 (s, 3 H, CH_3); ^{13}C NMR (125 MHz, $CDCl_3$) δ 170.4 (C=O), 169.5 (C=O), 169.2 (C=O), 165.9 (C=O), 164.9 (C=O), 159.4 ($ArOCH_3$), 137.9 (Ar), 133.5 (Ar), 133.2 (Ar), 130.1 (Ar), 129.8 (Ar), 129.6 (Ar), 129.5 (Ar), 129.4 (Ar), 128.9 (Ar), 128.5 (Ar), 128.4 (Ar), 128.4 (Ar), 127.7 (Ar), 113.8 (Ar), 105.3 (quaternary C *pyruvate*), 102.6 (C-1'), 98.1 (C-1), 76.1 (C-4), 74.6 (C-2), 74.5 (CH_3OPhCH_2O), 74.1 (C-3'), 73.1 ($PhCH_2O$), 72.6, 72.3 (C-4', C-5'), 70.6 (C-3), 69.9 (C-2'), 68.6 (C-5), 68.3 (C-6), 62.0 (C-6'), 55.2 (CH_3OPhCH_2O), 52.6 ($C(O)OCH_3$), 21.2 ($CH_3C(O)O$), 20.9 ($CH_3C(O)O$), 20.8 ($-CH_3$); ESI HRMS Calcd. for $C_{55}H_{58}O_{18}Na$ 917.3871. Found 917.3864; Anal. Calc'd. for $C_{55}H_{58}O_{18}$: C, 63.36; H, 5.64. Found: C, 63.02; H, 5.73.

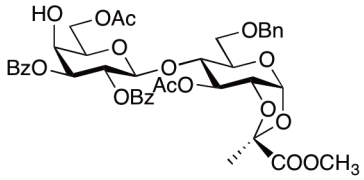

4.11

6-*O*-Acetyl-2,3-di-*O*-benzoyl-β-D-galactopyranosyl-(1→4)-3-*O*-acetyl-6-*O*-benzyl-1,2-*O*-[(*S*)-1-(methoxycarbonyl)ethylidene]-α-D-glucopyranoside (4.11):

Compound **4.10** (0.685 g, 0.737 mmol) was dissolved in anhydrous CH_2Cl_2 (24 ml) and placed under argon atmosphere. The stirred solution was cooled to -20 °C in a dry ice-acetone bath. TfOH (0.065 ml, 0.737 mmol) was added and the reaction instantly turned purple indicating a complete reaction. TLC (20 %, ethyl acetate-toluene) confirmed the reaction to be complete. The reaction mixture was neutralized with Et_3N until neutral and the contents were diluted with CH_2Cl_2. This crude mixture was washed with saturated aqueous sodium bicarbonate, distilled water and saturated aqueous sodium chloride. The organic phase was dried over anhydrous sodium sulfate, filtered and concentrated. The crude product was purified by flash column chromatography on silica gel (2:1, hexanes-ethyl acetate) to give the product **4.11** (0.483 g, 81 %) as a white foam; R_f 0.22 (20 %, ethyl acetate-toluene); $[a]_D$ +41.8 ^{o}(*c* 1.08, $CHCl_3$); ^{1}H NMR (500 MHz, $CDCl_3$) δ 7.99 (m, 2 H, ArH), 7.93 (m, 2 H, ArH), 7.54 (m, 2 H, ArH), 7.37 (m, 7 H, ArH), 7.22 (m, 2 H, ArH), 5.80 (d, 1 H, $J_{1,2}$ 5.1 Hz, H-1), 5.71 (dd, 1 H, $J_{1',2'}$ 7.9 Hz, $J_{2',3'}$ 10.4 Hz, H-2'), 5.57 (vt, 1 H, $J_{2,3}$ 2.8 Hz, $J_{3,4}$ 2.8 Hz, H-3), 5.24 (dd, 1 H, $J_{3',4'}$ 3.3 Hz, $J_{2',3'}$ 10.4 Hz, H-3'), 4.70 (d, 1 H, $J_{1',2'}$ 7.9 Hz, H-1'), 4.43 (dd, 1 H, $J_{5',6a'}$ 7.1 Hz, $J_{6a',6b'}$ 11.5 Hz, H-6a'), 4.40 (d, 1 H, J_{gem} 12.2 Hz,

PhC*H*$_2$O), 4.36 (ddd, 1 H, $J_{2,4}$ 1.2 Hz, $J_{2,3}$ 3.0 Hz, $J_{1,2}$ 5.2 Hz, H-2), 4.33 (dd, 1 H, $J_{5',6b'}$ 5.9 Hz, $J_{6a',6b'}$ 11.4 Hz, H-6b'), 4.27 (m, 1 H, $J_{3',4'}$ 3.1 Hz, H-4'), 4.18 (d, 1 H, J_{gem} 12.3 Hz, PhC*H*$_2$O), 3.94 (m, 1 H, H-4), 3.90 (m, 1 H, H-5'), 3.77 (s, 3 H, C(O)OC*H*$_3$), 3.73 (m, 1 H, H-5), 3.43 (dd, 1 H, $J_{5,6a}$ 2.4 Hz, $J_{6a,6b}$ 10.9 Hz, H-6a), 3.40 (dd, 1 H, $J_{5,6b}$ 3.5 Hz, $J_{6a,6b}$ 10.9 Hz, H-6b), 2.45 (d, 1 H, $J_{4',OH}$ 6.0 Hz, 4'-OH), 2.12 (s, 3 H, C*H*$_3$C(O)O), 2.11 (s, 3 H, C*H*$_3$C(O)O), 1.71 (s, 3 H, CH_3); ^{13}C NMR (125 MHz, $CDCl_3$) δ 170.9 (C=O), 169.5 (C=O), 169.3 (C=O), 165.8 (C=O), 164.9 (C=O), 137.9 (Ar), 133.5 (Ar), 133.3 (Ar), 129.9 (Ar), 129.7 (Ar), 129.3 (Ar), 129.0 (Ar), 128.5 (Ar), 128.4 (Ar), 127.8 (Ar), 105.4 (quaternary C *pyruvate*), 102.6 (C-1'), 98.2 (C-1), 76.1 (C-4), 74.0 (C-2, C-3'), 73.2 (Ph*C*H$_2$O), 72.2 (C-5'), 70.5 (C-3), 69.5 (C-2'), 68.7 (C-5), 68.3 (C-6), 67.1 (C-4'), 61.9 (C-6'), 52.6 (C(O)O*C*H$_3$), 21.2 (*C*H$_3$C(O)O), 20.9 (*C*H$_3$C(O)O), 20.8 (-CH$_3$); ESI HRMS Calcd. for $C_{41}H_{44}O_{17}Na$ 831.2471. Found 831.2473; Anal. Calc'd. for $C_{41}H_{44}O_{17}$: C, 60.89; H, 5.48; O, 33.63. Found: C, 61.06; H, 5.54.

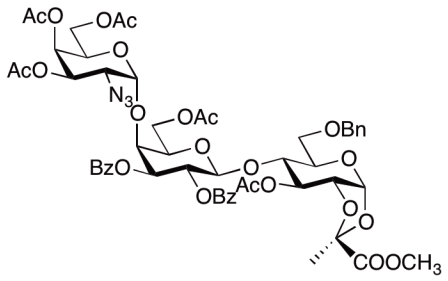

4.4

3,4,6-Tri-*O*-acetyl-2-azido-2-deoxy-α-D-galactopyranosyl-(1→4)-6-*O*-acetyl-2,3-di-*O*-benzoyl-β-D-galactopyranosyl-(1→4)-3-*O*-acetyl-6-*O*-benzyl-1,2-*O*-[(*S*)-1-(methoxycarbonyl)ethylidene]-α-D-glucopyranoside (4.4):

The acceptor **4.11** (0.203 g, 0.251 mmol) and 4Å molecular sieves (100 mg) were combined in a dry flask and dissolved in anhydrous Et_2O (2 ml). The reaction mixture was stirred for one hour under argon atmosphere, after which the activator TMSOTf (6.8 ml, 0.038 mmol) was added. The trichloroacetimidate donor **3.3** (0.478 g, 1.00 mmol) was dissolved in anhydrous Et_2O (2 ml) and added drop-wise at room temperature to the stirred solution. The reaction proceeded for two hours and reaction progress was monitored by TLC analysis (60 %, ethyl acetate-hexanes) at which point donor was consumed. The reaction was quenched with one drop of Et_3N, filtered through Celite and concentrated to dryness. The crude reaction mixture was purified by flash column chromatography in silica gel (1:1, ethyl acetate-hexanes) to provide the product **4.4** (0.134 g, 48 %) as a white foam; R_f 0.44 (60 %, ethyl acetate-toluene); $[a]_D$ +77.2 ^{o}(*c* 1.04, $CHCl_3$); ^{1}H NMR (500 MHz, $CDCl_3$) δ 7.95 (m, 2 H, ArH), 7.89 (m, 2 H, ArH), 7.49 (m, 2 H, ArH), 7.34 (m, 7 H, ArH), 7.20 (m, 2 H, ArH), 5.78 (d, 1 H, $J_{1,2}$ 5.2 Hz, H-1), 5.62 (dd, 1 H, $J_{1',2'}$ 7.9 Hz, $J_{2',3'}$ 10.7 Hz, H-2'), 5.54 (vt, 1 H, $J_{2,3}$ 2.5 Hz, $J_{3,4}$ 2.5 Hz, H-3), 5.43 (dd, 1 H, $J_{3'',4''}$ 3.1 Hz, $J_{2'',3''}$ 11.1 Hz, H-3''),

5.21 (dd, 1 H, $J_{3',4'}$ 3.1 Hz, $J_{2',3'}$ 10.7 Hz, H-3'), 5.01 (d, 1 H, $J_{1'',2''}$ 3.5 Hz, H-1''), 4.72 (d, 1 H, $J_{1',2'}$ 7.8 Hz, H-1'), 4.50 (m, 1 H, H-5''), 4.46 (m, 2 H, H-6ab'), 4.38 (m, 2 H, H-4', PhCH_2O), 4.34 (ddd, 1 H, $J_{2,4}$ 0.9 Hz, $J_{2,3}$ 3.1 Hz, $J_{1,2}$ 5.2 Hz, H-2), 4.18 (d, 1 H, J_{gem} 12.1 Hz, PhCH_2O), 3.92 (m, 2 H, H-4, H-5'), 3.81 (m, 2 H, H-2'', H-6a''), 3.75 (m, 4 H, H-5, C(O)OCH_3), 3.43 (m, 3 H, H-6ab, H-6b''), 2.12 (s, 3 H, CH_3C(O)O), 2.11 (s, 3 H, CH_3C(O)O), 2.07 (s, 3 H, CH_3C(O)O), 1.85 (s, 3 H, CH_3C(O)O), 1.70 (s, 3 H, CH_3); ^{13}C NMR (125 MHz, $CDCl_3$) δ 170.4 (C=O), 170.1 (C=O), 169.9 (C=O), 169.6 (C=O), 169.3 (C=O), 166.0 (C=O), 164.7 (C=O), 137.9 (Ar), 133.6 (Ar), 133.3 (Ar), 129.8 (Ar), 129.6 (Ar), 129.2 (Ar), 128.7 (Ar), 128.4 (Ar), 128.3 (Ar), 127.7 (Ar), 127.6 (Ar), 105.3 (quaternary C *pyruvate*), 102.4 (C-1'), 99.2 (C-1''), 98.1 (C-1), 76.2 (C-5'), 74.8 (C-4'), 74.3 (C-2), 73.5 (C-3'), 73.2 (Ph*C*H_2O), 72.1 (C-4), 70.7 (C-3), 69.5 (C-2'), 68.6, 68.5 (C-5, C-3''), 68.3 (C-6), 67.1, 67.0 (C-4'', C-5''), 61.4 (C-6'), 60.5 (C-6''), 58.2 (C-2''), 52.6 (*C*H_3OC(O)), 21.3 (*C*H_3C(O)O), 20.9 (*C*H_3C(O)O), 20.8 (*C*H_3C(O)O), 20.6 (*C*H_3C(O)O), 20.5(5) (*C*H_3C(O)O), 20.5(1) (*C*H_3C(O)O); ESI HRMS Calc'd. for $C_{53}H_{59}N_3O_{24}Na$ 1144.3381. Found 1144.3376; Anal. Calc'd. for $C_{53}H_{59}N_3O_{24}$: C, 56.73; H, 5.30; N, 3.74. Found: C, 56.86; H, 5.42; N, 3.44.

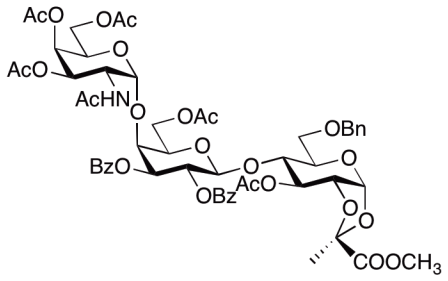

4.12

2-Acetamido-3,4,6-tri-*O*-acetyl-2-deoxy-α-D-galactopyranosyl-(1→4)-6-*O*-acetyl-2,3-di-*O*-benzoyl-β-D-galactopyranosyl-(1→4)-3-*O*-acetyl-6-*O*-benzyl-1,2-*O*-[(*S*)-1-(methoxycarbonyl)ethylidene]-α-D-glucopyranoside (4.12):

The azide **4.4** (0.297 g, 0.265 mmol) was placed in a dry flask dissolved in a 6:1 mixture of CH_3CN:Et_3N (8 ml) and placed under an argon atmosphere. DTT (0.163 g, 1.06 mmol) was added and the reaction proceeded at room temperature overnight. Subsequent TLC analysis (60 %, ethyl acetate-hexanes) showed no remaining starting material. A 1:1 mixture of acetic Ac_2O:Pyr was added to the reaction flask and again allowed to proceed overnight. The reaction mixture was then concentrated to dryness while co-evaporating with toluene. The crude product was then subjected to flash column chromatography on silica gel (40 %, acetone-hexanes) to provide the product **4.12** (0.262 g, 87 %) as a white foam; R_f 0.30 (1:1, acetone-hexanes); $[a]_D$ +77.2 ^{o}(*c* 1.12, $CHCl_3$); ^{1}H NMR (500 MHz, $CDCl_3$) δ 7.94 (m, 2 H, ArH), 7.91 (m, 2 H, ArH), 7.51 (m, 2 H, ArH), 7.41-7.31 (m, 7 H, ArH), 7.21 (m, 2 H, ArH), 6.05 (d, 1 H, $J_{2",NH}$ 9.5 Hz, N-H), 5.80 (d, 1 H, $J_{1,2}$ 5.1 Hz, H-1), 5.69 (dd, 1 H, $J_{1',2'}$ 7.9 Hz, $J_{2',3'}$ 10.5 Hz, H-2'), 5.61 (m, 1 H, H-3), 5.35 (m, 1 H, H-4"), 5.29 (dd, 1 H, $J_{3",4"}$ 3.1 Hz, $J_{2",3"}$ 11.5 Hz, H-3"), 5.24 (dd, 1 H, $J_{3',4'}$ 3.0 Hz, $J_{2',3'}$ 10.6 Hz, H-3'), 5.06 (d, 1 H, $J_{1",2"}$ 3.9 Hz, H-1"), 4.71 (d, 1 H, $J_{1',2'}$ 7.8 Hz, H-1'), 4.69 (ddd, 1 H, $J_{1",2"}$ 3.9 Hz, $J_{2",NH}$ 9.7 Hz, $J_{2",3"}$ 11.6 Hz, H-

2''), 4.47 (dd, 1 H, $J_{5',6a'}$ 6.2 Hz, $J_{6a',6b'}$ 11.2 Hz, H-6a'), 4.43 (d, 1 H, $J_{3',4'}$ 3.0 Hz, H-4'), 4.39 (m, 2 H, J_{gem} 12.2 Hz, H-5'', PhCH_2O), 4.33 (ddd, 1 H, $J_{2,4}$ 1.0 Hz, $J_{2,3}$ 2.5 Hz, $J_{1,2}$ 5.1 Hz, H-2), 4.19 (d, 1 H, J_{gem} 12.1 Hz, PhCH_2O), 4.02 (dd, 1 H, $J_{5',6b'}$ 8.2 Hz, $J_{6a',6b'}$ 11.2 Hz, H-6b'), 3.94 (m, 2 H, H-4, H-5'), 3.77 (s, 3 H, C(O)OCH_3), 3.74 (m, 1 H, H-5), 3.68 (dd, 1 H, $J_{5'',6a''}$ 8.5 Hz, $J_{6a'',6b''}$ 10.9 Hz, H-6a''), 3.46 (dd, 1 H, $J_{5,6a}$ 2.2 Hz, $J_{6a,6b}$ 10.9 Hz, H-6a), 3.40 (dd, 1 H, $J_{5,6b}$ 3.5 Hz, $J_{6a,6b}$ 10.8 Hz, H-6b), 3.20 (dd, 1 H, $J_{5'',6b''}$ 6.1 Hz, $J_{6a'',6b''}$ 10.9 Hz, H-6b''), 2.14 (s, 3 H, CH_3C(O)O), 2.12 (s, 3 H, CH_3C(O)O), 2.09 (s, 3 H, CH_3C(O)O), 2.08 (s, 3 H, CH_3C(O)O), 2.04 (s, 3 H, CH_3C(O)O), 1.77 (s, 3 H, CH_3C(O)NH), 1.73 (s, 3 H, CH_3); ^{13}C NMR (125 MHz, $CDCl_3$) δ 170.7 (C=O), 170.2 (C=O), 169.7 (C=O), 169.4 (C=O), 169.2 (C=O), 165.8 (C=O), 164.9 (C=O), 137.9 (Ar), 133.6 (Ar), 133.4 (Ar), 129.7 (Ar), 129.6 (Ar), 129.1 (Ar), 128.8 (Ar), 128.6 (Ar), 128.5 (Ar), 128.4 (Ar), 127.8 (Ar), 127.7 (Ar), 105.5 (quaternary C *pyruvate*), 102.6 (C-1'), 98.2 (C-1''), 97.9 (C-1), 76.4 (C-4), 74.1 (C-2), 73.2 (Ph*C*H_2O), 73.1 (C-3'), 72.2 (C-4'), 72.1 (C-5'), 70.0 (C-3), 69.6 (C-2'), 68.3 (C-5), 68.2 (C-6), 68.1 (C-3''), 66.8, 66.7 C-4'', -5''), 60.6, 60.5 (C-6', C-6''), 52.7 (*C*H_3OC(O)), 47.6 (C-2''), 23.2 (*C*H_3C(O)O), 21.2 (*C*H_3C(O)O), 20.9 (*C*H_3C(O)O), 20.8 (*C*H_3C(O)O), 20.7 (-*C*H_3), 20.5 (*C*H_3C(O)NH); ESI HRMS Calc'd. for $C_{55}H_{63}NO_{25}Na$ 1160.3581. Found 1160.3573; Anal. Calc'd. for $C_{55}H_{63}NO_{25}$: C, 58.04; H, 5.58; N, 1.23. Found: C, 57.76; H, 5.57; N, 1.28.

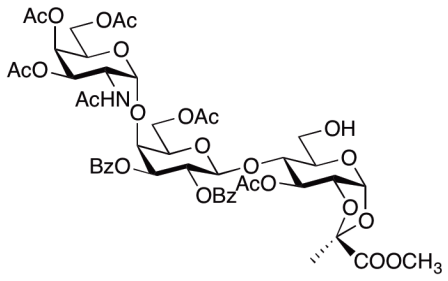

4.13

2-Acetamido-3,4,6-tri-*O*-acetyl-2-deoxy-α-D-galactopyranosyl-(1→4)-6-*O*-acetyl-2,3-di-*O*-benzoyl-β-D-galactopyranosyl-(1→4)-3-*O*-acetyl-1,2-*O*-[(*S*)-1-(methoxycarbonyl)ethylidene]-α-D-glucopyranoside (4.13):

The 6-*O*-benzyl trisaccharide derivative **4.12** (0.738 g, 0.648 mmol) was combined with 20 % wt. $Pd(OH)_2$ on charcoal (0.250 g) in the reaction flask and the starting material was dissolved in ethyl acetate (14 ml). The reaction vessel was placed under a hydrogen atmosphere and the hydrogenation reaction proceeded at room temperature for three hours. TLC analysis (1:1, acetone-hexanes) showed the reaction to be complete. The reaction mixture was filtered through a Millipore filter to remove the solid catalyst and the filtrate was subsequently concentrated to dryness to provide the product **4.13** (0.660 g, 97%) as a white foam; R_f 0.24 (1:1, acetone-hexanes); $[a]_D$ +81.6 ^{o}(*c* 1.11, $CHCl_3$); ^{1}H NMR (500 MHz, $CDCl_3$) δ 7.93 (m, 2 H, ArH), 7.90 (m, 2 H, ArH), 7.48 (m, 2 H, ArH), 7.36 (m, 4 H, ArH), 6.28 (d, 1 H, $J_{2",NH}$ 10.4 Hz, N-H), 5.74 (m, 2 H, H-1, H-2'), 5.50 (m, 1 H, H-3), 5.33 (m, 1 H, H-4"), 5.30 (dd, 1 H, $J_{3",4"}$ 3.2 Hz, $J_{2",3"}$ 11.4 Hz, H-3"), 5.24 (dd, 1 H, $J_{3',4'}$ 2.9 Hz, $J_{2',3'}$ 10.5 Hz, H-3'), 5.01 (d, 1 H, $J_{1",2"}$ 3.8 Hz, H-1"), 4.93 (d, 1 H, $J_{1',2'}$ 8.0 Hz, H-1'), 4.65 (ddd, 1 H, $J_{1",2"}$ 3.8 Hz, $J_{2",NH}$ 9.6 Hz, $J_{2",3"}$ 11.4 Hz, H-2"), 4.46 (dd, 1 H, $J_{5',6a'}$ 4.2 Hz, $J_{6a',6b'}$ 9.0 Hz, H-6a'), 4.42 (d, 1 H, $J_{3',4'}$ 2.9 Hz, H-4'), 4.38 (m, 1 H, H-5"), 4.32 (ddd, 1 H, $J_{2,4}$ 1.0 Hz, $J_{2,3}$ 2.6

Hz, $J_{1,2}$ 5.1 Hz, H-2), 4.00 (m, 3 H, H-4, H-5', H-6b'), 3.74 (s, 3 H, C(O)OC*H*$_3$), 3.66 (m, 3 H, H-5, H-6a, H-6a''), 3.49 (m, 1 H, H-6b), 3.10 (dd, 1 H, $J_{5'',6b''}$ 6.0 Hz, $J_{6a'',6b''}$ 10.9 Hz, H-6b''), 2.10 (s, 3 H, C*H*$_3$C(O)O), 2.09 (s, 3 H, C*H*$_3$C(O)O), 2.06 (s, 3 H, C*H*$_3$C(O)O), 2.05 (s, 3 H, C*H*$_3$C(O)O), 2.01 (s, 3 H, C*H*$_3$C(O)O), 1.76 (s, 3 H, C*H*$_3$C(O)NH), 1.72 (s, 3 H, CH_3); ^{13}C NMR (125 MHz, $CDCl_3$) δ 170.8 (C=O), 170.7 (C=O), 170.2 (C=O), 169.7 (C=O), 169.3 (C=O), 169.2 (C=O), 165.9 (C=O), 165.1 (C=O), 133.7 (Ar), 133.5 (Ar), 129.7 (Ar), 129.6 (Ar), 128.9 (Ar), 128.7 (Ar), 128.5 (Ar), 105.6 (quaternary C *pyruvate*), 102.3 (C-1'), 98.6 (C-1''), 97.8 (C-1), 75.3 (C-4), 73.9 (C-2), 73.5 (C-3'), 72.6 (C-4'), 72.3 (C-5'), 70.2 (C-3), 69.2, 68.9 (C-5, C-2'), 67.9 (C-3''), 66.8, 66.7 (C-4'', C-5''), 61.5 (C-6''), 60.6, 60.4 (C-6, C-6'), 52.7 (C(O)O*C*H$_3$), 47.7 (C-2''), 23.1 (*C*H$_3$C(O)O), 21.2 (*C*H$_3$C(O)O), 20.9 (*C*H$_3$C(O)O), 20.8 (*C*H$_3$C(O)O), 20.6 (*C*H$_3$C(O)NH), 20.5 (-CH$_3$); ESI HRMS Calc'd. for $C_{48}H_{57}NO_{25}Na$ 1070.3112. Found 1070.3105; Anal. Calc'd. for $C_{48}H_{57}NO_{25}$: C, 55.01; H, 5.48; N, 1.34. Found: C, 55.04; H, 5.65; N, 1.38.

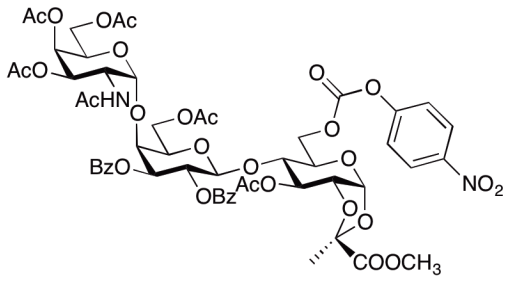

4.14

2-Acetamido-3,4,6-tri-*O*-acetyl-2-deoxy-α-D-galactopyranosyl-(1→4)-6-*O*-acetyl-2,3-di-*O*-benzoyl-β-D-galactopyranosyl-(1→4)-3-*O*-acetyl-6-(4-nitrophenylcarbonate)-1,2-*O*-[(*S*)-1-(methoxycarbonyl)ethylidene]-α-D-glucopyranoside (4.14):

The primary alcohol **4.13** (0.144 g, 0.137 mmol) was combined with 4-nitrophenyl chloroformate **4.16** (0.033 g, 0.165 mmol) and dissolved in dry CH_2Cl_2 (3 ml). Pyr (0.022 ml, 0.274 mmol) was then added and the reaction proceeded at room temperature for 10 min. TLC analysis (1:1, acetone-hexanes) showed no remaining starting material. The reaction was diluted with CH_2Cl_2 and washed with saturated aqueous sodium bicarbonate, distilled water and saturated aqueous sodium chloride. The organic layer was dried over anhydrous sodium sulfate, filtered and concentrated to dryness. The crude product was purified by flash column chromatography on silica gel (1:1, acetone-hexanes) to give the product **4.14** (0.165 g, 99 %) was a white foam; R_f 0.26 (1:1, acetone-hexanes); $[a]_D$ +92.2 ^{o}(*c* 1.08, $CHCl_3$); ^{1}H NMR (600 MHz, $CDCl_3$) δ 8.27 (m, 2 H, ArH), 7.93 (m, 4 H, ArH), 7.48 (m, 2 H, ArH), 7.38 (m, 2 H, ArH), 7.32 (m, 2 H, ArH), 7.28 (m, 2 H, ArH), 6.02 (d, 1 H, $J_{2'',NH}$ 9.5 Hz, N-H), 5.79 (d, 1 H, $J_{1,2}$ 5.2 Hz, H-1), 5.72 (dd, 1 H, $J_{1',2'}$ 7.7 Hz, $J_{2',3'}$ 10.5 Hz, H-2'), 5.64 (m, 1 H, H-3), 5.34 (m, 1 H, H-4''), 5.32 (dd, 1 H, $J_{3',4'}$ 3.1 Hz, $J_{2',3'}$ 10.6 Hz, H-3'), 5.29 (dd, 1 H, $J_{3'',4''}$ 3.2

Hz, $J_{2",3"}$ 11.6 Hz, H-3"), 5.06 (d, 1 H, $J_{1",2"}$ 3.9 Hz, H-1"), 4.94 (d, 1 H, $J_{1',2'}$ 7.8 Hz, H-1'), 4.66 (ddd, 1 H, $J_{1",2"}$ 3.8 Hz, $J_{2",NH}$ 9.6 Hz, $J_{2",3"}$ 11.5 Hz, H-2"), 4.50 (m, 1 H, H-6a'), 4.44 (d, 1 H, $J_{3',4'}$ 3.1 Hz, H-4'), 4.37 (m, 2 H, H-2, H-5"), 4.32 (dd, 1 H, $J_{5,6a}$ 2.2 Hz, $J_{6a,6b}$ 11.7 Hz, H-6a), 4.16 (dd, 1 H, $J_{5,6b}$ 4.9 Hz, $J_{6a,6b}$ 11.8 Hz, H-6b), 4.00 (m, 3 H, $J_{5,6a}$ 2.2 Hz, $J_{5,6b}$ 4.9 Hz, $J_{4,5}$ 9.5 Hz, H-5, H-5', H-6b'), 3.83 (m, 1 H, $J_{4,5}$ 9.5 Hz, H-4), 3.78 (s, 3 H, C(O)OC*H*$_3$), 3.67 (m, 1 H, $J_{5",6a"}$ 8.4 Hz, $J_{6a",6b"}$ 10.9 Hz, H-6a"), 3.21 (dd, 1 H, $J_{5",6b"}$ 6.1 Hz, $J_{6a",6b"}$ 11.0 Hz, H-6b"), 2.13 (s, 3 H, C*H*$_3$C(O)O), 2.12 (s, 3 H, C*H*$_3$C(O)O), 2.08 (s, 3 H, C*H*$_3$C(O)O), 2.07 (s, 3 H, C*H*$_3$C(O)O), 2.03 (s, 3 H, C*H*$_3$C(O)O), 1.78 (s, 3 H, C*H*$_3$C(O)NH), 1.76 (s, 3 H, CH_3); ^{13}C NMR (125 MHz, $CDCl_3$) δ 170.7 (C=O), 170.6 (C=O), 170.2 (C=O), 169.7 (C=O), 169.2 (C=O), 165.8 (C=O), 165.0 (Ar), 155.3 (Ar), 151.8 (Ar), 145.4 (Ar), 133.7 (Ar), 133.5 (Ar), 129.7 (Ar), 129.6 (Ar), 128.8 (Ar), 128.7 (Ar), 128.5 (Ar), 128.4 (Ar), 105.7 (quaternary C *pyruvate*), 102.5 (C-1'), 98.3 (C-1"), 97.7 (C-1), 77.0 (C-4), 74.2 (C-2), 73.1 (C-3'), 72.3, 72.2 (C-4', C-5'), 69.6, 69.5(9) (C-3, C-2'), 68.0 (C-3"), 67.4 (C-5), 66.8 (C-6), 66.6, 66.5 (C-4", C-5"), 60.6 (C-6"), 60.5 (C-6'), 52.7 (*C*H_3OC(O)), 47.7 (C-2"), 23.1 (*C*H_3C(O)O), 21.2 (*C*H_3C(O)O), 20.9 (*C*H_3C(O)O), 20.7(8) (*C*H_3C(O)O), 20.7(6) (*C*H_3C(O)O), 20.6 (*C*H_3C(O)NH), 20.5 (-CH_3); ESI HRMS Calc'd. for $C_{55}H_{60}N_2O_{29}Na$ 1235.3174. Found 1235.3167; Anal. Calc'd. for $C_{55}H_{60}N_2O_{29}$: C, 54.46; H, 4.99; N, 2.31. Found: C, 54.45; H, 5.22; N, 2.19.

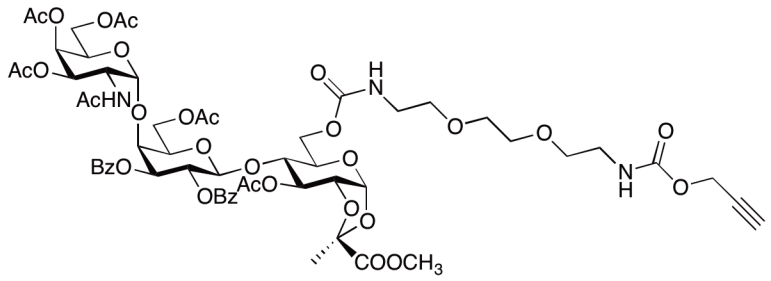

4.15

2-Acetamido-3,4,6-tri-*O*-acetyl-2-deoxy-α-D-galactopyranosyl-(1→4)-6-*O*-acetyl-2,3-di-*O*-benzoyl-β-D-galactopyranosyl-(1→4)-3-*O*-acetyl-6-*O*-(10-oxo-3,6,11-trioxa-9-azatetradec-13-ynyl)carbamoyl-1,2-*O*-[(*S*)-1-(methoxycarbonyl)ethylidene]-α-D-glucopyranoside (4.15):

The *p*-nitrophenylcarbamoyl derivative **4.14** (0.656 g, 0.541 mmol) was combined with the propargylated amine **4.5** (0.186 g, 0.811 mmol) and dissolved in dry CH_2Cl_2 (10 ml). Et_3N (0.151 ml, 1.08 mmol) was added and the reaction proceeded at room temperature for two hours. The reaction mixture was concentrated to dryness and the crude product purified by flash column chromatography on silica gel (1:1, acetone-hexanes) to provide the product **4.15** (0.706 g, 95 %) as a white foam; R_f 0.34 (1:1, acetone-hexanes); $[a]_D$ +70.7 ^{o}(*c* 1.00, $CHCl_3$); ^{1}H NMR (500 MHz, $CDCl_3$) δ 7.95 (m, 2 H, ArH), 7.92 (m, 2 H, ArH), 7.49 (m, 2 H, ArH), 7.37 (m, 4 H, ArH), 6.07 (d, 1 H, $J_{2'',NH}$ 9.3 Hz, N-H), 5.75 (d, 1 H, $J_{1,2}$ 5.2 Hz, H-1), 5.70 (dd, 1 H, $J_{1',2'}$ 7.8 Hz, $J_{2',3'}$ 10.5 Hz, H-2'), 5.64 (bs, 1 H, H-3), 5.40 (bs, 1 H, N-H linker), 5.34 (m, 1 H, $J_{3'',4''}$ 2.8 Hz, H-4''), 5.29 (t, 1 H, $J_{3'',4''}$ 2.8 Hz, H-3''), 5.26 (m, 1 H, H-3'), 5.04 (d, 1 H, $J_{1'',2''}$ 3.9 Hz, H-1''), 4.89 (d, 1 H, $J_{1',2'}$ 7.8 Hz, H-1'), 4.66 (m, 3 H, $J_{1'',2''}$ 3.8 Hz, H-2'', OCH_2C≡CH), 4.48 (dd, 1 H, $J_{5',6a'}$ 9.7 Hz, $J_{6a',6b'}$ 14.3 Hz, H-6a'), 4.43 (d, 1 H, $J_{3',4'}$ 3.1 Hz, H-4'), 4.37 (m, 1 H, H-5''), 4.31 (dd, 1 H, $J_{2,3}$ 2.5 Hz, $J_{1,2}$ 5.2 Hz, H-2), 4.18 (dd, 1 H,

$J_{5,6a}$ 4.2 Hz, $J_{6a,6b}$ 11.8 Hz, H-6a), 4.03 (dd, 1 H, $J_{5,6b}$ 1.2 Hz, $J_{6a,6b}$ 11.6 Hz, H-6b), 3.98 (m, 2 H, H-5', H-6b'), 3.82 (m, 1 H, H-5), 3.75 (s, 3 H, C(O)OCH_3), 3.72 (m, 1 H, H-4), 3.66 (dd, 1 H, $J_{5",6a"}$ 8.5 Hz, $J_{6a",6b"}$ 10.8 Hz, H-6a"), 3.60 (s, 4 H, OCH_2CH_2O *linker*), 3.55 (m, 4 H, HNCH$_2$CH_2O linker), 3.36 (m, 4 H, HNCH_2CH$_2$O), 3.15 (dd, 1 H, $J_{5",6b"}$ 6.0 Hz, $J_{6a",6b"}$ 10.8 Hz, H-6b"), 2.48 (t, 1 H, $J_{CH,CH2}$ 2.1 Hz, OCH$_2$C≡C*H*), 2.10 (s, 3 H, CH_3C(O)O), 2.09 (s, 3 H, CH_3C(O)O), 2.07 (s, 3 H, CH_3C(O)O), 2.06 (s, 3 H, CH_3C(O)O), 2.02 (s, 3 H, CH_3C(O)O), 1.75 (s, 3 H, -CH$_3$), 1.72 (s, 3 H, CH_3C(O)NH); ^{13}C NMR (125 MHz, CDCl$_3$) δ 170.7 (C=O), 170.6 (C=O), 170.2 (C=O), 170.1 (C=O), 169.7 (C=O), 169.3 (C=O), 168.9 (C=O), 165.8 (C=O), 165.1 (C=O), 155.8 (C=O), 155.5 (C=O), 133.6 (Ar), 133.3 (Ar), 129.7 (Ar), 129.7 (Ar), 129.6 (Ar), 128.9 (Ar), 128.7 (Ar), 128.5 (Ar), 128.4 (Ar), 105.6 (quaternary C *pyruvate*), 102.3 (C-1'), 98.4 (C-1"), 97.7 (C-1), 76.4 (C-4), 74.7 (OCH$_2$C≡*C*H), 73.9 (C-2), 73.3 (C-3"), 72.3, 72.1 (C-4', C-5'), 70.3, (CH$_2$, *linker)*, 70.0 (CH$_2$, *linker*), 69.9 CH$_2$ *linker*), 69.8 (C-3), 69.5 (C-2'), 68.0 (C-3'), 67.5 (C-5), 66.8, 66.7 (C-4", C-5"), 63.4 (C-6), 60.4 (C-6, C-6'), 52.7 (C(O)O*C*H$_3$), 52.4 (O*C*H$_2$C≡CH), 47.6 (C-2"), 40.9 (CH$_2$ *linker*), 23.1 (*C*H$_3$C(O)O), 21.1 (*C*H$_3$C(O)O), 20.9 (*C*H$_3$C(O)O), 20.8 (*C*H$_3$C(O)O), 20.6 (*C*H$_3$C(O)NH), 20.4 (-CH$_3$); ESI HRMS Calcd. for $C_{59}H_{73}N_3O_{30}Na$ 1326.4171. Found 1326.4159; Anal. Calc'd. for $C_{59}H_{70}N_3O_{30}$: C, 54.33; H, 5.64; N, 3.22. Found: C, 54.43; H, 5.79; N, 3.31.

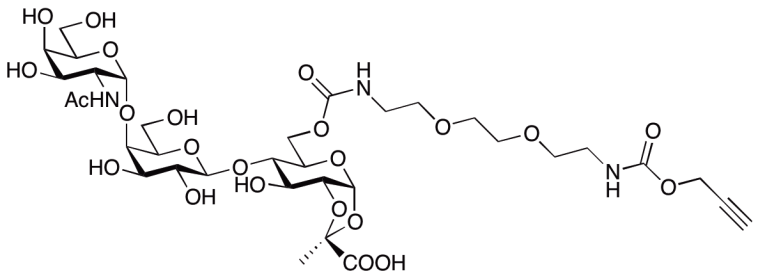

4.2

2-Acetamido-2-deoxy-α-D-galactopyranosyl-(1→4)-β-D-galactopyranosyl-(1→4)-6-O-(10-oxo-3,6,11-trioxa-9-azatetradec-13-ynyl)carbamoyl-1,2-*O*-[(*S*)-1-(carboxy)ethylidene]-α-D-glucopyranoside (4.2):

The acylated trisaccharide **4.15** (0.410 g, 0.314 mmol) was placed in a round bottom flask and dissolved in anhydrous CH_3OH (20 ml). A 1 M solution of CH_3ONa in CH_3OH was prepared and added (0.314 ml, 0.314 mmol) to the reaction flask. The reaction proceeded for two days at which point TLC (10 %, methanol-dichloromethane) showed the reaction was complete. The reaction mixture was concentrated to dryness and placed under high vacuum for two hours. The residue was subsequently dissolved in 20 ml MilliQ water and the pH checked and adjusted to ensure a pH ~8/9. The hydrolysis of the methyl ester was allowed to proceed for 15 min at which point TLC analysis (4:5:1:0.1, dichloromethane:methanol:water:acetic acid) showed no remaining starting material. The reaction was quenched by drop-wise addition of TFA until the pH was ~7. The reaction mixture was concentrate and lyophilized. The crude product was purified by HPLC on an X-Bridge C18 reverse-phase column (100 % water (0.1 %, TFA) → 100 % acetonitrile) and was once again lyophilized to provide the product **4.2** (0.242 g, 88 %) was a white powder; R_f 0.58 (4:5:1:0.1, dichloromethane:methanol:water:acetic acid); $[a]_D$ +79.4 ^{o}(*c* 1.20, H_2O); ^{1}H NMR

(700 MHz, D_2O) δ 5.77 (d, 1 H, $J_{1,2}$ 4.9 Hz, H-1), 4.90 (d, 1 H, $J_{1",2"}$ 3.9 Hz, H-1"), 4.62 (bs, 1 H, OCH_2C≡CH), 4.52 (d, 1 H, $J_{1',2'}$ 7.7 Hz, H-1'), 4.42 (m, 3 H, $J_{5,6a}$ 6.4 Hz, H-3, H-6a, H-5"), 4.37 (t, 1 H, $J_{1,2}$ 4.1 Hz, H-2), 4.24 (dd, 1 H, $J_{5,6b}$ 5.4 Hz, $J_{6a,6b}$ 11.9 Hz, H-6b), 4.21 (dd, 1 H, $J_{1",2"}$ 3.9 Hz, $J_{2",3"}$ 11.2 Hz, H-2"), 4.04 (m, 2 H, $J_{3",4"}$ 3.1 Hz, H-5, H-4"), 3.98 (m, 2 H, $J_{3',4'}$ 3.1 Hz, $J_{3",4"}$ 3.2 Hz, $J_{2",3"}$ 11.3 Hz, H-4', H-3"), 3.82 (d, 1 H, $J_{4,5}$ 9.4 Hz, H-4), 3.76 (m, 2 H, H-5', H-6a'), 3.72 (m, 4 H, $J_{3',4'}$ 3.1 Hz, $J_{2'3'}$ 10.4 Hz, H-3', H-6b', H-6ab"), 3.68 (s, 4 H, OCH_2CH_2O), 3.61 (m, 5 H, $J_{1',2'}$ 7.7 Hz, $J_{2',3'}$ 10.2 Hz, H-2', HNCH_2CH_2O(X2)), 3.34 (m, 4 H, HNCH_2CH_2O(X2)), 2.91 (bs, 1 H, OCH_2C≡C*H*), 2.09 (s, 3 H, CH_3C(O)NH), 1.76 (s, 3 H, CH_3); ^{13}C NMR (125 MHz, D_2O) δ 175.4 (C=O), 173.8 (C=O), 158.9 (C=O), 158.6 (C=O), 106.4 (quaternary C *pyruvate*), 106.3 (C-1'), 99.3 (C-1"), 98.0 (C-1), 79.6 (OCH_2*C*≡CH), 79.5 (C-4), 77.4 (OCH_2C≡*C*H), 76.7 (C-4'), 76.6 (C-5'), 76.2, (C-2), 73.1 (C-3'), 71.6 (C-2', C-5"), 70.4 (CH_2 *linker*), 70.2 (CH_2 *linker*), 70.1 (CH_2 *linker*), 69.8, 69.5 (C-3, C-5), 69.2 (C-4"), 68.2 (C-3"), 65.1 (C-6), 61.5, 61.3 (C-6', C-6"), 53.8 (O*C*H_2C≡CH), 51.0 (C-2"), 41.1 (CH_2-linker), 22.9 (*C*H_3C(O)NH), 21.8 (CH_3); ESI HRMS Calcd. for $C_{34}H_{52}N_3O_{23}[M-H]^-$ 870.2997. Found 870.3005.

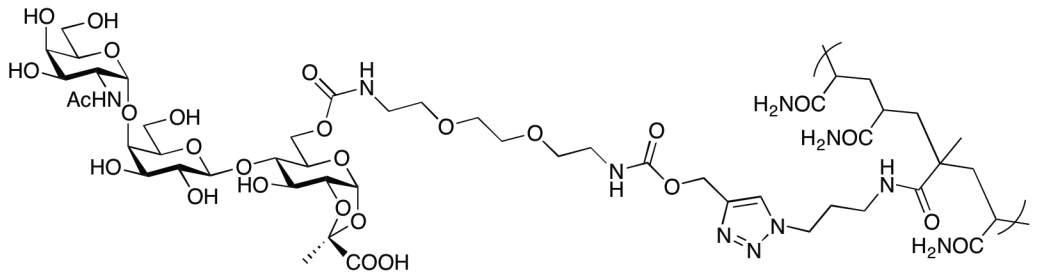

4.1

PolyBAIT-P^{k}NAc (4.1):

BAIT-P$_{k}$NAc **4.2** (0.113 g, 0.130 mmol) was combined with poly[acrylamide-co-(2-azidopropylmethacrylamide)] (27 KDa, PDI 1.29, 0.139 g, 0.0865 mmol) and the contents dissolved in degassed MilliQ water (0.5 ml). A 1.0 M solution of sodium ascorbate was prepared and added to the solution (125 μl) followed by the addition of a 0.005 M solution of $CuSO_4$ (250 μl). The reaction proceeded for two days with stirring and subsequent TLC (4:5:1:0.1, dichloromethane:methanol:water:acetic acid) showed the reaction to be incomplete. The pH of the reaction was checked and found to be neutral. Sodium bicarbonate was added until the pH was ~8 and the reaction continued for 24 hours at which point TLC analysis showed the reaction to be complete. The reaction product was isolated and purified *via* dialysis and the pure product lyophilized from water to give the PolyBAIT-P^{k}NAc **4.1** product as a white solid; Characterization of PolyBAIT-P^{k}NAc required comparison of spectra of starting monomer to that obtained of conjugated polymer. ^{1}H NMR analysis determined 5 % incorporation of the carbohydrate ligand to the polymer.

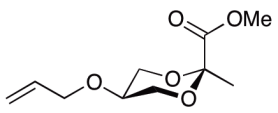

4.23

Methyl 5-(allyloxy)-2-methyl-1,3-dioxane-2-carboxylate (4.23):

The dimethyl amide **4.25** (5.20 g, 22.7 mmol) was dissolved in dry ethanol (30 ml) and 1.0 M NaOH in water (27.3 ml, 27.2 mmol). The reaction was refluxed at 100 ºC for 48 hours until ^{1}H NMR analysis showed the disappearance of two methyl amide peaks. The reaction was quenched by the addition of Dowex ion exchange resin (H^+) until pH acidic. The crude intermediate was concentrated to dryness and placed under high vacuum for 12 hours. The crude intermediate was dissolved in anhydrous CH_3OH (80 ml) and placed under argon atmosphere. $SOCl_2$ (3.30 ml, 45.4 mmol) was added and the reaction proceeded at room temperature. After 3.5 hours, TLC analysis (3:1, hexanes-ethyl acetate) showed maximum product formation. The reaction was quenched by the slow addition of saturated aqueous sodium bicarbonate until basic. The mixture was concentrated to dryness. The crude product was extracted into dichloromethane and the salts filtered off. The crude product was purified by flash column chromatography on silica gel (3:1, hexanes-ethyl acetate) to give the product **4.23** (2.26 g, 46 %) as a colorless syrup; R_f 0.48 (3:1, hexanes-ethyl acetate); FTIR found: 3081.80 cm^{-1} (sp^2 C-H stretch), 2978.87 cm^{-1}, 2955.59 cm^{-1}, 2885.47 cm^{-1} (sp^3 C-H stretch), 1746.63 cm^{-1} (C=O stretch), 1647.93 cm^{-1} (C=C stretch); ^{1}H NMR (500 MHz, $CDCl_3$) δ 5.84 (ddt, 1 H, $J_{CH,CH2}$ 5.8 Hz, J_{cis} 10.3 Hz, J_{trans} 17.2 Hz, -CH_2CH=CH_2), 5.26 (m, 1 H, -OCH_2CH=CH_2), 5.19 (m, 1 H, -OCH_2CH=CH_2), 4.09 (m, 2 H, *ring* -CH_2-), 4.01 (m, 2 H, -OCH_2CH=CH_2), 3.82 (s, 3 H,

C(O)OCH_3), 3.64 (m, 1 H, *ring* -C*H*-), 3.49 (m, 2 H, *ring* -CH_2-), 1.50 (s, 3 H, -CH_3); ^{13}C NMR (125 MHz, $CDCl_3$) δ 170.4 (*C*(O)OCH$_3$), 134.2 (-OCH$_2$*C*H=CH$_2$), 117.7 (-OCH$_2$CH=*C*H$_2$), 98.3 (quaternary C *ring*), 70.6 (-O*C*H$_2$CH=CH$_2$), 67.4 (*ring* -*C*H-), 66.1 (ring -*C*H$_2$- (x2)), 52.6 (C(O)O*C*H$_3$), 25.2 (-CH$_3$); ESI HRMS: calcd. for $C_{10}H_{16}O_5Na$ 239.0890. Found 239.0887.

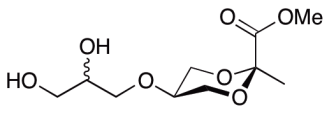

4.26

Methyl 5-(2,3-dihydroxypropoxy)-2-methyl-1,3-dioxane-2-carboxylate (4.26):

The olefin **4.23** (1.13 g, 5.21 mmol) and NMO (0.916 g, 7.82 mmol) were combined and dissolved in acetone (18 ml) and water (1 ml). The flask was placed under argon atmosphere. A solution of 1.0 M OsO_4 in *t*-butanol (0.52 ml, 0.52 mmol) was added and the reaction proceeded at room temperature for 24 hours. TLC analysis (1:1, acetone-dichloromethane) was done and no remaining starting material was detected. The reaction mixture was concentrated to dryness. The crude product was purified by flash column chromatography on silica gel (1:1, acetone-dichloromethane) to provide the product **4.26** (1.27 g, 97 %) as a clear colorless liquid; R_f 0.42 (1:1, acetone-dichloromethane); FTIR found: 3430.44 cm^{-1} (O-H bending), 2940.89 cm^{-1}, 2881.46 cm^{-1} (sp^3 stretch), 1742.95 cm^{-1} (C=O stretch); ^{1}H NMR (500 MHz, $CDCl_3$) δ 4.10 (m, 2 H, *ring* -CH_2-), 3.82 (s, 3 H, C(O)OCH_3), 3.79 (m, 1 H, -C*H*(OH)-), 3.67-3.60 (m, 2 H, *ring* -C*H*, HOCH_2CH(OH)CH$_2$O-), 3.58-3.52 (m, 3 H, HOCH_2CH(OH)CH$_2$O-, -CH(OH)CH_2O-), 3.48 (m, 2 H, *ring* -CH_2-), 1.49 (s, 3 H, -CH$_3$); ^{13}C NMR (125

MHz, $CDCl_3$) δ 170.4 (*C*(O)OCH_3), 98.2 (quaternary C *ring*), 70.8 (HO*C*H_2CH(OH)CH_2O-), 70.7 (HO*C*H_2CH(OH)CH_2O-), 68.8 (*ring* -*C*H-) 65.8 (*ring* -*C*H_2-), 65.7 (ring -*C*H_2-), 63.6 (HOCH_2CH(OH)*C*H_2O-), 52.7 (C(O)O*C*H_3), 24.9 (-CH_3); ESI HRMS: calcd. for $C_{10}H_{18}O_7Na$ 273.0945. Found 273.0942.

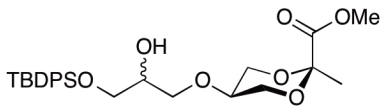

4.27

Methyl 5-(3-(*tert*-butyldiphenylsilyloxy)-2-hydroxypropoxy)-2-methyl-1,3-dioxane-2-carboxylate (4.27):

The diol **4.26** (0.112 g, 0.45 mmol) was dissolved in dry CH_2Cl_2 (2 ml) and placed under argon atmosphere. DMAP (2 mg, 0.014 mmol) was added and allowed to dissolve after which Et_3N (0.13 ml, 0.90 mmol) was added. TBDPSCl (0.14 ml, 0.54 mmol) was added slowly over 20 minutes and the reaction proceeded at room temperature overnight. TLC analysis (1:1, hexanes-ethyl acetate and 3:1, hexanes-ethyl acetate) showed no remaining starting material. The reaction mixture was washed with saturated aqueous sodium bicarbonate, and the organic layer dried over anhydrous sodium sulfate, filtered and concentrated to dryness. The crude product was purified by flash column chromatography on silica gel (3:1, hexanes-ethyl acetate) to provide the product **4.27** (0.160 g, 73 %) as a clear colorless film; R_f 0.24 (3:1, hexanes-ethyl acetate); FTIR found: 3515.20 cm^{-1} (O-H bending), 3071.47 cm^{-1}, 3049.04 cm^{-1} (aromatic sp^2 C-H stretch), 2998.93 cm^{-1}, 2954.34 cm^{-1}, 2931.90 cm^{-1}, 2858.76 cm^{-1} (sp^3 C-H stretch), 1747.95 cm^{-1} (C=O stretch); ^{1}H NMR (500 MHz, $CDCl_3$) δ 7.63 (m, 4 H,

ArH), 7.44 (m, 2 H, ArH), 7.39 (m, 4 H, ArH), 4.07 (m, 2 H, *ring* -CH_2-), 3.82 (s, 3 H, C(O)OCH_3), 3.73 (m, 1 H, -C*H*(OH)-), 3.67-3.51 (m, 5 H, *ring* -C*H*, TBDPSOCH_2-, -CH(OH)CH_2O), 3.45 (m, 2 H, *ring* -CH_2-), 2.37 (d, 1 H, $J_{CH,OH}$ 5.4 Hz, -CH(O*H*)-), 1.51 (s, 3 H, -CH_3), 1.05 (s, 9 H, -*C*H_3 *t*-butyl); ^{13}C NMR (125 MHz, $CDCl_3$) δ 170.4 (*C*(O)OCH$_3$), 135.5 (Ar), 135.4 (Ar), 132.9 (Ar), 129.9 (Ar), 129.8 (Ar), 127.7 (Ar), 98.3 (quaternary C *ring*), 70.8 (TBDPSOCH$_2$*C*H(OH)-), 70.2 (-CH(OH)*C*H$_2$O-), 68.6 (*ring* -*C*H-) 65.9 (*ring* -*C*H$_2$- (x2)), 64.3 (TBDPSO*C*H$_2$-), 52.7 (C(O)O*C*H$_3$), 26.8 (-*C*H$_3$ *t*-butyl), 25.2 (-CH$_3$), 19.2 (TBDPSO quaternary C); ESI HRMS: calcd. for $C_{26}H_{36}O_7SiNa$ 511.2123. Found 511.2117.

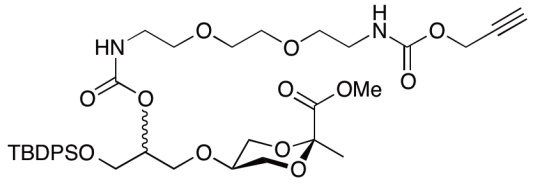

4.28

Methyl 5-(2-((*tert*-butyldiphenylsilyloxy)methyl)-4,15-dioxo-3,8,11,16-tetraoxa-5,14-diazanonadec-18-ynyloxy)-2-methyl-1,3-dioxane-carboxylate (4.28):

The alcohol **4.27** (0.139 g, 0.29 mmol) was dissolved in anhydrous CH_2Cl_2 (6 ml). 4-nitrophenyl chloroformate **4.16** (0.069 g, 0.34 mmol) was added to the reaction vessel and the contents placed under argon atmosphere. Pyr (0.05 ml, 0.58 mmol) was added after 30 minutes TLC analysis (3:1, hexanes-ethyl acetate) still showed some remaining starting material. The reaction proceeded for an additional 30 minutes after which TLC analysis showed the reaction to be

complete. The reaction mixture was quenched by the addition of saturated aqueous sodium bicarbonate. The contents were transferred to a separatory funnel and washed with saturated aqueous sodium bicarbonate, distilled water and saturated aqueous sodium chloride. The p-nitrophenyl ester intermediate (0.758 g, 1.16 mmol) and the propargylated amine **4.5** (0.488 g, 1.74 mmol) were combined and dissolved in anhydrous CH_2Cl_2 (10 ml) and the flask placed under argon atmosphere. Et_3N (0.32 ml, 2.32 mmol) was added and the reaction proceeded at room temperature for two hours. TLC analysis (10%, acetone-dichloromethane) showed no remaining starting material. The reaction mixture was concentrated to dryness and the crude product purified by flash column chromatography on silica gel (10 %, acetone-dichloromethane) to give the product **4.28** (0.799 g, 93 %) as a clear colorless syrup; R_f 0.35 (10%, acetone-dichloromethane); FTIR found: 3346.85 cm^{-1} (N-H bending), 3071.60 cm^{-1}, 3049.52 cm^{-1} (aromatic sp^2 C-H stretch), 2933.14 cm^{-1}, 2860.73 cm^{-1} (sp^3 C-H stretch), 2125.14 cm^{-1} (sp C≡C stretch), 1726.26 cm^{-1} (C=O stretch); ^{1}H NMR (500 MHz, $CDCl_3$) δ 7.63 (m, 4 H, ArH), 7.44-7.36 (m, 6 H, ArH), 5.36 (bs, 1 H, N-H), 5.17 (bs, 1 H, N-H), 4.89 (m, 1 H, TBDPSOCH$_2$C*H*(OR)-), 4.65 (d, 1 H, $J_{CH,CH2}$ 1.8 Hz, -OC*H*$_2$C≡CH$_2$), 4.09-4.03 (m, 2 H, *ring* -C*H*$_2$-), 3.81 (s, 3 H, C(O)OC*H*$_3$), 3.76-3.66 (m, 4 H, TBDPSOC*H*$_2$-, -CH(OR)C*H*$_2$O-), 3.63-3.57 (m, 5 H, *ring* -C*H*-, -OC*H*$_2$C*H*$_2$O-), 3.55-3.49 (m, 4 H, -OC*H*$_2$CH$_2$NH-), 3.43 (m, 2 H, ring -C*H*$_2$-), 3.36 (m, 4 H, -OCH$_2$C*H*$_2$NH-), 2.43 (t, 1 H, $J_{CH,CH2}$ 2.2 Hz, -OC*H*$_2$C≡CH), 1.49 (s, 3 H, -C*H*$_3$), 1.03 (s, 9 H, -CH$_3$ *t*-butyl); ^{13}C NMR (125 MHz, $CDCl_3$) δ 170.4 (*C*(O)OCH$_3$), 155.7 (-O*C*(O)NH-), 155.4 (-O*C*(O)NH-), 135.54 (Ar), 135.50 (Ar), 133.2 (Ar),

133.1 (Ar), 129.8 (Ar), 127.7 (Ar), 127.6 (Ar), 98.2 (quaternary C *ring*), 74.6 (-CH_2*C*≡CH), 73.3 (TBDPSOCH_2C*H*(OR)-), 70.3 (-O*C*H_2*C*H_2O-), 70.1 (-O*C*$H_2$$CH_2$NH-), 69.9 (-$OCH_2$C≡*C*H), 68.7 (*ring* -*C*H-), 68.1 (TBDPSO*C*H_2-), 66.0, 65.9 (*ring* -*C*H_2-), 62.1 (-CH(OR)*C*H_2O-), 52.7 (C(O)O*C*H_3), 52.4 (-O*C*H_2C≡CH), 40.9, 40.8 (-OCH_2*C*H_2NH-), 26.8 (-*C*H_3 *t*-butyl), 25.2 (-CH_3), 19.2 (*TBDPSO* quaternary C); ESI HRMS: calcd. for $C_{37}H_{52}N_2O_{12}SiNa$ 767.3182. Found 767.3168.

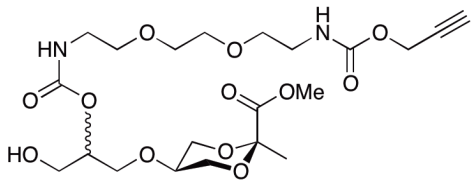

4.21

Methyl 5-(2-(hydroxymethyl)-4,15-dioxo-3,8,11,16-tetraoxa-5,14-diazanonadec-18-ynyloxy)-2-methyl-1,3-dioxane-carboxylate (4.21):

The silyl ether **4.28** (0.547 g, 0.734 mmol) was dissolved in Pyr (5.5 ml) in a polypropylene falcon tube. 30% HF-Pyr (1.1 ml) was added and the reaction proceeded under argon atmosphere, and room temperature overnight. Subsequent TLC analysis (1:1, acetone-dichloromethane) was done and the reaction found to be complete. The reaction mixture was diluted with CH_2Cl_2 and washed with saturated aqueous sodium bicarbonate, distilled water and saturated aqueous sodium chloride. The organic layer was dried over anhydrous sodium sulfate, filtered and concentrated to dryness. The crude product was purified by flash column chromatography on silica gel (1:1, acetone-dichloromethane) to give the product **4.21** (0.309 g, 83 %) as a clear colorless syrup; R_f 0.39 (50 %, acetone-

dichloromethane); FTIR found: 3349.98 cm^{-1} (O-H bending), 2939.34 cm^{-1}, 2878.29 cm^{-1} (sp^3 C-H stretch), 2126.53 cm^{-1} (sp C≡C stretch), 1714.62 cm^{-1} (C=O stretch); ^{1}H NMR (600 MHz, $CDCl_3$) δ 5.52 (bs, 1 H, N-H), 5.47 (bs, 1 H, N-H), 4.80 (m, 1 H, $HOCH_2CH$(OR)-), 4.67 (d, 1 H, $J_{CH,CH2}$ 2.2 Hz, -$OCH_2C{\equiv}CH_2$), 4.08 (m, 2 H, *ring* -CH_2-), 3.82 (s, 3 H, C(O)OCH_3), 3.77-3.66 (m, 4 H, $HOCH_2$-, -CH(OR)CH_2O-), 3.64-3.59 (m, 5 H, *ring* -CH-, -OCH_2CH_2O-), 3.56 (m, 4 H, -OCH_2CH_2NH-), 3.45 (m, 2 H, ring -CH_2-), 3.38 (m, 4 H, -OCH_2CH_2NH-), 2.58 (bs, 1 H, $HOCH_2$-), 2.48 (t, 1 H, $J_{CH,CH2}$ 2.4 Hz, -$OCH_2C{\equiv}CH$), 1.49 (s, 3 H, -CH_3); ^{13}C NMR (150 MHz, $CDCl_3$) δ 170.4 (C(O)OCH_3), 156.2 (-OC(O)NH-), 155.6 (-OC(O)NH-), 98.2 (quaternary C *ring*), 74.7 (-$CH_2C{\equiv}CH$), 74.1 ($HOCH_2CH$(OR)-), 70.2 (-OCH_2CH_2O-), 69.9 (-OCH_2CH_2NH-), 68.8 (*ring* -CH-), 68.5 ($HOCH_2$-), 65.8 (*ring* -CH_2-), 62.2 (-CH(OR)CH_2O-), 52.7 (C(O)OCH_3), 52.4 (-$OCH_2C{\equiv}CH$), 40.95, 40.91 (-OCH_2CH_2NH-), 25.1 (-CH_3); ESI HRMS: calcd. for $C_{21}H_{34}N_2O_{12}Na$ 529.2004. Found 529.2000.

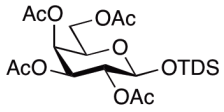

4.30

(Dimethyl)thexylsilyl 2,3,4,6-tetra-*O*-acetyl-β-D-galactopyranoside (4.30):

The 1-OH-galactose **4.29** (5.24 g, 15.1 mmol) was dissolved in anhydrous CH_2Cl_2 (60 ml) and the vessel placed under argon atmosphere. TDSCl (4.43 ml, 22.6 mmol) was added and the stirring solution cooled to 0 °C in an ice-water bath. Imidazole (2.56 g, 37.8 mmol) was added and the reaction proceeded for 24

hours while warming to room temperature. TLC analysis (2:1, hexanes-ethyl acetate) showed maximum product formation. The contents were diluted with CH_2Cl_2 and washed with distilled water and saturated aqueous sodium chloride. The organic layer was dried over anhydrous sodium sulfate, filtered and concentrated to dryness. The crude product was purified by flash column chromatography on silica gel (4:1 → 3:1, hexanes-ethyl acetate) to give the product **4.30** (7.04 g, 95%) as a clear colorless syrup; R_f 0.59 (2:1, hexanes-ethyl acetate); $[a]_D$ +1.98 ^{o}(*c* 1.04, $CHCl_3$); ^{1}H NMR (600 MHz, $CDCl_3$) δ 5.37 (d, 1 H, $J_{3,4}$ 3.3 Hz, H-4), 5.15 (dd, 1 H, $J_{1,2}$ 7.6 Hz, $J_{2,3}$ 10.5 Hz, H-2), 4.99 (dd, 1 H, $J_{3,4}$ 3.5 Hz, $J_{2,3}$ 10.5 Hz, H-3), 4.70 (d, 1 H, $J_{1,2}$ 7.6 Hz, H-1), 4.15 (dd, 1 H, $J_{5,6a}$ 7.2 Hz, $J_{6a,6b}$ 11.4 Hz, H-6a), 4.10 (dd, 1 H, $J_{5,6b}$ 6.2 Hz, $J_{6a,6b}$ 11.3 Hz, H-6b), 3.89 (m, 1 H, $J_{5,6a}$ 7.0 Hz, $J_{5,6b}$ 6.4 Hz, H-5), 2.16 (s, 3 H, C*H*$_3$C(O)O), 2.04 (s, 3 H, C*H*$_3$C(O)O), 2.03 (s, 3 H, C*H*$_3$C(O)O), 1.98 (s, 3 H, C*H*$_3$C(O)O), 1.60 (m, 1 H, -C*H*(CH$_3$)$_2$), 0.86 (m, 6 H, -CH(C*H*$_3$)$_2$), 0.84 (s, 3 H, -C(C*H*$_3$)$_2$CH-), 0.83 (s, 3 H, -C(C*H*$_3$)$_2$CH-), 0.17 (s, 3 H, -OSi(C*H*$_3$)$_2$-), 0.14 (s, 3 H, -OSi(C*H*$_3$)$_2$-); ^{13}C NMR (150 MHz, $CDCl_3$) δ 170.4 (*C*(O)OCH$_3$), 170.3 (*C*(O)OCH$_3$), 170.2 (*C*(O)OCH$_3$), 169.3 (*C*(O)OCH$_3$), 96.2 (C-1), 70.9, 70.8, 70.7 (C-2, C-3, C-5), 67.3 (C-4), 61.6 (C-6), 33.9 (-*C*H(CH$_3$)$_2$), 24.8 (-*C*(CH$_3$)$_2$CH-), 20.8 (*C*H$_3$C(O)O), 20.7 (*C*H$_3$C(O)O), 20.6 (*C*H$_3$C(O)O), 20.5 (*C*H$_3$C(O)O), 19.9 (-C(*C*H$_3$)$_2$CH-), 19.8 (-C(*C*H$_3$)$_2$CH-), 18.5 (-CH(*C*H$_3$)$_2$), 18.4 (-CH(*C*H$_3$)$_2$), -1.9 (-OSi(*C*H$_3$)$_2$-), -3.4 (-OSi(*C*H$_3$)$_2$-); ESI HRMS: calcd. for $C_{22}H_{38}O_{10}SiNa$ 513.2126. Found 513.2119; Anal. calcd for $C_{22}H_{38}O_{10}Si$: C, 53.86; H, 7.81. Found: C, 54.03; H, 7.86.

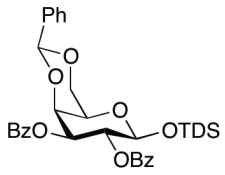

4.31

(Dimethyl)thexylsilyl 2,3-di-*O*-benzoyl-4,6-*O*-benzylidenyl-β-D-galactopyranoside (4.31):

The galactoside **4.30** (5.59 g, 11.4 mmol) was partially dissolved in anhydrous CH_3OH (60 ml). The stirring solution was cooled to -20 °C in a cooled ethanol bath. Na metal (catalytic) was added and the reaction proceeded overnight at -20 °C. Subsequent TLC analysis (20%, methanol-dichloromethane) showed no remaining starting material. The reaction was quenched with Dowex® 50-W-X8 ion exchange resin (H^+) until pH ~7. The mixture was filtered and concentrated to dryness. The crude product was used directly in the next step. The intermediate (4.30 g, 13.3 mmol) was suspended in anhydrous CH_3CN (60 ml). $PhCH(OCH_3)_2$ (2.4 ml, 16.0 mmol) was added followed by a catalytic amount of CSA (100 mg). The reaction proceeded at 30 °C and under mild vacuum to remove CH_3OH formed during the reaction. After 1.5 hours TLC analysis (10%, methanol-dichloromethane) showed maximum product formation. An excess of Pyr (20 ml) was added to neutralize and basicify the reaction mixture. BzCl (7.73 ml, 66.5 mmol) was added slowly to the reaction mixture while stirring and the reaction proceeded at room temperature overnight. Subsequent TLC analysis (5:1, hexanes-ethyl acetate) showed maximum product formation. The reaction mixture was concentrated to dryness while co-evaporating with toluene (3 x 20 ml). The crude product was diluted with CH_2Cl_2 and washed with distilled water and

saturated aqueous sodium chloride. The organic layer was dried over anhydrous sodium sulfate, filtered and concentrated to dryness. The crude product was purified by flash column chromatography on silica gel (5:1, hexanes-ethyl acetate) to give the product **4.31** (6.28 g, 76 % 3 steps) as a white foam; R_f 0.24 (5:1, hexanes-ethyl acetate); $[a]_D$ +93.1 ^{o}(*c* 1.04, $CHCl_3$); ^{1}H NMR (600 MHz, $CDCl_3$) δ 7.99 (m, 4 H, ArH), 7.54 (m, 2 H, ArH), 7.49 (m, 2 H, ArH), 7.39-7.34 (m, 7 H, ArH), 5.82 (dd, 1 H, $J_{1,2}$ 7.6 Hz, $J_{2,3}$ 10.4 Hz, H-2), 5.54 (s, 1 H, *benzylidene* C-*H*), 5.34 (dd, 1 H, $J_{3,4}$ 3.8 Hz, $J_{2,3}$ 10.4 Hz, H-3), 5.02 (d, 1 H, $J_{1,2}$ 7.7 Hz, H-1), 4.59 (d, 1 H, $J_{3,4}$ 3.5 Hz, H-4), 4.36 (dd, 1 H, $J_{5,6a}$ 1.3 Hz, $J_{6a,6b}$ 12.2 Hz, H-6a), 4.14 (dd, 1 H, $J_{5,6b}$ 1.8 Hz, $J_{6a,6b}$ 12.2 Hz, H-6b), 3.65 (m, 1 H, H-5), 1.54 (m, 1 H, -C*H*$(CH_3)_2$), 0.75 (m, 12 H, -C(C*H*$_3)_2$-, -CH(C*H*$_3)_2$), 0.23 (s, 3 H, -OSi(C*H*$_3)_2$-), 0.13 (s, 3 H, -OSi(C*H*$_3)_2$-); ^{13}C NMR (150 MHz, $CDCl_3$) δ 166.3 (Ph*C*(O)O), 165.2 (Ph*C*(O)O), 137.7 (Ar), 133.7 (Ar), 133.3 (Ar), 132.9 (Ar), 130.2 (Ar), 129.97 (Ar), 129.95 (Ar), 129.6 (Ar), 129.3 (Ar), 128.9 (Ar), 128.5 (Ar), 128.45 (Ar), 128.41 (Ar), 128.3 (Ar), 128.2 (Ar), 128.1 (Ar), 126.3 (Ar), 100.9 (*benzylidene C*-H), 96.3 (C-1), 73.7 (C-4), 72.8 (C-3), 71.2 (C-2), 69.2 (C-6), 66.5 (C-5), 33.9 (-*C*H$(CH_3)_2$), 24.8 (-*C*$(CH_3)_2$-), 19.95, 19.92, 18.4 (-C(*C*H$_3)_2$CH(*C*H$_3)_2$), -1.69 (-OSi(*C*H$_3)_2$-), -2.91 (-OSi(*C*H$_3)_2$); ESI HRMS: calcd. for $C_{35}H_{42}O_8SiNa$ 641.2541. Found 641.2527; Anal. calcd for $C_{35}H_{42}O_8Si$: C, 67.94; H, 6.84. Found: C, 68.13; H, 6.60.

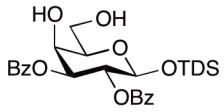

4.32

(Dimethyl)thexylsilyl 2,3-di-*O*-benzoyl-β-D-galactopyranoside (4.32):

The 4,6-*O*-benzylidene-galactoside **4.31** (3.29 g, 5.33 mmol) was suspended in an 80%, CH_3COOH-water mixture and placed in an oil bath. The reaction was heated to 80 °C and once the starting material was dissolved, the reaction proceeded for two hours. Subsequent TLC analysis (2:1, hexanes-ethyl acetate) showed no remaining starting material. The reaction was cooled to room temperature and diluted with CH_2Cl_2. The mixture was washed with saturated aqueous sodium bicarbonate, distilled water and saturated aqueous sodium chloride. The organic layer was dried over anhydrous sodium sulfate, filtered and concentrated. The crude product was purified by flash column chromatography on silica gel (2:1, hexanes-ethyl acetate) to give the product **4.32** (1.81 g, 64 %) as a white foam; R_f 0.24 (2:1, hexanes-ethyl acetate); $[a]_D$ +62.1 ^{o}(*c* 1.16, $CHCl_3$); ^{1}H NMR (500 MHz, $CDCl_3$) δ 7.96 (m, 4 H, ArH), 7.49 (m, 2 H, ArH), 7.36 (m, 2 H, ArH), 5.70 (dd, 1 H, $J_{1,2}$ 7.5 Hz, $J_{2,3}$ 10.4 Hz, H-2), 5.27 (dd, 1 H, $J_{3,4}$ 3.2 Hz, $J_{2,3}$ 10.4 Hz, H-3), 4.96 (d, 1 H, $J_{1,2}$ 7.5 Hz, H-1), 4.36 (m, 1 H, H-4), 4.00 (m, 1 H, H-6a), 3.89 (m, 1 H, H-6b), 3.77 (m, 1 H, H-5), 2.74 (d, 1 H, $J_{4,OH}$ 4.6 Hz, 4-OH), 2.14 (bt, 1 H, 6-OH), 1.51 (m, 1 H, -C*H*$(CH_3)_2$), 0.73 (m, 12 H, -C(C*H*$_3)_2$-, -CH(C*H*$_3)_2$), 0.18 (s, 3 H, -OSi(C*H*$_3)_2$-), 0.08 (s, 3 H, -OSi(C*H*$_3)_2$-); ^{13}C NMR (125 MHz, $CDCl_3$) δ 165.9 (Ph*C*(O)O), 165.3 (Ph*C*(O)O), 133.4 (Ar), 132.9 (Ar), 129.9 (Ar), 129.7 (Ar), 129.6 (Ar), 129.1 (Ar), 128.4 (Ar), 128.2 (Ar), 95.6 (C-1), 74.4, 74.3 (C-3, C-5), 71.6 (C-2), 68.3 (C-4), 62.4 (C-6), 33.8 (-*C*H$(CH_3)_2$), 24.7

(-*C*(CH_3)$_2$-), 19.9, 19.8, 18.4, 18.3 (-C(*C*H_3)$_2$CH(*C*H_3)$_2$), -1.75 (-OSi(*C*H_3)$_2$-), -3.28 (-OSi(*C*H_3)$_2$); ESI HRMS: calcd. for $C_{28}H_{38}O_8SiNa$ 553.2228. Found 553.2213; Anal. calcd for $C_{28}H_{38}O_8Si$: C, 63.37; H, 7.22. Found: C, 63.69; H, 7.46.

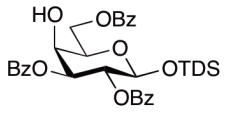

4.22

(Dimethyl)thexylsilyl 2,3,6-tri-*O*-benzoyl-β-D-galactopyranoside (4.22):

The 4,6-diol-galactoside **4.32** (1.03 g, 1.93 mmol) was dissolved in anhydrous CH_2Cl_2 (30 ml) and placed under argon atmosphere. Pyr (0.311 μl, 3.86 mmol) was added and the solution cooled to 0 °C in an ice-water bath. BzCl (0.258 ml, 2.13 mmol) was added slowly over 30 minutes to the stirring solution. The reaction proceeded overnight warming to room temperature. TLC analysis (2:1, hexanes-ethyl acetate) was done and showed maximum product formation. The reaction mixture was concentrated to dryness and the crude product was purified by flash column chromatography on silica gel (5 %, ethyl acetate-toluene) to give the product **4.22** (0.958 g, 78 %) was a white foam; R_f 0.59 (2:1, hexanes-ethyl acetate); $[a]_D$ +44.2 ^{o}(*c* 1.22, $CHCl_3$); ^{1}H NMR (500 MHz, $CDCl_3$) δ 8.06 (m, 2 H, ArH), 7.97 (m, 4 H, ArH), 7.58 (m, 1 H, ArH), 7.48 (m, 4 H, ArH), 7.37 (m, 4 H, ArH), 5.70 (dd, 1 H, $J_{1,2}$ 7.6 Hz, $J_{2,3}$ 10.4 Hz, H-2), 5.32 (dd, 1 H, $J_{3,4}$ 3.3 Hz, $J_{2,3}$ 10.4 Hz, H-3), 4.96 (d, 1 H, $J_{1,2}$ 7.6 Hz, H-1), 4.67 (dd, 1 H, $J_{5,6a}$ 5.6 Hz, $J_{6a,6b}$ 11.6 Hz, H-6a), 4.59 (dd, 1 H, $J_{5,6b}$ 7.2 Hz, $J_{6a,6b}$ 11.5 Hz, H-6b), 4.34 (m, 1 H, H-4), 4.07 (m, 1 H, H-5), 2.41 (d, 1 H, $J_{4,OH}$ 6.0 Hz, 4-OH), 1.49

(m, 1 H, -C*H*(CH_3)$_2$), 0.72 (m, 12 H, -C(C*H*$_3$)$_2$-, -CH(C*H*$_3$)$_2$), 0.16 (s, 3 H, -OSi(C*H*$_3$)$_2$-), 0.06 (s, 3 H, -OSi(C*H*$_3$)$_2$-); ^{13}C NMR (125 MHz, $CDCl_3$) δ 166.4 (Ph*C*(O)O), 165.8 (Ph*C*(O)O), 165.2 (Ph*C*(O)O), 133.4 (Ar), 133.3 (Ar), 132.9 (Ar), 129.9 (Ar), 129.8 (Ar), 129.7 (Ar), 129.6 (Ar), 129.1 (Ar), 128.5 (Ar), 128.4 (Ar), 128.2 (Ar), 96.4 (C-1), 74.1, 72.5 (C-5), 71.5 (C-2), 67.7 (C-4), 63.1 (C-6), 33.9 (-*C*H(CH_3)$_2$), 24.7 (-*C*(CH_3)$_2$-), 19.9, 19.8, 18.4, 18.3 (-C(*C*H$_3$)$_2$CH(*C*H$_3$)$_2$), -1.90 (-OSi(*C*H$_3$)$_2$-), -3.50 (-OSi(*C*H$_3$)$_2$); ESI HRMS: calcd. for $C_{35}H_{42}O_9SiNa$ 657.2490. Found 657.2494; Anal. calcd for $C_{35}H_{42}O_9Si$: C, 66.22; H, 6.67. Found: C, 66.42; H, 6.65.

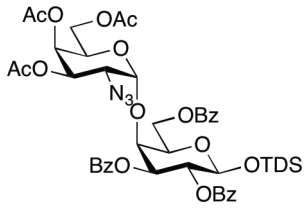

4.33

(Dimethyl)thexylsilyl 3,4,6-tri-*O*-acetyl-2-azido-2-deoxy-α-D-galactopyranosyl-(1→4)-2,3,6-tri-*O*-benzoyl-β-D-galactopyranoside (4.33):

The acceptor **4.22** (1.26 g, 1.99 mmol) and donor **3.3** (1.43 g, 3.0 mmol) were combined with pre-activated 3Å molecular sieves (0.78 g) and placed under argon atmosphere. The contents were dissolved in anhydrous CH_2Cl_2 (15 ml) and stirred at room temperature for one hour. The solution was cooled to -20 °C in a dry ice-acetone bath and once cool TMSOTf (0.072 ml, 0.40 mmol) was added. The reaction proceeded at -20 °C for 2.5 hours until TLC analysis (2:1, hexanes-ethyl acetate) showed no remaining donor. The reaction was neutralized by the

addition of Et_3N, filtered though Celite® and concentrated to dryness. The crude product was purified by flash column chromatography on silica gel (3:1, hexanes-ethyl acetate) to provide the product **4.33** (1.84 g, 97 %) as a white foam; R_f 0.36 (2:1, hexanes-ethyl acetate); $[a]_D$ +79.5 ^{o}(*c* 0.99, $CHCl_3$); ^{1}H NMR (500 MHz, $CDCl_3$) δ 8.07 (m, 2 H, ArH), 7.97 (m, 2 H, ArH), 7.92 (m, 2 H, ArH), 7.59 (m, 1 H, ArH), 7.47 (m, 4 H, ArH), 7.35 (m, 4 H, ArH), 5.63 (dd, 1 H, $J_{1,2}$ 7.5 Hz, $J_{2,3}$ 10.8 Hz, H-2), 5.48 (m, 2 H, $J_{3',4'}$ 3.2 Hz, H-3', H-4'), 5.30 (dd, 1 H, $J_{3,4}$ 3.0 Hz, $J_{2,3}$ 10.7 Hz, H-3), 5.04 (d, 1 H, $J_{1',2'}$ 3.5 Hz, H-1'), 4.98 (d, 1 H, $J_{1,2}$ 7.5 Hz, H-1), 4.74 (dd, 1 H, $J_{5,6a}$ 6.4 Hz, $J_{6a,6b}$ 11.4 Hz, H-6a), 4.68 (dd, 1 H, $J_{5,6b}$ 7.1 Hz, $J_{6a,6b}$ 11.4 Hz, H-6b), 4.56 (m, 1 H, H-5'), 4.46 (d, 1 H, $J_{3,4}$ 2.8 Hz, H-4), 4.10 (m, 1 H, H-5), 3.84 (m, 2 H, $J_{5',6a'}$ 7.8 Hz, $J_{6a',6b'}$ 10.9 Hz, H-2', H-6a'), 3.57 (dd, 1 H, $J_{5',6b'}$ 6.1 Hz, $J_{6a',6b'}$ 10.9 Hz, H-6b'), 2.07 (s, 3 H, CH_3C(O)O), 2.06 (s, 3 H, CH_3C(O)O), 1.87 (s, 3 H, CH_3C(O)O), 1.52 (m, 1 H, -CH(CH_3)$_2$), 0.73 (m, 12 H, -C(CH_3)$_2$-, -CH(CH_3)$_2$), 0.19 (s, 3 H, -OSi(CH_3)$_2$-), 0.08 (s, 3 H, -OSi(CH_3)$_2$-); ^{13}C NMR (150 MHz, $CDCl_3$) δ 170.2 (CH_3C(O)O), 169.9 (CH_3C(O)O), 169.6 (CH_3C(O)O), 166.2 (Ph*C*(O)O), 166.1 (Ph*C*(O)O), 165.1 (Ph*C*(O)O), 133.5 (Ar), 133.3 (Ar), 132.9 (Ar), 129.9 (Ar), 129.7 (Ar), 129.6 (Ar), 129.59 (Ar), 129.56 (Ar), 128.8 (Ar), 128.6 (Ar), 128.5 (Ar), 128.24 (Ar), 128.21 (Ar), 99.4 (C-1'), 96.5 (C-1), 75.8 (C-4), 73.5 (C-3), 72.5 (C-5), 71.5 (C-2), 68.9 (C-3'), 67.3, 67.2 (C-4', C-5'), 62.7 (C-6), 60.7 (C-6'), 58.5 (C-2'), 33.9 (-*C*H(CH_3)$_2$), 24.8 (-*C*(CH_3)$_2$-), 20.7 (*C*H_3C(O)O), 20.6 (*C*H_3C(O)O), 20.5 (*C*H_3C(O)O), 19.9, 19.8, 18.4, 18.3 (-C(*C*H_3)$_2$CH(*C*H_3)$_2$), -1.80 (-OSi(*C*H_3)$_2$-), -3.30 (-OSi(*C*H_3)$_2$); ESI

HRMS: calcd. for $C_{47}H_{57}N_3O_{16}SiNa$ 970.3400. Found 970.3394; Anal. calcd for $C_{47}H_{57}N_3O_{16}Si$: C, 59.54; H, 6.06; N, 4.43. Found: C, 59.91; H, 6.33; N, 4.59.

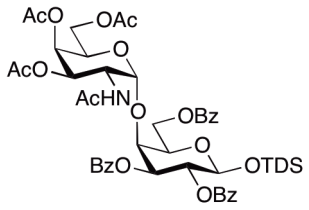

4.34

(Dimethyl)thexylsilyl 2-acetamido-3,4,6-tri-*O*-acetyl-2-deoxy-α-D-galactopyranosyl-(1→4)-2,3,6-tri-*O*-benzoyl-β-D-galactopyranoside (4.34):

The azide **4.33** (0.107 g, 0.113 mmol) was dissolved in a 6:1 mixture of CH_3CN:Et_3N (3.4 ml) and placed under argon atmosphere. DTT (0.070 g, 0.453 mmol) was added and the reaction proceeded overnight at room temperature. Subsequent TLC analysis (2:1, hexanes-ethyl acetate) showed no remaining starting material. A 1:1 mixture of Ac_2O:Pyr (8 ml) was added and the reaction proceeded for three hours until TLC analysis (1:1 hexanes-ethyl acetate) showed the reaction to be complete. The reaction mixture was concentrated to dryness while co-evaporating with toluene (3 x 10 ml). The crude product was purified by flash column chromatography (1:1, hexanes-ethyl acetate) to give the product **4.34** (0.094 g, 86 %) was a white foam; R_f 0.26 (1:1, hexanes-ethyl acetate); $[a]_D$ +101.9 ^{o}(*c* 1.07, $CHCl_3$); ^{1}H NMR (500 MHz, $CDCl_3$) δ 8.04 (m, 2 H, ArH), 7.93 (m, 4 H, ArH), 7.59 (m, 1 H, ArH), 7.47 (m, 4 H, ArH), 7.36 (m, 4 H, ArH), 6.28 (d, 1 H, $J_{NH,2'}$ 9.5 Hz, N-H), 5.69 (dd, 1 H, $J_{1,2}$ 7.4 Hz, $J_{2,3}$ 10.6 Hz, H-2), 5.35 (d, 1 H, $J_{3',4'}$ 3.2 Hz, H-4'), 5.33-5.29 (m, 2 H, H-3, H-3'), 5.12 (d, 1 H, $J_{1',2'}$ 3.8 Hz,

H-1'), 4.98 (d, 1 H, $J_{1,2}$ 7.4 Hz, H-1), 4.75 (dd, 1 H, $J_{5,6a}$ 7.7 Hz, $J_{6a,6b}$ 11.2 Hz, H-6a), 4.67 (ddd, 1 H, $J_{1',2'}$ 3.7 Hz, $J_{NH,2'}$ 9.4 Hz, $J_{2',3'}$ 11.4 Hz, H-2'), 4.49 (d, 1 H, $J_{3,4}$ 3.2 Hz, H-4), 4.37 (t, 1 H, $J_{5',6a'}$ 7.5 Hz, H-5'), 4.31 (dd, 1 H, $J_{5,6b}$ 6.1 Hz, $J_{6a,6b}$ 11.3 Hz, H-6b), 4.10 (m, 1 H, H-5), 3.60 (dd, 1 H, $J_{5',6a'}$ 7.8 Hz, $J_{6a',6b'}$ 10.9 Hz, H-6a'), 3.31 (dd, 1 H, $J_{5',6b'}$ 6.5 Hz, $J_{6a',6b'}$ 10.9 Hz, H-6b'), 2.07 (s, 3 H, CH_3C(O)O), 2.06 (s, 3 H, CH_3C(O)O), 2.03 (s, 3 H, CH_3(O)NH), 1.74 (s, 3 H, CH_3C(O)O), 1.51 (m, 1 H, -CH(CH_3)$_2$), 0.73 (m, 12 H, -C(CH_3)$_2$-, -CH(CH_3)$_2$), 0.16 (s, 3 H, -OSi(CH_3)$_2$-), 0.06 (s, 3 H, -OSi(CH_3)$_2$-); ^{13}C NMR (125 MHz, $CDCl_3$) δ 170.8 (CH_3*C*(O)NH), 170.5 (CH_3*C*(O)O), 170.2 (CH_3*C*(O)O), 169.8 (CH_3*C*(O)O), 165.8 (Ph*C*(O)O), 165.7 (Ph*C*(O)O), 165.2 (Ph*C*(O)O), 133.6 (Ar), 133.5 (Ar), 133.1 (Ar), 129.8 (Ar), 129.7 (Ar), 129.6 (Ar), 129.4 (Ar), 129.2 (Ar), 128.7 (Ar), 128.6 (Ar), 128.5 (Ar), 128.3 (Ar), 98.1 (C-1'), 96.5 (C-1), 73.0 (C-3), 72.6 (C-5), 72.4 (C-4), 71.4 (C-2), 68.1 (C-3'), 66.9 (C-4'), 66.8 (C-5'), 61.9 (C-6), 60.7 (C-6'), 47.8 (C-2'), 33.8 (-*C*H(CH_3)$_2$), 24.7 (-*C*(CH_3)$_2$-), 23.2 (*C*H_3C(O)NH), 20.8 (*C*H_3C(O)O), 20.6 (*C*H_3C(O)O), 20.4 (*C*H_3C(O)O), 19.8, 18.4, (-C(*C*H_3)$_2$CH(*C*H_3)$_2$), -1.89 (-OSi(*C*H_3)$_2$-), -3.42 (-OSi(*C*H_3)$_2$); ESI HRMS: calcd. for $C_{49}H_{61}NO_{17}SiNa$ 986.3601. Found 986.3593; Anal. calcd for $C_{49}H_{61}NO_{17}Si$: C, 61.04; H, 6.38; N, 1.45. Found: C, 60.92; H, 6.59; N, 1.57.

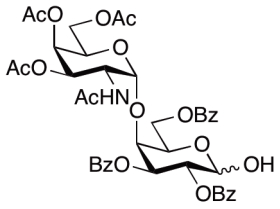

4.35

2-Acetamido-3,4,6-tri-*O*-acetyl-2-deoxy-α-D-galactopyranosyl-(1→4)-2,3,6-tri-*O*-benzoyl-α,β-D-galactopyranose (4.35):

The 1-OTDS disaccharide **4.34** (0.171 g, 0.178 mmol) was placed in a Falcon® tube and dissolved in anhydrous THF (2.2 ml). 33% HF-Pyr (0.065 ml) was added and the reaction proceeded overnight at room temperature. TLC analysis (1:1, ethyl acetate-toluene) showed the reaction to be complete. The crude mixture was diluted with CH_2Cl_2 and was with saturated aqueous sodium bicarbonate, distilled water and saturated aqueous sodium chloride. The organic layer was dried over anhydrous sodium sulfate, filtered and concentrated to dryness. The crude product was purified by flash column chromatography on silica gel (1:1, ethyl acetate-toluene) to give the product **4.35** (0.103 g, 71 %) as an inseparable mixture of isomers (3:1, α:β) and as a clear colorless syrup; R_f 0.24 (1:1, ethyl acetate-toluene); **For 4.35α:** ^{1}H NMR (600 MHz, $CDCl_3$) δ 8.04 (m, 2 H, ArH), 7.97 (m, 4 H, ArH), 7.60 (m, 1 H, ArH), 7.51 (m, 2 H, ArH), 7.47 (m , 2 H, ArH), 7.39-7.33 (m, 4 H, ArH), 6.12 (d, 1 H, $J_{NH,2'}$ 9.3 Hz, N-H), 5.85 (dd, 1 H, $J_{3,4}$ 3.1 Hz, $J_{2,3}$ 10.9 Hz, H-3), 5.80 (bs, 1 H, H-1), 5.68 (dd, 1 H, $J_{1,2}$ 3.7 Hz, $J_{2,3}$ 10.9 Hz, H-2), 5.37-5.34 (m, 2 H, H-3', H-4'), 5.18 (d, 1 H, $J_{1',2'}$ 3.6 Hz, H-1'), 4.75-4.67 (m, 3 H, H-5, H-6a, H-2'), 4.59 (d, 1 H, $J_{3,4}$ 3.1 Hz, H-4), 4.48 (m, 1 H, H-5'), 4.27 (m, 1 H, H-6b), 3.72 (bs, 1 H, 1-OH), 3.67 (dd, 1 H, $J_{5',6a'}$ 8.0

Hz, $J_{6a',6b'}$ 10.9 Hz, H-6a'), 3.33 (dd, 1 H, $J_{5',6b'}$ 6.4 Hz, $J_{6a',6b'}$ 10.9 Hz, H-6b'), 2.09 (s, 3 H, CH_3C(O)O), 2.06 (s, 3 H, CH_3C(O)O), 2.03 (s, 3 H, CH_3(O)NH), 1.72 (s, 3 H, CH_3C(O)O); ^{13}C NMR (125 MHz, $CDCl_3$) δ 171.1 (CH_3*C*(O)NH), 170.6 (CH_3*C*(O)O), 170.3 (CH_3*C*(O)O), 169.9 (CH_3*C*(O)O), 166.3 (Ph*C*(O)O), 166.0 (Ph*C*(O)O), 165.9 (Ph*C*(O)O), 133.8 (Ar), 133.6 (Ar), 133.56 (Ar), 133.54 (Ar), 133.4 (Ar), 129.9 (Ar), 129.84 (Ar), 129.8 (Ar), 129.7 (Ar), 129.6 (Ar), 129.2 (Ar), 129.1 (Ar), 129.0 (Ar), 128.8 (Ar), 128.7 (Ar), 128.6 (Ar), 128.5 (Ar), 128.48 (Ar), 128.47 (Ar), 128.3 (Ar), 98.5 (C-1'), 90.9 (C-1), 74.2 (C-4), 69.8 (C-3), 69.0 (C-2), 68.2 (C-5), 67.9 (C-3'), 66.9 (C-4'), 66.8 (C-5'), 61.6 (C-6), 60.8 (C-6'), 48.1 (C-2'), 23.3 (*C*H_3C(O)NH), 20.8 (*C*H_3C(O)O), 20.7 (*C*H_3C(O)O), 20.4 (*C*H_3C(O)O); **For 4.35β:** ^{1}H NMR (600 MHz, $CDCl_3$) δ 8.01 (m, 2 H, ArH), 7.93 (m, 4 H, ArH), 7.60 (m, 1 H, ArH), 7.51 (m, 2 H, ArH), 7.47 (m , 2 H, ArH), 7.39-7.33 (m, 4 H, ArH), 6.72 (d, 1 H, $J_{NH,2'}$ 9.2 Hz, N-H), 5.71 (dd, 1 H, $J_{1,2}$ 7.8 Hz, $J_{2,3}$ 10.6 Hz, H-2), 5.47 (dd, 1 H, $J_{3,4}$ 3.1 Hz, $J_{2,3}$ 10.6 Hz, H-3), 5.42 (dd, 1 H, $J_{3',4'}$ 3.2 Hz, $J_{2',3'}$ 11.7 Hz, H-3'), 5.37-5.34 (m, 1 H, H-4'), 5.23 (d, 1 H, $J_{1',2'}$ 3.6 Hz, H-1'), 5.12 (d, 1 H, $J_{OH,1}$ 7.9 Hz, 1-OH), 5.05 (t, 1 H, $J_{OH,1}$ 7.6 Hz, $J_{1,2}$ 7.6 Hz, H-1), 4.75-4.67 (m, 2 H, H-6a, H-2'), 4.51 (d, 1 H, $J_{3,4}$ 3.1 Hz, H-4), 4.49-4.45 (m, 2 H, H-6b, H-5'), 4.18 (t, 1 H, $J_{5,6a}$ 6.8 Hz, $J_{5,6b}$ 6.8 Hz, H-5), 3.65 (dd, 1 H, $J_{5',6a'}$ 8.1 Hz, $J_{6a',6b'}$ 10.4 Hz, H-6a'), 3.49 (dd, 1 H, $J_{5',6b'}$ 6.1 Hz, $J_{6a',6b'}$ 10.9 Hz, H-6b'), 2.10 (s, 3 H, CH_3C(O)O), 2.06 (s, 3 H, CH_3C(O)O), 2.04 (s, 3 H, CH_3(O)NH), 1.76 (s, 3 H, CH_3C(O)O); ^{13}C NMR (125 MHz, $CDCl_3$) δ 171.2 (CH_3*C*(O)NH), 170.8 (CH_3*C*(O)O), 170.2 (CH_3*C*(O)O), 170.0 (CH_3*C*(O)O), 165.9 (Ph*C*(O)O), 165.8 (Ph*C*(O)O), 165.7 (Ph*C*(O)O), 133.8 (Ar), 133.6 (Ar), 133.56 (Ar), 133.54

(Ar), 133.4 (Ar), 129.9 (Ar), 129.84 (Ar), 129.8 (Ar), 129.7 (Ar), 129.6 (Ar), 129.2 (Ar), 129.1 (Ar), 129.0 (Ar), 128.8 (Ar), 128.7 (Ar), 128.6 (Ar), 128.5 (Ar), 128.48 (Ar), 128.47 (Ar), 128.3 (Ar), 98.4 (C-1'), 96.3 (C-1), 73.1 (C-5), 72.9 (C-3), 72.7 (C-4), 71.6 (C-2), 67.9 (C-3'), 66.8 (C-4), 66.7 (C-5'), 61.6 (C-6), 60.9 (C-6'), 47.9 (C-2'), 23.1 (*C*H_3C(O)NH), 20.8 (*C*H_3C(O)O), 20.6 (*C*H_3C(O)O), 20.4 (*C*H_3C(O)O); **For 4.35α, 4.35β:** ESI HRMS: calcd. for $C_{41}H_{43}NO_{17}Na$ 844.2423. Found 844.2410; Anal. calcd for $C_{41}H_{43}NO_{17}$: C, 59.92; H, 5.27; N, 1.70. Found: C, 59.62; H, 5.43; N, 1.75.

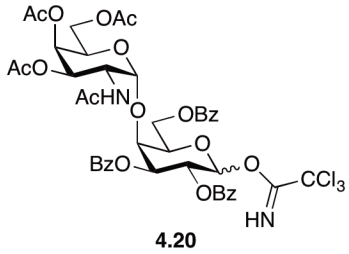

4.20

Trichloroacetimidate 2-acetamido-3,4,6-tri-*O*-acetyl-2-deoxy-α-D-galactopyranosyl-(1→4)-2,3,6-tri-*O*-benzoyl-α,β-D-galactopyranoside (4.20):

The 1-OH disaccharide **4.35** (0.0382 g, 0.0465 mmol) was dissolved in anhydrous CH_2Cl_2 (1 ml) and the reaction vessel placed under argon atmosphere. K_2CO_3 (0.013 g, 0.0930 mmol) was added followed by the addition of Cl_3CCN (0.023 ml, 0.233 mmol) and the reaction proceeded overnight at room temperature. TLC analysis (1:1, ethyl acetate-toluene) showed the reaction to be complete. The reaction mixture was filtered through Celite® and the filtrate concentrated. The crude product was purified by flash column chromatography on silica gel (1:1, ethyl acetate-toluene) to give the product **4.20** (0.0403 g, 81 %) as

an anomeric mixture (1.5:1, α:β) and as a white foam; **For 4.20α:** R_f 0.44 (1:1, ethyl acetate-toluene); ^{1}H NMR (500 MHz, $CDCl_3$) δ 8.61 (s, 1 H, *trichloroacetimidate* N-H), 8.04-7.92 (m, ArH), 7.60-7.54 (m, ArH), 7.53-7.31 (m, ArH), 6.80 (d, 1 H, $J_{1,2}$ 3.8 Hz, H-1), 6.02 (m, 1 H, N-H), 5.94 (dd, 1 H, $J_{1,2}$ 3.8 Hz, $J_{2,3}$ 10.9 Hz, H-2), 5.84 (dd, 1 H, $J_{3,4}$ 2.9 Hz, $J_{2,3}$ 10.9 Hz, H-3), 5.36-5.31 (m, 2 H, H-3', H-4'), 5.16 (d, 1 H, $J_{1',2'}$ 3.6 Hz, H-1'), 4.71-4.65 (m, 4 H, H-4, H-5, H-6a, H-2'), 4.43 (t, 1 H, $J_{5',6a'}$ 7.2 Hz, H-5'), 4.33 (dd, 1 H, $J_{5,6b}$ 4.7 Hz, $J_{6a,6b}$ 9.8 Hz, H-6b), 3.64 (dd, 1 H, $J_{5',6a'}$ 7.6 Hz, $J_{6a',6b'}$ 10.9 Hz, H-6a'), 3.37 (dd, 1 H, $J_{5',6b'}$ 6.5 Hz, $J_{6a',6b'}$ 10.9 Hz, H-6b'), 2.084 (s, 3 H, CH_3C(O)O), 2.081 (s, 3 H, CH_3C(O)O), 2.07 (s, 3 H, CH_3(O)NH), 1.73 (s, 3 H, CH_3C(O)O); ^{13}C NMR (125 MHz, $CDCl_3$) δ 170.8 (CH_3*C*(O)NH), 170.6 (CH_3*C*(O)O), 170.2 (CH_3*C*(O)O), 170.1 (CH_3*C*(O)O), 165.8 (Ph*C*(O)O), 165.6 (Ph*C*(O)O), 164.9 (Ph*C*(O)O), 160.9 (Cl_3C*C*(NH)O), 133.9 (Ar), 133.8 (Ar), 133.6 (Ar), 133.57 (Ar), 133.5 (Ar), 129.9 (Ar), 129.85 (Ar), 129.81 (Ar), 129.7 (Ar), 129.2 (Ar), 129.1 (Ar), 129.0 (Ar), 128.9 (Ar), 128.84 (Ar), 128.81 (Ar), 128.7 (Ar), 128.6 (Ar), 128.58 (Ar), 128.52 (Ar), 128.4 (Ar), 128.2 (Ar), 98.5 (C-1'), 93.6 (C-1), 73.3 (C-4), 71.12 (C-5), 71.1 (C-3), 68.0 (C-4'), 67.3 (C-2), 67.2 (C-3'), 66.9 (C-5'), 61.7 (C-6), 61.0 (C-6'), 47.9 (C-2'), 23.2 (*C*H_3C(O)NH), 20.8 (*C*H_3C(O)O), 20.7 (*C*H_3C(O)O), 20.4 (*C*H_3C(O)O); **For 4.20β:** R_f 0.32 (1:1, ethyl acetate-toluene); ^{1}H NMR (500 MHz, $CDCl_3$) δ 8.77 (s, 1 H, *trichloroacetimidate* N-H), 8.04-7.92 (m, ArH), 7.60-7.54 (m, ArH), 7.53-7.31 (m, ArH), 6.38 (d, 1 H, $J_{NH,2'}$ 9.5 Hz, N-H), 6.17 (d, 1 H, $J_{1,2}$ 6.8 Hz, H-1), 6.02 (m, 1 H, H-2), 5.51 (dd, 1 H, $J_{3,4}$ 3.1 Hz, $J_{2,3}$ 9.3 Hz, H-3), 5.36-5.31 (m, 2 H, H-3', H-4'), 5.22 (d, 1 H, $J_{1',2'}$ 3.7 Hz, H-1'), 4.89 (dd,

1 H, $J_{5,6a}$ 7.4 Hz, $J_{6a,6b}$ 11.4 Hz, H-6a), 4.71-4.65 (m, 1 H, H-2'), 4.58 (m, 1 H, H-4), 4.48 (m, 1 H, H-6b), 4.39-4.35 (t, 2 H, H-5, H-5'), 3.69 (m, 1 H, H-6a'), 3.47 (m, 1 H, H-6b'), 2.04 (s, 3 H, C*H*$_3$C(O)O), 2.03 (s, 3 H, C*H*$_3$C(O)O), 2.02 (s, 3 H, C*H*$_3$(O)NH), 1.76 (s, 3 H, C*H*$_3$C(O)O); ^{13}C NMR (125 MHz, $CDCl_3$) δ 170.9 (CH_3*C*(O)NH), 170.5 (CH_3*C*(O)O), 169.9 (CH_3*C*(O)O), 169.8 (CH_3*C*(O)O), 166.0 (Ph*C*(O)O), 165.7 (Ph*C*(O)O), 165.5 (Ph*C*(O)O), 160.6 (Cl_3C*C*(NH)O), 133.9 (Ar), 133.8 (Ar), 133.6 (Ar), 133.57 (Ar), 133.5 (Ar), 129.9 (Ar), 129.85 (Ar), 129.81 (Ar), 129.7 (Ar), 129.2 (Ar), 129.1 (Ar), 129.0 (Ar), 128.9 (Ar), 128.84 (Ar), 128.81 (Ar), 128.7 (Ar), 128.6 (Ar), 128.58 (Ar), 128.52 (Ar), 128.4 (Ar), 128.2 (Ar), 98.8 (C-1'), 96.2 (C-1), 73.4 (C-5), 72.2 (C-4), 72.1 (C-3), 68.3 (C-2), 67.9 (C-4'), 67.2 (C-3'), 66.8 (C-5'), 61.7 (C-6), 60.8 (C-6'), 48.1 (C-2'), 23.4 (*C*H_3C(O)NH), 20.8 (*C*H_3C(O)O), 20.7 (*C*H_3C(O)O), 20.4 (*C*H_3C(O)O); **For 4.20α, 4.20β:** ESI HRMS: calcd. for $C_{43}H_{43}Cl_3N_2O_{17}Na$ 987.1520. Found 987.1531.

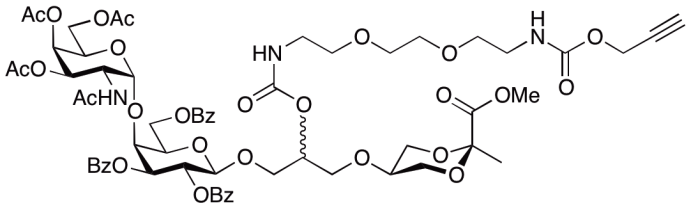

4.36

Methyl 5-(2-(2-acetamido-3,4,6-tri-*O*-acetyl-2-deoxy-α-D-galactopyranosyl-(1→4)-2,3,6-tri-*O*-benzoyl-β-D-galactopyranosyl)-4,15-dioxo-3,8,11,16-tetraoxa-5,14-diazanonadec-18-ynyloxy)-2-methyl-1,3-dioxane-carboxylate (4.36):

The donor **4.20** (0.0429 g, 0.0444 mmol) and the acceptor **4.21** (0.034 g, 0.0666 g) were combined with pre-activated 3Å molecular sieves (50 mg) and the contents dissolved in anhydrous CH_2Cl_2 (1 ml). The flask was placed under argon atmosphere and stirred for 1.5 hours at room temperature. The flask was subsequently cooled to -20 °C in a dry ice-acetone bath. Once cool, TMSOTf (0.0008 ml, 0.00444 mmol) was added and the reaction proceeded for 30 minutes until TLC analysis (1:1, acetone-hexanes) showed the reaction to be complete. A 1:1 mixture of Ac_2O:Et_3N was added (3 ml) and the reaction proceeded overnight. TLC analysis (1:1, acetone-hexanes) was done and the evolution of a new product was observed, assumed to be the acetylated acceptor. The reaction mixture was filtered through Celite® and concentrated to dryness while co-evaporating with toluene (3 x 10 ml). The crude product was purified by flash column chromatography on silica gel (1:1, acetone-hexanes) to give the product **4.36** (0.0509 g, 87 %) as an inseparable mixture of diastereoisomers and as a white foam; R_f 0.19 (1:1, acetone-hexanes); For the purposes of NMR characterization, where identifiable, signals corresponding to one isomer will be arbitrarily denoted

with *"r"*, while the other with *"s"*: ^{1}H NMR (700 MHz, $CDCl_3$) δ 8.04 (m, 4 H, ArH), 7.97-7.91 (m, 8 H, ArH), 7.61 (m, 2 H, ArH), 7.54-7.46 (m, 8 H, ArH), 7.41-7.36 (m, 8 H, ArH), 6.89 (d, 1 H, $J_{NH,2'}$ 8.9 Hz, N-H *"r"*), 6.46 (d, 1 H, $J_{NH,2'}$ 9.1 Hz, N-H *"s"*), 5.74-5.69 (m, 2 H, H-2 *"r"*, H-2 *"s"*), 5.41-5.32 (m, 6 H, H-3 *"r"*, H-3 *"s"*, H-3' *"r"*, H-3' *"s"*, H-4' *"r"*, H-4' *"s"*), 5.18 (d, 1 H, $J_{1',2'}$ 3.6 Hz, H-1' *"r"*), 5.15 (d, 1 H, $J_{1',2'}$ 3.0 Hz, H-1' *"s"*), 4.93 (m, 1 H, -OCH_2CH(OR)- *"r"*), 4.87-4.77 (m, 5 H, $J_{1,2}$ 7.4 Hz, -OCH_2CH(OR)- *"s"*, H-1 *"r"*, H-1 *"s"*, H-6a *"r"*, H-6a *"s"*), 4.72-4.66 (m, 6 H, H-2' *"r"*, H-2' *"s"*, -$OCH_2C{\equiv}CH$ *"r"*, -$OCH_2C{\equiv}CH$ *"s"*), 4.49 (m, 1 H, H-4 *"r"*, H-4 *"s"*), 4.42 (m, 2 H, H-5' *"r"*, H-5' *"s"*), 4.32 (m, 2 H, H-6b *"r"*, H-6b *"s"*), 4.15-4.11 (m, 2 H, H-5 *"r"*, H-5 *"s"*), 4.01-3.93 (m, 4 H, -OCH_2CH(OR)- *"r"*, *ring* -CH_2- *"r"*), 3.91-3.84 (m, 2 H, -OCH_2CH(OR)- *"s"*), 3.82-3.79 (m, 6 H, C(O)OCH_3 *"r"*, C(O)OCH_3 *"s"*), 3.72-3.64 (m, 4 H, -CH(OR)CH_2O- *"r"*, H-6a' *"r"*, H-6a' *"s"*), 3.62-3.46 (m, 20 H, *ring* C-H *"r"*, *ring* C-H *"s"*, *ring* -CH_2- *"s"*, -OCH_2CH_2O- *"r"*, -OCH_2CH_2O- *"s"*, -OCH_2CH_2NH- (x2) *"r"*, -OCH_2CH_2NH- (x2) *"s"*), 3.43-3.20 (m, 14 H, ring -CH_2- *"r"*, ring -CH_2- *"s"*, H-6b' *"r"*, H-6b' *"s"*, -OCH_2CH_2NH- (x2) *"r"*, -OCH_2CH_2NH- (x2) *"s"*), 2.48 (m, 2 H, -$OCH_2C{\equiv}CH$ *"r"*, -$OCH_2C{\equiv}CH$ *"s"*), 2.084 (s, 3 H, CH_3C(O)O), 2.081 (s, 6 H, CH_3C(O)O), 2.07 (s, 3 H, CH_3C(O)O), 2.03 (s, 3 H, CH_3C(O)NH), 2.02 (s, 3 H, CH_3C(O)NH), 1.76 (s, 3 H, CH_3C(O)O), 1.74 (s, 3 H, CH_3C(O)O), 1.48 (s, 3 H, -CH_3), 1.47 (s, 3 H, -CH_3); ^{13}C NMR (175 MHz, $CDCl_3$) δ 171.0, 170.8, 170.7, 170.6, 170.4, 170.3, 170.2, 170.1, 169.9, 169.7, 165.9, 165.84, 165.83, 165.81, 165.2, 155.6, 155.59, 155.51, 155.4, 133.7, 133.6, 133.59, 133.53, 133.4, 129.8, 129.7, 129.64, 129.6, 129.2, 129.13, 129.12,

129.0, 128.8, 128.7, 128.63, 128.62, 128.6, 128.56, 128.5, 101.7 (C-1), 101.4 (C-1), 98.8 (C-1'), 98.6 (C-1'), 98.1, 78.4, 74.7, 72.9, 72.7, 72.6, 72.5, 72.4, 71.8, 71.5, 70.3, 69.9, 69.5, 69.3, 68.7, 67.9, 67.85, 67.81, 67.6, 66.97, 66.9, 66.8, 66.7, 65.8, 65.7, 61.4, 61.3, 60.7, 60.6, 53.4, 52.7, 52.4, 47.9, 47.7, 40.9, 40.8, 40.7, 31.9, 29.7, 29.6, 29.4, 29.3, 25.1, 23.2, 22.9, 22.6, 20.8, 20.6, 20.4, 14.1; ESI HRMS: calcd. for $C_{62}H_{75}N_3O_{28}Na$ 1332.4429. Found 1332.4430; Anal. calcd for $C_{62}H_{75}N_3O_{28}$: C, 56.83; H, 5.77; N, 3.21. Found: C, 56.95; H, 5.96; N, 3.43.

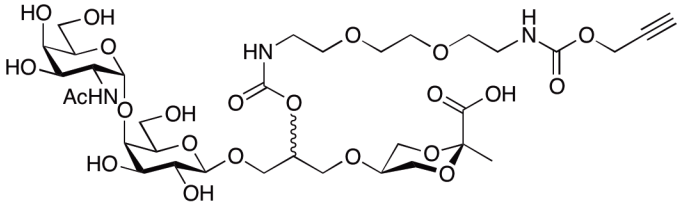

4.18

Methyl 5-(2-(2-acetamido-2-deoxy-α-D-galactopyranosyl-(1→4)-β-D-galactopyranosyl)-4,15-dioxo-3,8,11,16-tetraoxa-5,14-diazanonadec-18-ynyloxy)-2-methyl-1,3-dioxane-2-carboxylic acid (4.18):

The fully protected derivative **4.36** (0.0656 g, 0.0501 mmol) was dissolved in anhydrous CH_3OH (2 ml) and placed under argon atmosphere. 1.0 M CH_3ONa in CH_3OH (0.0501 ml, 0.0501 mmol) was added and the reaction proceeded overnight at room temperature. TLC analysis (4:3:0.5:0.1 dichloromethane:methanol:water:acetic acid) was done and the reaction found to be complete and was concentrated to dryness. The crude residue was dissolved in milliQ water (2 ml) and stirred and room temperature while monitoring with TLC. After one hour, TLC indicated remaining starting material. An additional equivalent of CH_3ONa in CH_3OH (0.0501 ml) was added and the reaction

proceeded for an additional two hours at which point TLC analysis showed the reaction to be complete. The crude reaction mixture was quenched with Dowex 50W-X8 ion exchange resin (H^+) and concentrated until dry. The crude product was purified using HPLC (100% H_2O (0.1% TFA) → 100% CH_3CN) and subsequently lyophilized to give the product **4.18** (0.04188 g, 97 %) as a soft white powder; R_f 0.32 (4:3:0.5:0.1, dichloromethane:methanol:water:acetic acid); FTIR found: 3363.15 cm^{-1} (O-H bending), 2938.63 cm^{-1}, 2885.16 cm^{-1} (sp^3 C-H stretch), 2125.04 cm^{-1} (sp C≡C stretch), 1708.94 cm^{-1} (C=O stretch); ^{1}H NMR (700 MHz, $CDCl_3$) δ 4.96 (m, 1 H, -OCH_2CH(OR)-), 4.86 (m, 1 H, $J_{1',2'}$ 2.6 Hz, H-1'), 4.64 (bs, 2 H, -OCH_2C≡CH), 4.39 (t, 1 H, $J_{1,2}$ 7.9 Hz, $J_{1,CH2}$ 7.9 Hz, H-1), 4.34 (t, 1 H, $J_{5',6a'}$ 6.5 Hz, H-5'), 4.18-4.13 (m, 3 H, *ring* -CH_2-, H-2'), 4.00-3.95 (m, 2 H, -OCH_2CH(OR)-, H-4'), 3.94-3.91 (m, 2 H, H-4, H-3'), 3.81-3.63 (m, 14 H, -OCH_2CH_2O-, -CH(OR)CH_2O-, -OCH_2CH(OR)-, ring C-H, H-5, H-6a, H-6b, H-6a', H-6b', H-3), 3.58 (t, 4 H, $J_{CH2,CH2}$ 5.4 Hz, -OCH_2CH_2NH- (x2)), 3.54-3.48 (m, 3 H, *ring* -CH_2-, H-2), 3.34-3.24 (m, 2 H, -OCH_2CH_2NH-), 2.87 (bs, 1 H, -OCH_2C≡C*H*), 2.04 (s, 3 H, CH_3C(O)NH), 1.49 (s, 3 H, -CH_3); ^{13}C NMR (175 MHz, D_2O) δ 174.52 (CH_3C(O)NH), 174.51 (CH_3C(O)NH), 163.1 (*C*(O)OH), 162.9 (*C*(O)OH), 157.8 (-O*C*(O)NH-), 157.7 (-O*C*(O)NH-), 157.6 (-O*C*(O)NH-), 103.6 (C-1), 103.3 (C-1), 98.6 (C-1'), 98.5 (C-1'), 98.3 (quaternary C *pyruvate*), 78.6 (-OCH_2C≡CH), 76.8 (C-4), 75.7 (-OCH_2C≡*C*H), 75.4 (*ring* C-H), 72.6 (-OCH_2CH(OR)-), 72.4 (C-3), 72.2 (C-2), 71.9 (C-5'), 70.7 (C-5), 69.5 (-OCH_2CH_2O-), 69.3 (-OCH_2CH_2NH-), 69.5 (-OCH_2CH_2NH-), 68.8, 68.7, 68.4, 68.3 (-OCH_2CH(OR)CH_2O-), 68.2 (C-4'), 67.2 (C-3'), 65.1 (ring -CH_2-), 64.9

(ring -CH_2-), 60.5, 60.2, 60.1 (C-6, C-6'), 52.8 (-OCH_2C≡CH), 50.1 (C-2'), 40.2 (-OCH_2CH_2NH-), 23.1 (CH_3C(O)NH), 21.9 (-CH_3); ESI HRMS: calcd. for $[C_{34}H_{54}N_3O_{22}]^-$ 856.3204. Found 856.3184.

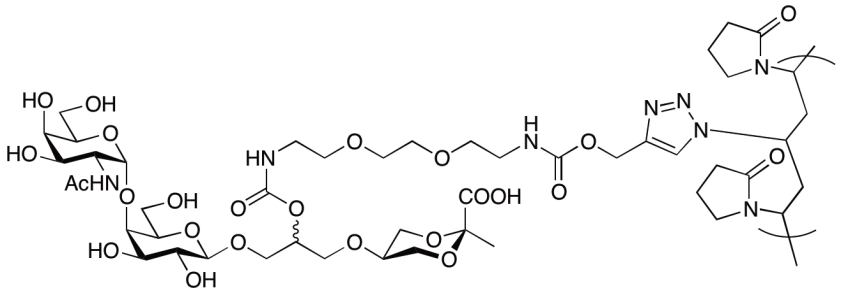

4.17

PolyBAIT-*di*NAc (4.17):

The disaccharide derivative **4.18** (39.24 mg, 45.74 μmol) and the aza-povidone polymer **4.19** (61.99 mg, 22.87 μmol) were combined and dissolved in de-gassed MilliQ water (4 ml). A 0.1 M solution of $CuSO_4$ was made and added to the starting materials (100 μl) followed by 1 M sodium ascorbate in water (100 μl). The reaction solution was basicified *via* the addition of sodium bicarbonate until pH ~8. The reaction proceeded for three days at which point TLC analysis (4:5:0.5:0.1, dichloromethane:methanol:water:acetic acid) showed a disappearance in starting material. The reaction mixture was transferred to a dialysis bag and dialyzed for four days with 0.5 M EDTA (1 ml/1 L water). The last two washes were without the addition of EDTA. The contents of the bag were subsequently lyophilized to provide the product **4.17** as a white solid; Degree of incorporation was determined using ^{1}H NMR spectroscopy and found to be

approximately 9-10%; FTIR found: 3405.62 cm^{-1} (O-H bending), 2948.70 cm^{-1}, 2882.63 cm^{-1} (sp^3 C-H stretch), 11675.31 cm^{-1} (C=C stretch).

Chapter 7

Bibliography

1. Drasar, B. S.; Hill, M. J. *Human intestinal flora.*; Academic Press London, 1974.
2. Levine, M. M. *J. Infect. Dis.* **1987**, *155*, 377-389.
3. Nataro, J. P.; Kaper, J. B. *Clin. Microbiol. Rev.* **1998**, *11*, 142-201.
4. Lior, H. In *Escherichia coli in domestic animals and humans*; Gyles, C. L., Ed.; CAB International: Wallingford, United Kingdom, 1996, p 31-72.
5. Kauffmann, F. *Acta Pathol. Microbiol. Scand.* **1944**, *21*, 20-45.
6. Edelman, R.; Levine, M. M. *J. Infect. Dis.* **1983**, *147*, 1108-1118.
7. Stewart, I.; Schluter, P. J.; Shaw, G. R. *Environ. Health* **2006**, *5*, 7.
8. Bardy, S. L. *Microbiology* **2003**, *149*, 295-304.
9. Kauffmann, F. *J. Immunol.* **1947**, *57*, 71-100.
10. Neter, E. *J. Pediatr.* **1959**, *55*, 223-239.
11. Nataro, J. P.; Levine, M. M. In *Escherichia coli in Domestic Animals and Humans*; Gyles, C. L., Ed.; CAB International: Wallingford, United Kingdom, 1996, p 285-333.
12. Donnenberg, M. S.; Kaper, J. B. *Infect. Immun.* **1992**, *60*, 3953-3961.

13. Cravioto, A.; Gross, R. J.; Scotland, S. M.; Rowe, B. *Curr. Microbiol.* **1979**, *3*, 95-99.

14. Baldini, M. M.; Kaper, J. B.; Levine, M. M.; Candy, D. C.; Moon, H. W. *J. Pediatr. Gastroenterol. Nutr.* **1983**, *2*, 534-538.

15. Baldwin, T. J.; Ward, W.; Aitken, A.; Knutton, S.; Williams, P. H. *Infect. Immun.* **1991**, *59*, 1599-1604.

16. Baldwin, T. J.; Lee-Delaunay, M. B.; Knutton, S.; Williams, P. H. *Infect. Immun.* **1993**, *61*, 760-763.

17. Field, M.; Rao, M. C.; Chang, E. B. *N. Engl. J. Med.* **1989**, *321*, 800-806.

18. Field, M.; Rao, M. C.; Chang, E. B. *N. Engl. J. Med.* **1989**, *321*, 879-883.

19. Jerse, A. E.; Yu, J.; Tall, B. D.; Kaper, J. B. *Proc. Natl. Acad. Sci. U. S. A.* **1990**, *87*, 7839-7843.

20. Donnenberg, M. S.; Tacket, C. O.; James, S. P.; Losonsky, G.; Nataro, J. P.; Wasserman, S. S.; Kaper, J. B.; Levine, M. M. *J. Clin. Invest.* **1993**, *92*, 1412-1417.

21. Kenny, B.; Lai, L. C.; Finlay, B. B.; Donnenberg, M. S. *Mol. Microbiol.* **1996**, *20*, 313-323.

22. Donnenberg, M. S.; Yu, J.; Kaper, J. B. *J. Bacteriol.* **1993**, *175*, 4670-4680.

23. Kenny, B.; Finlay, B. B. *Proc. Natl. Acad. Sci. U. S. A.* **1995**, *92*, 7991-7995.

24. Lai, L. C.; Wainwright, L. A.; Stone, K. D.; Donnenberg, M. S. *Infect. Immun.* **1997**, *65*, 2211-2217.

25. Foubister, V.; Rosenshine, I.; Donnenberg, M. S.; Finlay, B. B. *Infect. Immun.* **1994**, *62*, 3038-3040.

26. Sixma, T. K.; Kalk, K. H.; van Zanten, B. A.; Dauter, Z.; Kingma, J.; Witholt, B.; Hol, W. G. *J. Mol. Biol.* **1993**, *230*, 890-918.

27. Streatfield, S. J.; Sandkvist, M.; Sixma, T. K.; Bagdasarian, M.; Hol, W. G.; Hirst, T. R. *Proc. Natl. Acad. Sci. U. S. A.* **1992**, *89*, 12140-12144.

28. Teneberg, S.; Hirst, T. R.; Angström, J.; Karlsson, K. A. *Glycoconj. J.* **1994**, *11*, 533-540.

29. Lencer, W. I.; Constable, C.; Moe, S.; Jobling, M. G.; Webb, H. M.; Ruston, S.; Madara, J. L.; Hirst, T. R.; Holmes, R. K. *J. Cell Biol.* **1995**, *131*, 951-962.

30. Sears, C. L.; Kaper, J. B. *Microbiol. Rev.* **1996**, *60*, 167-215.

31. Fishman, P. In *ADP-Ribosylating Toxins and G-Proteins*; Vaughan, M., Moss, J., Eds.; American Society for Microbiology: Washington, D.C., 1990, p 127-140.

32. Dubreuil, J. D. *Curr. Issues Mol. Biol.* **2012**, *14*, 71-82.

33. Gyles, C. L. In *Escherichia coli in Domestic Animals and Humans*; Gyles, C. L., Ed.; CAB International: Wallingford, United Kigndom, 1996, p 337-364.

34. Lazure, C.; Seidah, N. G.; Pélaprat, D.; Chrétien, M. *Can. J. Biochem. Cell Biol.* **1983**, *61*, 501-515.

35. de Sauvage, F. J.; Horuk, R.; Bennett, G.; Quan, C.; Burnier, J. P.; Goeddel, D. V. *J. Biol. Chem.* **1992**, *267*, 6479-6482.

36. Vaandrager, A. B.; van der Wiel, E.; Hom, M. L.; Luthjens, L. H.; de Jonge, H. R. *J. Biol. Chem.* **1994**, *269*, 16409-16415.

37. Dreyfus, L. A.; Urban, R. G.; Whipp, S. C.; Slaughter, C.; Tachias, K.; Kupersztoch, Y. M.; Drefus, L. A. *Mol. Microbiol.* **1992**, *6*, 2397-2406.

38. Dreyfus, L. A.; Harville, B.; Howard, D. E.; Shaban, R.; Beatty, D. M.; Morris, S. J. *Proc. Natl. Acad. Sci. U. S. A.* **1993**, *90*, 3202-3206.

39. DuPont, H. L.; Formal, S. B.; Hornick, R. B.; Snyder, M. J.; Libonati, J. P.; Sheahan, D. G.; LaBrec, E. H.; Kalas, J. P. *N. Engl. J. Med.* **1971**, *285*, 1-9.

40. van den Beld, M. J. C.; Reubsaet, F. A. G. *Eur. J. Clin. Microbiol. Infect. Dis.* **2012**, *31*, 899-904.

41. Harris, J. R.; Wachsmuth, I. K.; Davis, B. R.; Cohen, M. L. *Infect. Immun.* **1982**, *37*, 1295-1298.

42. Hale, T. L.; Sansonetti, P. J.; Schad, P. A.; Austin, S.; Formal, S. B. *Infect. Immun.* **1983**, *40*, 340-350.

43. Sansonetti, P. J.; Kopecko, D. J.; Formal, S. B. *Infect. Immun.* **1982**, *35*, 852-860.

44. Sansonetti, P. J. *Rev. Infect. Dis.* **1991**, *13 Suppl 4*, S285-292.

45. Hale, T. L. *Microbiol. Rev.* **1991**, *55*, 206-224.

46. Scaletsky, I. C.; Silva, M. L.; Trabulsi, L. R. *Infect. Immun.* **1984**, *45*, 534-536.

47. Nataro, J. P.; Scaletsky, I. C.; Kaper, J. B.; Levine, M. M.; Trabulsi, L. R. *Infect. Immun.* **1985**, *48*, 378-383.

48. Nataro, J. P.; Kaper, J. B.; Robins-Browne, R.; Prado, V.; Vial, P.; Levine, M. M. *Pediatr. Infect. Dis. J.* **1987**, *6*, 829-831.

49. Weintraub, A. *J. Med. Microbiol.* **2007**, *56*, 4-8.

50. Andrade, J. A. B. d.; Freymüller, E.; Fagundes-Neto, U. *Arq. Gastroenterol.* **2011**, *48*, 199-204.

51. Konno, T.; Yatsuyanagi, J.; Saito, S. *FEMS Immunol. Med. Microbiol.* **2012**, *64*, 314-320.

52. Navarro-Garcia, F. *Future Microbiol.* **2010**, *5*, 1005-1013.

53. Marin-Esteban, V.; Turbica, I.; Dufour, G.; Semiramoth, N.; Gleizes, A.; Gorges, R.; Beau, I.; Servin, A. L.; Lievin-Le Moal, V.; Sandré, C.; Chollet-Martin, S. *Infect. Immun.* **2012**, *80*, 1891-1899.

54. Konowalchuk, J.; Speirs, J. I.; Stavric, S. *Infect. Immun.* **1977**, *18*, 775-779.

55. Riley, L. W.; Remis, R. S.; Helgerson, S. D.; McGee, H. B.; Wells, J. G.; Davis, B. R.; Hebert, R. J.; Olcott, E. S.; Johnson, L. M.; Hargrett, N. T.; Blake, P. A.; Cohen, M. L. *N. Engl. J. Med.* **1983**, *308*, 681-685.

56. Karmali, M. A.; Steele, B. T.; Petric, M.; Lim, C. *Lancet* **1983**, *1*, 619-620.

57. O'Brien, A. D.; Thompson, M. R.; Gemski, P.; Doctor, B. P.; Formal, S. B. *Infect. Immun.* **1977**, *15*, 796-798.

58. O'Brien, A. D.; LaVeck, G. D.; Griffin, D. E.; Thompson, M. R. *Infect. Immun.* **1980**, *30*, 170-179.

59. O'Brien, A. D.; LaVeck, G. D.; Thompson, M. R.; Formal, S. B. *J. Infect. Dis.* **1982**, *146*, 763-769.

60. O'Brien, A. D.; Lively, T. A.; Chang, T. W.; Gorbach, S. L. *Lancet* **1983**, *2*, 573.

61. Johnson, W. M.; Lior, H.; Bezanson, G. S. *Lancet* **1983**, *1*, 76.

62. Karmali, M. A.; Petric, M.; Lim, C.; Fleming, P. C.; Steele, B. T. *Lancet* **1983**, *2*, 1299-1300.

63. Bergan, J.; Dyve Lingelem, A. B.; Simm, R.; Skotland, T.; Sandvig, K. *Toxicon* **2012**, *60*, 1085-1107.

64. Mead, P. S.; Griffin, P. M. *Lancet* **1998**, *352*, 1207-1212.

65. Strockbine, N. A.; Jackson, M. P.; Sung, L. M.; Holmes, R. K.; O'Brien, A. D. *J. Bacteriol.* **1988**, *170*, 1116-1122.

66. Calderwood, S. B.; Auclair, F.; Donohue-Rolfe, A.; Keusch, G. T.; Mekalanos, J. J. *Proc. Natl. Acad. Sci. U. S. A.* **1987**, *84*, 4364-4368.

67. Jackson, M. P.; Newland, J. W.; Holmes, R. K.; O'Brien, A. D. *Microb. Pathog.* **1987**, *2*, 147-153.

68. Zhang, W.; Bielaszewska, M.; Kuczius, T.; Karch, H. *J. Clin. Microbiol.* **2002**, *40*, 1441-1446.

69. Bürk, C.; Dietrich, R.; Açar, G.; Moravek, M.; Bülte, M.; Märtlbauer, E. *J. Clin. Microbiol.* **2003**, *41*, 2106-2112.

70. Jackson, M. P.; Neill, R. J.; O'Brien, A. D.; Holmes, R. K. *FEMS Microbiol. Lett.* **1987**, *44*, 109-114.

71. Piérard, D.; Muyldermans, G.; Moriau, L.; Stevens, D.; Lauwers, S. *J. Clin. Microbiol.* **1998**, *36*, 3317-3322.

72. Schmitt, C. K.; McKee, M. L.; O'Brien, A. D. *Infect. Immun.* **1991**, *59*, 1065-1073.

73. Teel, L. D.; Melton-Celsa, A. R.; Schmitt, C. K.; O'Brien, A. D. *Infect. Immun.* **2002**, *70*, 4282-4291.

74. Gyles, C. L.; De Grandis, S. A.; MacKenzie, C.; Brunton, J. L. *Microb. Pathog.* **1988**, *5*, 419-426.

75. Schmidt, H.; Scheef, J.; Morabito, S.; Caprioli, A.; Wieler, L. H.; Karch, H. *Appl. Environ. Microbiol.* **2000**, *66*, 1205-1208.

76. Leung, P. H. M.; Peiris, J. S. M.; Ng, W. W. S.; Robins-Browne, R. M.; Bettelheim, K. A.; Yam, W. C. *Appl. Environ. Microbiol.* **2003**, *69*, 7549-7553.

77. Fraser, M. E.; Chernaia, M. M.; Kozlov, Y. V.; James, M. N. *Nat. Struct. Biol.* **1994**, *1*, 59-64.

78. Ling, H.; Boodhoo, A.; Hazes, B.; Cummings, M. D.; Armstrong, G. D.; Brunton, J. L.; Read, R. J. *Biochemistry* **1998**, *37*, 1777-1788.

79. Shimizu, H.; Field, R. A.; Homans, S. W.; Donohue-Rolfe, A. *Biochemistry* **1998**, *37*, 11078-11082.

80. Endo, Y.; Mitsui, K.; Motizuki, M.; Tsurugi, K. *J. Biol. Chem.* **1987**, *262*, 5908-5912.

81. Tesh, V. L. *Future Microbiol.* **2010**, *5*, 431-453.

82. O'Brien, A. D.; Newland, J. W.; Miller, S. F.; Holmes, R. K.; Smith, H. W.; Formal, S. B. *Science* **1984**, *226*, 694-696.

83. Allison, H. E.; Sergeant, M. J.; James, C. E.; Saunders, J. R.; Smith, D. L.; Sharp, R. J.; Marks, T. S.; McCarthy, A. J. *Infect. Immun.* **2003**, *71*, 3409-3418.

84. Law, D.; Kelly, J. *Infect. Immun.* **1995**, *63*, 700-702.

85. Cornick, N. A.; Booher, S. L.; Moon, H. W. *Infect. Immun.* **2002**, *70*, 2704-2707.

86. Judge, N. A.; Mason, H. S.; O'Brien, A. D. *Infect. Immun.* **2004**, *72*, 168-175.

87. McKee, M. L.; Melton-Celsa, A. R.; Moxley, R. A.; Francis, D. H.; O'Brien, A. D. *Infect. Immun.* **1995**, *63*, 3739-3744.

88. Melton-Celsa, A.; Mohawk, K.; Teel, L.; O'Brien, A. In *Ricin and Shiga Toxins*; Mantis, N., Ed.; Springer Berlin Heidelberg: Berlin, Heidelberg, 2011; Vol. 357, p 67-103.

89. Engedal, N.; Skotland, T.; Torgersen, M. L.; Sandvig, K. *Microb. Biotechnol.* **2011**, *4*, 32-46.

90. Sandvig, K.; Bergan, J.; Dyve, A.-B.; Skotland, T.; Torgersen, M. L. *Toxicon* **2010**, *56*, 1181-1185.

91. Sandvig, K.; Pust, S.; Skotland, T.; van Deurs, B. *Curr. Opin. Cell Biol.* **2011**, *23*, 413-420.

92. Sandvig, K.; Olsnes, S.; Brown, J. E.; Petersen, O. W.; van Deurs, B. *J. Cell Biol.* **1989**, *108*, 1331-1343.

93. Sandvig, K.; Prydz, K.; Ryd, M.; van Deurs, B. *J. Cell Biol.* **1991**, *113*, 553-562.

94. Sandvig, K.; Garred, O.; Prydz, K.; Kozlov, J. V.; Hansen, S. H.; Vandeurs, B. *Nature* **1992**, *358*, 510-512.

95. Donta, S. T.; Tomicic, T. K.; Donohue-Rolfe, A. *J. Infect. Dis.* **1995**, *171*, 721-724.

96. Valderrama, F.; Durán, J. M.; Babià, T.; Barth, H.; Renau-Piqueras, J.; Egea, G. *Traffic* **2001**, *2*, 717-726.

97. Endo, Y.; Tsurugi, K.; Yutsudo, T.; Takeda, Y.; Ogasawara, T.; Igarashi, K. *Eur. J. Biochem.* **1988**, *171*, 45-50.

98. Jandhyala, D. M.; Thorpe, C. M.; Magun, B. *Curr. Top. Microbiol. Immunol.* **2012**, *357*, 41-65.

99. Mayer, C. L.; Leibowitz, C. S.; Kurosawa, S.; Stearns-Kurosawa, D. J. *Toxins* **2012**, *4*, 1261-1287.

100. Obrig, T. G.; Louise, C. B.; Lingwood, C. A.; Boyd, B.; Barley-Maloney, L.; Daniel, T. O. *J. Biol. Chem.* **1993**, *268*, 15484-15488.

101. Gould, L. H.; Demma, L.; Jones, T. F.; Hurd, S.; Vugia, D. J.; Smith, K.; Shiferaw, B.; Segler, S.; Palmer, A.; Zansky, S.; Griffin, P. M. *Clin. Infect. Dis.* **2009**, *49*, 1480-1485.

102. Fukushima, H.; Hashizume, T.; Morita, Y.; Tanaka, J.; Azuma, K.; Mizumoto, Y.; Kaneno, M.; Matsuura, M.; Konma, K.; Kitani, T. *Pediatr. Int.* **1999**, *41*, 213-217.

103. Frank, C.; Werber, D.; Cramer, J. P.; Askar, M.; Faber, M.; an der Heiden, M.; Bernard, H.; Fruth, A.; Prager, R.; Spode, A.; Wadl, M.; Zoufaly, A.; Jordan, S.; Kemper, M. J.; Follin, P.; Müller, L.; King, L. A.; Rosner, B.; Buchholz, U.; Stark, K.; Krause, G. *N. Engl. J. Med.* **2011**, *365*, 1771-1780.

104. Buchholz, U.; Bernard, H.; Werber, D.; Böhmer, M. M.; Remschmidt, C.; Wilking, H.; Deleré, Y.; an der Heiden, M.; Adlhoch, C.; Dreesman, J.; Ehlers, J.; Ethelberg, S.; Faber, M.; Frank, C.; Fricke, G.; Greiner, M.; Höhle, M.; Ivarsson, S.; Jark, U.; Kirchner, M.; Koch, J.; Krause, G.; Luber, P.; Rosner, B.; Stark, K.; Kühne, M. *N. Engl. J. Med.* **2011**, *365*, 1763-1770.

105. Garg, A. X.; Suri, R. S.; Barrowman, N.; Rehman, F.; Matsell, D.; Rosas-Arellano, M. P.; Salvadori, M.; Haynes, R. B.; Clark, W. F. *JAMA* **2003**, *290*, 1360-1370.

106. Oakes, R. S.; Kirkham, J. K.; Kirkhamm, J. K.; Nelson, R. D.; Siegler, R. L. *Pediatr. Nephrol.* **2008**, *23*, 1303-1308.

107. Wong, C. S.; Mooney, J. C.; Brandt, J. R.; Staples, A. O.; Jelacic, S.; Boster, D. R.; Watkins, S. L.; Tarr, P. I. *Clin. Infect. Dis.* **2012**, *55*, 33-41.

108. Kimmitt, P. T.; Harwood, C. R.; Barer, M. R. *Emerg. Infect. Dis.* **2000**, *6*, 458-465.

109. Hauswaldt, S.; Nitschke, M.; Sayk, F.; Solbach, W.; Knobloch, J. K.-M. *Curr. Infect. Dis. Rep.* **2013**, *15*, 4-9.

110. Rasko, D. A.; Sperandio, V. *Nat. Rev. Drug Discovery* **2010**, *9*, 117-128.

111. Cegelski, L.; Marshall, G. R.; Eldridge, G. R.; Hultgren, S. J. *Nat. Rev. Microbiol.* **2008**, *6*, 17-27.

112. Ivarsson, M. E.; Leroux, J.-C.; Castagner, B. *Angew. Chem., Int. Ed. Engl.* **2012**, *51*, 4024-4045.

113. Bai, Y.; Watt, B.; Wahome, P. G.; Mantis, N. J.; Robertus, J. D. *Toxicon* **2010**, *56*, 526-534.

114. Wahome, P. G.; Bai, Y.; Neal, L. M.; Robertus, J. D.; Mantis, N. J. *Toxicon* **2010**, *56*, 313-323.

115. Miller, D. J.; Ravikumar, K.; Shen, H.; Suh, J.-K.; Kerwin, S. M.; Robertus, J. D. *J. Med. Chem.* **2002**, *45*, 90-98.

116. Mukhopadhyay, S.; Linstedt, A. D. *Science* **2012**, *335*, 332-335.

117. Mukhopadhyay, S.; Bachert, C.; Smith, D. R.; Linstedt, A. D. *Mol. Biol. Cell* **2010**, *21*, 1282-1292.

118. Mukhopadhyay, S.; Linstedt, A. D. *Proc. Natl. Acad. Sci. U. S. A.* **2011**, *108*, 858-863.

119. Nishikawa, K.; Watanabe, M.; Kita, E.; Igai, K.; Omata, K.; Yaffe, M. B.; Natori, Y. *FASEB J.* **2006**, *20*, 2597-2599.

120. Watanabe-Takahashi, M.; Sato, T.; Dohi, T.; Noguchi, N.; Kano, F.; Murata, M.; Hamabata, T.; Natori, Y.; Nishikawa, K. *Infect. Immun.* **2010**, *78*, 177-183.

121. Armstrong, G. D.; Fodor, E.; Vanmaele, R. *J. Infect. Dis.* **1991**, *164*, 1160-1167.

122. Trachtman, H.; Cnaan, A.; Christen, E.; Gibbs, K.; Zhao, S.; Acheson, D. W. K.; Weiss, R.; Kaskel, F. J.; Spitzer, A.; Hirschman, G. H.; Trial, I. o. t. H.-S. P. M. C. *JAMA* **2003**, *290*, 1337-1344.

123. Paton, A. W.; Morona, R.; Paton, J. C. *Nat. Rev. Microbiol.* **2006**, *4*, 193-200.

124. Paton, A. W.; Morona, R.; Paton, J. C. *Nat. Med.* **2000**, *6*, 265-270.

125. Dohi, H.; Nishida, Y.; Mizuno, M.; Shinkai, M.; Kobayashi, T.; Takeda, T.; Uzawa, H.; Kobayashi, K. *Bioorg. Med. Chem.* **1999**, *7*, 2053-2062.

126. Matsuoka, K.; Terabatake, M.; Esumi, Y.; Terunuma, D.; Kuzuhara, H. *Tetrahedron Lett.* **1999**, *40*, 7839-7842.

127. Nishikawa, K.; Matsuoka, K.; Kita, E.; Okabe, N.; Mizuguchi, M.; Hino, K.; Miyazawa, S.; Yamasaki, C.; Aoki, J.; Takashima, S.; Yamakawa, Y.; Nishijima, M.; Terunuma, D.; Kuzuhara, H.; Natori, Y. *Proc. Natl. Acad. Sci. U. S. A.* **2002**, *99*, 7669-7674.

128. Nishikawa, K.; Matsuoka, K.; Watanabe, M.; Igai, K.; Hino, K.; Hatano, K.; Yamada, A.; Abe, N.; Terunuma, D.; Kuzuhara, H.; Natori, Y. *J. Infect. Dis.* **2005**, *191*, 2097-2105.

129. Watanabe, M.; Matsuoka, K.; Kita, E.; Igai, K.; Higashi, N.; Miyagawa, A.; Watanabe, T.; Yanoshita, R.; Samejima, Y.; Terunuma, D.; Natori, Y.; Nishikawa, K. *J. Infect. Dis.* **2004**, *189*, 360-368.

130. Kitov, P. I.; Sadowska, J. M.; Mulvey, G.; Armstrong, G. D.; Ling, H.; Pannu, N. S.; Read, R. J.; Bundle, D. R. *Nature* **2000**, *403*, 669-672.

131. Mulvey, G. L.; Marcato, P.; Kitov, P. I.; Sadowska, J.; Bundle, D. R.; Armstrong, G. D. *J. Infect. Dis.* **2003**, *187*, 640-649.

132. Solomon, D.; Kitov, P.; Paszkiewicz, E.; Grant, G.; Sadowska, J.; Bundle, D. *Org. Lett.* **2005**, *7*, 4369-4372.

133. Ho, J. G. S.; Kitov, P. I.; Paszkiewicz, E.; Sadowska, J.; Bundle, D. R.; Ng, K. K. S. *J. Biol. Chem.* **2005**, *280*, 31999-32008.

134. Fan, E.; Zhang, Z.; Minke, W. E.; Hou, Z.; Verlinde, C. L. M. J.; Hol, W. G. J. *J. Am. Chem. Soc.* **2000**, *122*, 2663-2664.

135. Kitov, P. I.; Lipinski, T.; Paszkiewicz, E.; Solomon, D.; Sadowska, J. M.; Grant, G. A.; Mulvey, G. L.; Kitova, E. N.; Klassen, J. S.; Armstrong, G. D.; Bundle, D. R. *Angew. Chem., Int. Ed. Engl.* **2008**, *47*, 672-676.

136. Kitova, E. N.; Kitov, P. I.; Paszkiewicz, E.; Kim, J.; Mulvey, G. L.; Armstrong, G. D.; Bundle, D. R.; Klassen, J. S. *Glycobiology* **2007**, *17*, 1127-1137.

137. Mammen, M.; Choi, S. K.; Whitesides, G. M. *Angew. Chem., Int. Ed. Engl.* **1998**, *37*, 2755-2794.

138. Lee, R. T.; Lee, Y. C. *Glycoconj. J.* **2000**, *17*, 543-551.

139. Lundquist, J. J.; Toone, E. J. *Chem. Rev.* **2002**, *102*, 555-578.

140. Helg, A.; Mueller, M. S.; Joss, A.; Pöltl-Frank, F.; Stuart, F.; Robinson, J. A.; Pluschke, G. *J. Immunol. Methods* **2003**, *276*, 19-31.

141. Mattes, M. J. *J. Immunol. Methods* **1997**, *202*, 97-101.

142. Jencks, W. P. *Proc. Natl. Acad. Sci. U. S. A.* **1981**, *78*, 4046-4050.

143. Kitov, P.; Bundle, D. *J. Am. Chem. Soc.* **2003**, *125*, 16271-16284.

144. Chakrabarti, C. G.; De, K. *Internat. J. Math., Math. Sci.* **2000**, *23*, 243-251.

145. Boerlin, P.; McEwen, S.; Boerlin-Petzold, F.; Wilson, J.; Johnson, R.; Gyles, C. *J. Clin. Microbiol.* **1999**, *37*, 497-503.

146. Fraser, M. E.; Fujinaga, M.; Cherney, M. M.; Melton-Celsa, A. R.; Twiddy, E. M.; O' Brien, A. D.; James, M. N. G. *J. Biol. Chem.* **2004**, *279*, 27511-27517.

147. Kale, R. R.; McGannon, C. M.; Fuller-Schaefer, C.; Hatch, D. M.; Flagler, M. J.; Gamage, S. D.; Weiss, A. A.; Iyer, S. S. *Angew. Chem., Int. Ed. Engl.* **2008**, *47*, 1265-1268.

148. Bertozzi, C. R.; Kiessling, L. L. *Science* **2001**, *291*, 2357-2364.

149. Kiessling, L. L.; Splain, R. A. *Annu. Rev. Biochem.* **2010**, *79*, 619-653.

150. Demchenko, A. V. *Lett. Org. Chem.* **2005**, *2*, 580-589.

151. Crich, D. *Acc. Chem. Res.* **2010**, *43*, 1144-1153.

152. Huang, M.; Garrett, G. E.; Birlirakis, N.; Bohé, L.; Pratt, D. A.; Crich, D. *Nature Chem.* **2012**, *4*, 663-667.

153. Mydock, L. K.; Demchenko, A. V. *Org. Biomol. Chem.* **2010**, *8*, 497-510.

154. Stick, R. V. *Carbohydrates: the sweet molecules of life*; Academic Press; London; UK, 2001.

155. Fisher, E. *Ber. Dtsch. Chem. Ges.* **1893**, *26*, 2400-2412.

156. Keonigs, W.; Knorr, E. *Ber. Dtsch. Chem. Ges.* **1901**, *34*, 957-981.

157. Meloncelli, P. J.; Martin, A. D.; Lowary, T. L. *Carbohydr. Res.* **2009**, *344*, 1110-1122.

158. Hadd, M. J.; Gervay, J. *Carbohydr. Res.* **1999**, *320*, 61-69.

159. Gervay, J.; Hadd, M. J. *J. Org. Chem.* **1997**, *62*, 6961-6967.

160. Lemieux, R. U.; Hendriks, K. B.; Stick, R. V.; James, K. *J. Am. Chem. Soc.* **1975**, *97*, 4056-4062.

161. Lemieux, R. U.; Driguez, H. *J. Am. Chem. Soc.* **1975**, *97*, 4063-4069.

162. Lemieux, R. U.; Driguez, H. *J. Am. Chem. Soc.* **1975**, *97*, 4069-4075.

163. Lemieux, R. U.; Bundle, D. R.; Baker, D. A. *J. Am. Chem. Soc.* **1975**, *97*, 4076-4083.

164. Pougny, J. R.; Jacquinet, J. C.; Nassr, M.; Duchet, D.; Milat, M. L.; Sinay, P. *J. Am. Chem. Soc.* **1977**, *99*, 6762-6763.

165. Schmidt, R. R.; Kinzy, W. *Adv. Carbohydr. Chem. Biochem.* **1994**, *50*, 21-123.

166. Yu, B.; Tao, H. *Tetrahedron Lett.* **2001**, *42*, 2405-2407.

167. Yu, B.; Tao, H. *J. Org. Chem.* **2002**, *67*, 9099-9102.

168. Fischer, E.; Delbrück, K. *Ber. Dtsch. Chem. Ges.* **1909**, *42*, 1476-1482.

169. Schmidt, R. R.; Castro-Palomino, J. C. *Pure and applied ...* **1999**.

170. Charbonnier, F.; Penadés, S. *Eur. J. Org. Chem.* **2004**, *2004*, 3650-3656.

171. Tran, A.-T.; Burden, R.; Racys, D. T.; Galan, M. C. *Chem. Commun.* **2011**, *47*, 4526-4528.

172. Garegg, P. J. *Adv. Carbohydr. Chem. Biochem.* **1997**, *52*, 179-205.

173. Tatai, J.; Fügedi, P. *Org. Lett.* **2007**, *9*, 4647-4650.

174. Crich, D.; Smith, M. *J. Am. Chem. Soc.* **2001**, *123*, 9015-9020.

175. Crich, D.; Li, H. *J. Org. Chem.* **2002**, *67*, 4640-4646.

176. Codée, J. D. C.; Litjens, R. E. J. N.; den Heeten, R.; Overkleeft, H. S.; van Boom, J. H.; van der Marel, G. A. *Org. Lett.* **2003**, *5*, 1519-1522.

177. Dinkelaar, J.; Codée, J. D. C.; van den Bos, L. J.; Overkleeft, H. S.; van der Marel, G. A. *J. Org. Chem.* **2007**, *72*, 5737-5742.

178. Konradsson, P.; Udodong, U. E.; Fraser-Reid, B. *Tetrahedron Lett.* **1990**, *31*, 4313-4316.

179. Veeneman, G. H.; van Leeuwen, S. H.; van Boom, J. H. *Tetrahedron Lett.* **1990**, *31*, 1331-1334.

180. Lemieux, R. U.; Koto, S. *Tetrahedron* **1974**, *30*, 1933-1944.

181. Lemieux, R. U.; Chü, N. J. *Abstr. Pap. Am. Chem. Soc.* **1955**, *133*, 31N.

182. Edward, J. T. *Chem. Ind. (London)* **1955**, 1102-1104.

183. Kabayama, M. A.; Patterson, D. *Can. J. Chem.* **1958**, *36*, 563-573.

184. Romers, C.; Altona, C.; Buys, H. R.; Havinga, E. *Topics in Stereochemistry*; Wiley-Interscience: New York, 1969; Vol. 4.

185. Radom, L.; Hehre, W. J.; Pople, J. A. *J. Am. Chem. Soc.* **1972**, *94*, 2371-2381.

186. Zhu, X.; Yu, B.; Hui, Y.; Schmidt, R. R. *Eur. J. Org. Chem.* **2004**, 965-973.

187. Gorin, P. A. J.; Perlin, A. S. *Can. J. Chem.* **1961**, *39*, 2474-2485.

188. Paulsen, H.; Lockhoff, O. *Tetrahedron Lett.* **1978**, 4027-4030.

189. Garegg, P. J.; Iversen, T. *Carbohydr. Res.* **1979**, *70*, C13-C14.

190. Wulff, G.; Röhle, G. *Angew. Chem., Int. Ed. Engl.* **1974**, *13*, 157-170.

191. Ratcliffe, A. J.; Fraser-Reid, B. *J. Chem. Soc., Perkin Trans. 1* **1990**, 747-750.

192. Crich, D.; Sun, S. *J. Am. Chem. Soc.* **1997**, *119*, 11217-11223.

193. Lu, S.-R.; Lai, Y.-H.; Chen, J.-H.; Liu, C.-Y.; Mong, K.-K. T. *Angew. Chem., Int. Ed. Engl.* **2011**, *50*, 7315-7320.

194. Udodong, U.; Fraser-Reid, B. *J. Am. Chem. Soc.* **1988**, *110*, 5583-5584.

195. Fraser-Reid, B.; Udodong, U. E.; Wu, Z. K.; Ottosson, H.; Merritt, J. R.; Rao, C. S.; Madsen, R. *Synlett* **1992**, 927-942.

196. Zhang, Z.; Ollmann, I. R.; Ye, X.-S.; Wischnat, R.; Baasov, T.; Wong, C.-H. *J. Am. Chem. Soc.* **1999**, *121*, 734-753.

197. Kitov, P. I.; Paszkiewicz, E.; Wakarchuk, W. W.; Bundle, D. R. *Methods Enzymol.* **2003**, *362*, 86-105.

198. Betaneli, V. I.; Ovchinnikov, M. V.; Backinowsky, L. V.; Kochetkov, N. K. *Carbohydr. Res.* **1979**, *68*, C11-C13.

199. Ferro, V.; Mocerino, M.; Stick, R. V.; Tilbrook, D. *Aust. J. Chem.* **1988**, *41*, 813-815.

200. Sakagami, M.; Hamana, H. *Tetrahedron Lett.* **2000**, *41*, 5547-5551.

201. Urban, F. J.; Moore, B. S.; Breitenbach, R. *Tetrahedron Lett.* **1990**, *31*, 4421-4424.

202. Du, Y.; Wei, G.; Cheng, S.; Hua, Y.; Linhardt, R. J. *Tetrahedron Lett.* **2006**, *47*, 307-310.

203. Ludek, O. R.; Gu, W.; Gildersleeve, J. C. *Carbohydr. Res.* **2010**, *345*, 2074-2078.

204. Chaudhary, S. K.; Hernandez, O. *Tetrahedron Lett.* **1979**, *20*, 99-102.

205. Nicolaou, K. C.; Seitz, S. P.; Pavia, M. R.; Petasis, N. A. *J. Org. Chem.* **1979**, *44*, 4011-4013.

206. Kitov, P. I.; Mulvey, G. L.; Griener, T. P.; Lipinski, T.; Solomon, D.; Paszkiewicz, E.; Jacobson, J. M.; Sadowska, J. M.; Suzuki, M.; Yamamura, K. I.; Armstrong, G. D.; Bundle, D. R. *Proc. Natl. Acad. Sci. U. S. A.* **2008**, *105*, 16837-16842.

207. Gamage, S. D.; McGannon, C. M.; Weiss, A. A. *J. Bacteriol.* **2004**, *186*, 5506-5512.

208. Zhang, J.; Kowal, P.; Fang, J.; Andreana, P.; Wang, P. G. *Carbohydr. Res.* **2002**, *337*, 969-976.

209. Meyer, B.; Peters, T. *Angew. Chem., Int. Ed.* **2003**, *42*, 864-890.

210. Koeller, K. M.; Smith, M. E.; Wong, C. H. *Bioorg. Med. Chem.* **2000**, *8*, 1017-1025.

211. Helferich, B.; Zirner, J. *Ber. Dtsch. Chem. Ges.* **1962**, *95*, 2604-2611.

212. DeNinno, M. P.; Etienne, J. B.; Duplantier, K. C. *Tetrahedron Lett.* **1995**, *36*, 669-672.

213. Schmidt, R. R.; Toepfer, A. *Tetrahedron Lett.* **1991**, *32*, 3353-3356.

214. Paulsen, H.; Merz, G.; Brockhausen, I. *Liebigs Ann. Chem.* **1990**, *1990*, 719-739.

215. McCloskey, C. M. *Adv. Carbohydr. Chem.* **1957**, *12*, 137-156.

216. Philips, K. D.; Žemlička, J.; Horwitz, J. P. *Carbohydr. Res.* **1973**.

217. Mayer, M.; Meyer, B. *Angew. Chem., Int. Ed.* **1999**, *38*, 1784-1788.

218. Kitova, E.; Kitov, P.; Bundle, D.; Klassen, J. *Glycobiology* **2001**, *11*, 605-611.

219. Gao, L.; Liu, Q.; Ren, S.; Wan, S.; Jiang, T.; Wong, I. L. K.; Chow, L. M. C.; Wang, S. *J. Carbohydr. Chem.* **2012**, *31*, 620-633.

220. Meloncelli, P. J.; Lowary, T. L. *Carbohydr. Res.* **2010**, *345*, 2305-2322.

221. Pagé, D.; Roy, R. *Bioorg. Med. Chem. Lett.* **1996**, *6*, 1765-1770.

222. Hällgren, C.; Hindsgaul, O. *J. Carbohydr. Chem.* **1995**, *14*, 453-464.

223. von Itzstein, M.; Jenkins, I. D. *J. Chem. Soc., Perkin Trans. 1* **1986**, 437.

224. Rodriguez, E. B.; Stick, R. V. *Aust. J. Chem.* **1990**, *43*, 665-679.

225. Kitov, P. I.; Railton, C.; Bundle, D. R. *Carbohydr. Res.* **1998**, *307*, 361-369.

226. Flagler, M. J.; Mahajan, S. S.; Kulkarni, A. A.; Iyer, S. S.; Weiss, A. A. *Biochemistry* **2010**, *49*, 1649-1657.

227. Fuller, C. A.; Pellino, C. A.; Flagler, M. J.; Strasser, J. E.; Weiss, A. A. *Infect. Immun.* **2011**, *79*, 1329-1337.

228. Armstrong, G. D.; Mulvey, G. L.; Marcato, P.; Griener, T. P.; Kahan, M. C.; Tennent, G. A.; Sabin, C. A.; Chart, H.; Pepys, M. B. *J. Infect. Dis.* **2006**, *193*, 1120-1124.

229. Griener, T. P.; Strecker, J. G.; Humphries, R. M.; Mulvey, G. L.; Fuentealba, C.; Hancock, R. E. W.; Armstrong, G. D. *PLoS One* **2011**, *6*, e21457.

230. Jacobson, J. M.; Kitov, P. I.; Bundle, D. R. *Carbohydr. Res.* **2013**, *378*, 4-14.

231. Rostovtsev, V. V.; Green, L. G.; Fokin, V. V.; Sharpless, K. B. *Angew. Chem., Int. Ed.* **2002**, *41*, 2596-2599.

232. Tornøe, C. W.; Christensen, C.; Meldal, M. *J. Org. Chem.* **2002**, *67*, 3057-3064.

233. Kitov, P. I.; Paszkiewicz, E.; Sadowska, J. M.; Deng, Z.; Ahmed, M.; Narain, R.; Griener, T. P.; Mulvey, G. L.; Armstrong, G. D.; Bundle, D. R. *Toxins* **2011**, *3*, 1065-1088.

234. Ferrier, R. J.; Furneaux, R. H. *Carbohydr. Res.* **1976**, *52*, 63-68.

235. Daragics, K.; Fügedi, P. *Tetrahedron Lett.* **2009**, *50*, 2914-2916.

236. Komarova, B. S.; Tsvetkov, Y. E.; Pier, G. B.; Nifantiev, N. E. *Carbohydr. Res.* **2012**, *360*, 56-68.

237. Kimura, T.; Tani, S.; Matsumoto Yi, Y.; Takeda, T. *J. Biol. Chem.* **2001**, *276*, 41576-41579.

238. Snedeker, K. G.; Shaw, D. J.; Locking, M. E.; Prescott, R. J. *BMC Infect. Dis.* **2009**, *9*, 144.

239. Muniesa, M.; Hammerl, J. A.; Hertwig, S.; Appel, B.; Bruessow, H. *Appl. Environ. Microbiol.* **2012**, *78*, 4065-4073.

240. Rojas, R. L. G.; Gomes, P. A. D. P.; Bentancor, L. V.; Sbrogio-Almeida, M. E.; Costa, S. O. P.; Massis, L. M.; Ferreira, R. C. C.; Palermo, M. S.; Ferreira, L. C. S. *Clin. Vaccine Immunol.* **2010**, *17*, 529-536.

241. Gelas, J.; Thiallier, A. *Carbohydr. Res.* **1973**, *30*, 21-34.

242. INC., Theracarb. 2004; Vol. WO2004/99173 A1.

243. Harper, J. L.; Hayman, C. M.; Larsen, D. S.; Painter, G. F.; Singh-Gill, G. *Bioorg. Med. Chem.* **2011**, *19*, 917-925.

244. Lassaletta, J. M.; Meichle, M.; Weiler, S.; Schmidt, R. R. *J. Carbohydr. Chem.* **1996**, *15*, 241-254.

245. Kitov, P. I.; Kotsuchibashi, Y.; Paszkiewicz, E.; Wilhelm, D.; Narain, R.; Bundle, D. R. *Org. Lett.* **2013**, *15*, 5190-5193.